GAZI MEDICAL JOURNAL

GAZİ UNIVERSITY
Gazi
1926

IV

GAZI MEDICAL JOURNAL

medicaljournal.gazi.edu.tr

GAZİ UNIVERSITY · Gazi · 1926

CONTENTS

Original Investigations - Özgün Araştırmalar

GAZI MEDICAL JOURNAL

medicaljournal.gazi.edu.tr

GAZİ UNIVERSITY
Gazi
1926

CONTENTS

GAZI MEDICAL JOURNAL

medicaljournal.gazi.edu.tr

GAZİ UNIVERSITY · 1926

CONTENTS

Investigation of the Effect of Antenatal Family Planning Counseling in Primary Care on Postpartum Family Planning Method Use

Birinci Basamakta Verilen Doğum Öncesi Aile Planlaması Danışmanlığının Doğum Sonrası Aile Planlaması Yöntemi Kullanımına Etkisinin İncelenmesi

Asiye Sezer Olgun[1], İrem Medeni[2]

[1]Department of Family Medicine, Kastamonu University Faculty of Medicine, Kastamonu, Türkiye
[2]Department of Employee Health, General Directorate of Public Health, Republic of Türkiye Ministry of Health, Ankara, Türkiye

ABSTRACT

Objective: This study aimed to assess the effect of family planning (FP) counseling provided to pregnant women who attended a family health center on their use of FP after pregnancy.

Methods: The antenatal and postpartum records of 219 of 225 women registered at a family health centre in Kastamonu between 2017 and 2022, whose follow-up was complete and without missing information, were retrospectively examined. The patients' sociodemographic data, obstetric information, the FP method they planned to use after birth (recorded at the third and fourth antenatal follow-ups), and information on postpartum FP method use were recorded.

Results: The mean age of the participants in this study was 29.6 years, and 41.5% were university graduates. The study reported an unplanned pregnancy rate of 16.4%. When asked about the FP method they would use in the postpartum period during the third antenatal visit (28–32 weeks), 52.5% of participants were undecided, 42.0% preferred a modern method, and participants were then provided FP method counselling. At the fourth antenatal follow-up (36–38 weeks), the rate of undecided individuals decreased significantly to 35.6%, while the rate of those preferring a modern method increased significantly to 59.4% (p < 0.001). At the postpartum follow-up (30–42 days after birth), 95% of women had started using FP methods: condoms were the most commonly used modern method (63.9%) and injections were the least used (1.9%).

Conclusion: FP consultancy services provided during the antenatal period facilitate women's ability to make informed choices in the

ÖZ

Amaç: Bu çalışmada aile sağlığı merkezinde gebelik döneminde verilen aile planlaması danışmanlığının, gebelik sonrası aile planlaması kullanım durumuna etkisinin incelenmesi amaçlanmıştır.

Yöntemler: 2017–2022 yılları arasında Kastamonu'daki bir aile sağlığı merkezine kayıtlı olan 225 kadından, izlemleri tam ve eksik bilgi olmayan 219 kadının gebe-lohusa izlem dosyaları retrospektif olarak incelendi. Hastaların sosyodemografik verileri, obstetrik bilgileri, doğumdan sonra kullanmayı planladıkları aile planlaması (AP) yöntemi (üçüncü ve dördüncü antenatal izlemde kaydedilen) ve postpartum AP yöntem kullanımı hakkında bilgiler kaydedilmiştir.

Bulgular: Çalışmaya katılanların ortalama yaşı 29,6 ve %41,5'i üniversite mezunuydu. Çalışmada, plansız gebelik oranı %16,4 bulundu. Üçüncü antenatal izlemde yapılan gebe izlemde (28–32 hafta) postpartum dönemde kullanacakları AP yöntemi sorulduğunda, katılımcıların %52,5'i kararsızdı, modern yöntem tercih edenlerin oranı %42,0 olarak bulundu, sonrasında AP yöntem danışmanlığı verildi. Dördüncü antenatal izlemde (36-38 hafta), kararsızların oranı anlamlı olarak azalmış (%35,6) ve modern yöntem tercih edenlerin oranı ise anlamlı olarak artmıştı (%59,4) (p < 0,001). Doğumdan 30-42 gün sonra yapılan lohusa izleminde, kadınların %95'i aile planlaması yöntemini kullanmaya başladı; kondom en çok tercih edilen modern yöntemdi (%63,9), enjeksiyon ise en az tercih edilen yöntemdi (%1,9).

Sonuç: Antenatal dönemde verilen AP danışmanlık hizmetleri, kadınların doğum sonrası dönemde bilinçli seçimler yapabilmelerini kolaylaştırarak hem kendi sağlıklarını hem de yeni doğan bebeklerinin sağlığının korunmasına katkıda bulunur.

Address for Correspondence/Yazışma Adresi: Asiye Sezer Olgun, Department of Family Medicine, Kastamonu University Faculty of Medicine, Kastamonu, Türkiye
E-mail / E-posta: dr.asiye33@gmail.com
ORCID ID: orcid.org/0009-0000-6499-0320

Gazi Med J 2026;37(1):1-6

Sezer Olgun and Medeni. The Impact of Prenatal Family Planning Counseling on Postnatal Contraception

ABSTRACT

postpartum period, thereby contributing to the protection of both their own health and that of their newborns.

Keywords: Family planning counselling, postpartum contraception, family planning, modern family planning

ÖZ

Anahtar Sözcükler: Aile planlaması danışmanlığı, doğum sonrası kontrasepsiyon, aile planlaması, modern aile planlaması

INTRODUCTION

Family planning (FP) refers to the conscious effort of a couple to limit the number of children they will have or to determine the intervals between births, typically through the use of contraceptive methods (1). The most important goals of FP are to protect and improve maternal and fetal health, to inform couples, to prevent unwanted pregnancies, and to provide assistance to individuals who cannot have children (2). FP affects the reproductive health of the mother, fetus, and the whole family by promoting adequate birth intervals for the mother, reducing unwanted pregnancies and abortions, and preventing sexually transmitted diseases (3).

FP methods are classified into modern and traditional contraceptive methods (4). Modern contraceptive methods include male and female sterilization, intrauterine devices (IUDs), implants, injectables, oral contraceptive pills, male and female condoms, and vaginal barrier methods (diaphragm, cervical cap, and spermicidal foam). In contrast, traditional contraceptive methods include the calendar method and withdrawal (5).

As long as humanity exists, the need for FP will persist; there will be girls and boys who reach sexual maturity and people who require FP and other health services (6). According to a study conducted by the United Nations in 2022, among 1.9 billion women of reproductive age (15-49 years), approximately 874 million women use modern contraceptive methods, while 92 million women use traditional FP methods (7). In Türkiye, FP services were legalized in 1965, and their use has become increasingly widespread since then (8). According to the results of the 2018 Türkiye Demographic and Health Survey, the most commonly used FP methods are withdrawal (20%), male condom (19%), IUD (14%), and tubal ligation (10%) (9).

If women become pregnant again during the early postpartum period, problems may occur for maternal and infant health (10). An important aspect of maternal care during the postpartum period is FP (11). According to the Prenatal Care Guidelines and Postpartum Care Guidelines of the Ministry of Health of the Republic of Türkiye, FP education and counseling are provided to pregnant women in primary health care institutions during the third (28–32 weeks) and fourth (36–38 weeks) antenatal follow-ups and in the postpartum period (12,13). During these follow-ups at health centers, family physicians and nurses provide both personalized general and method-specific counseling.

This study aimed to examine the effect of FP education, provided to pregnant women who applied to a family health center, on their use of FP after pregnancy.

MATERIALS AND METHODS

This study examined the antenatal and postpartum records of women who gave birth between 2017 and 2022 and who were registered at a family medicine center in Kastamonu Province. According to the "Prenatal Care Management Guide" published by the General Directorate of Public Health, each pregnant woman should have at least four follow-up visits, and counseling on reproductive health methods should be provided at the 3rd (28–32 weeks) and 4th (36–38 weeks) visits and during the postpartum period (12).

In this retrospective cross-sectional study, all antenatal and postpartum records from the relevant institution within the specified date range were included. The inclusion criteria for the study included access to all prenatal and postnatal records of 225 women who were registered at the family health center and who applied for prenatal follow-up between 2017 and 2022. However, six participants were excluded from the study due to missing information in their files. The study included 219 women whose follow-up was complete from the beginning of pregnancy through the puerperium and who had no missing information in the antenatal and postpartum records.

The patients' sociodemographic data, obstetric information the FP method they planned to use after birth (at the 3rd and 4th antenatal follow-ups), and information on postpartum FP method use were recorded.

Statistical Analysis

In this study, all statistical analyses were performed using Pearson's chi-square test and Fisher's exact test to compare categorical variables, which were presented as numbers and percentages in the descriptive results section, using IBM SPSS Statistics version 22 (IBM Corp.). The threshold for statistical significance was established at $p < 0.05$.

RESULTS

Sociodemographic information and the percentage distribution of participants, based on data from 219 antenatal and postpartum records included in the study, are presented in Table 1. Participants' ages ranged from 18 to 42 years (mean: 29.6 ± 5.0 years). 41.5% of the participants were university graduates, 68.5% were housewives, and 83% were from nuclear families. Twenty-seven (12.3%) of the participants reported having a chronic disease before pregnancy, and 18 (8.2%) reported smoking during pregnancy. Participants' ages at first marriage ranged from 16 to 36 years, with a mean age of 23.6 ± 3.8 years.

Information on FP use and the obstetric history of the participants is shown in Table 2. Among the 219 participants, 83.6% did not use any FP method during the pre-pregnancy period because they were planning to become pregnant, and became pregnant unintentionally while using a FP method. Unplanned pregnancies (n = 36) occurred primarily during condom use (55.6%) and secondarily during withdrawal (38.9%).

Gazi Med J 2026;37(1):1-6

Sezer Olgun and Medeni. The Impact of Prenatal Family Planning Counseling on Postnatal Contraception

During the study, 32.4% of the participants had their first pregnancy, 37.4% had their second pregnancy, 4 participants (1.8%) had multiple pregnancies, 26.5% had experienced a miscarriage before their current pregnancy, 41.6% had no living children, and 44.3% had one living child.

During the pregnancy follow-up at 28–32 weeks, when asked which FP method they planned to use in the postpartum period, 52.5% responded "uncertain", 25.6% chose condom, 9.1% chose IUD, and 5.9% chose tubal ligation. At the 36–38-week pregnancy follow-up, 35.6% reported "uncertain", 35.6% reported condom use, 11.4% reported IUD use, and 8.7% reported tubal ligation.

In the postpartum follow-up conducted between days 30 and 42 after birth, 5% of the participants had not yet started using a FP

Table 1. Descriptive characteristics of the participants.

	n	%
Age (n = 219)		
18–23	33	15.1
24–29	72	32.9
30–35	91	41.6
36 and over	23	10.5
Occupation (n = 219)		
Housewife	150	68.5
Teacher	22	10.0
Worker	17	7.8
Other*	30	13.7
Educational status (n = 219)		
Not completed any school	1	0.5
Primary school graduate	29	13.2
Middle school graduate	32	14.6
High school graduate	63	28.8
University graduate	91	41.5
Master's/PhD	3	1.4
Smoking (n = 219)		
No	201	91.8
Yes	18	8.2
Chronic disease (n = 219)		
No	192	87.7
Yes	27	12.3
Types of family (n = 219)		
Nuclear family	183	83.6
Extended family	36	16.4
Marriage age (n = 219)		
16–21	69	31.5
22–27	118	53.9
28–33	29	13.2
34 and over	3	1.4
Number of people living in the household n = 219		
2	79	36.1
3	82	37.4
4	28	12.8
5 and more	30	13.7

*Other: Academician, nurse, officer

Table 2. Distribution of some reproductive and FP use characteristics of the participants.

	(n)	(%)
Total number of pregnancies(n = 219)		
1	71	32.4
2	82	37.4
3	37	16.9
4	20	9.1
5 and over	9	4.2
Total number of living children (n = 219)		
0	91	41.6
1	97	44.3
2	25	11.4
3	6	2.7
Miscarriage/abortion status (n = 219)		
No	161	73.5
Yes	58	26.5
Multiple pregnancy status (n = 219)		
No	215	98.2
Yes	4	1.8
Blood type incompatibility (n = 219)		
No	205	93.6
Yes	14	6.4
Use of FP before pregnancy (n = 219)		
Does not use	183	83.6
Is using	36	16.4
FP method used before pregnancy (n = 36)		
Withdrawal	14	38.9
Condom	20	55.6
Oral contraceptive pills	1	2.8
Injectables	1	2.8
The decision to use the FP method in the postpartum period was made after the first interview (n = 219)		
Uncertain	115	52.5
Condom	56	25.6
IUD	20	9.1
Tubal ligation	13	5.9
Withdrawal	10	4.6
Injectables	2	0.9
Oral contraceptive pills	1	0.5
Does not want to use	1	0.5

Gazi Med J 2026;37(1):1-6

Sezer Olgun and Medeni. The Impact of Prenatal Family Planning Counseling on Postnatal Contraception

Table 2. Continued.

	(n)	(%)
The decision to use the FP method in the postpartum period was made after the second interview (n = 219)		
Uncertain	78	35.6
Condom	78	35.6
IUD	25	11.4
Tubal ligation	19	8.7
Withdrawal	9	4.1
Injectables	4	1.8
Oral contraceptive pills	3	1.4
Does not want to use	1	0.5
The status of postpartum FP use (n = 219)		
No	11	5.0
Yes	208	95.0
FP method used after pregnancy (n =2 08)		
Condom	133	63.9
Tubal ligation	19	9.1
Withdrawal	22	10.6
IUD	15	7.2
Oral contraceptive pills	6	2.9
Injectables	4	1.9
Lactational amenorrhea	9	4.3

IUD: Intrauterine device

method, while 95% had; among the 209 method users, condoms were the most preferred (63.9%) and injections the least (1.9%).

Table 3 shows the FP methods used before and after the training. In our study, participants were asked during the third pregnancy follow-up which FP method they planned to use in the postpartum period. The 53.4% of the participants stated that they were uncertain or would not use a method; 4.6% that they; and 42.0% that they would prefer modern methods. Subsequently, FP counseling was provided as part of the third and fourth pregnancy follow-up visits. When participants were asked at the fourth pregnancy follow-up which FP method they planned to use during the postpartum period, the proportion who were uncertain or who said they would not use a method decreased to 36.5%. The rate of those who preferred the withdrawal method decreased to 4.1%, while the rate of those who preferred modern methods increased to 59.4%. As a result of FP

Table 3. Distribution of FP methods used before and after education

	Before education		After education		
	n	%	n	%	
Traditional methods	10	4.6	9	4.1	**p < 0.001**
Modern methods	92	42.0	130	59.4	**p < 0.001**
Uncertain/unwilling	117	53.4	80	36.5	**p < 0.001**

counseling, there was a significant increase in plans to use modern methods and a significant decrease in the rate of uncertainty or unwillingness p < 0.001.

In our study, no significant relationship was found between postpartum FP method use and either age or educational status.

DISCUSSION

This study assesses the current use of FP methods among women who gave birth at a family health center by comprehensively analyzing five-year follow-up slips for pregnant and postpartum women. The findings show that women who were educated about the subject during the antenatal period had increased use of modern methods.

Worldwide, 42% of pregnancies are unintended (14). Unintended pregnancy rates were 55% in Papua New Guinea, 27% in Middle Eastern and North African countries, 33.9% in sub-Saharan African countries, and 31% in Sweden (15–18). In a study conducted in Türkiye, the unplanned pregnancy rate was 30%; of these pregnancies, 38.5% occurred in women who did not use FP methods and 47.2% occurred in women who used traditional FP methods. In our study, the rate of unplanned pregnancies was 16.4% (19). These rates indicate that unintended pregnancies are a significant public health problem in both developed and developing countries. The reason our study's results were lower than those of other studies may be the high level of education among the participants.

According to World Health Organization data, 95% of women do not want to become pregnant again in the first year after delivery; however, 70% of these women do not use any contraceptive method (20). A study conducted in England found that 71.1% used the FP method at the 8th postpartum week; a study conducted in Brazil found 87.9% at the 3rd postpartum month; and a study conducted in Ethiopia found 16% at the 6th postpartum week (21–23). In a study conducted in Türkiye among women 6–12 months postpartum, 84.8% were using the FP method, while nearly half (49.3%) were using modern methods (24). In our study, the FP method use rate at the 6-week postpartum follow-up was 95%. The high rate of FP use during the postpartum period among the women who participated in our study was associated with the provision of FP counseling during the 3rd and 4th antenatal follow-ups. These differing rates in the literature may be due to variation in the time elapsed since birth across studies and to differences in participants' sociodemographic characteristics. In a study conducted in China, the rates of knowledge and use of effective postpartum methods were higher, and the rate of unintended pregnancy was lower in the group that received postpartum FP counseling intervention within 1 year after delivery compared to the control group (25). Studies conducted in Kenya, Zambia, and Tanzania found that the intention to use postpartum contraception and the use of effective methods would increase with the integration of FP counseling into prenatal follow-up (26,27). In another study, conducted in Uganda, the plans to use postpartum modern methods during pregnancy follow-up were 87% in the intervention group and 71% in the control group (28). In a study conducted in Southern Ethiopia, 69.7% of women received FP counseling during pregnancy; the rate of postpartum FP use was 1.79 times higher in those who received counseling (29). In our study, the use of modern FP methods increased from 42% before the

Gazi Med J 2026;37(1):1-6

Sezer Olgun and Medeni. The Impact of Prenatal Family Planning Counseling on Postnatal Contraception

training to 59.1% after the training; this difference was statistically significant p < 0.001. These results suggest that FP counseling during pregnancy can increase awareness of the use of modern FP methods in the postpartum period.

Study Limitations

A limitation of this study is that it was conducted at a single center, which may limit the generalizability of the findings to the national level. However, this study reveals the contribution of family medicine to women's and community health and will guide similar studies on this subject.

CONCLUSION

The protection and promotion of maternal and infant health are critical to the sustainability of public health. Correct and regular use of FP methods prevents unintended pregnancies, reduces the health risks of both mother and baby, and enables fertility control. The rate at which women use FP methods, especially in the postpartum period, is directly related to the counseling provided by healthcare providers. These counseling services, provided during the antenatal period, enable women to make informed choices in the postpartum period and contribute to protecting both their own health and that of their newborns. According to the results of our study, women who receive FP counseling are more likely to use modern FP methods appropriately and safely during the postpartum period. Family physicians should provide individualized, comprehensive, and holistic information and counseling on FP, taking into account the sociodemographic and cultural characteristics of women they serve. Community-based studies should be conducted to assess public knowledge and attitudes, and national and regional policies should be developed.

Ethics

Ethics Committee Approval: Ethical approval for the study was obtained from Kastamonu University Clinical Research Ethics Committee (approval number: 2002-KAEK92, date: 16.11.2022).

Informed Consent: It is retrospective cross-sectional study.

Footnotes

Authorship Contributions

Surgical and Medical Practices: A.S.O., İ.M., Concept: A.S.O., İ.M., Design: A.S.O., İ.M., Data Collection or Processing: A.S.O., İ.M., Analysis or Interpretation: A.S.O., İ.M., Literature Search: A.S.O., İ.M., Writing: A.S.O., İ.M.,

Conflict of Interest: No conflict of interest was declared by the authors.

Financial Disclosure: The authors declared that this study received no financial support.

REFERENCES

1. Omar AA, Ahmed DA. Knowledge and practice of family planning methods among the married women of reproductive age group attending SOS Hospital in Mogadishu Somalia. Turkish Journal of Health Science and Life. 2022; 5: 62–8.

2. Doğru HY, Oktay G, İşgüder ÇK, Özsoy AZ, Çakmak B, Delibaş İB, et al. The overview of women by age groups on the family planning and the evaluation of preferred methods: a tertiary center experience. Dicle Medical Journal. 2016; 43: 413–8.

3. Ali S, Hassan S, El-Nemer A. Assessment of family planning knowledge and practice among married couples. Mansoura Nurs J. 2020; 7(2): 214–26.

4. Alenezi GG, Haridi HK. Awareness and use of family planning methods among women in northern Saudi Arabia. Middle East Fertil Soc J. 2021; 26: 8.

5. Kantorová V, Wheldon MC, Ueffing P, Dasgupta ANZ. Estimating progress towards meeting women's contraceptive needs in 185 countries: a Bayesian hierarchical modelling study. PLoS Med. 2020; 17: e1003026.

6. World Health Organization; Department of Reproductive Health and Research; Johns Hopkins Bloomberg School of Public Health, Center for Communication Programs (INFO Project). *Family planning: a global handbook for providers: evidence-based guidance developed through worldwide collaboration* [Internet]. Baltimore (MD): CCP; Geneva: WHO; 2007 [cited 2026 Jan 7]. Available from: https://repository.stikesbcm.ac.id/id/eprint/335/1/Family%20Planning%20a%20Global%20Handbook%20for%20Providers%202007.pdf

7. United Nations, Department of Economic and Social Affairs, Population Division. *World family planning 2022: meeting the changing needs for family planning: contraceptive use by age and method* [Internet]. New York: United Nations; 2022 [cited 2026 Jan 7]. (UN DESA/POP/2022/TR/NO.4). Available from: https://desapublications.un.org/file/1128/download

8. Gavas E, İnal S. The family planning methods using status and attitudes of women in Türkiye: A systematic review. J Health Life Sci. 2019; 1: 37–43.

9. Hacettepe Üniversitesi Nüfus Etütleri Enstitüsü; T.C. Cumhurbaşkanlığı Strateji ve Bütçe Başkanlığı; TÜBİTAK. *2018 Türkiye Nüfus ve Sağlık Araştırması* [Internet]. Ankara (Turkey): Hacettepe Üniversitesi Nüfus Etütleri Enstitüsü; 2019 Nov [cited 2026 Jan 7]. Available from: https://fs.hacettepe.edu.tr/hips/dosyalar/Ara%C5%9Ft%C4%B1rmalar%20-%20raporlar/2018%20TNSA/TNSA2018_ana_Rapor_compressed.pdf

10. Alp Yılmaz F, Höbek Akarsu R, Tosun Güleroğlu F. Determination of preference family planning of postpartum women. Bozok Tıp Dergisi. 2018; 8: 21–5.

11. Thiel de Bocanegra H, Chang R, Howell M, Darney P. Interpregnancy intervals: impact of postpartum contraceptive effectiveness and coverage. Am J Obstet Gynecol. 2014; 210: 311.e1–8.

12. T.C. Sağlık Bakanlığı, Halk Sağlığı Genel Müdürlüğü, Kadın ve Üreme Sağlığı Dairesi Başkanlığı. *Doğum öncesi bakım yönetim rehberi* [Internet]. Ankara (Turkey): T.C. Sağlık Bakanlığı; 2018 [cited 2026 Jan 7]. Available from: https://dosyamerkez.saglik.gov.tr/Eklenti/28085,dogumoncesibakimyonetimrehberipdf.pdf

13. T.C. Sağlık Bakanlığı, Halk Sağlığı Genel Müdürlüğü, Kadın ve Üreme Sağlığı Dairesi Başkanlığı. *Doğum sonu bakım yönetim rehberi* [Internet]. Ankara (Türkiye): T.C. Sağlık Bakanlığı; 2018 [cited 2026 Jan 7]. Available from: https://platform.who.int/docs/default-source/mca-documents/policy-documents/guideline/TUR-MN-48-04-GUIDELINE-2018-tur-Postnatal-Care-Management-Guidelines.pdf

14. Valerio C, Norby M, Kremsreiter P. Options for unintended pregnancies. Am Fam Physician. 2025; 111: 352–60.

15. Peach E, Morgan C, Scoullar MJL, Fowkes FJI, Kennedy E, Melepia P, et al. Risk factors and knowledge associated with high unintended pregnancy rates and low family planning use among pregnant women in Papua New Guinea. Sci Rep. 2021; 11: 1222.

16. Islam N, Mahmood S, Kabir H, Chowdhury SR, Elshaikh U, Alhussaini N, et al. Prevalence of unintended pregnancy in the MENA region: a systematic review and meta-analysis. BMJ Open. 2025; 15: e084016.

Gazi Med J 2026;37(1):1-6

Sezer Olgun and Medeni. The Impact of Prenatal Family Planning Counseling on Postnatal Contraception

17. Bain LE, Zweekhorst MBM, de Cock Buning T. Prevalence and determinants of unintended pregnancy in sub-Saharan Africa: a systematic review. Afr J Reprod Health. 2020; 24: 187–205.

18. Carlander A, Hultstrand JN, Reuterwall I, Jonsson M, Tydén T, Kullinger M. Unplanned pregnancy and the association with maternal health and pregnancy outcomes: a Swedish cohort study. PLoS One. 2023; 18: e0286052.

19. Bayer A, Taşpınar A. Frequency of unplanned pregnancies and effect on body image. J Samsun Health Sci. 2023;8:77–90.

20. World Health Organization. *Programming strategies for postpartum family planning* [Internet]. Geneva: World Health Organization; 2013 Nov 7 [cited 2026 Jan 7]. Available from: https://www.who.int/publications/i/item/9789241506496

21. Moffat M, Jackowich R, Möller-Christensen C, Sullivan C, Rankin J. Demographic and pregnancy-related predictors of postnatal contraception uptake: a cross-sectional study. BJOG. 2024; 131: 1360–7.

22. Moreira LR, Ewerling F, Bertoldi AD, Silveira MF. Use of modern contraceptive methods and pregnancy planning: a cohort study. Rev Saude Publica. 2025; 59: e14.

23. Jima GH, Stekelenburg J, Fekadu H, Sendekie TY, Biesma R. Effect of contacts with health professionals on modern contraceptives uptake during the first 6 weeks after child birth: a prospective cohort study in Arsi Zone. Contracept Reprod Med. 2023; 8: 37.

24. Bilge Ç, Kaydırak M, Altınsoy B, Yakıt Ak E, Öztürk S. Women's attitudes toward family planning in the postpartum period and affecting factors: Turkiye sample. J Transcult Nurs. 2025; 36: 271–8.

25. Yin A, Zhou X, Qian X, Zhang L, Wang X, Yang H, et al. Integrating a postpartum contraception intervention in the maternal and child health care system of China: a randomized clinical trial. JAMA Netw Open. 2024; 7: e2450635.

26. Do M, Hotchkiss D. Relationships between antenatal and postnatal care and post-partum modern contraceptive use: evidence from population surveys in Kenya and Zambia. BMC Health Serv Res. 2013; 13: 6.

27. Keogh SC, Urassa M, Kumogola Y, Kalongoji S, Kimaro D, Zaba B. Postpartum contraception in northern tanzania: patterns of use, relationship to antenatal intentions, and impact of antenatal counseling. Stud Fam Plann. 2015; 46: 405–22.

28. Ayiasi RM, Muhumuza C, Bukenya J, Orach CG. The effect of prenatal counselling on postpartum family planning use among early postpartum women in Masindi and Kiryandongo districts, Uganda. Pan Afr Med J. 2015; 21: 138.

29. Sirage N, Desalegn Z, Wako WG, Yimer A, Bizuneh FK, Feleke SF, et al. Family planning utilization among postpartum women in the Bule Hora District, southern Ethiopia. Front Glob Womens Health. 2024; 5: 1323024.

Calorie Restriction: The Elixir of Youth for Kidneys and Testicles?

Kalori Kısıtlaması: Böbrekler ve Testisler için Gençlik İksiri mi?

Ayça Coşkun[1], Esra Toker[2], Arzu Keskin Aktan[3], Saadet Özen Akarca Dizakar[4], Kazime Gonca Akbulut[2]

[1]Department of Physiotherapy and Rehabilitation, Sakarya University Faculty of Health Sciences, Sakarya, Türkiye
[2]Department of Physiology, Gazi University Faculty of Medicine, Ankara, Türkiye
[3]Department of Physiology, Afyonkarahisar Health Sciences University Faculty of Medicine, Afyonkarahisar, Türkiye
[4]Department of Histology and Embryology, İzmir Bakırçay University Faculty of Medicine, İzmir, Türkiye

ABSTRACT

Objective: Reactive oxygen species that accumulate during aging can cause oxidative stress in kidney and testicular tissues, contributing to the progression of chronic kidney disease and to male infertility. Caloric restriction (CR) is considered the most effective non-pharmacological method to promote healthy aging through multiple mechanisms, including modulation of oxidative stress. This study aimed to investigate the effects of short-term CR on kidney and testicular tissues during aging.

Methods: Twenty-eight rats were divided into four groups: young control, young CR, old control, and old CR. Control groups were fed ad libitum, whereas CR groups received approximately one-third of their daily caloric intake. After 10 weeks, blood parameters [creatinine (Cre), blood urea nitrogen, uric acid (UA), testosterone levels], oxidative stress markers [malondialdehyde (MDA) and glutathione (GSH)], and histological changes were analyzed.

Results: Aging was associated with increased body and kidney weights and a reduced testicular index p < 0.005. CR reduced body and kidney weights and increased kidney and testicular indices (p <0.005). Renal function markers (Cre and UA) increased with age but were significantly reduced by CR (p <0.005). Aging increased MDA levels and decreased GSH levels in both renal and testicular tissues. Aging increased inflammatory cell infiltration and fibrosis in the kidney and testicular tissues, whereas CR significantly reduced the fibrosis percentage in aged rats.

ÖZ

Amaç: Yaşlanma sırasında biriken reaktif oksijen türleri, böbrek ve testis dokularında oksidatif strese neden olarak kronik böbrek hastalığının ve erkek kısırlığının ilerlemesine katkıda bulunabilir. Kalori kısıtlaması (CR), oksidatif stresin modülasyonu da dahil olmak üzere çeşitli mekanizmalar aracılığıyla sağlıklı yaşlanmayı destekleyen en etkili farmakolojik olmayan yöntem olarak kabul edilir. Bu çalışma, kısa süreli CR'nin yaşlanma sırasında böbrek ve testis dokuları üzerindeki etkilerini araştırmayı amaçlamıştır.

Yöntemler: Yirmi sekiz sıçan, dört gruba ayrıldı: genç kontrol, genç CR, yaşlı kontrol ve yaşlı CR. Kontrol grupları al-libitum olarak beslenirken, CR grupları günlük kalori alımlarının yaklaşık üçte birini tüketti. On hafta sonra, kan parametreleri [kreatinin (Cre), kan üre azotu, ürik asit (UA), testosteron düzeyleri], oksidatif stres belirteçleri [malondialdehit (MDA) ve glutatyon (GSH)] ve histolojik değişiklikler analiz edildi.

Bulgular: Yaşlanma, vücut ve böbrek ağırlıklarında artış ve testis indeksinde azalma ile ilişkiliydi p < 0,005. CR, vücut ve böbrek ağırlıklarında azalma ve böbrek ve testis indekslerinde artış gösterdi (p < 0.005). Böbrek fonksiyon belirteçleri (Cre ve UA) yaşla birlikte artmış, ancak CR ile anlamlı olarak azalmıştı (p <0,005). Yaşlanma, hem böbrek hem de testis dokularında MDA düzeylerini artırdı ve GSH düzeylerini düşürdü. Yaşlanma, böbrek ve testis dokularında inflamatuar hücre infiltrasyonunu ve fibrozisi artırırken, CR yaşlı sıçanlarda fibrozis yüzdesini anlamlı şekilde azalttı.

Address for Correspondence/Yazışma Adresi: Ayça Coşkun, Department of Physiotherapy and Rehabilitation, Sakarya University Faculty of Health Sciences, Faculty of Health Sciences, Sakarya, Türkiye
E-mail / E-posta: aycacoskun@subu.edu.tr
ORCID ID: orcid.org/0000-0002-7670-8668

Gazi Med J 2026;37(1):7-14

Coşkun et al. Calorie Restriction in Aging Testis and Kidney

ABSTRACT

Conclusion: Short-term CR may alleviate structural and functional impairments in the kidney and testis during aging by reducing oxidative stress.

Keywords: Caloric restriction, aging, kidney, testis, oxidative stress, infertility

ÖZ

Sonuç: Kısa süreli CR, oksidatif stresi azaltarak yaşlanma sırasında böbrek ve testisteki yapısal ve fonksiyonel bozuklukları hafifletebilir.

Anahtar Sözcükler: Kalori kısıtlaması, yaşlanma, böbrek, testis, oksidatif stres, infertilite

INTRODUCTION

Aging causes morphological and functional changes in various organs, increasing the risk of many important diseases, including neurodegenerative and cardiovascular diseases, as well as renal failure (1). Advancing age is associated with a significant decline in kidney function and in male fertility. The gradual decline in kidney glomerular filtration rate (GFR) and blood flow contributes to impaired renal function (2). In addition, the age-related loss of nephrons-the essential functional and structural units of the kidney-contributes to reduced renal capacity (3). This condition elevates the risk of developing chronic kidney disease (CKD) in older adults (4). CKD is 3–13 times more common in older individuals (5) and is anticipated to become the fifth most prevalent cause of death worldwide by 2040 (6).

Infertility is a significant health issue affecting 10–15% of couples worldwide. The etiology of this problem, which is male-related in 25–50% of cases, is largely unknown (7). Different levels of kidney disease in men have been associated with azoospermia, oligospermia, and low testosterone levels (8). Therefore, assessing reproductive and renal functions during aging is essential for preventing age-related disorders and promoting healthy aging (2).

Age-related dysfunction in organs such as the kidneys and testes results from an imbalance between reactive oxygen species (ROS) and the antioxidant defense system, leading to increased oxidative stress (9). Renal tissue is susceptible to oxidative damage due to age-related decreases in renal blood flow and GFR (10). Similarly, testicular tissue is vulnerable to oxidative stress due to its high metabolic activity, low antioxidant defenses, and abundant unsaturated fatty acids (11).

Caloric restriction (CR), in which total caloric intake is reduced while adequate intake of essential nutrients is maintained, is the most effective non-pharmacological strategy to support metabolic health (12). CR has been reported to improve kidney function by lowering levels of blood urea nitrogen (BUN), creatinine (Cre), and urinary protein. Thus, it delays the onset and progression of CKD, the risk of which increases with age (13). In addition, short-term CR has been shown to reduce glomerulosclerosis, urinary protein excretion, and renal fibrosis (14,15). It also reduces oxidative stress and supports testosterone production in the testes (16). In obese mice, CR increases the testicular organ index and serum testosterone levels by reducing oxidative stress levels and also regulates sperm morphology (17).

Various interventions that slow the aging process may help prevent organ damage. Our research examines the potential protective effects of CR against age-related changes in renal and testicular tissues, using markers of organ function, oxidative stress parameters, and histological assessments.

MATERIALS AND METHODS

Animals and the Experimental Group

The experimental procedures were approved by the Gazi University Animal Experiments Ethics Committee (approval number: #G.Ü.ET-25.068, date: 18.07.2025). All procedures involving rats were conducted in accordance with the European Convention (ETS 123) guidelines. Twenty-eight male Wistar albino rats obtained from the Gazi University Experimental Animal Research and Application Center were included in the study. The rats were kept under standardized laboratory conditions at 23 °C, with a 12-hour light-12-hour dark cycle from 08:00 to 20:00. A total of 28 rats were divided into two age groups: young (3 months old) and old (20 months old). They were further divided into four subgroups: young control (YC) (YC, n = 6); young experimental [young calorie restriction (YCR), n = 6]; old control (OC), n = 8]; and old experimental [old calorie restriction (OCR), n = 8].

The control group was fed standard chow ad libitum for 10 weeks. To ensure that the effects of short-term CR were achieved, the Altromin C-1012 diet (Altromin Spezialfutter GmbH, Germany) was administered to the CR group for the same period [30% of daily caloric intake (~1,303 kcal/kg)] (18). Rats' weights were monitored weekly throughout the experiment. At the end of the 10-week period, after a 12-hour fast, all rats were anesthetized with 10% ketamine and 2% xylazine. Subsequently, cardiac blood was collected, and the rats were decapitated. The right testis and right kidney were removed, and wet organ weights were measured.

The organ index for the kidney and testis was calculated as (organ weight/body weight) × 100. For histological evaluation, tissue samples were placed in 10% formaldehyde, whereas the remaining tissue samples were washed with PBS and immediately frozen in liquid nitrogen. Then they were stored at -80 °C until further analysis.

Evaluation of MDA and GSH Levels in Tissue Samples

Testis and kidney tissues were homogenized using rotor-stator tissue homogenizer in trichloroacetic acid (TCA) [200 mg tissue and 1.8 mL TCA (10% w/v)]. Supernatants obtained by centrifugation at 4,000 rpm for 15 minutes were analyzed for malondialdehyde (MDA, an indicator of lipid peroxidation, using the thiobarbituric acid-reactive substances assay (19). The supernatants were mixed with butylated hydroxytoluene [1% (w/v)] and thiobarbituric acid [(TBA, 0.67% (w/v)] in glass tubes and then boiled at 100 °C for 15 minutes. The resulting mixtures were transferred to plates and analyzed spectrophotometrically at 532 nm.

To assess antioxidant defense capacity in tissue samples, glutathione (GSH) levels were measured using the modified Ellman method (20). Supernatants from tissues homogenized at room temperature were reacted with 0.3 M disodium hydrogen phosphate (Na_2HPO_4)

Gazi Med J 2026;37(1):7-14

Coşkun et al. Calorie Restriction in Aging Testis and Kidney

and 5,5'-dithiobis-(2-nitrobenzoic acid) (0.4 mg/mL in 1% sodium citrate). The mixtures were then transferred to plates and analyzed spectrophotometrically at 412 nm.

Evaluation of Kidney Parameters and Plasma Testosterone Levels

Prior to sacrifice, blood samples were collected from the rats via cardiac puncture and then centrifuged at 4,000 rpm for 15 minutes. Plasma BUN, Cre, and uric acid (UA) levels were measured in the supernatants using colorimetric methods on a Siemens Advia Chemistry XPT (Siemens Healthcare Diagnostics, Tarrytown, NY, USA), and plasma testosterone levels were measured in the supernatants using chemiluminescent immunoassay on a Siemens Advia Centaur XPT at the Gazi University Hospital Biochemistry Central Laboratory.

Histological Analysis

Morphometric Measurements and Histological Staining

Tissue sections (5 μm thick) were prepared from renal and testicular samples using a microtome (Slee, CUT 5062, Germany). Histological analyses of kidney tissue were performed using hematoxylin-Eosin (H&E) and Masson's Trichrome (M&T) stains. Stained sections were evaluated under a ZEISS Axiolab 5 computer-assisted light microscope (Germany) using ZEN Blue 3.4 software. After M&T staining, the fibrotic area ratio was quantified in randomLy selected kidney sections. The fibrotic area ratio (%), glomerular diameters (μm) in kidney sections, and seminiferous tubule diameters (μm) in testicular sections were evaluated using ImageJ software.

Additionally, testicular tissue was analyzed histologically using H&E, following the same protocol. After staining, the samples were examined microscopically, and histological evaluations of the seminiferous tubules and interstitial space were performed.

Johnsen Testis Score Evaluation

Histopathological assessment of spermatogenesis was performed using the Johnsen testicular biopsy score. Scores were calculated from 100 randomLy selected seminiferous tubules per group (21). Only scores in the range of 7–10 were observed in testicular sections from the evaluated groups. The scoring system for testicular biopsies was as follows: 10 (complete spermatogenesis); 9 (numerous late spermatids, irregular epithelial cells); 8 (fewer than five spermatocytes per tubule, few late spermatids); and 7 (no spermatocytes, no late spermatids, numerous early-stage spermatids).

Statistical Analysis

Study data were analyzed using SPSS 22. Data are presented as group mean ± standard deviation. One-way ANOVA (post-hoc LSD) was used for group comparisons, and a paired-sample t-test was used to compare weight changes. Pearson's r was also calculated to examine the relationship between variables. Statistical significance was set at $p < 0.05$.

RESULTS

Effects of CR on Weight Change, Right Testis/Body Weight Ratio, and Right Kidney/Body Weight Ratio

Initially, the body weights of older rats were greater than those of younger rats YC: 179.50 ± 6.60, YCR: 185.33 ± 7.94, OC: 360.50 ± 30.18, OCR: 351.38 ± 37.05; $p < 0.001$). While weight gain was observed in the OC group at the end of 10 weeks, significant weight loss was observed in young and old rats due to CR (YCR: 167.33 ± 16.40, $p < 0.001$; OCR: 258.88 ± 42.82, $p < 0.001$) (Figure 1A). Kidney weight was significantly higher in the OC group compared to the YC group (1.27 ± 0.11, 0.87 ± 0.1, $p < 0.001$, respectively), while CR reduced kidney weight in both young and elderly rats (0.70 ± 0.06, 0.97 ± 0.08, $p < 0.001$, $p < 0.001$, respectively) (Figure 1B). There was no difference in the kidney index between the control groups, whereas CR increased the kidney index in both young and old rats (0.41 ± 0.04, $p = 0.001$; 0.39 ± 0.04, $p = 0.024$, respectively) (Figure 1C). There was no significant difference in testis weight between the YC and OC groups. Testicular weight was lower in the OCR group than in the OC group (1.35 ± 0.28 and 1.61 ± 0.17, respectively; $p = 0.013$) (Figure 1D). The testicular index was lower in the OC group than in the YC group (OC: 0.44 ± 0.03; YC: 0.56 ± 0.06; $p < 0.001$). CR significantly increased the testicular index in both young and aged rats (0.84 ± 0.06, $p < 0.001$; 0.52 ± 0.04, $p = 0.004$, respectively) (Figure 1E).

The Effect of CR on Kidney Function

Serum Cre was significantly elevated in the OC group (0.44 ± 0.06; $p = 0.019$); CR decreased Cre in both the YCR and OCR groups (0.29 ± 0.07 and 0.26 ± 0.03; $p = 0.009$ and $p < 0.001$, respectively) (Figure 2A). BUN levels were significantly higher in aged rats (YC: 16.67 ± 3.61, YCR: 16.83 ± 2.48, OC: 25.13 ± 1.95, OCR: 24.25 ± 0.49, $p < 0.001$), whereas CR had no significant effect in either young or aged rats (Figure 2B). Serum UA levels were significantly elevated in aged rats (YC: 0.44 ± 0.05; OC: 15.63 ± 0.20; $p < 0.001$), and CR decreased UA levels in aged rats (OCR: 0.39 ± 0.07; $p < 0.001$) (Figure 2C).

Effect of CR on Blood Testosterone Levels

Plasma testosterone levels were significantly decreased in the OC group (63.75 ± 14.62, $p < 0.001$). CR reduced testosterone levels in both young and old rats [YCR: 26.29 ± 14.35 ($p < 0.001$); OCR: 33.89 ± 15.55 ($p = 0.032$)] (Figure 3).

Effect of CR on MDA and GSH Status in Kidney and Testicular Tissue

Aging significantly increased kidney MDA levels (YC: 12.44 ± 1.25, OC: 19.15 ± 3.95, $p < 0.001$), whereas CR significantly decreased MDA levels in aged rats (12.41 ± 3.24, $p < 0.001$; Figure 4A). Kidney GSH levels declined with age in control rats (YC: 2.69 ± 0.29, OC: 2.31 ± 0.15, $p = 0.006$), and CR increased GSH levels in aged rats (2.62 ± 0.29, $p = 0.016$) (Figure 4B). Kidney MDA levels were negatively correlated with GSH and positively correlated with Cre, BUN, and UA ($r = -0.38$, $p = 0.046$; $r = 0.435$, $p = 0.021$; $r = 0.452$, $p = 0.016$; $r = 0.788$, $p < 0.001$, respectively). Testicular MDA levels were significantly higher and GSH levels were lower in aged rats compared to young rats (MDA; YC: 2.05 ± 0.33, OC: 3.50 ± 1.15, $p = 0.002$; GSH; YC: 2.40 ± 0.17, OC: 2.11 ± 0.05, $p = 0.005$). CR significantly decreased testicular MDA levels in aged rats (2.44 ± 0.52; $p = 0.024$;

Gazi Med J 2026;37(1):7-14

Coşkun et al. Calorie Restriction in Aging Testis and Kidney

Figure 4C), whereas GSH levels remained unchanged (Figure 4D). Furthermore, tissue MDA levels were negatively correlated with the organ index (r = -0.455, p = 0.029).

Histological Findings

H&E staining of kidney tissue showed a normal histological architecture in young rats, whereas aged rats showed inflammatory cell infiltration, tubular dilatation, and vacuolar degeneration in some areas. No statistically significant differences were observed between the YC and YCR groups (p = 1.000). M&T staining revealed an increase in the fibrotic area in both the OC and OCR groups compared with the YC group (p = 1.000). M&T staining revealed an increase in the fibrotic area in both the OC and OCR groups compared with the YC group (p < 0.001 and p = 0.006, respectively). The fibrotic area in OCR kidneys was lower than in OC kidneys (p
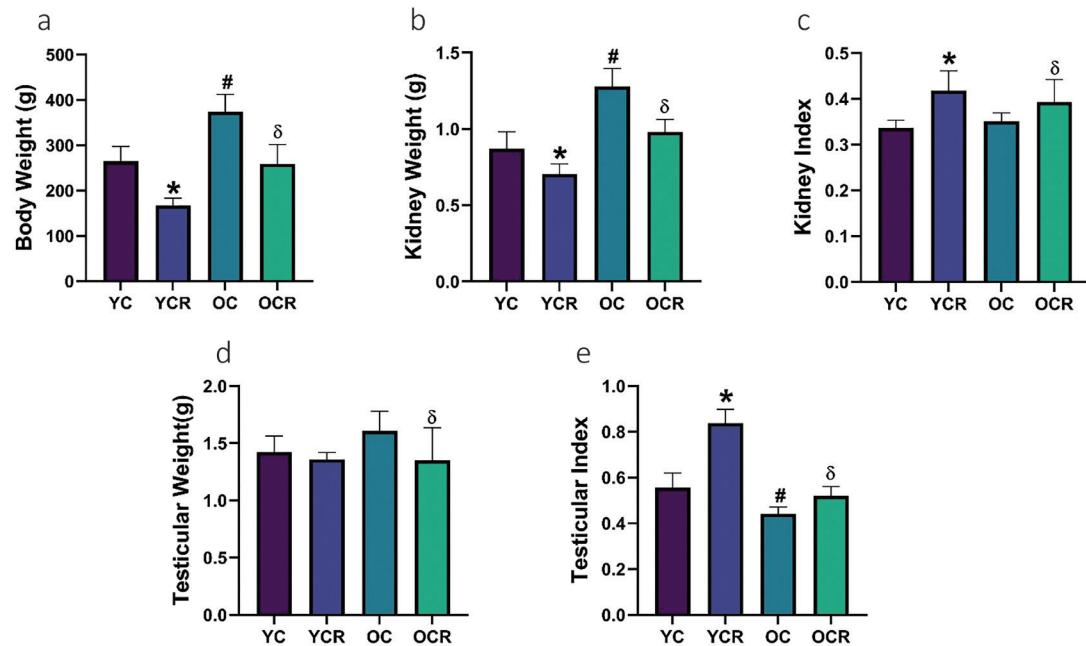
Figure 1. Effect of caloric restriction on body weight (a), kidney weight (b), kidney organ indices (c), testicular weight (d) and testicular indices (e) in young (YC, YCR) and old (OC, OCR) rats.

*p < 0.05 compared with the YC group; #p < 0.05 compared with the YC and YCR groups; δp < 0.05 compared with the OC group.
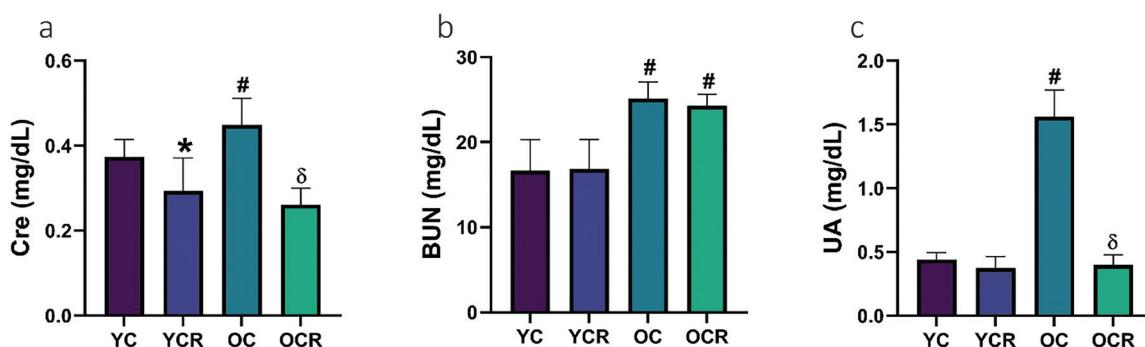
Figure 2. Effect of CR on serum Cre (a), BUN (b) and UA (c) levels in young (YC, YCR) and old (OC, OCR) rats.

*p < 0.05 compared with the YC group; #p < 0.05 compared with the YC and YCR groups; δp < 0.05 compared with the OC group.

Gazi Med J 2026;37(1):7-14

Coşkun et al. Calorie Restriction in Aging Testis and Kidney

< 0.020), whereas the fibrotic area in YCR kidneys was lower than in OCR kidneys (p < 0.001). CR reduced fibrosis in aged rats (p < 0.005). Glomerular diameter in the YCR, OC, and OCR groups decreased compared with the YC group (p < 0.001, p < 0.001, and p = 0.001, respectively).

Testicular histology in YC rats revealed a normal interstitium and normal seminiferous tubules. In OC rats, seminiferous tubules were dilated, spermatogenic cells showed atrophic changes, interstitial edema increased, Leydig cell degeneration was observed. The seminiferous tubule diameter was significantly lower in the YC group compared with the OC and OCR groups (p < 0.001 for both comparisons). The Johnsen score was significantly higher in the YC compared with the OC (p < 0.001). CR significantly decreased the Johnsen score in young rats and increased it in aged rats (p < 0.001 and p = 0.011, respectively). The Johnsen score was positively correlated with plasma testosterone levels and inversely correlated with BUN and UA (p = 0.013, p < 0.001, and p < 0.001, respectively) (Table 1).

DISCUSSION

Aging, a gradual and pathological process, affects many organs and systems (22). Our findings suggest that aging decreases testicular index while increasing kidney weight. Imaging studies in healthy individuals without kidney disease report age-related reductions in

Figure 3. Effect of CR on plasma testosterone levels in young (YC, YCR) and old (OC, OCR) rats.

*p < 0.05 compared with the YC group; δp < 0.05 compared with the OC group.

kidney volume (23,24). Findings from experimental animal models support these results (25,26).

Gonadal aging involves morphological, hormonal, and metabolic changes that impair reproductive function and quality of life. It is also associated with an increased risk of age-related diseases, including diabetes, renal dysfunction, cardiovascular failure, and cancer (27). Aging is commonly associated with decreased testicular volume in men (28). Studies show that men aged over 75 years have a lower average testicular volume than men aged 18–40 years (29). Similarly, our study observed a reduction in testicular weight in aged rats.

The literature indicates that aging impairs renal and testicular function. It increases Cre, BUN, and UA and decreases testosterone levels (26,30–32). It has been reported that testosterone levels begin to decline in the third decade of life and continue to decrease gradually throughout life (33). Consistent with these data, our study found higher levels of kidney function markers (Cre, UA) and lower levels of serum testosterone with aging.

Because of their high oxygen consumption, the kidneys are particularly vulnerable to ROS-induced damage (34). ROS-induced oxidative stress, along with tissue damage and structural deterioration, is a key factor in premature aging associated with CKD (35). Moreover, increased oxidative stress, influenced by endogenous and environmental factors, leads to irreversible changes in the kidneys and testes (36,37). These changes predispose them to various pathologies (38).

ROS contribute to several physiological processes, including spermatogenesis, sperm capacitation, and acrosomal activity. However, controlled ROS levels are essential for healthy sperm function and, consequently, successful fertilization (39). Elevated ROS levels impair sperm function and increase DNA fragmentation in the sperm nucleus (40), both of which contribute to male infertility (41). Previous studies have reported elevated ROS concentrations in the semen of 25–40% of infertile men (42). Furthermore, lower levels of antioxidant enzymes are detected in the seminal plasma of these individuals compared than in controls (43). ROS found in seminal plasma have been shown to be primarily the superoxide anion, the hydroxyl radical, and hydrogen peroxide (44). Our earlier research demonstrated that aging in male Wistar rats increases oxidative stress in testicular tissue, leading to a decline in testosterone and GSH levels (36). Moreover, a study of 66 men at
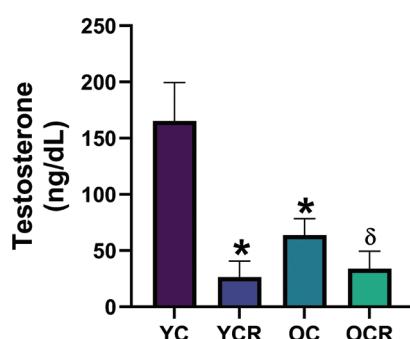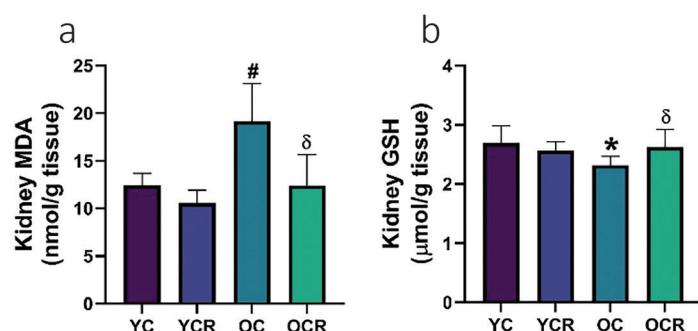
Figure 4. Effect of CR on MDA (a-c) and GSH (b-d) levels in kidney and testicular tissue in young (YC, YCR)and old (OC, OCR) rats.

*p < 0.05 compared with the YC group; #p < 0.05 compared with the YC and YCR groups; δp < 0.05 compared with the OC group.

Gazi Med J 2026;37(1):7-14

Coşkun et al. Calorie Restriction in Aging Testis and Kidney

Table 1. Histological evaluation results.

	Young		Old	
	Control	CR	Control	CR
Renal fibrotic area (%)	1.68 ± 0.22	1.23 ± 0.12	9.89 ± 0.66*	4.86 ± 0.63*[#δ]
Glomerular diameter (μm)	64.25 ± 0.79	57.51 ± 0.47*	58.44 ± 1.07*	60.51 ± 1.04*
Seminiferous tubule diameter (μm)	216.11 ± 1.71	222.54 ± 1.79	273.49 ± 1.60*	249.62 ± 1.47*[#]
Johnsen score (0–10)	9.63 ± 0.12	9.17 ± 0.13*	8.28 ± 0.07*	8.51 ± 0.26*[#]

*$p < 0.05$, compared with the YC group; #$p < 0.05$, compared with the OC group; δ$p < 0.05$, compared with the YCR group.

various stages of kidney disease revealed a significant association between reduced testosterone levels and progressive loss of kidney function (45).

Changes associated with aging are not limited to biochemical and inflammatory processes; they also encompass morphological alterations. Morphological changes with aging include a reduced number of glomeruli in the kidneys as well as an increase in glomerular volume and fibrosis (14). Other changes observed in the testis include reduced tubular diameter, increased basement membrane thickness, fibrosis, and decreased numbers of sertoli and spermatogenic cells (2). These structural deteriorations reduce the Johnsen score, a marker of male fertility (36).

CR is an effective dietary strategy to mitigate age-related degenerative changes. It functions by reducing oxidative stress, inflammation, and metabolic disorders through the limitation of energy intake (46). In our study, CR resulted in decreased organ weight and body weight regardless of age, whereas renal and testicular indices increased significantly. Evidence from other studies suggests that CR may increase the organ index, leading to a compensatory mechanism against mass reduction (47,48). CR has also been shown to slow the progression of CKD in rodents. It lowers blood markers, such as Cre, BUN, and UA, and delays disease onset, thereby increasing survival (49,50). CR suppresses oxidative damage to lipids, proteins, and DNA that is associated with aging, while enhancing cellular defense mechanisms against oxidative stress (51). CR also reduces mitochondrial ROS formation in the cardiac and skeletal muscles and the liver (52). In the kidney, CR decreases levels of MDA, a marker of oxidative stress, and increases levels of GSH, an important antioxidant (53). In mice, 60% CR for 2 months increased GSH levels and decreased levels of oxidized GSH and GSH peroxidase in the kidneys (54). In rats, short-term 60% CR decreased body weight, triacylglycerol levels, glomerular volume, fibrosis, and cellular senescence (14,15). Furthermore, CR decreases the incidence of histopathological nephropathy and improves renal function (14,15). Although CR prolongs lifespan (55), it can have adverse effects on reproduction (56). Studies in adult rats have demonstrated that CR can decrease body, testicular, epididymal, and prostate weights (57). Short-term CR decreases blood testosterone levels in rats, whereas long-term CR increases testosterone levels compared with rats fed ad libitum (58). While these results are consistent with our findings, the observed differences may be attributable to the duration of CR application, age, and hormonal status.

Study Limitations

Although our study is preliminary and suggests that CR may protect kidney and testicular tissues by reducing oxidative stress during ageing, it is limited by the lack of measurements of oxidative stress parameters (such as superoxide dismutase and GSH oxidase) and hormone levels (such as FSH and LH). However, renal and reproductive dysfunctions may coexist and should be considered during follow-up.

CONCLUSION

In conclusion, our findings show that CR during aging helps preserve the structural and functional integrity of the kidney and testis. These effects are demonstrated by reduced oxidative stress, increased antioxidant defenses, and reduced fibrosis on histology. However, further histological and molecular analyses are needed to clarify the underlying mechanisms and their interactions.

Ethics

Footnotes

Authorship Contributions

Concept: A.C., K.G.A., Design: A.C., K.G.A., Data Collection or Processing: A.C., E.T., Analysis or Interpretation: A.K.A, S.Ö.A.D., Literature Search: A.C., K.G.A., Writing: A.C., K.G.A.

Conflict of Interest: No conflict of interest was declared by the authors.

REFERENCES

1. López-Otín C, Blasco MA, Partridge L, Serrano M, Kroemer G. Hallmarks of aging: an expanding universe. Cell. 2023; 186: 243–78.
2. Alshinnawy AS, El-Sayed WM, Taha AM, Sayed AA, Salem AM. Astragalus membranaceus and Punica granatum alleviate infertility and kidney dysfunction induced by aging in male rats. Turk J Biol. 2020; 44: 166–75.

Gazi Med J 2026;37(1):7-14

Coşkun et al. Calorie Restriction in Aging Testis and Kidney

3. Denic A, Lieske JC, Chakkera HA, Poggio ED, Alexander MP, Singh P, et al. The substantial loss of nephrons in healthy human kidneys with aging. J Am Soc Nephrol. 2017; 28: 313–20.

4. Wang X, Garrett MR. Nephron number, hypertension, and CKD: physiological and genetic insight from humans and animal models. Physiol Genomics. 2017; 49: 180–92.

5. Minutolo R, Borrelli S, De Nicola L. CKD in the Elderly: kidney senescence or blood pressure-related nephropathy? Am J Kidney Dis. 2015; 66: 184–6.

6. Foreman KJ, Marquez N, Dolgert A, Fukutaki K, Fullman N, McGaughey M, et al. Forecasting life expectancy, years of life lost, and all-cause and cause-specific mortality for 250 causes of death: reference and alternative scenarios for 2016-40 for 195 countries and territories. Lancet. 2018; 392: 2052–90.

7. Eisenberg ML, Lathi RB, Baker VL, Westphal LM, Milki AA, Nangia AK. Frequency of the male infertility evaluation: data from the national survey of family growth. J Urol. 2013; 189: 1030–4.

8. Lehtihet M, Hylander B. Semen quality in men with chronic kidney disease and its correlation with chronic kidney disease stages. Andrologia. 2015; 47: 1103–8.

9. Weir CP, Robaire B. Spermatozoa have decreased antioxidant enzymatic capacity and increased reactive oxygen species production during aging in the Brown Norway rat. J Androl. 2007; 28: 229–40.

10. Daskalova E, Pencheva M, Denev P. Black chokeberry (aronia melanocarpa) juice supplementation improves oxidative stress and aging markers in testis of aged rats. Curr Issues Mol Biol. 2024; 46: 4452–70.

11. Antinozzi C, Di Luigi L, Sireno L, Caporossi D, Dimauro I, Sgrò P. Protective role of physical activity and antioxidant systems during spermatogenesis. Biomolecules. 2025; 15: 478.

12. Das SK, Balasubramanian P, Weerasekara YK. Nutrition modulation of human aging: the calorie restriction paradigm. Mol Cell Endocrinol. 2017; 455: 148–57.

13. Xu XM, Cai GY, Bu R, Wang WJ, Bai XY, Sun XF, et al. Beneficial effects of caloric restriction on chronic kidney disease in rodent models: a meta-analysis and systematic review. PLoS One. 2015; 10: e0144442.

14. Ning YC, Cai GY, Zhuo L, Gao JJ, Dong D, Cui S, et al. Short-term calorie restriction protects against renal senescence of aged rats by increasing autophagic activity and reducing oxidative damage. Mech Ageing Dev. 2013; 134: 570–9.

15. Afsar B, Afsar RE, Copur S, Sag AA, Ortiz A, Kanbay M. The effect of energy restriction on development and progression of chronic kidney disease: review of the current evidence. Br J Nutr. 2021; 125: 1201–14.

16. Martins AD, Jarak I, Morais T, Carvalho RA, Oliveira PF, Monteiro MP, et al. Caloric restriction alters the hormonal profile and testicular metabolome, resulting in alterations of sperm head morphology. Am J Physiol Endocrinol Metab. 2020; 318: E33–43.

17. Zhang S, Zhang M, Sun S, Wei X, Chen Y, Zhou P, et al. Moderate calorie restriction ameliorates reproduction via attenuating oxidative stress-induced apoptosis through SIRT1 signaling in obese mice. Ann Transl Med. 2021; 9: 933.

18. Vidal A, Rios R, Pineda C, Lopez I, Raya AI, Aguilera-Tejero E, et al. Increased 1,25(OH)2-Vitamin D concentrations after energy restriction are associated with changes in skeletal muscle phenotype. Nutrients. 2021; 13: 607.

19. Casini AF, Ferrali M, Pompella A, Maellaro E, Comporti M. Lipid peroxidation and cellular damage in extrahepatic tissues of bromobenzene-intoxicated mice. Am J Pathol. 1986; 123: 520–31.

20. Aykaç G, Uysal M, Yalçin AS, Koçak-Toker N, Sivas A, Oz H. The effect of chronic ethanol ingestion on hepatic lipid peroxide, glutathione, glutathione peroxidase and glutathione transferase in rats. Toxicology. 1985; 36: 71–6.

21. Johnsen SG. Testicular biopsy score count--a method for registration of spermatogenesis in human testes: normal values and results in 335 hypogonadal males. Hormones. 1970; 1: 2–25.

22. Tian YE, Cropley V, Maier AB, Lautenschlager NT, Breakspear M, Zalesky A. Heterogeneous aging across multiple organ systems and prediction of chronic disease and mortality. Nat Med. 2023; 29: 1221–31.

23. Emamian SA, Nielsen MB, Pedersen JF, Ytte L. Kidney dimensions at sonography: correlation with age, sex, and habitus in 665 adult volunteers. AJR Am J Roentgenol. 1993; 160: 83–6.

24. Gourtsoyiannis N, Prassopoulos P, Cavouras D, Pantelidis N. The thickness of the renal parenchyma decreases with age: a CT study of 360 patients. AJR Am J Roentgenol. 1990; 155: 541–4.

25. Hassawi WW, Al-sammak MA-J. Impact of aging on kidneys of male Wistar albino rats: the protective antiaging role of resveratrol. J Appl Nat Sci. 2023; 15: 926–36.

26. Melchioretto EF, Zeni M, Veronez DA, Martins EL Filho, Fraga Rd. Quantitative analysis of the renal aging in rats. Stereological study. Acta Cir Bras. 2016; 31: 346–52.

27. Appt SE, Ethun KF. Reproductive aging and risk for chronic disease: insights from studies of nonhuman primates. Maturitas. 2010; 67: 7–14.

28. Paniagua R, Nistal M, Amat P, Rodriguez MC, Martin A. Seminiferous tubule involution in elderly men. Biol Reprod. 1987; 36: 939–47.

29. Mahmoud AM, Goemaere S, El-Garem Y, Van Pottelbergh I, Comhaire FH, Kaufman JM. Testicular volume in relation to hormonal indices of gonadal function in community-dwelling elderly men. J Clin Endocrinol Metab. 2003; 88: 179–84.

30. Song F, Ma Y, Bai XY, Chen X. The expression changes of inflammasomes in the aging rat kidneys. J Gerontol A Biol Sci Med Sci. 2016; 71: 747–56.

31. Han B, Zhang Y, Liu C, Ji P, Xing Z, Geng X, et al. Renal inflammation combined with renal function reserve reduction accelerate kidney aging via pentose phosphate pathway. iScience. 2024; 27: 110045.

32. Vermeulen A, Goemaere S, Kaufman JM. Testosterone, body composition and aging. J Endocrinol Invest. 1999; 22: 110–6.

33. Kaufman JM, Vermeulen A. The decline of androgen levels in elderly men and its clinical and therapeutic implications. Endocr Rev. 2005; 26: 833–76.

34. Daenen K, Andries A, Mekahli D, Van Schepdael A, Jouret F, Bammens B. Oxidative stress in chronic kidney disease. Pediatr Nephrol. 2019; 34: 975–91.

35. Verma S, Singh P, Khurana S, Ganguly NK, Kukreti R, Saso L, et al. Implications of oxidative stress in chronic kidney disease: a review on current concepts and therapies. Kidney Res Clin Pract. 2021; 40: 183–93.

36. Muratoğlu S, Akarca Dizakar OS, Keskin Aktan A, Ömeroğlu S, Akbulut KG. The protective role of melatonin and curcumin in the testis of young and aged rats. Andrologia. 2019; 51: e13203.

37. Zhao D, Fayyaz S, Yi Z, Liu Z, Wang Y, Cai P, et al. Metabolic profile changes of kidney aging and protective effects of Polygonatum sibiricum polysaccharides on D-galactose-induced aging mice. Digital Chinese Medicine. 2023; 6: 328–40.

38. Gunes S, Hekim GN, Arslan MA, Asci R. Effects of aging on the male reproductive system. J Assist Reprod Genet. 2016; 33: 441–54.

39. Wagner H, Cheng JW, Ko EY. Role of reactive oxygen species in male infertility: an updated review of literature. Arab J Urol. 2017; 16: 35–43.

Gazi Med J 2026;37(1):7-14

Coşkun et al. Calorie Restriction in Aging Testis and Kidney

40. Iwasaki A, Gagnon C. Formation of reactive oxygen species in spermatozoa of infertile patients. Fertil Steril. 1992; 57: 409–16.

41. Takeshima T, Usui K, Mori K, Asai T, Yasuda K, Kuroda S, et al. Oxidative stress and male infertility. Reprod Med Biol. 2020; 20: 41–52.

42. Agarwal A, Sharma RK, Sharma R, Assidi M, Abuzenadah AM, Alshahrani S, et al. Characterizing semen parameters and their association with reactive oxygen species in infertile men. Reprod Biol Endocrinol. 2014; 12: 33.

43. Eid Hammadeh M, Filippos A A, Faiz Hamad M. Reactive oxygen species and antioxidant in seminal plasma and their impact on male fertility. International Journal of Fertility and Sterility. 2009; 3: 87–110.

44. Agarwal A, Saleh RA, Bedaiwy MA. Role of reactive oxygen species in the pathophysiology of human reproduction. Fertil Steril. 2003; 79: 829–43.

45. Habashy E. Chronic kidney disease and male factor infertility. Kidney News. 2023; 15: 12-. Available from: https://www.kidneynews.org/view/journals/kidney-news/15/8/article-p12_7.xml

46. López-Lluch G, Hunt N, Jones B, Zhu M, Jamieson H, Hilmer S, et al. Calorie restriction induces mitochondrial biogenesis and bioenergetic efficiency. Proc Natl Acad Sci U S A. 2006; 103: 1768–73.

47. Hamden K, Silandre D, Delalande C, El Feki A, Carreau S. Age-related decrease in aromatase and estrogen receptor (ERalpha and ERbeta) expression in rat testes: protective effect of low caloric diets. Asian J Androl. 2008; 10: 177–87.

48. Weindruch R, Walford RL, Fligiel S, Guthrie D. The retardation of aging in mice by dietary restriction: longevity, cancer, immunity and lifetime energy intake. J Nutr. 1986; 116: 641–54.

49. Kim MJ, Hwang T, Ha S, Kim H, Kim J, Kim D, et al. Calorie restriction exacerbates folic acid-induced kidney fibrosis by altering mitochondria metabolism. J Nutr Biochem. 2024; 134: 109765.

50. Walford RL, Mock D, Verdery R, MacCallum T. Calorie restriction in biosphere 2: alterations in physiologic, hematologic, hormonal, and biochemical parameters in humans restricted for a 2-year period. J Gerontol A Biol Sci Med Sci. 2002; 57: B211–24.

51. Merry BJ. Oxidative stress and mitochondrial function with aging--the effects of calorie restriction. Aging Cell. 2004; 3: 7–12.

52. Gredilla R, Phaneuf S, Selman C, Kendaiah S, Leeuwenburgh C, Barja G. Short-term caloric restriction and sites of oxygen radical generation in kidney and skeletal muscle mitochondria. Ann N Y Acad Sci. 2004;1019:333–42.

53. Fang D, Wang Y, Zhang Z, Yang D, Gu D, He B, et al. Calorie restriction protects against contrast-induced nephropathy via SIRT1/GPX4 activation. Oxid Med Cell Longev. 2021; 2021: 2999296.

54. Cadenas S, Rojas C, Pérez-Campo R, López-Torres M, Barja G. Caloric and carbohydrate restriction in the kidney: effects on free radical metabolism. Exp Gerontol. 1994; 29: 77–88.

55. Bartke A, Masternak MM, Al-Regaiey KA, Bonkowski MS. Effects of dietary restriction on the expression of insulin-signaling-related genes in long-lived mutant mice. Interdiscip Top Gerontol. 2007; 35: 69–82.

56. Masoro EJ. Caloric restriction and aging: an update. Exp Gerontol. 2000; 35: 299–305.

57. Santos AM, Ferraz MR, Teixeira CV, Sampaio FJ, da Fonte Ramos C. Effects of undernutrition on serum and testicular testosterone levels and sexual function in adult rats. Horm Metab Res. 2004; 36: 27–33.

58. Chen H, Luo L, Liu J, Brown T, Zirkin BR. Aging and caloric restriction: effects on Leydig cell steroidogenesis. Exp Gerontol. 2005; 40: 498–505.

Possible Relationships of Ferritin and Inflammatory Cytokines with Metabolic Syndrome: A Case Control Study

Ferritin ve Enflamatuvar Sitokinlerin Metabolik Sendrom ile Olası İlişkileri: Bir Olgu Kontrol Çalışması

 Hatice Tuğçe Berberoğlu[1], Burcu Baba[2], Cem Onur Kıraç[3], Bahadır Öztürk[4], Aysun Hacışevki[5]

[1]Department of Nutrition and Dietetics, KTO Karatay University Faculty of Health Sciences, Konya, Türkiye
[2]Department of Medical Biochemistry, Yüksek İhtisas University Faculty of Medicine, Ankara, Türkiye
[3]Division of Endocrinology and Metabolism, Clinic of lnternal Medicine, HG Hospital, Kahramanmaraş, Türkiye
[4]Department of Medical Biochemistry, Selçuk University Faculty of Medicine, Konya, Türkiye,
[5]Department of Biochemistry, Gazi University Faculty of Pharmacy; Health Sciences Institute, Sports Pharmacy Program, Gazi University, Ankara, Türkiye

ABSTRACT

Objective: Metabolic syndrome (MetS) is characterized by the coexistence of several risk factors, including abdominal obesity, elevated blood pressure, glucose intolerance, and dyslipidemia. MetS has become a significant public health concern worldwide, and its prevalence is steadily increasing in Türkiye. It has been suggested that serum ferritin concentrations are higher in individuals with MetS and that inflammation plays a crucial role in the pathogenesis of the syndrome. The aim of this study was to evaluate serum ferritin levels and inflammatory cytokine levels in individuals with and without MetS.

Methods: A total of 150 individuals who presented to the endocrinology unit were included in the study. According to the National Cholesterol Education Program/Adult Treatment Panel III (NCEP ATP III) criteria, participants were divided into two groups: those with MetS (n = 75) and those without MetS (n = 75). Fasting serum ferritin, interleukin (IL)-1α, IL-10, and interferon (IFN)-γ levels were analyzed using commercial enzyme-linked immunosorbent assay (ELISA) kits. Demographic characteristics, anthropometric measurements, and biochemical parameters of the participants were also evaluated.

Results: Serum levels of ferritin, IL-1α, and IFN-γ were significantly higher in individuals with MetS than in the control group (p < 0.05). Although IL-10 levels were also higher in the MetS group, the difference was not statistically significant. Furthermore, fasting blood glucose, triglycerides, blood pressure, and waist circumference were

ÖZ

Amaç: Metabolik sendrom (MetS) abdominal obezite, artmış kan basıncı, glukoz intoleransı ve dislipidemi gibi risk faktörlerinden oluşan bir durum olarak tanımlanmaktadır. MetS dünya çapında önemli bir halk sağlığı sorunudur ve Türkiye'de MetS prevalansı giderek artmaktadır. Serum ferritin konsantrasyonunun MetS'li bireylerde daha yüksek ve enflamasyonun, MetS patogenezinde önemli bir rol oynadığı öne sürülmüştür. Bu çalışmanın amacı MetS olan ve olmayan bireylerde serum ferritin ve enflamatuvar sitokin düzeylerini değerlendirmektir.

Yöntemler: Endokrinoloji ünitesine başvuran 150 kişi, Ulusal Kolesterol Eğitim Programı/Yetişkin Tedavi Paneli (NCEP ATP III) MetS kriterleri temel alınarak her grupta 75 kişi olacak şekilde iki gruba ayrılmıştır. Açlık serum ferritin, interlökin (IL)-1α, IL-10 ve interferon (IFN)-γ düzeyleri ticari enzim bağlantılı immünosorbent test (ELISA) yöntemi ile analiz edilmiştir. Ayrıca demografik parametreler, antropometrik ölçümler ve biyokimyasal parametreler değerlendirilmiştir.

Bulgular: MetS'li bireylerde serum ferritin, IL-1α ve IFN-γ düzeyleri kontrol grubuna kıyasla anlamlı düzeyde yüksek bulunmuştur (p < 0,05). IL-10 düzeyleri hastalarda daha yüksek olmasına rağmen, bu artış istatistiksel olarak anlamlı bulunmamıştır. Ayrıca MetS grubunda, kontrol grubuna göre açlık kan şekeri, trigliserit, kan basıncı, bel çevresi değerleri anlamlı şekilde yüksek; yüksek yoğunluklu lipoprotein-kolesterol düzeyleri ise anlamlı şekilde düşük saptanmıştır.

ABSTRACT

significantly higher, whereas high-density lipoprotein cholesterol levels were significantly lower in the MetS group than in controls.

Conclusion: The findings suggest that inflammatory markers such as ferritin, IL-1α, and IFN-γ may serve as biomarkers for the diagnosis and management of MetS, thereby contributing to a better understanding of its pathogenesis and early detection. Further large-scale studies are required to validate these findings and clarify the roles of these parameters in MetS.

Keywords: Ferritin, inflammation, metabolic syndrome, interleukin-1alpha, interleukin-10, interferon-gamma

ÖZ

Sonuç: Bulgular, ferritin, IL-1α ve IFN-γ gibi enflamatuvar belirteçlerin MetS tanı ve yönetiminde potansiyel biyobelirteçler olarak hizmet edebileceğini, patogenezinin daha iyi anlaşılmasına ve erken teşhisine katkıda bulunabileceğini göstermektedir. Bu bulguların doğrulanması için bu değişkenlerin dikkate alındığı daha geniş örneklemli çalışmalara ihtiyaç duyulmaktadır.

Anahtar Sözcükler: Ferritin, enflamasyon, metabolik sendrom, interlökin-1alfa, interlökin-10, interferon-gama

INTRODUCTION

Metabolic syndrome (MetS) is a worldwide clinical challenge characterized by a cluster of risk factors, including abdominal obesity, insulin resistance, glucose intolerance, diabetes mellitus, dyslipidemia, and hypertension (1). According to the International Diabetes Federation, one-quarter of the global population has MetS (2). The Turkish Adult Risk Factor study reported that the prevalence of MetS among adults aged over 40 years in Türkiye was 53% (3). Obesity, low educational level, physical inactivity, hypertension, elevated total cholesterol levels, older age, and higher body mass index (BMI) are also strong risk factors for the development of MetS (4). Although the precise pathogenic pathways underlying MetS remain to be elucidated, the interaction among obesity, low-grade inflammation, and insulin resistance is considered to play a vital role in its development (5). The association between MetS and inflammation has not been fully explained; however, adipose tissue is thought to mediate the relationship between MetS and inflammation (6).

Obesity, an important risk factor for the development of MetS, is characterized by low-grade inflammation leading to adipose tissue dysfunction. Adipose tissue is an endocrine organ that secretes various bioactive substances, such as adipocytokines. An imbalance between the production of anti-inflammatory and pro-inflammatory adipocytokines in obese adipose tissue contributes to the pathophysiology of MetS (7). Ferritin, an acute-phase reactant, is a recognized biomarker of acute or chronic inflammation and is non-specifically elevated in various inflammatory conditions, including acute infection, malignancy, chronic kidney disease, rheumatoid arthritis, and other autoimmune disorders (8). Despite this, it remains unclear whether serum ferritin is involved in an inflammatory cycle or whether it causes or reflects inflammation (9). This study aimed to contribute to this growing area of research by exploring serum levels of ferritin, interleukin (IL)-1α, IL-10, and interferon (IFN)-γ as inflammatory markers and by examining the relationships among them in individuals with and without MetS.

MATERIALS AND METHODS

Study Population

Overweight or obese subjects were recruited from the Endocrinology and Metabolism Unit of Selçuk University Medical Faculty Hospital. This cross-sectional study was conducted in Konya Province, Türkiye, with 150 adults (114 women, 36 men) aged 19-65 yearsin Konya province, Türkiye. In this case-control study, 75 subjects diagnosed with MetS according to the National Cholesterol Education Program/Adult Treatment Panel III (NCEP ATP III) criteria constituted the patient group (mean age 40.4 ± 1.5 years; mean BMI: 34.5 ± 0.8 kg/m²), and 75 subjects without MetS constituted the control group (mean age 28.1 ± 1.0 years; mean BMI: 29.8 ± 0.6 kg/m²). Individuals were excluded from the study if they met any of the following criteria: age outside the 19-65-year age range; use of antioxidants or specialized nutritional supplements; presence of inflammatory conditions (e.g., connective tissue diseases, cancer, infection, inflammatory bowel disease, rheumatoid arthritis, lupus, tuberculosis); diagnosis of any chronic or genetic disease other than diabetes mellitus or hypertension; pregnancy or lactation; or use of medications that affect nutritional status.

BMI was calculated as weight in kilograms divided by the square of height in metres (kg/m²). BMI categories were defined as follows (10):

Normal weight: 18.5-24.9 kg/m²

Overweight: 25-29.9 kg/m²

Obesity: ≥30 kg/m²

Obesity class I: 30-34.9 kg/m²

Obesity class II: 35-39.9 kg/m²

Obesity class III: ≥40 kg/m²

The classification of MetS was based on the NCEP ATP III guidelines. According to the NCEP ATP III definition, a diagnosis of MetS requires the presence of at least three of the following five components: waist circumference >102 cm for men and >88 for women; triglycerides ≥150 mg/dL; high-density lipoprotein cholesterol (HDL)-C <40 mg/dL for men, and <50 mg/dL for women; systolic blood pressure ≥130 mmHg or diastolic blood pressure ≥85 mmHg; and fasting glucose ≥110 mg/dL] (11).

Laboratory Analysis

Blood samples were collected after an overnight fast. Serum samples were separated by centrifugation at 3000 rpm for 10 minutes at room temperature and stored at -80 °C until analysis. Serum ferritin (DiaMetra, DK0039), IL-1α (Elabscience, E-EL-H0088), IL-10 (Elabscience, E-EL-H6154), and IFN-γ (Elabscience, E-EL-H0108) levels were analyzed using commercial enzyme-linked immunosorbent

assay (ELISA) kits. Biochemical parameters were analyzed at the Pharmaceutical Biochemistry Laboratory of Gazi University.

Blood pressure was measured twice on the participant's right arm using a mercury sphygmomanometer after a 20-minute rest. The mean of the two measurements was used for statistical analysis.

The study was approved by the Medical Ethics Committee of Selçuk University (approval number: 2016/304, dated: 21.12.2016). Written informed consent was obtained from all participants prior to study enrollment.

Statistical Analysis

Numerical variables were expressed as mean ± standard error and categorical variables as percentages. Unequal gender group sizes can affect test power when group variances are heterogeneous but have minimal impact when group variances are homogeneous. Therefore, Levene's test was used to assess the homogeneity of variances. When variances were not homogeneous, Welch's t test was applied; otherwise, Student's t-test or ANOVA was used for parametric variables. For nonparametric variables, the Mann-Whitney U test or the Kruskal-Wallis test was employed. Correlations were evaluated using either Pearson or Spearman correlation coefficients. A p-value of <0.05 was considered statistically significant. All analyses were performed using SPSS (Statistical Package for the Social Sciences) version 24.0.

RESULTS

A total of 150 subjects participated in the present study. participants were divided into two subgroups based on the NCEP ATP III criteria for the diagnosis of MetS. The patient group included individuals with at least three MetS components: 31.3% (n = 47) had three components; 14.7% (n = 22) had four components; and 4% (n = 6) had all five components. The control group comprised individuals with no MetS components or with only one or two components: 7.3% (n = 11) had none; 17.3% (n = 26) had one component; and 25.3% (n = 38) had two components.

The general characteristics of the study participants, including age and BMI ranges, gender distribution, education level, smoking status, and alcohol consumption status, are summarized in Table 1.

Across the patient group (aged 40-65 years) and the control group (aged 18-24 years), the participation rate was 52% (n = 39). The mean ages of the patient and control groups were 40.4 ± 1.5 and 28.1 ± 1.0 years, respectively. Individuals diagnosed with MetS were significantly older than those without MetS (p=0.000; data not shown). Among patients, 33.3% (n = 25) had first-degree obesity, whereas among controls, 58.7% (n = 44) were overweight. BMI was significantly higher in patients than in controls (34.5 ± 0.8 and 29.8 ± 0.6, respectively; p < 0.001; data not shown). In terms of education, most patients (53.3%) were elementary school graduates, while most controls (48%) were high school graduates. The majority of participants reported never smoking and never consuming alcohol (77.3% and 91.3%, respectively).

Demographic characteristics, anthropometric measurements, biochemical data, and other measured parameters for each group are summarized in Table 2.

Anthropometric measurements, including hip circumference and mid-upper arm circumference, were significantly higher in patients than in controls (p = 0.000 for both). Biochemical analysis revealed that homeostatic model assessment-insulin resistance and levels of total cholesterol, alanine transaminase (ALT), urea, and insulin were significantly higher, whereas the estimated glomerular filtration rate (e-GFR) was significantly lower in patients compared with controls (p = 0.000, p = 0.001, p = 0.001, p = 0.000, p = 0.000, and p = 0.000, respectively). MetS components identified in patients included increased waist circumference, elevated fasting blood glucose, elevated systolic and diastolic blood pressure, elevated triglycerides, and reduced HDL-C levels. Recent evidence suggests that MetS accelerates eGFR decline, thereby increasing the risk of chronic kidney disease and end-stage renal disease (12). Although no prior study has specifically examined the relationship between urea and MetS, it is hypothesized that MetS may elevate serum urea levels by impairing renal function. Serum ferritin, IL-1α, IL-10, and IFN-γ levels for each group are presented in Table 3.

In the present study, serum levels of ferritin, IFN-γ, and IL-1α were significantly higher in patients than in controls. Although serum IL-10 levels were also higher in individuals with MetS, this difference did not reach statistical significance. The distribution of the measured parameters by gender is presented in Table 4.

This study revealed that serum ferritin concentrations were statistically significantly higher in men than in women in both the control and patient groups.

DISCUSSION

The main finding of this study was that the concentrations of serum ferritin, IL-1α, and IFN-γ were significantly higher in participants with MetS than in healthy controls. Although serum IL-10 levels were also higher in patients, the difference was not statistically significant. These results suggest that ferritin, IL-1α, and IFN-γ may serve as biomarkers for MetS.

Although the precise pathogenic mechanisms underlying MetS remain unclear, the interplay between obesity, low-grade inflammation, and insulin resistance is thought to play a vital role in its development (5). In particular, chronic low-grade inflammation is considered a central factor in the pathogenesis of MetS (13).

Ferritin plays a critical role in iron homeostasis and serves as a clinical biomarker for both iron deficiency and hemochromatosis (14). Recent studies have reported higher serum ferritin concentrations in individuals with MetS compared with healthy controls (13,15). This finding supports the idea that serum ferritin may serve as a marker for the development of MetS. Although the underlying mechanisms linking ferritin and MetS are not fully understood, several hypotheses have been proposed, including the Fenton reaction (16), the iron dysregulation and dormant microbes hypothesis (17), the lipolytic effect of excessive iron concentrations (18), and the increased hypersensitivity of pancreatic cells to reactive oxygen species (19). Nevertheless, some studies have reported conflicting results regarding the association between serum ferritin and MetS. These discrepancies have been attributed to small sample sizes, confounding factors, and differences in study populations (20).

Table 1. General characteristics of study participants.

		Total individuals n (%)	Patients n (%)	Controls n (%)
Age range	18-24 years	50 (33.3%)	11 (14.7%)	**39 (52%)**
	25-39 years	50 (33.3%)	25 (33.3%)	25 (33.3%)
	40-65 years	50 (33.3%)	**39 (52%)**	11 (14.7%)
Gender	Male	36 (24%)	23 (30.7%)	13 (17.3%)
	Female	114 (76%)	52 (69.3%)	62 (82.7%)
BMI range	Overweight	65 (43.3%)	21 (28%)	**44 (58.7%)**
	1st degree obesity	46 (30.7%)	**25 (33.3%)**	21 (28%)
	2nd degree obesity	26 (17.3%)	18 (24%)	8 (10.7%)
	3rd degree obesity	13 (8.7%)	11 (14.7%)	2 (2.7%)
Level of education	Literate	8 (5.3%)	4 (5.3%)	4 (5.3%)
	Elementary	57 (38%)	**40 (53.3%)**	17 (22.7%)
	High school	53 (35.3%)	17 (22.7%)	**36 (48%)**
	University	28 (18.7%)	12 (16%)	16 (21.3%)
	Postgraduate	4 (2.7%)	2 (2.7%)	2 (2.7%)
Smoking status	Current	20 (14%)	13 (17.3%)	7 (10.7%)
	Never	116 (77.3%)	54 (72%)	**62 (82.7%)**
	Former	13 (8.7%)	8 (10.7%)	5 (6.7%)
Alcohol consumption	Current	7 (4.7%)	3 (4%)	4 (5.3%)
	Never	137 (91.3%)	68 (90.7%)	**69 (92%)**
	Former	6 (4%)	4 (5.3%)	2 (2.7%)

BMI: Body mass index.

Adipose tissue, which is currently recognised as an endocrine organ (21), undergoes hypertrophy and hyperplasia in response to excessive caloric intake (22). This increase in adipose tissue mass leads to elevated adipokine production by pre-adipocytes and macrophages, thereby contributing to the development of inflammation (23). Therefore, the accumulation of visceral adipose tissue, a characteristic feature of MetS, may alter the vascular and lymphatic microenvironment, thereby creating lethal conditions for adipocytes that are distant from blood vessels. In addition, hypoxia and lipotoxicity may occur in adipocytes, thereby triggering the release of fatty acids and substrates that activate pro-inflammatory pathways in tissues (22). Although the pathogenesis of MetS has not yet been fully elucidated, it is hypothesised that an imbalance between antioxidant and pro-oxidant activities plays a vital role in its development (24). Furthermore, a chronic inflammatory state is considered the primary mechanism underlying MetS pathophysiology (21). Chronic low-grade inflammation, resulting from the accumulation of excess adipose tissue, is generally regarded as a key factor in the development of insulin resistance and may play an important role in the pathobiology of MetS (24,25).

Nicoară et al. (26) demonstrated the diagnostic value of the systemic immune-inflammatory response index for distinguishing MetS in obese children. Another study found a pronounced increase in pro-inflammatory cytokines in men with MetS and a decrease in anti-inflammatory adipokines in women with MetS (27). IFN-γ suppresses the expression of Sirtuin-1 (SIRT1), leading to metabolic dysfunction and the development of T2DM (28). Increased IFN-γ levels reduce insulin activity, disrupt metabolic homeostasis and insulin signaling

in skeletal muscle, and induce tumor necrosis factor (TNF)-α and Nuclear Factor Kappa B (NF-kB). IFN-γ also contributes to T-cell modulation, diet-associated insulin resistance, T2DM, and obesity by activating the JAK-STAT pathway, ultimately leading to insulin resistance (28). IFN-γ cytokine levels were found to be significantly higher in individuals diagnosed with MetS than in healthy adults (29), and increased serum IFN-γ concentrations were associated with insulin resistance and MetS components in obese children (30). These findings indicate that elevated IFN-γ levels are related to insulin resistance and MetS in pediatric population. Therefore, IFN-γ concentration may serve as a clinical biomarker for MetS and T2DM development and is considered a potential therapeutic target for improving these pathologies (31). Similar to previous studies, we found that serum IFN-γ concentrations were significantly higher in patiens with MetS compared to healthy counterparts.

IL-1, which includes IL-1α, IL-1β, and IL-1 receptor, is produced and secreted by hepatocytes and various other cellss, including vascular smooth muscle cells, endothelial cells, and macrophages/monocytes (32). Elevated serum IL-1α concentrations have been identified as vital parameters in the development of MetS (29). Lower IL-1α concentrations were associated with reduced adiposity and improved glucose tolerance in diet-induced obese mice, suggesting that inhibition of IL-1α may help maintain glucose tolerance and protect against obesity-related comorbidities (33). In another study, IL-1α treatment was shown to impair insulin signaling (34) by increasing IL-6 production in 3T3-L1 adipocytes, thereby contributing to insulin resistance. Other mechanisms have been suggested, including disruption of insulin signalling via STAT phosphorylation, SOCS3

Table 2. Demographic, anthropometric, and clinical data of study participants.

	Patients mean ± SE	Controls mean ± SE	p-value
Age	40.4 ± 1.5	28.1 ± 1.0	0.000*
BMI	34.5 ± 0.8	29.8 ± 0.6	0.000*
Hip circumference (cm)	119.8 ± 1.6	112.5 ± 1.3	0.000*
Mid upper arm circumference (cm)	37.9 ± 0.5	34.2 ± 0.5	0.000*
Waist circumference (cm)	115.9 ± 1.8	99.8 ± 1.9	0.000*
SBP (mmHg)	128.5 ± 2.4	110.8 ± 1.5	0.000*
DBP (mmHg)	80.2 ± 1.4	72.7 ± 1.2	0.000*
Fasting blood glucose (mg/dL)	118.5 ± 5.7	88.7 ± 0.9	0.000*
Insulin (mU/L)	18.6 ± 1.3	12.7 ± 0.7	0.000*
HOMA-IR	4.6 ± 0.3	2.8 ± 0.2	0.000*
Total cholesterol (mg/dL)	200.5 ± 5.6	178.2 ± 3.9	0.000*
Triglycerides (mg/dL)	203.5 ± 10.8	90.7 ± 4.1	0.000*
HDL-C (mg/dL)	44.7 ± 1.1	53.6 ± 1.2	0.000*
LDL-C (mg/dL)	117.2 ± 4.6	106.5 ± 2.9	0.051
e-GFR (mL/min)	117.6 ± 2.2	131.4 ± 1.6	0.000*
ALT (U/L)	25.5 ± 1.5	19.5 ± 1.4	0.001*
Creatinine (mg/dL)	0.73 ± 0.02	0.68 ± 0.01	0.178
Urea (mg/dL)	26.2 ± 0.9	22.3 ± 0.6	0.000*
Vitamin B$_{12}$ (ng/L)	292.0 ± 11.2	307.7 ± 13.5	0.684
TSH (mU/L)	2.1 ± 0.1	2.3 ± 0.2	0.403

*p < 0.05, HOMA-IR: Homeostatic model assessment-insulin resistance, SE: Standard error, BMI: Body mass index, SBP: systolic blood pressure, DBP: Diastolic blood pressure, HDL-C: High denstiy lipoprotein cholesterol, LDL-C: Low density lipoprotein cholesterol, ALT: Alanine aminotransferase, TSH: Thyroid-stimulating hormone.

Table 3. Evaluation of measured parameter levels in participants according to MetS status.

	Patients Mean ± SE	Controls Mean ± SE	p-value
Ferritin (ng/mL)	60.8 ± 4.2	37.1 ± 3.4	0.000*
IL-1α (pg/mL)	3.3 ± 0.2	2.7 ± 0.1	0.011*
IL-10 (pg/mL)	3.9 ± 0.1	3.7 ± 0.1	0.089
IFN-γ (pg/mL)	3.0 ± 0.1	2.8 ± 0.0	0.001*

*p < 0.05.

IL-1α: Interleukin-1α, IL-10: Interleukin 10, IFN-γ: Interferon-γ, SE: Standard error.

induction (35), and downregulation of insulin receptor substrate-1 in the presence of IL-6 (28). Consistent with previous research (29), the present study found that serum IL-1α concentrations were significantly higher in patients than in controls.

IL-10, an anti-inflammatory cytokine, plays an important role in regulating the immune system and in inhibiting the production and expression of pro-inflammatory cytokines (25). IL-10 is produced by macrophages and lymphocytes and exerts its anti-inflammatory and insulin signalling-modulating effects by inhibiting kappa B inhibitor kinase activity, suppressing TNF-induced nuclear factor kappa B activation (36), inhibiting NADPH oxidase-mediated oxidative stress, and downregulating TNF-α and IL-6 concentrations (37).

High circulating IL-10 levels help counter chronic inflammation in obesity and T2DM (38,39). Serum IL-10 has been found to be inversely associated with metabolic disorders, including elevated blood pressure, dyslipidemia, glucose intolerance (40), and MetS (25,38). Freitas et al. (41) reported that subjects with the IL-10 AA genotype, which is associated with lower IL-10 levels, had a higher risk of developing MetS. Serum IL-10 concentration has been linked to improvements in MetS and obesity by reducing BMI and body fat mass, reducing insulin resistance, and improving adipose tissue function in both human and animal models (42,43). Reduced IL-10 concentrations in adipose tissue and serum have been observed in subjects with obesity and type 2 diabetes (44,45). Interestingly, increased serum IL-10 concentrations have been found in obese women compared to non-obese women (38); this was attributed to a compensatory increase in IL-10 aimed at downregulating pro-inflammatory cytokines (38), as well as in children and adolescents (46). Some studies have also reported higher serum IL-10 concentrations in subjects with MetS compared with healthy counterparts (29,47). In our study, serum IL-10 concentrations were higher in patients; however, the difference between the two groups was not statistically significant. Although the underlying mechanism is not fully understood, a compensatory increase in IL-10 in response to the pro-inflammatory state may explain these findings (29). Additionally, genetic factors are thought to contribute to variability in cytokine production (48), and genetic differences

Table 4. Evaluation of measured parameters according to gender in controls and patient groups.

Measured parameters in controls	n	Meant ± SE	p-value
Ferritin			
Female	62	30.7 ± 2.1	0.03*
Male	13	67.7 ± 14.6	
IL-1α			
Female	62	2.6 ± 0.1	0.317
Male	13	3.0 ± 0.3	
IL-10			
Female	62	3.7 ± 0.1	0.905
Male	13	3.7 ± 0.2	
IFN-γ			
Female	62	2.8 ± 0.0	0.413
Male	13	2.8 ± 0.0	
Measured parameters in patients			
Ferritin			
Female	52	52.7 ± 4.1	0.011*
Male	23	79.2 ± 9.0	
IL-1α			
Female	52	3.2 ± 0.2	0.899
Male	23	3.4 ± 0.4	
IL-10			
Female	52	3.8 ± 0.1	0.140
Male	23	4.0 ± 0.1	
IFN-γ			
Female	52	3.1 ± 0.1	0.411
Male	23	3.0 ± 0.1	

*$p < 0.05$.
IL, IL-1α: Interleukin-1α, IL-10: Interleukin 10, IFN-γ: Interferon-γ, SE: Standard error.

among individuals in our study may account for the higher serum IL-10 concentrations observed in patients with MetS compared with those in the control group.

Gender is considered a significant factor that potentially influences differences in serum ferritin levels. A review of the literature has revealed that studies report inconsistent results (49). The discrepancies observed across studies may be attributed to differences in study population characteristics, sample size, and factors influencing serum ferritin levels. Physiologically, women tend to have lower serum ferritin concentrations than men due to iron loss through menstruation. In men, increased visceral adiposity and metabolic disorders may elevate serum ferritin levels by promoting the production of inflammatory cytokines. In our study, consistent with previous research (50), Levene's test indicated that variances across groups were not homogeneous. Therefore, Welch's t-test was applied, and only serum ferritin concentrations were higher in men than in women in both the patient and the control groups.

Study Limitations

Although this study was successfully completed, several limitations should be considered. First, the small sample size and the cross-sectional design of the study may limit the generalizability of the findings. Prospective studies with larger sample sizes are needed to clarify the causal relationships between serum ferritin, inflammatory cytokines, and MetS. Another limitation is that menopausal status was not considered, which may have influenced serum ferritin levels.

CONCLUSION

To the best of our knowledge, this is the first study in Türkiye to evaluate levels of serum ferritin and other inflammatory cytokines in individuals with and without MetS. The main finding was that serum concentrations of ferritin, IL-1α, and IFN-γ were significantly higher in participants diagnosed with MetS than in healthy controls. Although serum IL-10 levels were also higher in patients, the difference was not statistically significant. These findings indicate that individuals with MetS have elevated serum levels of pro-inflammatory cytokines and ferritin, which may be clinically relevant to the pathogenesis of the syndrome. Identifying new determinants of MetS could facilitate earlier diagnosis and more effective treatment. A better understanding of the roles of inflammation and ferritin in MetS may also contribute to improved prevention strategies. Prospective studies with larger cohorts are needed to further elucidate the relationship between cytokines and MetS.

REFERENCES

1. Neeland IJ, Lim S, Tchernof A, Gastaldelli A, Rangaswami J, Ndumele CE, et al. Metabolic syndrome. Nat Rev Dis Primers. 2024; 10: 77.

2. International Diabetes Federation. The IDF consensus worldwide definition of the Metabolic Syndrome [Internet]. Brussels: IDF; 2023 [cited 2024 Jun 7]. Available from: https://idf.org/media/uploads/2023/05/attachments-30.pdf

3. Onat A, Yüksel M, Köroğlu B, Gümrükçüoğlu HA, Aydın M, Cakmak HA, et al. TEKHARF 2012: Turkish Adult Risk Factor Study survey 2012: overall and coronary mortality and trends in the prevalence of metabolic syndrome. Turk Kardiyol Dern Ars. 2013; 41: 373–8.

4. Mollaoğlu M, Kars Fertelli T, Özkan Tuncay F. The risk levels of metabolic syndrome and related factors among adults admitted at a village clinic. 2010; 18: 72–9.

5. Serbis A, Giapros V, Galli-Tsinopoulou A, Siomou E. Metabolic syndrome in children and adolescents: ıs there a universally accepted definition? Does it matter? Metab Syndr Relat Disord. 2020; 18: 462–70.

6. Hacışevki A, Berberoğlu HT. Activation of inflammatory signaling pathways in metabolic syndrome: changes in adipokines and cytokines. In: Yucel D, ed. Current Biochemical Studies. Ankara, Akademisyen Kitabevi; 2020: 15–36.

7. Coelho M, Oliveira T, Fernandes R. Biochemistry of adipose tissue: an endocrine organ. Arch Med Sci. 2013; 9: 191–200.

8. Wang W, Knovich MA, Coffman LG, Torti FM, Torti SV. Serum ferritin: past, present and future. Biochim Biophys Acta. 2010; 1800: 760–9.

9. Mahroum N, Alghory A, Kiyak Z, Alwani A, Seida R, Alrais M, et al. Ferritin- from iron, through inflammation and autoimmunity, to COVID-19. J Autoimmun. 2022; 126: 102778.

10. Weir CB, Jan A. BMI classification percentile and cut off points. In: StatPearls [Internet]. Treasure island (FL): StatPearls Publishing; 2025 [cited 2025 Nov 05]. Available from: https://www.ncbi.nlm.nih.gov/books/NBK541070/.

11. National Cholesterol Education Program. Third report of the National Cholesterol Education Program (NCEP) expert panel on detection, evaluation, and treatment of high blood cholesterol in adults (Adult Treatment Panel III) final report [Internet]. Bethesda (MD): National Heart, Lung, and Blood Institute; 2002 [cited 2018 Jun 20]. Available from: https://www.nhlbi.nih.gov/files/docs/resources/heart/atp-3-cholesterol-full-report.pdf

12. Valizadeh A, Nikoohemmat M, Ebadinejad A, Soltani S, Tape PMK, Sohrabi A, et al. Metabolic syndrome as a risk factor for the development of kidney dysfunction: a meta-analysis of observational cohort studies. J Diabetes Metab Disord. 2023; 23: 215–27.

13. Srivastav SK, Mir IA, Bansal N, Singh PK, Kumari R, Deshmukh A. Serum ferritin in metabolic syndrome-mechanisms and clinical applications. Pathophysiology. 2022; 29: 319–25.

14. Heeney MM, Andrews NC. Iron homeostasis and inherited iron overload disorders: an overview. Hematol Oncol Clin North Am. 2004; 18: 1379–403.

15. Tran TN, Tran HD, Tran-Huu TT, Tran DM, Tran QN. A cross-sectional study of serum ferritin levels in vietnamese adults with metabolic syndrome. Diabetes Metab Syndr Obes. 2022; 15: 1517–23.

16. Shim YS, Kang MJ, Oh YJ, Baek JW, Yang S, Hwang IT. Association of serum ferritin with insulin resistance, abdominal obesity, and metabolic syndrome in Korean adolescent and adults: The Korean National Health and Nutrition Examination Survey, 2008 to 2011. Medicine (Baltimore). 2017; 96: e6179.

17. Kell DB, Pretorius E. No effects without causes: the ıron dysregulation and dormant microbes hypothesis for chronic, inflammatory diseases. Biol Rev Camb Philos Soc. 2018; 93: 1518–57.

18. Moore Heslin A, O'Donnell A, Buffini M, Nugent AP, Walton J, Flynn A, et al. Risk of ıron overload in obesity and ımplications in metabolic health. Nutrients. 2021; 13: 1539.

19. Eguchi N, Vaziri ND, Dafoe DC, Ichii H. The role of oxidative stress in pancreatic β Cell dysfunction in diabetes. Int J Mol Sci. 2021; 22: 1509.

20. Kilani N, Vollenweider P, Waeber G, Marques-Vidal P. Iron metabolism and incidence of metabolic syndrome. Nutr Metab Cardiovasc Dis. 2015; 25: 1025–32.

21. Dutta D, Maisnam I, Mukhopadhyay S, Raychaudhuri SK, Raychaudhuri SP. Systemic inflammation in psoriasis: sequel of metabolic syndrome. In: Mukhopadhyay S, Mondal S, eds. Metabolic syndrome: from mechanisms to interventions. Academic Press; 2024: 621-33. Available from: https://www.elsevier.com/books/metabolic-syndrome-from-mechanisms-to-interventions/mukhopadhyay/978-0-323-85732–1.

22. Debnath M, Agrawal S, Agrawal A, Dubey GP. Metaflammatory responses during obesity: Pathomechanism and treatment. Obes Res Clin Pract. 2016; 10: 103–13.

23. Guarner V, Rubio-Ruiz ME. Low-grade systemic inflammation connects aging, metabolic syndrome and cardiovascular disease. Interdiscip Top Gerontol. 2015; 40: 99–106.

24. Vona R, Gambardella L, Cittadini C, Straface E, Pietraforte D. Biomarkers of Oxidative Stress in Metabolic Syndrome and Associated Diseases. Oxid Med Cell Longev. 2019; 2019: 8267234.

25. Choi KM, Ryu OH, Lee KW, Kim HY, Seo JA, Kim SG, et al. Serum adiponectin, interleukin-10 levels and inflammatory markers in the metabolic syndrome. Diabetes Res Clin Pract. 2007; 75: 235–40.

26. Nicoară DM, Munteanu AI, Scutca AC, Mang N, Juganaru I, Brad GF, et al. Assessing the relationship between systemic immune-inflammation index and metabolic syndrome in children with obesity. Int J Mol Sci. 2023; 24: 8414.

27. Ter Horst R, van den Munckhof ICL, Schraa K, Aguirre-Gamboa R, Jaeger M, Smeekens SP, et al. Sex-specific regulation of inflammation and metabolic syndrome in obesity. Arterioscler Thromb Vasc Biol. 2020; 40: 1787–800.

28. Li P, Zhao Y, Wu X, Xia M, Fang M, Iwasaki Y, et al. Interferon gamma (IFN-γ) disrupts energy expenditure and metabolic homeostasis by suppressing SIRT1 transcription. Nucleic Acids Res. 2012; 40: 1609–20.

29. Mirhafez SR, Pasdar A, Avan A, Esmaily H, Moezzi A, Mohebati M, et al. Cytokine and growth factor profiling in patients with the metabolic syndrome. Br J Nutr. 2015; 113: 1911–9.

30. Pacifico L, Di Renzo L, Anania C, Osborn JF, Ippoliti F, Schiavo E, et al. Increased T-helper interferon-γ-secreting cells in obese children. Eur J Endocrinol. 2006; 154: 691–7.

31. Reinehr T, Roth CL. Inflammation markers in type 2 diabetes and the metabolic syndrome in the pediatric population. Curr Diab Rep. 2018; 18: 131.

32. Kamari Y, Werman-Venkert R, Shaish A, Werman A, Harari A, Gonen A, et al. Differential role and tissue specificity of interleukin-1alpha gene expression in atherogenesis and lipid metabolism. Atherosclerosis. 2007; 195: 31–8.

33. Almog T, Kandel Kfir M, Levkovich H, Shlomai G, Barshack I, Stienstra R, et al. Interleukin-1α deficiency reduces adiposity, glucose intolerance and hepatic de-novo lipogenesis in diet-induced obese mice. BMJ Open Diabetes Res Care. 2019; 7: e000650.

34. Ballak DB, Stienstra R, Tack CJ, Dinarello CA, van Diepen JA. IL-1 family members in the pathogenesis and treatment of metabolic disease: focus on adipose tissue inflammation and insulin resistance. Cytokine. 2015; 75: 280–90.

35. Uno T, He J, Usui I, Kanatani Y, Bukhari A, Fujisaka S, et al. Long-term interleukin-1alpha treatment inhibits insulin signaling via IL-6 production and SOCS3 expression in 3T3-L1 adipocytes. Horm Metab Res. 2008; 40: 8–12.

36. de Luca C, Olefsky JM. Inflammation and insulin resistance. FEBS Lett. 2008; 582: 97–105.

37. Srikanthan K, Feyh A, Visweshwar H, Shapiro JI, Sodhi K. Systematic review of metabolic syndrome biomarkers: a panel for early detection, management, and risk stratification in the West Virginian population. Int J Med Sci. 2016; 13: 25–38.

38. Esposito K, Pontillo A, Giugliano F, Giugliano G, Marfella R, Nicoletti G, et al. Association of low interleukin-10 levels with the metabolic syndrome in obese women. J Clin Endocrinol Metab. 2003; 88: 1055–8.

39. Barry JC, Shakibakho S, Durrer C, Simtchouk S, Jawanda KK, Cheung ST, et al. Hyporesponsiveness to the anti-inflammatory action of interleukin-10 in type 2 diabetes. Sci Rep. 2016; 6: 21244.

40. Kulshrestha H, Gupta V, Mishra S, Mahdi AA, Awasthi S, Kumar S. Interleukin-10 as a novel biomarker of metabolic risk factors. Diabetes Metab Syndr. 2018; 12: 543–7.

41. Freitas RS, de Souza Silva CM, Ferreira Fratelli C, Ramos de Lima L, Morato Stival M, Schwerz Funghetto S, et al. IL-10 and IL-1β serum levels, genetic variants, and metabolic syndrome: ınsights into older adults' clinical characteristics. Nutrients. 2024; 16: 1241.

42. Gao M, Zhang C, Ma Y, Bu L, Yan L, Liu D. Hydrodynamic delivery of mIL10 gene protects mice from high-fat diet-induced obesity and glucose intolerance. Mol Ther. 2013; 21: 1852–61.

43. Cintra DE, Pauli JR, Araújo EP, Moraes JC, de Souza CT, Milanski M, et al. Interleukin-10 is a protective factor against diet-induced insulin resistance in liver. J Hepatol. 2008; 48: 628–37.

44. Rodrigues KF, Pietrani NT, Bosco AA, Campos FMF, Sandrim VC, Gomes KB. IL-6, TNF-α, and IL-10 levels/polymorphisms and their association with type 2 diabetes mellitus and obesity in Brazilian individuals. Arch Endocrinol Metab. 2017; 61: 438–46.

45. Medeiros NI, Mattos RT, Menezes CA, Fares RCG, Talvani A, Dutra WO, Rios-Santos F, Correa-Oliveira R, Gomes JAS. IL-10 and TGF-β unbalanced levels in neutrophils contribute to increase inflammatory cytokine expression in childhood obesity. Eur J Nutr. 2018; 57: 2421–30.

46. Calcaterra V, De Amici M, Klersy C, Torre C, Brizzi V, Scaglia F, et al. Adiponectin, IL-10 and metabolic syndrome in obese children and adolescents. Acta Biomed. 2009; 80: 117–23.

47. Yeldu MH, Mus'ab A. Serum biochemical and inflammatory cytokines in a rat model of metabolic syndrome. Asian J Med Sci. 2020; 11: 46–52.

48. Westendorp RG, Langermans JA, Huizinga TW, Elouali AH, Verweij CL, Boomsma DI, et al. Genetic influence on cytokine production and fatal meningococcal disease. Lancet. 1997; 349: 170–3.

49. Alqahtani SAM, Alsaleem MA, Ghazy RM. Association between serum ferritin level and lipid profile among diabetic patients: A retrospective cohort study. Medicine (Baltimore). 2024; 103: e37631.

50. Badenhorst CE, Forsyth AK, Govus AD. A contemporary understanding of iron metabolism in active premenopausal females. Front Sports Act Living. 2022; 4: 903937.

The Forensic Medical Significance of Nasal Bone Fractures: A Clinical and Medico-Legal Retrospective Analysis

Burun Kemiği Kırıklarının Adli Tıbbi Önemi: Klinik ve Medikolegal Retrospektif Bir Analiz

Ⓘ Emre Gürkan Bulutluöz[1], Ⓘ Burak Kaya[2]

[1]Clinic of Forensic Medicine, Çankırı State Hospital, Çankırı, Türkiye
[2]Council of Forensic Medicine, Artvin Branch Office, Artvin, Türkiye

ABSTRACT

Objective: This study aims to evaluate nasal bone fractures, the most frequently encountered injuries in maxillofacial trauma, from a forensic medicine perspective and to contribute to the objectivity of the medicolegal analysis of such cases.

Methods: A total of 205 patients with nasal bone fractures who presented to Çankırı State Hospital between 2022 and 2025 and were reported as forensic cases were retrospectively analyzed. Age, sex, etiology of trauma, fracture type, associated injuries, physical examination findings, and imaging methods used were evaluated. Data were analyzed using descriptive and comparative statistical methods.

Results: The prevalence of nasal fractures among forensic cases was 1.15%, and 82.9% of the patients were male. The most common etiological factor was assault (57.1%), followed by traffic accidents (33.7%). Of the fractures, 62% were displaced, 31.2% were linear, and 6.8% were comminuted/depressed; 92.2% were closed, and 7.8% were open. Open fractures were significantly more common during in-vehicle traffic accidents. Additional skeletal fractures were detected in 31.2% of cases. Computed tomography was the most frequently used imaging modality (63.4%).

Conclusion: Nasal fractures are more frequently observed in young adult males and are commonly associated with assault-related trauma. The presence of accompanying fractures reflects the severity of the trauma. These findings are expected to contribute to the standardization and objectivity of forensic medical evaluation processes.

Keywords: Nasal bone, forensic medicine, facial injuries, wounds and injuries, maxillofacial injuries, violence

ÖZ

Amaç: Bu çalışma maksillofasiyal travmalar içerisinde en sık karşılaşılan nazal kemik kırıklarını adli tıp açısından değerlendirmeyi ve bu olguların medikolegal analizini objektifleştirmeyi amaçlamaktadır.

Yöntemler: 2022-2025 yılları arasında Çankırı Devlet Hastanesi'ne başvuran, adli olgu bildirimi yapılan ve nazal kırık saptanan 205 olgu retrospektif olarak incelenmiştir. Olguların yaş, cinsiyet, travma etiyolojisi, kırık tipi, eşlik eden yaralanmalar, muayene bulguları ve kullanılan görüntüleme yöntemleri incelenmiştir. Veriler tanımlayıcı ve karşılaştırmalı istatistiklerle analiz edilmiştir.

Bulgular: Nazal fraktür görülme sıklığı %1,15 olarak saptanmış, olguların %82,9'unu erkekler oluşturmuştur. En sık etiyolojik nedenin darp (%57,1) olduğu belirlenmiş, bunu trafik kazaları (%33,7) takip etmiştir. Kırıkların %62'si deplase, %31,2'si lineer, %6,8'i parçalı/çökme tipi olup; %92,2'si kapalı, %7,8'i açık kırıklardan oluşmaktadır. Özellikle araç içi trafik kazalarında açık kırık oranı anlamlı düzeyde daha yüksek bulunmuştur. Olguların %31,2'sinde eşlik eden başka kemik kırıkları tespit edilmiştir. Bilgisayarlı tomografi en sık kullanılan görüntüleme yöntemi olarak saptanmıştır (%63,4).

Sonuç: Nazal kırıklar genç erişkin erkeklerde ve darp kaynaklı travmalarda daha sık görülmekte olup, eşlik eden kırıkların varlığı travma şiddetini yansıtmaktadır. Bulgular, adli tıbbi değerlendirme süreçlerinin objektifleştirilmesine katkı sunacaktır.

Anahtar Sözcükler: Burun kemiği, adli tıp, yüz yaralanmaları, yaralar ve travmalar, maksillofasiyal yaralanmalar, şiddet

Gazi Med J 2026;37(1):23-30

Bulutluöz and Kaya. The Forensic Medical Significance of Nasal Bone Fractures

INTRODUCTION

The maxillofacial region is among the most frequently affected anatomical areas in traumatic incidents because of its location and exposure to the external environment (1). Among injuries involving this region, the nasal bone is one of the most commonly fractured structures, because it is the most prominent part of the face and has the weakest supporting tissue (2). The unprotected structure of the nasal bone makes it susceptible to fracture even under forces that may be insufficient to cause fractures of other facial bones (3).

Nasal bone fractures are frequently associated with forensic cases, such as assaultassaults, and with accidental causes, including falls, traffic accidents, and occupational or domestic injuries (4). Clinically and radiologically, they are typically classified as linear (non-displaced), displaced, or comminuted fractures. Moreover, depending on whether the integrity of the skin overlying the fracture line is compromised, they may also be classified as closed or open (5). Clinical findings commonly include nasal deviation, nasal depression, tenderness, edema, crepitus, and epistaxis (6). Imaging modalities such as plain radiography or computed tomography (CT) are used to confirm the diagnosis and guide treatment planning (7).

Nasal bone fractures require specialized evaluation not only from a medical perspective but also from forensic and legal perspectives (8). According to the Turkish Penal Code, injuries resulting in bone fractures are punishable by imprisonment for one to six years, depending on the extent to which the fracture affects vital bodily functions (9).

In this context, the Guide for the Forensic Medical Evaluation of Injuries Defined in the Turkish Penal Code (10) classifies bone fractures as mild (1), moderate (2-3), and severe (4-6) according to their impact on vital bodily functions. In the forensic assessment of nasal bone fractures, the fracture type serves as a primary parameter. A linear fracture or avulsion of the nasal bone is considered to have a mild (1) effect on vital functions, whereas more complex fractures, such as comminuted or depressed nasal fractures, are deemed to have a moderate (2) effect on vital functions.

Although nasal fractures may occur as isolated injuries, they are often accompanied by fractures of other facial bones or of bones in other regions of the body, particularly in high-energy trauma cases (11). The presence of multiple fractures is regarded as a significant indicator of increased trauma severity (12).

The aim of this study is to elucidate the role of nasal bone fractures in forensic medicine and to contribute to standardization of criteria and diagnostic methods used to evaluate such cases. Additionally, the study seeks to enhance the forensic medical assessment of nasal bone fractures and expand the body of knowledge in this area.

MATERIALS AND METHODS

Data from cases presenting to Çankırı State Hospital between 2022 and 2025 and reported as forensic incidents were retrospectively reviewed, and cases in which a nasal bone fracture was identified were included in the study. For each included case, general forensic examination reports, patient discharge summaries (epicrises), and radiological images were evaluated. The following variables were examined: age, sex, time of injury, cause of the incident, physical examination findings, type of fracture, presence of accompanying fractures, and diagnostic investigations performed to establish the clinical diagnosis.

This study was approved by the Ethics Committee of Health Sciences of Çankırı Karatekin University (meeting number: 22, date: 14.07.2025). The research was conducted in accordance with the principles of the Declaration of Helsinki.

Statistical Analysis

Statistical analyses were conducted using IBM SPSS Statistics version 26 (IBM Corp., Armonk, NY, USA). Descriptive statistics were presented as frequencies, percentages, means, standard deviations, minimum and maximum values. The differences between categorical variables were analyzed using the Pearson chi-square test. Additionally, a chi-square goodness-of-fit test was employed to assess whether a categorical variable was uniformly distributed across categories by comparing the observed distribution with the expected distribution under equal proportions. The expected frequencies in some cells were less than 5. A p-value of <0.05 was considered statistically significant.

RESULTS

A total of 17,810 cases reported as forensic incidents and assessed as involving medico-legal injuries were reviewed. Among these, 205 cases were identified as having nasal fractures and were included within the scope of the study. The prevalence of nasal fractures among all forensic cases was 1.15%.

Of the 205 cases included in our study, 82.9% (n = 170) were male and 17.1% (n = 35) were female. The number of male cases was significantly higher than that of female cases (χ^2=88.90, p <0.001).

The ages of the cases evaluated in the study ranged from 2 to 87 years, with a mean age of 35.51±16.42 years. The distribution of cases by age group is presented in Table 1. The highest number of cases was observed in the 26-40 age group (34.6%, n = 71), followed by the 18-25 age group (25.9%, n = 53) and the 41-64 age group (25.9%, n = 53). Additionally, 5.9% (n = 12) of the cases were in the 13-17 age group, 5.4% (n = 11) were aged 65 and above, 1.5% (n = 3) were in the 7-12 age group, and 1% (n = 2) were aged 0-6 years. Nasal bone fractures in forensic incidents were significantly concentrated in the 18-25 and 26-40 age groups (χ^2=168.46, p <0.001).

The monthly distribution of nasal fractures is presented in Figure 1. The highest number of cases was recorded in October (14.1%, n = 29), followed by January (10.2%; n = 21), May (9.8%; n = 20), and July (9.8%; n = 20). The lowest number of cases was observed in December (3.9%; n = 8).

Regarding seasonal distribution the highest number of cases occurred in autumn (32.2%; n = 66) followed by summer (25.4%; n = 52), spring (24.4%; n = 50), and winter (18.0%; n = 37). While the monthly distribution was not statistically significant (χ^2=18.43; p=0.072), the seasonal variation was found to be significant (χ^2=8.25; p=0.041). A notable increase in forensic nasal fractures was observed particularly during the autumn season.

The distribution of injury mechanisms is presented in Table 1. The most common cause of nasal fractures was physical assault (57.1%; n = 117). This was followed by in-vehicle traffic accidents (21.5%; n = 44), out-of-vehicle traffic accidents (12.2%; n = 25), falls from height

Gazi Med J 2026;37(1):23-30

Bulutluöz and Kaya. The Forensic Medical Significance of Nasal Bone Fractures

(7.3%; n = 15), and other types of accidents (e.g., occupational or domestic/environmental incidents) (2%; n = 4). The notably high proportion of assault-related cases was found to be statistically significant (χ^2=197.22; p <0.001).

The distribution of injury mechanisms by sex is presented in Table 2. Among males the most common cause of injury was physical assault (62.4%; n = 106), followed by in-vehicle traffic accidents (17.6%; n = 30), out-of-vehicle traffic accidents (11.2%; n = 19), falls from height (7.6%; n = 13), and other accidents (1.2%; n = 2). In female cases the leading causes were in-vehicle traffic accidents (40.0%; n = 14) and physical assault (31.4%; n = 11), followed by out-of-vehicle traffic accidents (17.1%; n = 6), falls from height (5.7%; n = 2), and other accidents (5.7%; n = 2). The distribution of injury mechanisms differed significantly between sexes (χ^2=15.68; p=0.003).

The distribution of fracture types among the cases is presented in Table 3. The most frequently observed fracture type was displaced fractures (62.0%; n = 127) followed by linear fractures (31.2%; n =

64) and comminuted/depressed fractures (6.8%; n = 14). Bilateral nasal bone fractures were identified in 67.3% of cases (n = 138) while unilateral fractures were observed in 32.7% (n = 67). A total of 92.2% (n = 189) of the fractures were classified as closed and 7.8% (n = 16) as open fractures. The proportion of open fractures was significantly higher in in-vehicle traffic accidents compared to other causes (χ^2=26.91; p <0.001).

Upon examination of clinical findings, crepitation over the nasal dorsum was detected in 35.6% of the cases (n = 73) whereas no such finding was observed in 64.4% (n = 132). Additionally active epistaxis was present in 48.3% of the cases (n = 99) in the remaining 51.7% (n = 106) either no nasal bleeding was observed or active epistaxis was absent.

Regarding imaging modalities 63.4% of the cases (n = 130) were evaluated using only CT, 26.3% (n = 54) underwent both CT and plain radiography and 10.2% (n = 21) were assessed with plain radiography solely.
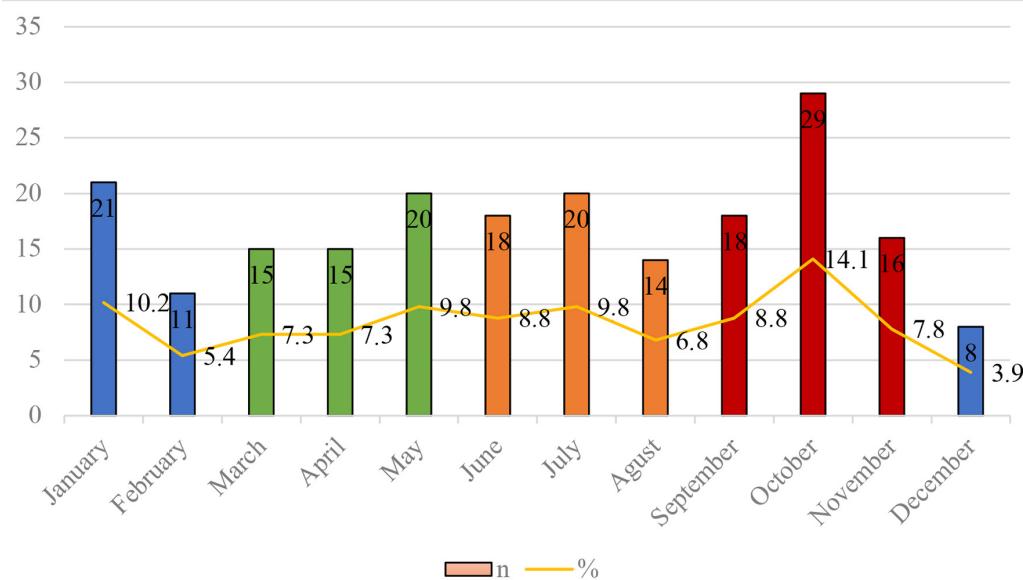
Figure 1. The monthly and seasonal distribution of nasal fractures.

Table 1. Distribution of injury mechanisms by age group.

Age group	Injury mechanisms					Total, n (%)	χ^2	p
	Physical assault	IVTA	OVTA	Falls	Other accidents			
	n (%)	n (%)	n (%)	n (%)	n (%)			
0-6	-	-	1 (50%)	1 (50%)	-	2 (1%)	168.46	<0.001
7-12	2 (66.7%)	-	1 (33.3%)	-	-	3 (1.5%)		
13-17	7 (58.3%)	3 (25%)	2 (16.7%)	-	-	12 (5.9%)		
18-25	34 (64.2%)	9 (17%)	4 (7.5%)	1 (1.9%)	5 (9.4%)	53 (25.9%)		
26-40	46 (64.8%)	12 (16.9%)	7 (9.9%)	1 (1.4%)	5 (7%)	71 (34.6%)		
41-64	25 (47.2%)	15 (28.3%)	8 (15.1%)	2 (3.8%)	3 (5.7%)	53 (25.9%)		
65+	3 (27.3%)	5 (45.5%)	2 (18.2%)	-	1 (9.1%)	11 (5.4%)		
Total	117 (57.1%)	44 (21.5%)	25 (12.2%)	4 (2%)	15 (7.3%)	205 (100%)		

IVTA: in-Vehicle traffic accidents, OVTA: Out-of-vehicle traffic accidents, Falls: Falls from height, Other accidents: Occupational or domestic/environmental incidents.

Gazi Med J 2026;37(1):23-30

Bulutluöz and Kaya. The Forensic Medical Significance of Nasal Bone Fractures

During the forensic evaluation process clinical management approaches revealed that 37.6% of the cases (n = 77) were referred for consultation with an otorhinolaryngology (Ear, Nose, and Throat; ENT) specialist while 62.4% (n = 128) were directed to outpatient follow-up. When consultation rates were examined according to fracture type it was found that 21.9% (n = 14) of cases with linear fractures, 40.9% (n = 52) of those with displaced fractures, and 78.6% (n = 11) of those with comminuted fractures were referred for specialist consultation. It was determined that Consultation rates increased significantly with the severity of the fracture (χ^2=17.37, p <0.001).

In accordance with our hospital's protocol for forensic cases blood ethanol levels are routinely assessed in all presenting patients. Ethanol was detected in blood samples in only 10.2% of the cases (n = 21).

In 31.2% (n = 64) of cases with nasal bone fractures additional fractures in other parts of the body were also identified. The distribution of these accompanying fractures is detailed in Table 4. The most frequently additional fractures involved facial bones (20.0%; n = 41) followed by extremity fractures (14.1%; n = 29), vertebral fractures (5.4%; n = 11), rib fractures (4.9%; n = 10), and cranial fractures (4.9%; n = 10). Fractures of the facial bones were found to be significantly more common than other types of accompanying fractures (χ^2=39.74, p <0.001). Furthermore the rate of accompanying fractures was significantly higher in both in-vehicle and out-of-vehicle traffic accidents compared to other types of incidents (χ^2=41.05; p < 0.001).

DISCUSSION

Maxillofacial injuries are among the most common types of physical trauma (1). The nose, the most prominent part of the face, accounts for approximately half of all maxillofacial fractures resulting from trauma (5). To determine the legal penalty for the perpetrator of an assault, it is essential to assess, from a forensic-medical perspective, the severity of these injuries and the conditions they cause.

In our study, the mean age of cases with nasal fractures was 35.51 years. The age group most frequently affected was 26-40 years (34.6%), followed by the 18-25 age group (25.9%). According to our findings, approximately 60.5% of nasal fractures occurred during young adulthood, indicating that individuals in this age range are at higher risk of nasal trauma-related fractures. The data obtained in this study are largely consistent with findings reported in the literature. Previous studies have documented that the mean age of patients with nasal bone fractures ranges from 25.9 to 34 years, and the majority of nasal fractures occur between the ages of 18 and 40

(2,11,13-16). Young adults are more frequently exposed to traumatic circumstances because of lifestyle factors. In particular, sports-related injuries, incidents of physical assault, and occupational and traffic accidents are more common in this age group (17). Moreover, factors such as increased social activity, participation in nightlife, presence in crowded environments, and a tendency toward risk-taking behaviors may further elevate the likelihood of trauma in this population.

Regarding the sex distribution of nasal fractures, the literature consistently reports that nasal fractures occur significantly more frequently in males than in females. Numerous studies have indicated that 72.5% to 88% of nasal fracture cases occur in males (2,15,16,18-21). In a study conducted by Karbeyaz et al. (18), the prevalence of nasal fractures was also found to be significantly higher in males than in females. Similarly, in our study, the vast majority of cases of nasal bone fractures (82.9%) were male, which is consistent with the existing literature. The higher incidence of nasal fractures in males is thought to be primarily due to increased exposure to physical trauma (such as traffic accidents and acts of violence), greater activity levels among younger males, influenced by sociocultural factors, and more frequent presence in outdoor or high-risk environments (1).

In our study, physical assault was identified as the most common cause of nasal fractures, accounting for 57.1% of cases. Assault was followed by in-vehicle traffic accidents (21.5%) and out-of-vehicle traffic accidents (12.2%). Overall, traffic accidents accounted for 33.7% of all nasal fractures. These findings are largely consistent with data reported in the literature. Previous studies have indicated that nasal fractures most frequently result from assault, with rates ranging from 32% to 90%, followed by traffic accidents reported at rates ranging from 7% to 38.4% (4,8,19,22,23). The high prevalence of assault-related nasal fractures may be attributed to the anatomical vulnerability of the nose, which is the most prominent and exposed part of the face, making it particularly susceptible to trauma (24). Attacks targeting the facial region often result in a direct impact to the nasal bone. In cases of interpersonal violence, physical aggression frequently begins with blows to the face, which may explain the predominance of assault as a mechanism of injury in nasal fractures. That traffic accidents rank second may be related to the direct exposure of the head and neck region to trauma during both in-vehicle and out-of-vehicle collisions.

The etiology of nasal fractures demonstrates a marked difference according to sex, a finding supported by various studies in the literature. Karbeyaz et al. (18) reported that physical assault was the most common cause of nasal fractures among males, whereas traffic accidents were the most common cause among females. The study also noted that this difference was statistically significant.

Table 2. Sex-based distribution of injury mechanisms.

Gender	Injury mechanisms					Total n (%)	χ^2	p
	Physical assault	IVTA	OVTA	Falls	Other accidents			
	n (%)	n (%)	n (%)	n (%)	n (%)			
Male	106 (62.4%)	30 (17.6%)	19 (11.2%)	13 (7.6%)	2 (1.2%)	170 (82.9%)	15.68	0.003
Famale	11 (31.4%)	14 (40%)	6 (17.1%)	2 (5.7%)	2 (5.7%)	35 (17.1%)		
Total	117 (57.1%)	44 (21.5%)	25 (12.2%)	15 (7.3%)	4 (2%)	205 (100%)		

IVTA: in-Vehicle traffic accidents, OVTA: Out-of-vehicle traffic accidents, Falls: Falls from height, Other accidents: Occupational or domestic/environmental incidents.

Gazi Med J 2026;37(1):23-30

Bulutluöz and Kaya. The Forensic Medical Significance of Nasal Bone Fractures

Table 3. Fracture typing and distribution.

Fracture type	n	%
Linear	64	31.2
Displaced	127	62
Comminuted	14	6.8
Broken side		
Unilateral	67	32.7
Bilateral	138	67.3
Skin integrity		
Open fractures	16	7.8
Closed fractures	189	92.2

Similarly, Hwang et al. (4) found that the most frequent cause of nasal fractures among male patients was assault (66.7%), whereas among female patients, accidents (52.7%) were the most common; this difference was also reported to be statistically significant. In our study, consistent with the aforementioned literature, similar results were observed. When all cases were analyzed collectively, regardless of sex, assault emerged as the most common etiological factor. However, a more detailed examination by sex revealed that among female cases, in-vehicle traffic accidents were the leading cause of nasal fractures (40%), followed by assault (31.4%). In contrast, among male cases, assault was the most frequent cause (62.4%), followed by in-vehicle traffic accidents (17.6%) and out-of-vehicle traffic accidents (11.2%). This difference was statistically significant (χ^2=15.68, p=0.003). This variation is likely attributable to differences between genders in societal roles, behavioral patterns, and exposure to violence. Although social structure, gender roles, and the prevalence of violence may vary across countries and regions (25), the findings of our study are consistent with previously reported data in the literature.

In our study, the evaluation of nasal bone fracture types revealed that displaced fractures were the most common type (62%). This was followed by linear fractures (31.2%) and comminuted/depressed fractures (6.8%). Our findings are consistent with those of several studies in the literature. Hosukler et al. (15) reported that 56.5% of nasal fractures were displaced; Bütün et al. (19) also identified displaced fractures as the most prevalent type (45.8%).

The high proportion of displaced fractures may be associated with the severity of the trauma. Although the majority of our cases were assault-related, high-energy trauma mechanisms such as traffic accidents also constituted a substantial proportion and may have contributed to the increased rate of displaced fractures. While linear fractures are more commonly observed in low-energy injuries, high-energy injuries are more likely to result in displaced fractures that are severe enough to cause deformity. Some studies, however, have reported a higher frequency of linear fractures. For example, Balandız et al. (1) found linear nasal fractures in 77.9% of cases, and Toygar et al. (8) reported a rate of 95%. These discrepancies may be attributed to differences in the characteristics of the study populations, the diversity and severity of trauma mechanisms, the diagnostic methods employed, and the criteria used for fracture classification.

The vast majority of nasal fractures were closed (92.2%), while the proportion of open fractures was 7.8%. Moreover, the rate of open fractures was significantly higher in in-vehicle traffic accidents than in other types of incidents (χ^2=26.91, p <0.001). These findings are largely consistent with the existing literature. Sayın et al. (14) reported that 92.9% of nasal bone fractures were closed, whereas only 7.1% were open. Similarly, Hosukler et al. (15) noted that the rate of open nasal fractures was 11.4%. These data suggest that most fractures tend to be closed due to the anatomical structure of the nasal region; however, as trauma severity increases, soft-tissue integrity may also be compromised. The higher frequency of open fractures during in-vehicle traffic accidents may be associated with the high kinetic energy involved in such incidents. In these cases, the force generated by the impact velocity is often transmitted directly to the facial region, typically causing collisions with hard surfaces such as the steering wheel or windshield, or with the airbag. This mechanism may result in skin lacerations, leading to open fractures (26). In contrast, in cases of assault or low-energy trauma, soft tissue often serves as a buffer overlying the bone, helping to preserve skin integrity and resulting in a closed fracture.

Evaluation of clinical symptoms associated with nasal fractures revealed that crepitation was present in 35.6% of cases, while epistaxis was observed in 48.3% of cases. When compared with findings reported in the literature, these rates show some variation. Gupta et al. (22) reported crepitation in 80% and active epistaxis in 76.8% of nasal fracture cases. Similarly, Akdag et al. (3) reported

Table 4. Distribution of fractures accompanying nasal bone fractures according to injury mechanisms.

Accompanying fractures	Injury mechanisms					Total	χ^2	p
	Physical assault	IVTA	OVTA	Falls	Other accidents	n (%)		
	n (%)	n (%)	n (%)	n (%)	n (%)			
Facial fractures	13 (11.1%)	14 (31.8%)	9 (36%)	4 (26.7%)	1 (25%)	41 (20%)	41.05	<0.001
Cranial fractures	-	5 (11.4%)	2 (8%)	3 (20%)	-	10 (4.9%)		
Extremity fractures	3 (2.6%)	13 (29.5%)	7 (28%)	5 (33.3%)	1 (25%)	29 (14.1%)		
Vertebral fractures	1 (0.9%)	8 (18.2%)	2 (8%)	-	-	11 (5.4%)		
Rib fractures	-	8 (18.2%)	-	-	2 (13.3%)	10 (4.9%)		

IVTA: in-Vehicle traffic accidents, OVTA: Out-of-vehicle traffic accidents, Falls: falls from height, Other accidents: Occupational or domestic/environmental incidents.

Gazi Med J 2026;37(1):23-30

Bulutluöz and Kaya. The Forensic Medical Significance of Nasal Bone Fractures

a crepitation rate of 75.3%. In contrast, Ersoy et al. (27) identified epistaxis in 45% and crepitation in 27.5% of cases, whereas Hosukler et al. (15), in their study based on medical record review, reported these rates as 19.4% and 11.7%, respectively. This variability suggests that the identification and documentation of symptoms of nasal fractures are influenced by several factors, including the severity of the trauma, the time elapsed since the incident, the patient's condition at the time of presentation, and variations in clinical practice. Additionally, during the retrospective review of medical records, the extent to which symptoms were thoroughly documented by the physician may affect the reported rates. Crepitation, in particular, is a clinical finding that can vary depending on the examiner's level of experience and examination technique; it is not always assessed in a standardized manner.

CT is currently regarded as the gold-standard imaging modality for diagnosing facial trauma (5). CT provides high-resolution cross-sectional images, offering significant advantages in evaluating the fracture line, the degree of displacement, and any concomitant facial bone injuries. However, plain radiographs (direct X-rays) are still used in some centers, with factors such as cost, accessibility, and radiation exposure influencing this preference. The literature reveals considerable variability in imaging methods used to diagnose nasal fractures. For instance, Hosukler et al. (15) reported using both CT and direct radiography in 76.5% of cases and direct radiography alone in 14.6% of cases. Similarly, Akdag et al. (3) used CT in 46.8% of cases and direct radiography in 53.2% of cases for fracture detection. In our study, nasal bone fractures were evaluated using CT alone in 63.4% of cases, both CT and direct radiography in 26.3% of cases, and direct radiography alone in only 10.2% of cases. These findings suggest a markedly greater reliance on CT. One likely explanation for this trend is the increased accessibility of CT in modern clinical practice. Furthermore, the limited sensitivity of plain radiographs—particularly in detecting minimally displaced fractures—has led clinicians to favor CT as a more reliable diagnostic tool. The use of both CT and plain radiography may reflect cases in which initial evaluation with plain radiography was followed by CT to confirm the diagnosis. The low proportion of cases evaluated solely with direct radiography further supports the view that this modality is no longer considered sufficient as a standalone diagnostic tool in the assessment of nasal fractures.

In the preparation of medico-legal reports for forensic cases the expert opinion of a specialist physician in the relevant field becomes increasingly important to provide detailed scientific data. Karakuş et al. (28) reported that nasal fractures were observed in 23.2% of forensic cases referred to the Department of ENT. In our study, an ENT specialist consultation was requested in 37.6% of cases, and the consultation rate also increased significantly with fracture severity (χ^2=17.37, p <0.001). (χ^2=17.37, p <0.001). In more severe cases in which both forensic reporting and therapeutic management become more complex, the involvement of ENT specialists is both expected and necessary to ensure a valid and objective evaluation.

Alcohol consumption is known to be a significant risk factor for trauma-related injuries (29). Maxillofacial trauma, in particular, occurs more frequently as a result of risk-taking behavior associated with alcohol intake. This association increases susceptibility not only to accidents but also to violence-related incidents. In a previous study (29), ethanol was detected in the blood of 36.5% of patients with trauma-related maxillofacial injuries. In contrast, in our study, blood ethanol positivity was detected in 10.2% of forensic nasal fracture cases. This rate appears to be lower than those reported in studies of facial trauma in general. One likely explanation is that our study was limited to nasal fractures . Maxillofacial trauma involves a broad anatomical region and is often associated with more severe mechanisms of injury. Therefore, behavioral risk factors such as alcohol use may be reported at higher rates in studies including a wider range of facial injuries.

Nasal bone fractures are among the most frequently encountered in maxillofacial trauma. Although they are often considered isolated injuries, they are frequently accompanied by additional damage to adjacent anatomical structures. The literature reports that fractures of other facial bones, such as the maxilla, nasal septum, and orbital walls, coexist with nasal fractures in 10%-35.6% of cases (30-32). This variation is influenced by the mechanism and severity of the trauma (24). In our study, consistent with the literature, 31.2% of cases of nasal bone fractures also had fractures in other body regions. This finding supports the notion that nasal fractures frequently occur as part of broader, more complex trauma patterns. The likelihood of such associations is particularly high in high-energy trauma. Upon examining the accompanying fractures in our study, extremity fractures were identified in 14.1% of cases, vertebral fractures in 5.4%, rib fractures in 4.9%, and cranial fractures in 4.9%. These data indicate that nasal fractures, especially those resulting from high-energy mechanisms, may be part of multisystem injury patterns. Similar findings have been reported in the literature. Kim et al. (33) emphasized that in high-energy trauma, such as traffic accidents, nasal fractures are often observed in conjunction with injuries to the head, spine, and extremities. This underscores the importance of identifying associated injuries during forensic reporting, as they play a critical role in determining the nature of the incident and assessing the severity of the trauma.

Study Limitations

Due to the retrospective design of this study, data were evaluated solely on the basis of existing medical records and forensic documents. Incomplete or non-standardized documentation may have affected the accuracy of certain findings. The study was conducted at a single center and included only cases that had been officially reported as forensic incidents. This limits the generalizability of the results and excludes milder or unreported cases within the broader population. Furthermore, the absence of data on the treatment process and long-term outcomes of the fractures limited the ability to thoroughly assess the relationship between clinical management and forensic implications.

CONCLUSION

This study aimed to contribute to both the anatomical and clinical understanding of nasal fractures and their systematic evaluation in forensic medicine. Our findings revealed that nasal fractures most commonly occur in young adult males and are predominantly associated with forensic incidents, such as physical assault. The majority of fractures were identified as displaced and closed, suggesting that the trauma often involved direct but moderate-intensity force.

Gazi Med J 2026;37(1):23-30

Bulutluöz and Kaya. The Forensic Medical Significance of Nasal Bone Fractures

However, the presence of accompanying fractures of the facial bones, extremities, vertebrae, and cranium indicates that nasal fractures are frequently associated with high-energy trauma rather than occurring as isolated injuries. Regarding diagnostic imaging, the predominant use of CT reinforces its role as the standard modality in current clinical practice, highlighting its advantages in providing a detailed evaluation.

The findings of this study emphasize the necessity of evaluating nasal fractures in forensic medicine based not solely on the presence of a fracture but also on the fracture type, associated injuries, etiology of the incident, and clinical findings. Moreover, it was concluded that forensic reporting of nasal fractures should be grounded in objective criteria that reflect the extent of the injury.

Future large-scale, multicenter studies conducted across different geographical regions and sociocultural contexts may significantly contribute to the development of standardized guidelines and the revision of existing protocols for the forensic assessment of nasal fractures. Furthermore, collaboration between clinical and forensic experts will enhance both patient management and the accuracy of legal processes. The results obtained in this study serve as a valuable reference for both healthcare professionals and forensic authorities, supporting the development of more reliable and scientifically grounded forensic reports.

Ethics

Ethics Committee Approval: This study was approved by the Ethics Committee of Health Sciences of Çankırı Karatekin University (meeting number: 22, date: 14.07.2025). The research was conducted in accordance with the principles of the Declaration of Helsinki.

Informed Consent: Retrospective study.

Footnotes

Authorship Contributions

Surgical and Medical Practices: E.G.B., B.K., Concept: E.G.B., B.K., Design: E.G.B., B.K., Data Collection or Processing: E.G.B., B.K., Analysis or Interpretation: E.G.B., B.K., Literature Search: E.G.B., B.K., Writing: E.G.B., B.K.

Conflict of Interest: No conflict of interest was declared by the authors.

Financial Disclosure: The authors declared that this study received no financial support.

REFERENCES

1. Balandız H, Aydogan HC, Kaya B, Özsever S, Özsoy S. Comprehensive examination of etiological factors and clinical manifestations of maxillofacial traumas in forensic cases: a five-year retrospective study. Ulus Travma Acil Cerrahi Derg. 2024; 30: 677–84.

2. Gökgöz MC, Ersoy Mirici M. Density mapping of nasal fracture: a new epidemiological perspective of nasal fractures in a pilot city. J Ear Nose Throat Head Neck Surg. 2022; 30: 31–7.

3. Akdag M, Dursun R, Gül A, Hattapoglu S, Meriç F, Topcu I. Retrospective analysis of nasal fractures in the emergency clinic. Eurasian J Emerg Med. 2014; 13: 139–42.

4. Hwang K, Ki SJ, Ko SH. Etiology of nasal bone fractures. J Craniofac Surg. 2017; 28: 785–8.

5. Epstein S, Ettinger RE. Nasal and naso-orbito-ethmoid fractures. Semin Plast Surg. 2021; 35: 263–8.

6. Atan Y, Akbaba M, Tataroğlu Z, Daş V, Yuluğ E. What approach should be taken towards maxillofacial trauma in terms of The Turkish Penal Code 87/1-2.? A Case Report. Ankara Med J. June 2019; 19: 434–8.

7. İzci A, Acar K, Çakmak V, Arslanergül M, Kurtuluş Dereli A. An example of multidisciplinary approach in the medicolegal evaluation of cases applying to the forensic medicine polyclinic: forensic medicine and radiology joint study model. Bull Leg Med. 2025; 30: 38–44.

8. Toygar M, Şenol E, Can İÖ, Karahatay S, Durmaz A, Tuğcu H, et al. Evaluation of nasal fractures in the aspect of forensic medicine. Turkiye Klinikleri J Foren Med. 2007; 4: 17-22. Available from: https://www.turkiyeklinikleri.com/journal/journal-of-forensic-medicine-and-forensic-sciences/15/issue/2007/4/1-0/en-index.html.

9. Çelik C, Ata U. About medicolegal evaluation of the effects of bone fracture/dislocation on life functions. Bull Leg Med. 2022; 27: 93–101.

10. Balcı Y, Çolak B, Gürpınar K, Anolay NN. Türk Ceza Kanunu'nda tanımlanan yaralama suçlarının adli tıp açısından değerlendirilmesi rehberi. İstanbul: Adli Tıp Uzmanları Derneği; Adli Tıp Kurumu Başkanlığı; Adli Tıp Derneği; 2019. Available from: https://www.atk.gov.tr/tckyaralama24-06-19.pdf

11. Jin KS, Lee H, Sohn JB, Han YS, Jung DU, Sim HY, et al. Fracture patterns and causes in the craniofacial region: an 8-year review of 2076 patients. Maxillofac Plast Reconstr Surg. 2018; 40: 29.

12. Canverenler S, Ünüvar Göçeoğlu Ü, Balcı Y. Evaluation of bone fractures in patients admitted to the forensic medicine outpatient clinic: descriptive research. Turkiye Klinikleri J Foren Sci Leg Med. 2022; 19: 20–9.

13. El Shehaby DM, Ragaey MA, Omeran GA. Medico-legal aspects of otorhinolaryngeal, face and neck injuries in Upper Egypt: a prospective analysis and retrospective evaluation of claimed disabilities. Egypt J Forensic Sci Appl Toxicol. 2019 Sep 1; 19: 103-20. Available from: https://doi.org/10.21608/ejfsat.2019.14358.1082.

14. Sayın İ, Ekizoğlu O, Erdim İ, Kayhan FT. Evaluation of nasal fractures and forensic medicine approach. Bull Leg Med. 2010; 15: 99-103.

15. Hosukler E, Erkol Z, Er G. Forensic medical evaluation of nasal trauma cases. Ann Med Res. 2022; 29: 639–43.

16. Kafadar H, Kafadar S. Investigation of nasale bone fractures in the framework of the Turkish penal code. Bull Leg Med. 2013; 18: 20–4.

17. Kowalczewska J, Rzepczyk S, Okła M, Nijakowski K, Słowik Ł, Makuch A, et al. Characteristics of e-scooter-related maxillofacial injuries over 2019-2022-retrospective study from Poznan, Poland. J Clin Med. 2023; 12: 3690.

18. Karbeyaz K, Düzer S, Düzer S, Balcı Y. The Evaluation of judicial report process of 1306 patients with nasal fracture. Bull Leg Med. 2015; 20: 99–103.

19. Bütün C, Altuntaş E, Beyaztaş F, Özen B, Durmuş K. Analysis of forensic reports prepared by the collaboration of forensic medicine and ear nose and throat departments. Cumhuriyet Med. J. 2011; 33: 189-94. Available from: https://dergipark.org.tr/tr/download/article-file/47797

20. Sener MT, Kok AN, Kara C, Anci Y, Sahingoz S, Emet M. Diagnosing isolated nasal fractures in the emergency department: are they missed or overdiagnosed? Ten years experience of 535 forensic cases. Eur J Trauma Emerg Surg. 2014; 40: 715–9.

21. El Shehaby DM, Farahat AMA, Shahine MS, Mohammed HM. Medico-legal evaluation and trend of the different patterns of maxillofacial fractures concomitant with closed head injury in Upper Egypt: retrospective study. Egypt J Forensic Sci. 2020; 10: 11.

22. Gupta A, Mahajan V, Jamwal PS. A clinical study of nasal bone fractures: a retrospective study. Int J Sci Study. 2019; 7: 122–5.

23. Basheeth N, Donnelly M, David S, Munish S. Acute nasal fracture management: A prospective study and literature review. Laryngoscope. 2015; 125: 2677–84.

Gazi Med J 2026;37(1):23-30

Bulutluöz and Kaya. The Forensic Medical Significance of Nasal Bone Fractures

24. Li L, Zang H, Han D, Yang B, Desai SC, London NR. Nasal Bone Fractures: Analysis of 1193 cases with an emphasis on coincident adjacent fractures. Facial Plast Surg Aesthet Med. 2020; 22: 249–54.

25. Koposov R, Isaksson J, Vermeiren R, Schwab-Stone M, Stickley A, Ruchkin V. Community violence exposure and school functioning in youth: cross-country and gender perspectives. Front Public Health. 2021; 9: 692402.

26. Giuvara CR, Costan VV, Boisteanu O, Armencia A, Ciofu M, Cernei ER, Balcos C, Iliescu B, Calin G, Hurjui LL. An Observational study on the management of medico-legal maxillofacial trauma cases by general practitioners. Healthcare (Basel). 2024; 12: 1803.

27. Ersoy S, Tursem Tokmak T, Dadalı Y, Çalışkan HM, Avcu M. Use of bedside ultrasonography for diagnosis of nasal fractures in emergency service. Eurasian J. Emerg. Med. 2021; 20: 236–40.

28. Karakuş MF, Yaşar Teke H. Analysis of forensic medicine consultations evaluated by the tertiary otorhinolaryngology Clinic. J Ear Nose Throat Head Neck Surg. 2024; 32: 111–7.

29. Yadav SK, Mandal BK, Karn A, Sah AK. Maxillofacial trauma with head injuries at a tertiary care hospital in Chitwan, Nepal: clinical, medico-legal, and critical care concerns. Turk J Med Sci. 2012; 52: 1505–12.

30. Park WY, Kim YH. A clinical study of the nasal bone fracture according to stranc classification. J. Korean Soc. Plast. Reconstr. Surg. 2008; 35: 289–94.

31. Pandher M, Mukherjee TJ, Halsey JN, Luthringer MM, Povolotskiy R, Hoppe IC, et al. A single center review of pediatric nasal bone fractures - an analysis of concomitant injuries, management, and outcomes. Eplasty. 2021; 21: e4.

32. Kitaya S, Ohta N, Saito Y, Tateda Y, Noguchi N, Yamazaki M, et al. Clinical analysis of nasal bone fracture. Nippon J. Ear Nose Throat Soc. 2020;123(11):1283-9. Available from: https://doi.org/10.3950/jibiinkoka.123.1283.

33. Kim KS, Lee HG, Shin JH, Hwang JH, Lee SY. Trend analysis of nasal bone fracture. Arch Craniofac Surg. 2018; 19: 270–4.

Interactive Pharmacokinetics: A Software for Discovery, Analysis, and Simulation

İnteraktif Farmakokinetik: Keşif, Analiz ve Simülasyon Yazılımı

Ⓞ Muhammed Cihan Güvel, Ⓞ Canan Uluoğlu

Department of Medical Pharmacology, Gazi University Faculty of Medicine, Ankara, Türkiye

ABSTRACT

Objective: We aimed to develop "interactive pharmacokinetics (PK)", an open-source, Python-based software package with a user-friendly graphical user interface. Our main goal was to overcome the cost and complexity barriers to industry-standard PK modeling tools and to facilitate the practical application of theoretical PK principles for students and researchers.

Methods: The software employs one, two, and three-compartment models, solving systems of differential equations to simulate drug concentration-time profiles. Parameter estimation is performed using non-linear optimization algorithms to minimize the sum of squared logarithmic errors. The platform is developed in Python, using NumPy and SciPy for core computations and the multiprocessing library for parallel processing of population data.

Results: A fully integrated, functional software application with a user-friendly graphical user interface was created. The platform enables users to run simulations and visualize results, including key parameters such as C_{max} and T_{max}. It performs *de novo* parameter estimation from patient data for one-compartment models and generates novel two- and three-compartment models using a priori data.

Conclusion: The software provides an accessible, no-cost tool for fundamental PK simulation and modeling. It serves as both a valuable pedagogical instrument for pharmacology education and a capable platform for preliminary research, particularly in resource-limited environments. Future work should focus on comprehensive validation against established software.

Keywords: Pharmacokinetic modelling, scientific software, drug development, clinical research

ÖZ

Amaç: Kullanıcı dostu bir grafiksel kullanıcı arayüzüne sahip, açık kaynak kodlu ve Python tabanlı bir yazılım paketi olan "interaktif farmakokinetiki (FK)" geliştirmeyi amaçladık. Temel hedefimiz, endüstri standardı FK modelleme araçlarına erişimdeki maliyet ve karmaşıklık engellerini aşmak; öğrenciler ve araştırmacılar için teorik FK prensiplerinin pratik uygulamasını kolaylaştırmaktır.

Yöntemler: Yazılım, ilaç konsantrasyon-zaman profillerini simüle etmek için diferansiyel denklem sistemlerini çözerek bir, iki ve üç kompartmanlı modelleri kullanmaktadır. Parametre tahmini, logaritmik hata kareleri toplamını en aza indirmek için doğrusal olmayan optimizasyon algoritmaları kullanılarak gerçekleştirilir. Platform; temel hesaplamalar için NumPy ve SciPy kütüphanelerini, popülasyon verilerinin paralel işlenmesi için ise multiprocessing kütüphanesini kullanarak Python dilinde geliştirilmiştir.

Bulgular: Kullanıcı dostu bir grafik kullanıcı arayüzüne sahip, tam entegre ve işlevsel bir yazılım uygulaması oluşturuldu. Platform, kullanıcıların simülasyonlar yürütmesine ve C_{max} ile T_{max} gibi temel parametreler dahil olmak üzere sonuçları görselleştirmesine olanak tanımaktadır. Yazılım, tek kompartmanlı modeller için hasta verilerinden sıfırdan parametre tahmini gerçekleştirebilmekte ve önceden sağlanan verileri kullanarak yeni iki ve üç kompartmanlı modelleri oluşturabilmektedir.

Sonuç: Bu yazılım, temel FK simülasyonu ve modellemesi için erişilebilir ve ücretsiz bir araç sunmaktadır. Araç, özellikle kaynakların kısıtlı olduğu ortamlarda, hem farmakoloji eğitimi için değerli bir pedagojik enstrüman hem de ön araştırmalar için yetenekli bir platform görevi görmektedir. Gelecekteki çalışmalar, kabul görmüş yazılımlara karşı kapsamlı bir validasyon gerçekleştirilmesine odaklanmalıdır.

Anahtar Sözcükler: Farmakokinetik modelleme, bilimsel yazılım, ilaç geliştirme, klinik araştırma

Address for Correspondence/Yazışma Adresi: Muhammed Cihan Güvel, Department of Medical Pharmacology, Gazi University Faculty of Medicine, Ankara, Türkiye

E-mail / E-posta: guvelmd@gmail.com
ORCID ID: orcid.org/0000-0002-8097-0853

INTRODUCTION

Pharmacokinetics (PK) is a fundamental discipline of pharmacology that studies the disposition of a drug in the body, encompassing the processes of absorption, distribution, metabolism, and excretion (ADME). PK modeling, in turn, utilizes a mathematical framework to define and predict these ADME processes. These models provide key information on a drug's efficacy and safety by predicting its time-concentration profile within the body *in silico* and are used to optimize therapeutic outcomes preclinically (1).

The model-based drug development (MBDD) approach, conducted through PK modeling, aims to reduce the high failure rates in clinical trials by providing better predictions about drug exposure-response relationships. Another important aspect of this approach is its acceptance not only by scientists but also by regulatory bodies. Leading regulatory agencies like the US Food and Drug Administration and the European Medicines Agency actively encourage the use of MBDD and view it as a critical component of marketing authorization applications (2).

The growing importance of PK modeling has led to the development of various specialized software platforms designed to perform these analyses. This ecosystem consists of both commercial and open-source tools, each specializing in specific types of analysis and is adapted to different user profiles.

Non-linear mixed-effects modeling (NONMEM) is a software package that has long been considered the gold standard for population PK/pharmacodynamic analyses. Its primary function is to analyze typically sparse data from patient populations to investigate the sources of variability in drug response (3).

Physiologically based PK (PBPK) modeling is an approach that mechanistically predicts ADME properties based on fundamental physiological and biochemical principles. The Simcyp simulator stands out as the most prominent platform in this field. It is known for its comprehensive libraries of diverse virtual populations and its ability to predict complex scenarios, such as drug-drug interactions (4).

Even though the current landscape of PK modeling software rests on a strong foundation, certain challenges and limitations present significant opportunities for developing new tools. These challenges include a lack of usability, accessibility, and integration with modern scientific computing platforms. All of these are directly linked to a broader issue encountered in pharmacology education. Students and young researchers find it difficult to translate theoretical principles into practical applications, a process known as "contextual learning transfer" (5). Software with complex interfaces deepens this educational gap and makes it difficult for the next generation of scientists to adopt these critical methods (6).

All the dominant platforms that are considered industry standards are commercial products. This restricts access for academic institutions, small biotechnology companies, and, in particular, researchers in low- and middle-income countries.

In this study, we developed an open-source, Python-based software package named "interactive PKs" for PK modeling and simulation to address these challenges. Our goal is to provide a powerful experimental tool open to further development by experienced pharmacologists and an intuitive learning platform for students and researchers new to the field.

MATERIALS AND METHODS

The software developed in this study was designed as an integrated platform that combines two fundamental components of PK analysis—simulation and parameter optimization—on a modern computational infrastructure.

Libraries Used

The software is based on Python 3.13, chosen for its rich ecosystem of scientific libraries. Tkinter, Python's standard interface library, was used to provide a desktop user experience and to make the software easily accessible to a wide audience. Two critical functions at the core of the software—solving differential equations and non-linear optimization—are handled by the NumPy and SciPy libraries. The industry-standard Matplotlib library was used to generate simulation results and graphics.

The multiprocessing library was employed to accelerate computationally intensive tasks, such as parameter estimation from population data, via processor-level parallelism.

Simulation

The software used a compartmental modeling approach to simulate the drug concentration-time profiles in the body. One-, two, and three-compartment models were represented as systems of differential equations describing the movement of the drug within the body. The equations used were based on differential pharmacological equations and on compartment-based PK models presented in Chapter 3 of Oğuz Kayaalp's Medical Pharmacology, 14th edition (7).

$$C(t) = \frac{fD}{v_d}\left(\frac{k_a}{k_a - k_e}\right)\left(e^{-k_e t} - e^{-k_a t}\right)$$

Equation 1. Basic concentration-time equation

The concentration equation for the central compartment was linked to those of the peripheral compartments through the intercompartmental transfer constants k_{12}, k_{21}, k_{13}, and k_{31}. Parameters for the percentages of free and bound drug were determined for each compartment.

The compartmental relationships described by differential equations were simplified by reducing the number of compartments. A three-compartment model was created first, followed by two-compartment and single-compartment models.

The fundamental operating mechanism of the software is based on object-based and event-based programming, combined with solving differential equations. The software uses a numerical solver (solve_ivp from SciPy) to simulate the process over small time intervals.

The solver works by following these steps:

1. Starts at time 0: It knows the initial drug concentrations in each compartment.

2. Rate calculation: It uses differential equations to compute the instantaneous rate of change.

3. Steps forward: It takes a small "time step" (e.g., 1 minute) and determines the updated amount of drug in each compartment based on the calculated rates.

4. Repeats: Steps 2 and 3 are repeated until the end of the simulation period.

This process creates the concentration-time curve point by point. At the end of the process, an interactive concentration-time curve is displayed.

Parameter Estimation

In addition to simulations, the software includes parameter-estimation functions that predict key PK parameters [k_a, k_e, volume of distribution (V_d), etc.] from patient concentration-time data. This process is treated as a non-linear optimization problem.

The objective of the optimization algorithms is to minimize the difference between model-predicted concentrations (C_{pred}) and observed concentrations (C_{obs}). To achieve this, our software uses the sum of squared logarithmic errors as its primary function. This function is expressed mathematically in equation 2.

$$Error = \sum \left(\log(C_{obs}) - \log(C_{pred}) \right)^2$$

Equation 2. Sum of squared logarithmic errors

The aim of the optimization process is to find the model parameters that make the predicted curve match the actual patient data as closely as possible.

1. Initial Estimate: The process begins with an estimate of the parameters.

2. Simulation: Using these estimated parameters, a simulation is run to generate a predicted concentration curve.

3. Error Calculation (Loss Function): The predicted curve is compared with the actual patient data points to compute a single error (loss) value.

4. Adjust and Repeat: An optimization function (scipy.optimize. minimize) adjusts the parameter estimates to reduce the error. The gradient-based trust-constr and L–BFGS-B optimization algorithms are used to optimize this function. This "simulate-compare-adjust" loop is repeated until the error can no longer be reduced. The final parameters are those that produce the best-fitting curve.

When working with population data, calculating the error function for each individual can significantly slow processing. To overcome this computational bottleneck, our software leverages the multiprocessing library. This method allows for parallel computations on multiple processor cores. The goal of this approach is to make the analysis of large datasets more practical by significantly accelerating the optimization process compared with single-core processing.

Using a parameter-estimation approach, four functions were integrated into the software.

1. Creation of single-compartment parameters from real patient data: users can input patient concentration-time data to determine parameters for a one-compartment analysis.

2. Assessment of the fit of existing patient data to pre-existing two- or three-compartment model data: after entering patient concentration-time data, the system evaluates how well the data fit an a priori reference model.

3. New models are developed from existing patient concentration-time data using a pre-existing two- or three-compartment model: users enter the concentration-time data, and a new model is created by optimization against an a priori reference model.

4. Generation of two-compartment model parameters from a single-compartment model: unlike the first three methods, this function uses both optimization and a heuristic approach to generate those parameters.

Attempt to Estimate Two-Compartment Model Data from One-Compartment Model Data

Attempting to generate parameters of a two-compartment model from one-compartment data represents the most experimental aspect of our software. For this purpose, a heuristic equation was developed.

$$k_{12} = \left(\frac{k_{e1comp}}{R^2} \right) * \left(\left(\frac{V_c}{V_{p)}} \right) * K_p \right) * (e^{(R-1)*2.5})$$

Equation 3. Heuristic equation for estimating two-compartment parameters from single-compartment parameters. (*Equation Parameters:* K_{e1comp}: Elimination constant from the one-compartment model; V_c: Tissue compartment volume; V_p: Plasma compartment volume; V_d: Virtual distribution volume; K_p: Ratio of free drug ratio in plasma to free drug ratio in tissue; R: Ratio of V_d to (V_c+V_p); e: Euler's number).

This equation generates a two-compartment model from single-compartment data, using a formula derived from several assumptions. The known variables in this equation are manually entered values for V_d and ke1comp the free drug fraction in plasma, and the calculated values for V_c and V_p based on body weight. The goal is to obtain an approximate value of k_{12} using these values.

We can explain this equation step-by-step as follows:

1. The calculation of $[(V_c/V_p)*K_p]$ in the middle of the equation involves dividing the amounts of free drug in the two compartments. The purpose of this calculation is to determine approximately whether the drug is more likely to move from plasma to tissue or from tissue to plasma. At steady state, we obtain the ratio of the total drug amount in the tissue compartment to that in the central compartment. This combined ratio is used to establish a balance between k_{12} (the rate of transfer from plasma to tissue) and k_{21} (the rate of return from tissue to plasma). The K_p value, which is calculated based on the drug-binding rate in tissue, is derived from the equation $V_d = V_p + [V_c * $ (plasma free drug fraction/tissue free drug fraction)]. This formula is based on the assumption that "as the free drug fraction in plasma increases and the free fraction in tissue decreases, the drug is expected to bind more extensively in tissue, thereby increasing the V_d.

2. The value of R is calculated by dividing the virtual V_d, already known from the single-compartment model, by the total physiological volume (V_p + V_c), which is calculated from body weight. This ratio serves as an approximate measure of how much of a drug is retained in the tissues. For example, if the ratio is 5, it means the drug behaves as if it's distributed in a volume five times the physical volume. Therefore, the calculation $e^{(R-1)*2.5}$ suggests that, as R exceeds 1, the accumulation rate in the tissue will increase and k_{12} will increase proportionally as well.

3. However, based on the k_{e1comp}/R^2 calculation in the equation, the drug's elimination must decrease in proportion to R^2. The drug's tendency to remain in the plasma decreases as R increases. Making k_{12} proportional to k_{e1comp} in this equation ensures the consistency of the two-compartment model. Assuming that a rapidly eliminated drug also distributes rapidly and that a slowly eliminated drug

distributes slowly, a more balanced model can be created. If there were no such relationship between k_{12} and k_{e1komp}, it would be possible to produce strange and illogical models in which a drug is eliminated very quickly but enters tissues extremely slowly.

This equation is merely a heuristic estimate and cannot directly simulate real-life situations. We observed that attempts to use this approach were unsuccessful. Two-compartment model predictions generated by this equation were unsuccessful.

Subsequently, the curve estimated by this equation was considered a hypothetical model. The single-compartment and the hypothetical two-compartment model curves were optimized relative to one another. When an optimization approach was applied to the two curves, substantially more successful estimation curves were obtained. The partial success achieved at this stage was retained in the software as a basis for further experimentation and development. This is currently at an experimental stage and requires further mathematical development and testing in a real-world environment.

Finally, all the simulation and parameter estimation functions within the software have been integrated and presented to the user through a user-friendly interface.

This research focuses on the design and implementation of an open-source computational tool for PK modeling. The study methodology relies entirely on mathematical algorithms and theoretical data processing. As no human subjects, animal models, or biological samples were utilized or collected during the development and testing of this software, no ethical approval was sought or required for this work.

RESULTS

Based on the approaches applied, an integrated environment with a user-friendly interface was created. When the program is launched, the screen shown in Figure 1 appears.

The first feature on the interface is a control for selecting the number of compartments. Users can choose among one-, two-, and three-compartment models (Figure 1a). This is followed by the section for entering model parameters (Figure 1b). For the single-compartment model, the required parameters are the virtual V_d, plasma protein binding rate, simulation duration, simulation time step (calculation frequency), and steady-state concentration tolerance, which determines the precision of the steady-state concentration. The model-parameter screen shows minor differences between the two- and three-compartment models. For instance, in the two-compartment model, the user must determine the transfer coefficients from plasma to tissue (k_{12}) and from tissue to plasma (k_{21}), and the percentage of protein binding in the tissue (Figure 2).

Next, the user is prompted to select the route of administration, with options for oral, IV bolus, and IV infusion. Here, the user also determines whether elimination will follow first-order or zero-order kinetics (Figure 1c).

In the block below, the elimination parameters are entered according to the chosen elimination type. If first-order kinetics is selected, the elimination constant (K_e) is required; if zero-order kinetics is selected, the user must provide the V_{max} and K_m values (Figure 1d).

The next block, which is optional, is for a loading dose. If this option is selected, the user is prompted to provide the loading dose (Figure 1e).

Finally, the user is prompted to specify the dose, number of doses, dosing interval, absorption rate, intestinal bioavailability, and hepatic bioavailability (Figure 1f).

After the "start simulation" button is clicked, a concentration-time graph will be generated (Figure 3). Additionally, the estimated half-life, T_{max}, C_{max}, clearance, steady-state concentration, and time to reach the steady-state concentration will be calculated (Figure 1g).

Additionally, the software's capabilities extend beyond mere visualization of differential equations.

De Novo Estimation Function from Patient Data

The software can create population data and estimate K_a and K_e using only patient blood concentration-time data and the provided volume of distribution and plasma protein-binding rates. Furthermore, it can generate concentration-time population curves based on these parameter estimates.

To use this function, the user inputs the patient number, dose, blood sampling time, and concentration values into the interface (Figure 4). The system then iteratively applies optimization algorithms. This process can take a relatively long time (30 minutes to 1 hour), depending on how close the initial estimates are to the correct values. Following this process, goodness-of-fit graphs can be generated at the user's request. The operation concludes with the estimation of model parameters and the visualization of the predicted concentration–time profile based on these parameters (Figure 5).

Estimation from Patient Data: Two- and Three-Compartment Models

Because of the large number of unknown variables in the two- and three-compartment models, new values could only be obtained through optimization based on a previously prepared model. Therefore, an a priori model must first be entered into the system. The system then attempts to determine new parameter estimates for these patients using the patient concentration-time data provided to the software (Figure 6).

This method not only builds a new model from an a priori model but also evaluates how well the entered data fit the pre-existing predictive model.

Estimation from Single-Compartment Model Data to Two-Compartment Model Parameters

When the estimated curve resulting from the heuristic equation was treated as a hypothetical model, the single-compartment and hypothetical two-compartment model curves were optimized relative to each other. It was observed that optimizing the fit between the two curves produced substantially more accurate prediction curves than the initial attempt (Figure 7). Here, the criterion for success was the similarity between the curve of the single-compartment model and the newly created optimization curve; no mathematical similarity analysis was conducted. This point is still in the experimental stage and needs to be further developed mathematically and tested in a real-world environment.
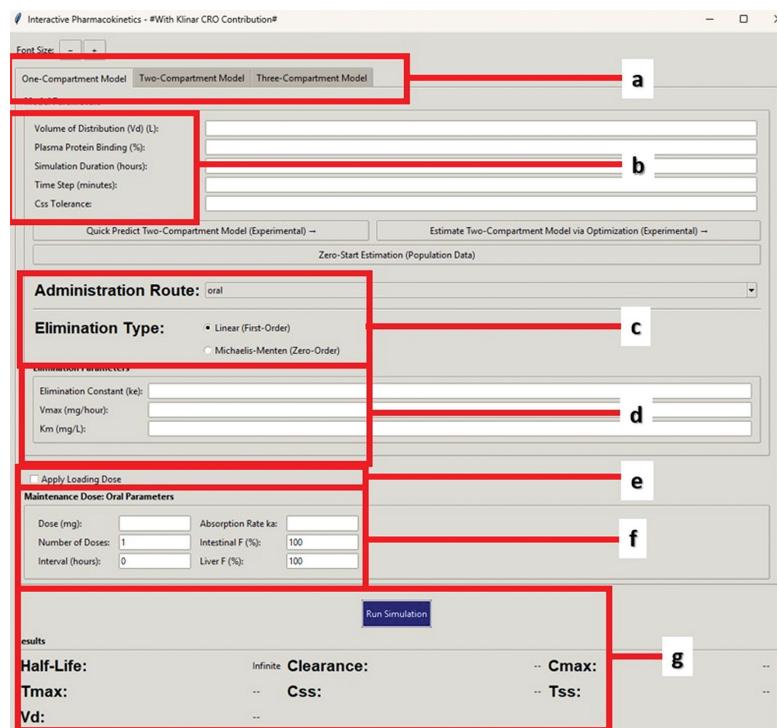
Figure 1. Main User Interface. (a) Selection of the number of compartments. (b) Model parameters. (c) Selection of the drug administration route and elimination type. (d) Determination of elimination parameters. (e) Selection of a loading dose. (f) Dose parameters, absorption rate, and bioavailability. (g) Calculated parameters.
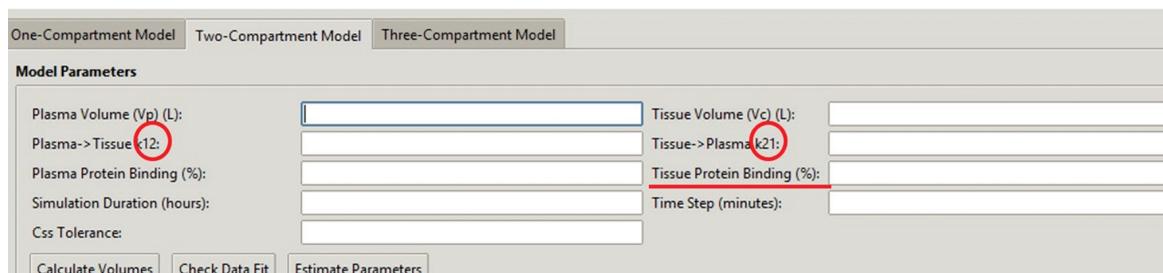
Figure 2. View in a two-compartment model.
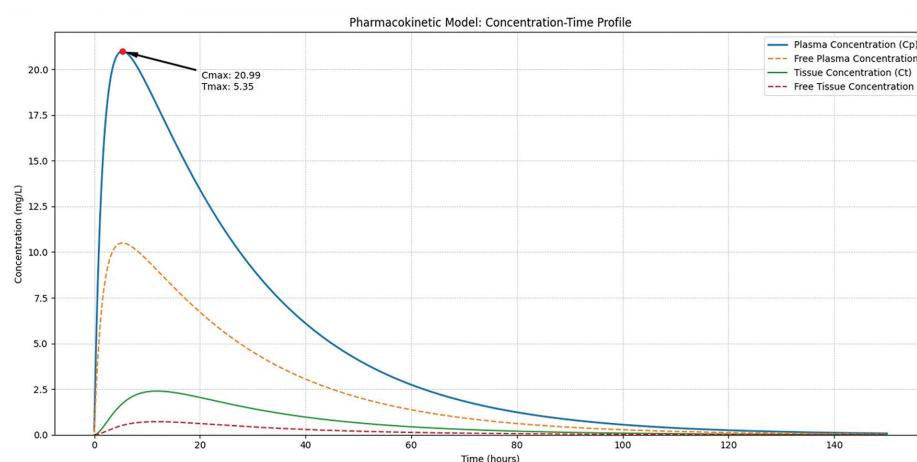
Figure 3. Concentration-time graph resulting from a two-compartment model calculation (the dark blue line: total plasma concentration. The light blue line: Free plasma concentration. The dark green line: total tissue concentration. The light green line: free tissue concentration).
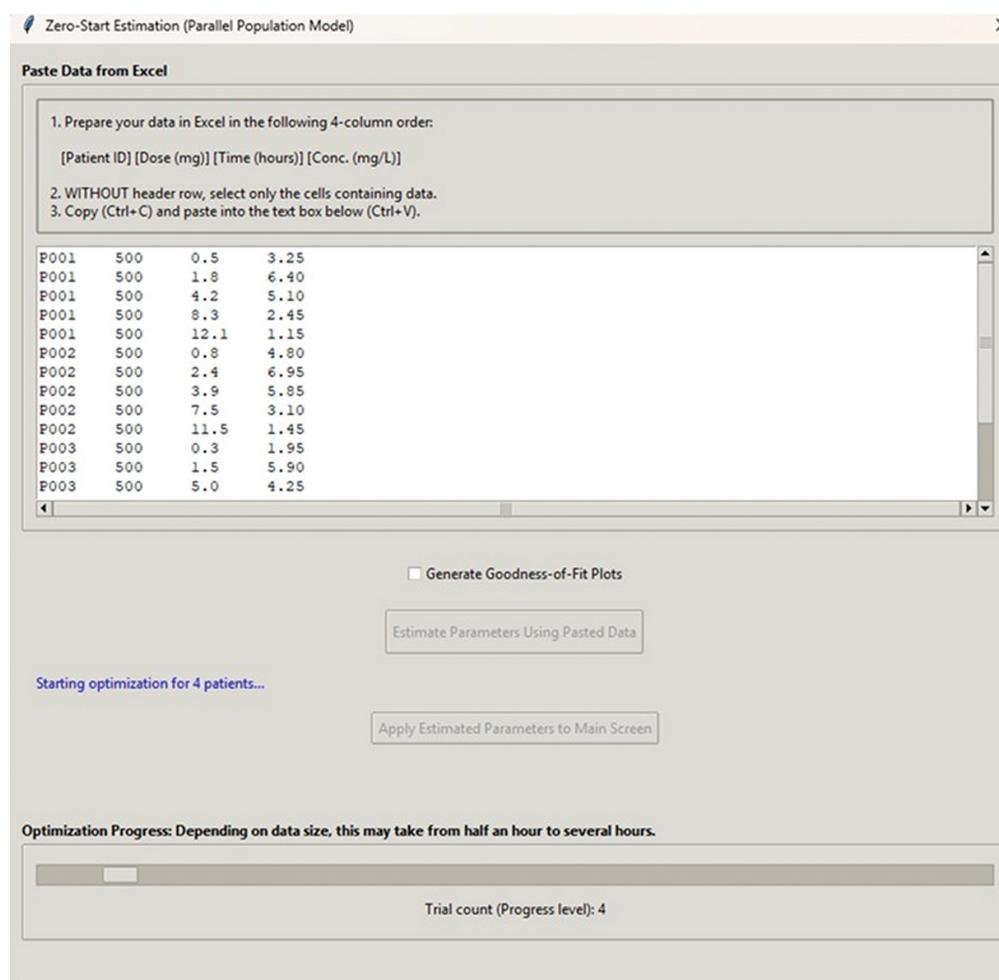
Figure 4. *De novo* estimation function from patient data.
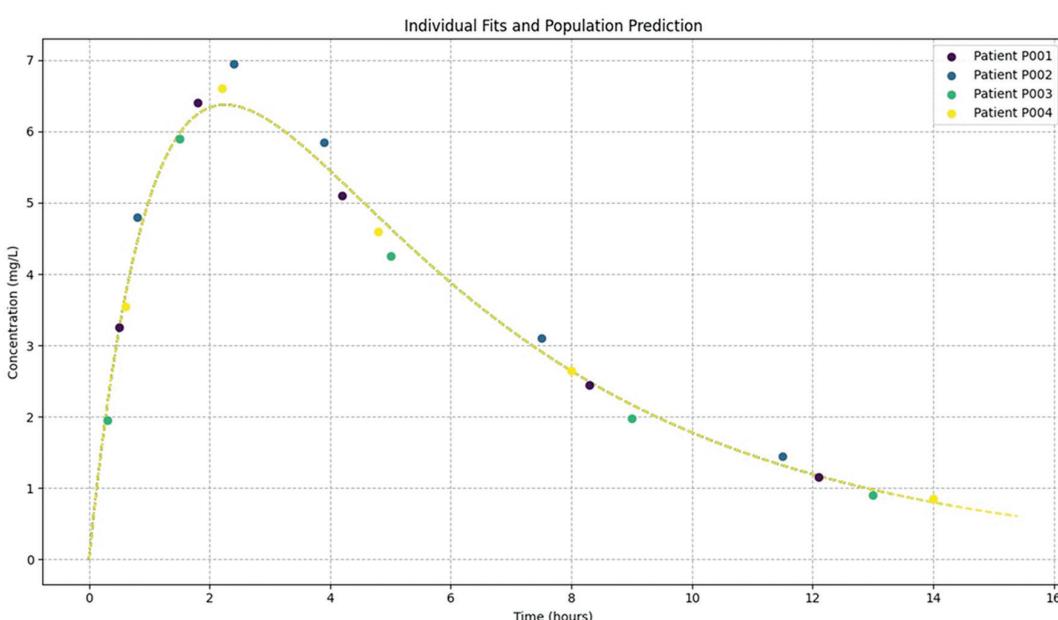
Figure 5. Visualization of the results from the *de novo* estimation function using patient data.
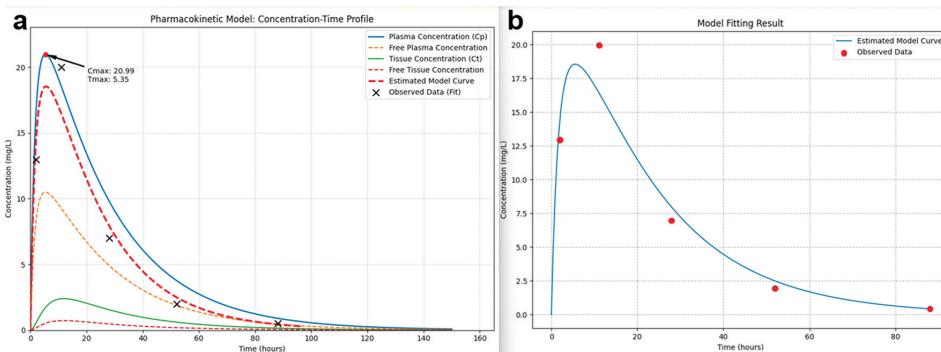
Figure 6. Visualization of the new concentration-time model estimated from patient data in a two-compartment modelç (a: the "x" marks show the patient data, while the dashed red line represents the new model curve created through optimization; b: the red dots indicate the new patient data entered, and the blue line shows the estimated model curve).
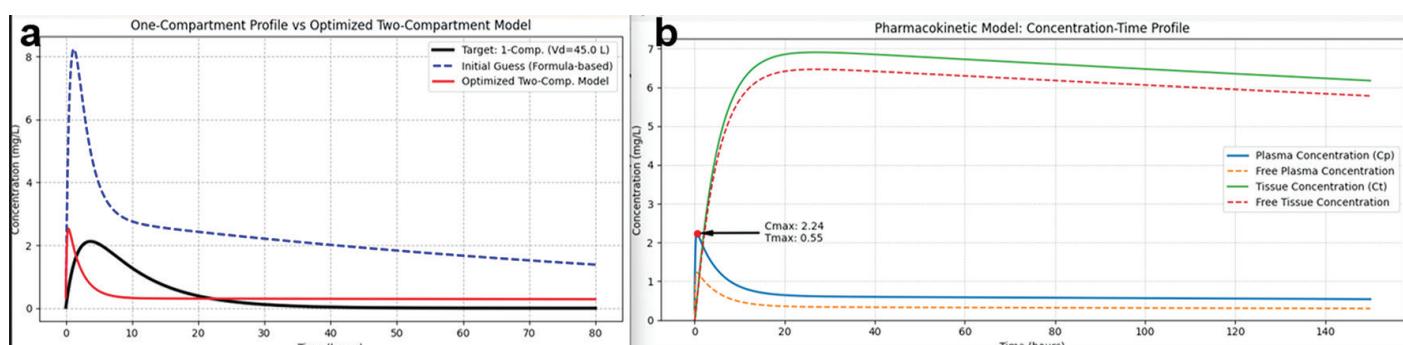
Figure 7. Estimation of two-compartment model parameters from single-compartment model data. (a) The dashed blue line represents the model resulting from the heuristic formula, the black line shows the single-compartment model, and the red line is the curve of the common model that emerged from optimization. (b) Panel b shows the new parameters created through optimization being tested in a two-compartment model simulation.

DISCUSSION

In this study, a software tool was developed to simulate and predict fundamental PK analyses. This software platform was designed to meet the needs of both educational and research fields.

The software interface is the most crucial element for ensuring accessibility and ease of use, which is our claim. In this context, the software's features should be regarded as a curated set of the most fundamental and frequently used tools in PKs. This highlights our strategic approach during the design phase. Rather than competing with the highly specializedand comprehensive features of commercial giants, our study focused on addressing the core curriculum of PK education and the fundamental needs of exploratory research. Therefore, the success of this work should be evaluated not by "what it can do", but by "whom it empowers".

Historically, the field of pharmacometric modeling has been dominated by powerful yet costly commercial software such as NONMEM and Simcyp. While these tools are considered industry standards, they create significant financial barriers. This makes them largely inaccessible to academic institutions, researchers in low-income countries, and small-scale companies. The open-source, free nature of the developed software is intended to completely eliminate this financial obstacle.

A second obstacle is the complexity and steep learning curve. Tools such as NONMEM are command-line-based and require in-depth knowledge of specialized programming languages or complex control files for effective use (8). In contrast, our software's user-friendly graphical interface removes this barrier, allowing users to focus on PK principles without struggling with the software.

However, strong alternatives exist within the open-source domain. The most prominent of these is the nlmixr2 package, which is based on the R programming language. nlmixr2 is a code-based solution that requires programming proficiency (9). Additionally, user-interface add-ons like shinyMixR, which have been developed for this package, indicate a need for user-friendly platforms within this ecosystem (10).

Basing this software on Python places it in a unique position regarding its linguistic foundation. While R has deep roots in statistics and bioinformatics, Python is increasingly the dominant language for scientific computing, data science, and machine learning. Its larger talent pool and ability to integrate more smoothly into large-scale corporate or web-based workflows make Python an attractive choice for modern scientific software development (11). Consequently, this software is positioned not only as a PK tool but also as a potential component of a broader Python-based scientific workflow.

The software's value should also be assessed by its potential to transform how PKs is taught and applied. Its accessibility and ease of use have the potential to foster pedagogical innovation in education and to provide equal opportunities for researchers. The software transforms abstract equations into an interactive visual experience. It allows learners to change parameters such as dose,

clearance, and volume of distribution and instantly see the results on the concentration-time curve, providing a dynamic, intuitive way to learn how these concepts are interrelated. This type of hands-on, simulation-based learning is a powerful active learning strategy that can increase understanding and retention more effectively than static textbook examples. Therefore, it can be confidently stated that this tool can make the learning process more engaging and effective by allowing students to explore theory in a gamified manner and to observe the results immediately.

Study Limitations

The software is more than a simulator; it is also a predictive tool that incorporates several optimization functions, some of which are more effective, while others remain experimental. At this point, it is important to highlight the effort required to calculate the transition from a single-compartment model to a two-compartment model. Initially, a heuristic equation-based approach was attempted but proved unsuccessful. This failure is, in itself, a significant finding because it provides evidence of the non-linear nature of the relationship between single-compartment and two-compartment model parameters. While the second approach, based on optimization between two curves, was more successful, this feature is not yet mature.

On the other hand, the software's current capabilities must be evaluated within certain limitations. One of the most significant limitations is its focus on standard compartmental models in its current form. This excludes more complex and mechanistic modeling paradigms, such as PBPKs, which play a central role in modern drug development. This situation defines the boundaries of the software's current applicability.

Another critical limitation is the lack of a comprehensive official validation study. While the software is functional, its outputs have not yet been compared with those of established software or with standard reference datasets accepted by regulatory agencies. This step is indispensable for the software to be accepted as a reliable research tool. This validation is essential for adoption of the software by the scientific community and should be the top development priority for future work.

CONCLUSION

In this study, new open-source PK-modeling software built within the Python ecosystem was developed. The platform offers a package of fundamental simulation and parameter estimation tools within an accessible graphical user interface.

The primary and most novel contribution of this work is not the invention of new modeling algorithms. Instead, existing numerical methods have been holistically integrated into a platform that aims to overcome critical barriers—such as cost, complexity, and usability—that limit access to industry-standard tools. This approach is intended to make PK modeling capabilities accessible to a wider audience.

In doing so, the study makes a dual contribution to the field: on the one hand, it provides a powerful pedagogical tool to bridge the gap between theory and practice in pharmacology education, and on the other hand, it empowers researchers in resource-limited environments with a capable platform for preliminary modeling and hypothesis testing. We also believe that our work will make significant contributions to postgraduate and lifelong learning in pharmacology. These capabilities require further improvement and validation through future development efforts.

Ethics

Ethics Committee Approval: This research focuses on the design and implementation of an open-source computational tool for pharmacokinetic modeling. The study methodology relies entirely on mathematical algorithms and theoretical data processing. As no human subjects, animal models, or biological samples were utilized or collected during the development and testing of this software, no ethical approval was sought or required for this work.

Informed Consent: Not required for this study.

Footnotes

Authorship Contributions

Surgical and Medical Practices: M.C.G., C.U., Concept: M.C.G., C.U., Design: M.C.G., C.U., Data Collection or Processing: M.C.G., C.U., Analysis or Interpretation: M.C.G., C.U., Literature Search: M.C.G., C.U., Writing: M.C.G., C.U.

Conflict of Interest: No conflict of interest was declared by the authors.

Financial Disclosure: The authors declared that this study received no financial support.

REFERENCES

1. Ahmad AM. Recent advances in pharmacokinetic modeling. Biopharm Drug Dispos. 2007; 28: 135–43.

2. Kimko H, Pinheiro J. Model-based clinical drug development in the past, present and future: a commentary. Br J Clin Pharmacol. 2015; 79: 108–16.

3. Park WS. Pharmacometric models simulation using NONMEM, Berkeley Madonna and R. Transl Clin Pharmacol. 2017; 25: 125–33.

4. Jamei M, Marciniak S, Feng K, Barnett A, Tucker G, Rostami-Hodjegan A. The simcyp population-based ADME simulator. Expert Opin Drug Metab Toxicol. 2009; 5: 211–23.

5. Brackett C, Reuning R. Teaching pharmacokinetics using a student-centered, modified mastery-based approach. Am J Pharm Educ. 1999; 63.

6. Fasinu PS, Wilborn TW. Pharmacology education in the medical curriculum: challenges and opportunities for improvement. Pharmacol Res Perspect. 2024; 12: e1178.

7. Onaran O. Temel farmakokinetik kavramlar. In: Kayaalp SO, Gümüşel B, Babaoğlu MÖ, Melli M, editors. Oğuz Kayaalp Tıbbi Farmakoloji. 14th ed. Ankara: Güneş Tıp Kitabevleri; 2024.

8. Bauer RJ, Guzy S, Ng C. A survey of population analysis methods and software for complex pharmacokinetic and pharmacodynamic models with examples. AAPS J. 2007; 9: E60-E83.

9. Fidler M, Wilkins JJ, Hooijmaijers R, Post TM, Schoemaker R, Trame MN, et al. Non-linear mixed-effects model development and simulation using nlmixr and related r open-source packages. CPT Pharmacometrics Syst Pharmacol. 2019; 8: 621–33.

10. Hooijmaijers R. Introduction to the shinyMixR package [Internet]. CRAN; Available from: https://cran.r-project.org/web/packages/shinyMixR/vignettes/getting_started.html Accessed 2025 Oct 11.

11. Pittard WS, Li S. The essential toolbox of data science: Python, R, Git, and Docker. Methods Mol Biol. 2020; 2104: 265–311.

The Impact of Law No. 6331 on Work-Related Incidents in Türkiye (2007–2023): Standardization Analysis of City-Level Data for Compulsory Insured Workers

Türkiye'de 6331 Sayılı Kanun'un İş Sağlığı Olaylarına Etkisi (2007–2023): İl Düzeyinde Zorunlu Sigortalı Çalışan Verilerinin Standardizasyon Analizi

Osman Faruk Bayramlar[1], Halim İşsever[2]

[1]Public Health Specialist, Occupational Physician, Ziraat Bank, Ataşehir, Türkiye
[2]Department of Public Health, İstanbul University-İstanbul Faculty of Medicine, İstanbul, Türkiye

ABSTRACT

Objective: This study examined the effects of the occupational health and safety (OHS) Law No. 6331, enacted in Türkiye in 2013. It analyzed the rates of work-related accidents (WrAs), occupational diseases (ODs), and work-related mortalities (WrMs) among compulsorily insured workers from 2007 to 2023. Additionally, it aimed to reveal the situation prior to the the introduction of compulsory OHS services for public institutions and low-risk workplaces with fewer than 50 workers in 2025. Pre-2025 before became mandatory.

Methods: Using data from Türkiye's social security institution, trends across 81 cities were examined in an epidemiological, observational, descriptive study.The research evaluated trends across 81 provinces usingobtained) withapproach. An indirect standardization technique was applied to adjust for changes in the number of "4-1/a compulsory insured" workers, allowing for comparisons of standardized ($_s$) WrA, $_s$OD, and $_s$WrM ratios between cities.

Results: Between 2007 and 2023, the number of insured workers in Türkiye nearly doubled. Regional disparities became evident, with sWrA ratios higher in western provinces and sWrM ratios elevated in the east. Inequalities $_s$WrAs concentrated, while $_s$WrMs were higher in eastern regions. The cities with the highest ratios of $_s$WrA, $_s$OD, included Zonguldak, Bilecik, Kütahya, Manisa, Bartın, Karabük, and Kocaeli following the after the law's implementation, $_s$WrA rose in the black sea region, while a modest rise in $_s$OD was detected in Marmara. Of Law No. 6331, $_s$WrAs increased significantly, especially. While $_s$ODs remained low nationwide, notable ratio increaserecordedthe region,

ÖZ

Amaç: Bu çalışma, 2013 yılında Türkiye'de yürürlüğe giren iş sağlığı ve güvenliği (İSG) kanunu no. 6331'in etkilerini incelemiştir. Zorunlu sigortalı çalışanlar arasında 2007–2023 yılları arasındaki iş kazası (WrA), meslek hastalığı (OD) ve iş yeri ölüm oranlarını (WrM) analiz etmiştir. Ayrıca, 2025'te kamu kurumları ve 50'den az çalışanı olan düşük riskli iş yerleri için iş sağlığı ve güvenliği hizmetlerinin zorunlu hale gelmesinden önceki durumu ortaya koymayı amaçlamıştır.

Yöntemler: Araştırma, Türkiye Sosyal Güvenlik Kurumu'ndan elde edilen verileri kullanarak 81 ildeki eğilimleri değerlendirmiş, epidemiyolojik, gözlemsel ve tanımlayıcı bir yaklaşım benimsemiştir. "4-1/a zorunlu sigortalı" çalışan sayısındaki değişiklikleri ayarlamak için dolaylı standartizasyon ($_s$) tekniği uygulanmış, böylece iller arasında $_s$WrA, $_s$OD ve $_s$WrM oranlarının karşılaştırılması sağlanmıştır.

Bulgular: 2007–2023 yılları arasında Türkiye'deki sigortalı çalışan sayısı neredeyse iki katına çıkmıştır. Bölgesel eşitsizlikler belirgin hale gelmiş, $_s$WrA oranları batı illerinde yoğunlaşırken, $_s$WrM oranları doğu bölgelerinde daha yüksek olmuştur. $_s$WrA, $_s$OD ve $_s$WrM oranlarının en yüksek olduğu iller arasında Zonguldak, Bilecik, Kütahya, Manisa, Bartın, Karabük ve Kocaeli bulunmaktadır. Kanun no. 6331'n uygulanmasının ardından, özellikle Karadeniz bölgesinde $_s$WrA oranlarında önemli bir artış gözlemlenmiştir. OD oranları ülke genelinde düşük kalırken, Marmara bölgesinde dikkate değer bir artış kaydedilmiş ve Doğu Karadeniz bölgesinde $_s$WrM oranlarında önemli artışlar gözlemlenmiştir.

Address for Correspondence/Yazışma Adresi: Osman Faruk Bayramlar, Public Health Specialist, Occupational Physician, Ziraat Bank, Ataşehir, Türkiye

E-mail / E-posta: obayramlar@gmail.com

ORCID ID: orcid.org/0000-0001-7311-3258

Gazi Med J 2026;37(1):39-48

Bayramlar and İşsever. Impact of Law No. 6331 on Work-Related Incidents

ABSTRACT

and significant increases in ₅WrMs werePeaks in ₅WrM occurred in various cities, with clustering observed in the Eastern Black Sea. region

Conclusion: This study provided critical insights into occupational health indicators in Türkiye, highlighting systemic deficiencies and regional disparities. Significant improvements were expected in these data with the upcoming 2025 expansion of Law No. 6331 provides an opportunity for improvement; however, persistent underreporting, limited diagnostic capacity for ODs, and uneven implementation across regions suggest that significant structural gaps remain.6331 in 2025.

Keywords: Work-related accident, work accident, OD, work-related mortality, occupational health and safety, OHS, Türkiye, city, province, region, standardization, 6331

ÖZ

Sonuç: Bu çalışma, Türkiye'deki iş sağlığı göstergeleri hakkında kritik bilgiler sunmuş, sistemik eksiklikleri ve bölgesel farklılıkları vurgulamıştır. 2025'te kanun no. 6331'in kapsamının genişletilmesiyle birlikte bu verilerde önemli iyileşmeler beklenmektedir.

Anahtar Sözcükler: İşle ilgili kaza, iş kazası, OD, işe bağlı mortalite, iş sağlığı ve güvenliği, İSG, Türkiye, şehir, il, bölge, standardizasyon, 6331

INTRODUCTION

In Türkiye's recent history, significant reforms in occupational health and safety (OHS) have been initiated, beginning with the social security reform of 2006. This reform unified previously separate social security institutions (SSI), including those for self-employed individuals and civil servants, under a single framework. As part of this reform, social security Law No. 5510 was enacted, mandating the reporting of all work-related accidents (WrAs) to the SSI. Since 2007, the ministry of labor and social security has made annual statistical data, compiled in accordance with International Labor Organization (ILO) definitions and European Union (EU) sustainability criteria, publicly accessible (1,2) and shared with relevant stakeholders (2).

Despite these advancements, the ILO reported in 2009 that OHS practices remained inadequate in 33 countries, including Türkiye (3). In response, OHS Law No. 6331 was introduced in 2013 (4), which requires employers to appoint occupational safety experts and workplace physicians, conduct risk assessments, provide OHS training, and designate worker representatives. This law also imposes penalties for non-compliance and mandates the preparation of emergency response plans. Following its implementation, reported WrAs tripled in 2013 (5,6), indicating increased awareness and reporting of workplace incidents. However, despite these improvements, the Ministry recognized the need for further interventions to enhance OHS practices (7). In the National OHS Policy Document-III, In response, OHS Law No. 6331, introduced in 2013 (5), requires employers to appoint occupational safety experts and workplace physicians, conduct risk assessments, provide OHS training, and designate worker representatives. Following its implementation, reported WrAs tripled in 2013 (6,7), indicating increased awareness and reporting of workplace incidents. In the National OHS Policy Document-III (8,9), published immediately after this law, OD set a target to achieve a significant increase in diagnosis rates, published immediately after this law, OD set a target for a significant increase in diagnosis rates.

Since its inception, The law was intended to require OHS services for public institutions and low-risk workplaces with fewer than 50 workers. However, due to infrastructural deficiencies, its implementation was postponed until 2025 (10). Following the publication of the 2023 SSI annual statistical data, a comprehensive dataset covering 17 years (2007–2023) is now available online (2), enabling in-depth analysis of long-term trends in OHS.

The purpose of this study is to evaluate the effects of the OHS Law No. 6331, which entered into force in Türkiye in 2013 by analyzing the standardized ratios (s) of WrAs, occupational diseases (ODs), and work-related mortalities (WrMs). Aimsexamineimpactenacted in 2013) among compulsory insured workers from 2007 to 2023. Additionally, it seeks to elucidate the conditions prior to 2025, when OHS services will become compulsory for public institutions and low-risk workplaces employing fewer than 50 workers, thereby informing potential future interventions by the Ministry of Labor and Social Security.

MATERIALS AND METHODS

Research Method

This study was designed as an epidemiological, observational, and descriptive study. The incidence rates of WrAs, ODs, and WrMs were standardized, and the resulting data were utilized for targeted evaluations.

Inclusion and Exclusion Criteria

The study included workers classified under the "4–1/a insurance" status, which refers to individuals employed under a service contract and whose social security contributions are paid by their employer. This group was selected due to their comprehensive and reliable dataset, as well as their higher risk of WrAs and ODs.

This study included workers classified under the "4–1/a insurance" status, as defined by article 4, paragraph 1(a) of the Law No. 5510 (1,11). This category specifically refers to individuals described as "worked by one or more workers under a service contract", for whom social security contributions are paid by their workers. This group was selected because of its comprehensive, reliable dataset, regular workups, and higher risks of WrAs and ODs (11,12).

• Excluded groups include interns, trainees, apprentices, partially insured workers, voluntary insured workers due to their lower exposure to hazardous tasks, and the groups mentioned below.

• Insured in agricultural sector: High levels of informal employment and seasonal work.

• Collective insured: Data unrelated to workplaces in Türkiye.

Gazi Med J 2026;37(1):39-48

Bayramlar and İşsever. Impact of Law No. 6331 on Work-Related Incidents

Furthermore, ODs diagnosed after insurance coverage began were not reported prior to Law No. 6331. Therefore, those reported after enactment of the law were also excluded to maintain consistency. Moreover, these data lacked city-specific information and were therefore excluded from the standardization analysis to maintain comparability and consistency across results.

Data Sources

Data were obtained from all statistical yearbooks published to date by Türkiye's SSI. The analysis covers a 17-year period (2007–2023) and includes data from 81 cities, allowing detailed examination of trends (2). Since the dataset for 2024 has not yet been published, it could not be included in the analysis.

Statistical Analysis

The indirect standardization technique was chosen because it does not require detailed age-specific rates or information on other confounding factors, making it appropriate for datasets in which such information is unavailable (11-13). This method is particularly advantageous for adjusting for variations in the number of insured workers and for ensuring comparability of incidence rates across cities (14,15). This approach adjusted for city-level differences in the number of insured workers, accounted for regional variations, and enabled more accurate comparisons of WrAs, ODs, and WrM incidence rates.

The analysis used the "standardized ratio formula" to compare observed and expected rates. The following formulas were applied to calculate standardized ratios for WrAs, ODs, and WrMs:

• National WrA or OD or WrM (incidence) Rate (only for WrA x 1,000) = Türkiye's observed WrAs/Türkiye's number of workers x 100,000.

• Expected incident = city's number of workers × national WrA or OD or WrM rate.

• Standardized ($_s$) city's WrA or OD or WrM incidence ($_s$WrA or $_s$OD or $_s$WrM) ratio = (city's observed/expected incident) × 100.

Statistical analyses were performed using SPSS 25 (IBM Corp., Armonk, NY, USA) and visualizations were generated using Excel and Flourish Studio (available at https://flourish.studio).

Interpretation of Standardized Ratios

A normal incidence rate is , for example, as the "WrA rate", while a standardized incidence rate is referred to as the "$_s$WrA ratio" and is typically expressed as a percentage. A "$_s$WrA ratio" of 100% represents the national average. For instance, in 2015, Şırnak's $_s$WrM ratio was 1,080%, representing a 9.8-fold increase relative to the national average. This indicates that while 17 fatalities were observed in Şırnak that year, only 2 expected based on the national WrM rate and the number of insured workers in Şırnak.

In other words, large standardized ratios highlight unexpected developments in specific cities during certain years. Identifying and analyzing these deviations can provide critical insights into their underlying causes and help develop targeted solutions.

Presentation Method - Tables

The results of the standardization analyses for WrAs, ODs, and work-related mortality (WrM) are presented in three supplementary tables (Supplementary Tables 1–4), which provide a comprehensive list of all cities and their respective ratios. The effective date of OHS Law No. 6331 is highlighted. Because these tables are extensive, a summary is provided for clarity and emphasis:

• Cities that ranked in the top six for WrAs in any year during the 17-year period are included in Table 1.

• Cities that ranked in the top three for ODs in any year were included in Table 2.

• Cities that ranked first for WrMs in any year are shown in Table 3.

Table 1. Cities appearing in the top six for standardized work-related accident (swra) ratios in any year from 2007 to 2023.

City (%)*	2007	2008	2009	2010	2011	2012	2013	2014	2015	2016	2017	2018	2019	2020	2021	2022	2023
Zonguldak	565	587	974	970	788	774	340	295	278	252	212	174	221	239	225	211	216
Bilecik	527	416	387	506	514	244	360	350	316	287	293	267	291	283	289	271	258
Karabük	576	614	635	616	607	454	267	252	252	216	198	165	184	183	201	159	149
Manisa	376	532	446	549	501	593	339	312	233	223	208	213	201	196	207	204	205
Karaman	122	94	155	132	153	173	205	217	198	277	354	277	229	243	203	189	146
Kütahya	167	244	288	179	301	262	158	179	155	150	159	156	137	147	148	157	134
Kocaeli	272	145	119	152	207	122	193	202	215	193	185	175	176	183	183	183	178
Eskişehir	201	252	210	270	291	93	203	179	180	172	149	145	145	148	143	140	141
Kayseri	226	243	184	20	227	215	213	204	184	174	165	149	158	171	176	162	159
Bartın	157	146	239	367	362	177	175	145	143	138	125	131	119	126	139	136	133
Denizli	169	216	210	245	248	251	175	161	156	147	136	125	123	125	128	127	115
Bolu	136	121	179	205	194	165	151	149	138	149	135	143	164	176	192	187	173
Yalova	90	106	154	63	97	138	98	114	136	156	164	160	230	253	266	241	251
Bursa	198	197	188	249	162	262	158	154	157	142	125	117	115	112	112	119	118
*Standardized ratio percentage	1st		2nd		3rd		4th		5th		6th			OHS Law No. 6331			

Gazi Med J 2026;37(1):39-48

Bayramlar and İşsever. Impact of Law No. 6331 on Work-Related Incidents

Table 2. Cities appearing in the top three for standardized occupational disease (ₛOD) ratios in any year from 2007 to 2023.

City (%)*	2007	2008	2009	2010	2011	2012	2013	2014	2015	2016	2017	2018	2019	2020	2021	2022	2023
Zonguldak	9900	7615	5316	2201	3158	8279	4921	1246	3737	3355	1269	1883	872	706	458	704	302
Kütahya	26	28	0	0	5788	267	231	381	364	434	1508	1601	1334	340	131	511	147
Bilecik	22	52	0	56	169	77	1347	3764	176	625	612	1138	1798	900	334	728	48
Kocaeli	39	5	207	129	9	83	218	366	447	198	384	339	420	330	657	535	0
Çankırı	146	334	1060	102	0	271	1303	0	146	0	104	144	124	69	152	62	0
Bartın	42	0	0	0	0	494	0	189	519	478	272	762	349	0	50	0	0
Yalova	0	0	0	0	0	0	0	0	71	62	307	410	619	384	486	728	0
İzmir	128	242	110	458	31	80	35	61	52	128	116	55	204	91	86	82	612
Sakarya	35	477	100	0	99	0	0	125	85	91	211	205	264	372	299	197	0
Çorum	0	0	0	0	0	0	0	0	251	913	138	297	0	129	49	235	63
Ankara	17	26	199	414	260	187	53	40	140	81	127	102	76	53	39	38	7
Samsun	0	52	0	17	0	0	0	0	23	20	32	0	0	22	8	19	1016
Artvin	0	0	0	0	0	131	0	0	0	0	0	0	61	410	262	292	30
Erzincan	0	195	559	0	0	0	0	0	0	0	261	0	0	0	0	0	0

*Standardized ratio percentage   1ˢᵗ   2ⁿᵈ   3ʳᵈ   OHS Law No. 6331

Table 3. Cities ranked first for standardized work-related mortality (ₛWrM) ratios in any year from 2007 to 2023.

City (%)*	2007	2008	2009	2010	2011	2012	2013	2014	2015	2016	2017	2018	2019	2020	2021	2022	2023
Şırnak	168	305	93	517	457	124	344	440	1080	331	441	135	201	527	335	403	131
Hakkâri	131	267	255	383	209	444	0	156	153	474	507	347	352	204	0	229	70
Artvin	208	131	86	252	214	348	347	253	134	260	208	257	338	126	422	82	137
Bartın	0	118	211	103	146	196	106	184	116	144	201	168	138	84	147	1622	23
Zonguldak	115	269	122	626	267	278	229	116	211	151	231	147	144	162	192	146	128
Siirt	155	157	220	176	419	344	182	43	190	870	151	28	122	78	35	67	209
Gümüşhane	0	785	277	68	55	240	210	66	223	73	223	122	259	232	149	68	90
Manisa	86	66	80	153	86	107	125	1232	63	105	110	99	68	133	109	122	165
Tunceli	468	0	302	376	110	0	0	138	144	479	111	0	0	132	248	0	365
Karabük	140	131	157	50	128	147	312	202	86	185	138	347	68	67	180	194	113
Batman	36	112	129	185	468	304	139	158	89	101	60	142	179	124	127	118	130
Nevşehir	202	177	90	338	124	47	394	86	55	55	115	161	118	252	73	130	116
Bingöl	110	0	354	99	341	359	95	0	220	130	63	166	239	82	187	0	77
Bayburt	388	0	0	0	125	223	0	0	0	144	98	111	462	0	247	119	113

*Standardized ratio percentage   1ˢᵗ   OHS Law No. 6331

This approach limits each table to 14 cities, ensuring a concise presentation while effectively conveying key patterns and trends in the data.

Presentation Method - Figures

To present the extensive dataset simply and effectively, the results of the standardization analysis were visualized using figures. The visualization process followed a hierarchical approach, starting with national-level analyses and progressively focusing on specific city-level trends. The Figures 1–8 were structured as follows:

Figure 1

This figure illustrates the annual changes in the number of workers, workplaces, WrAs, ODs, and WrMs across Türkiye. It emphasizes trends at the national level and highlights the effective date of OHS Law No. 6331. This figure is particularly significant as it visualizes the five key work-related risk parameters in a single graph. To achieve this, two Y-axes were utilized: parameters marked with an asterisk (*) correspond to the left Y-axis, while those represented with dashed lines correspond to the right Y-axis, which uses a logarithmic scale. This dual-axis approach ensures clarity and allows for the simultaneous presentation of multiple parameters within a single figure.

Gazi Med J 2026;37(1):39-48

Bayramlar and İşsever. Impact of Law No. 6331 on Work-Related Incidents

Figure 2

This figure illustrates the "National WrA, OD, and WrM Rates" over a 17-year period, with the effective date of Law No. 6331 highlighted.

Figures 3–5

This heatmaps of Türkiye were created to visualize the 17-year standardization analyses, illustrating the average standardized ratio percentages for 81 cities over the study period. In the top left corner of the figures, there is a scale for the standardized work incidence ratio range (%), along with a second scale indicating the percentage increase represented by the upward arrows. These arrows highlight cities that exhibited an increasing trend in these ratios following Law No. 6331, effectively representing both the magnitude and direction of the correlation (Spearman). This approach was limited to the highest 14 cities in order to attract attention.

Figures 6–8

These figures provide detailed analyses of the top 7 cities with the highest standardized ratio percentages of WrAs, ODs, and WrMs over the 17-year period, particularly in the context of the implementation of Law No. 6331. This approach allows for a closer examination of specific cities while maintaining the general-to-specific flow of the study. Figures 6–8 utilize a logarithmic scale on the Y-axis but presenting values in their original. This method effectively displays both small and large standardization ratios, ensuring that variations across the dataset are clearly visible and comparable.

RESULTS

National Level

Between 2007 and 2023, the number of 4-1/a compulsorily insured workers in Türkiye increased from 8,505,390 to 16,406,420; the number of workplaces rose from 1,116,638 to 2,179,123; WrA cases increased from 80,602 to 681,401; OD diagnoses decreased from 1,208 to 945; and WrM cases rose from 1,043 to 1,966 (Figure 1).

The number of WrAs nearly tripled within one year of the implementation of Law No. 6331, and this increase continued steadily in subsequent years.WrA In contrast, the number of ODs exhibited a delayed response, showing a consistent upward trend one year after the law's enactment. This trend persisted until the onset of the COVID-19 pandemic, when the ratios fluctuated. Conversely, WrM cases followed a fluctuating pattern; however, when averaged over time, they demonstrated a stable trajectory (Figure 1).

Examination of the National Incidence Rates (Figure 2), which are more reliable than the numbers in Figure 1, showed that although no difference in the WrA trajectory was detected that would alter the interpretation, the increase observed in OD rates in Figure 1 was, in fact, minimal. Furthermore, while no significant difference in WrM rates was observed before and after the implementation of the law in Figure 1, a notable decrease in these rates was recorded in the period following the law's enactment, in Figure 2.

Region Level

WrA reports were predominantly located in the western half of the country. However, when examined the 14 cities that experienced the most significant increase in sWrAs (range: 70%-96.4%) as a

result of Law No. 6331, a clustering pattern of this upward trend was identified in the black sea region (Figure 3).

In terms of sODs, consistently high percentages and ranking positions were notable in cities such as Zonguldak, Kütahya, and Bilecik. Additionally, when examined the 14 cities with the largest increase in OD diagnoses (range: 61.5%-96.1%) as a result of Law No. 6331, a clustering pattern was identified in the marmara region (Figure 4).

In contrast to ODs, high sWrM ratios were not confined to a limited area but were widespread across the country. When the 14 cities with the highest sWrMs (range: 35.5%–58.2%) that resulted from Law No. 6331 were examined, it was evident that these high rates were concentrated in the Eastern Black Sea region (Figure 5).
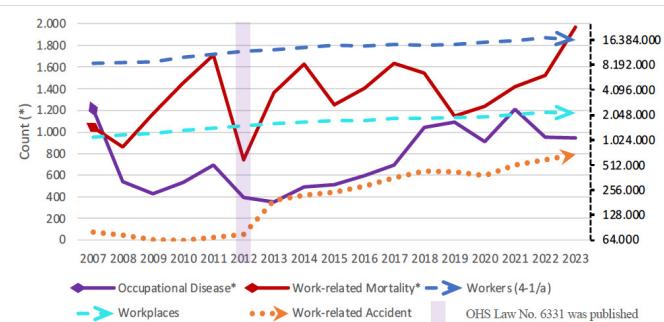
Figure 1. The count of workers, workplaces and work-related incidents in Türkiye (2007–2023).
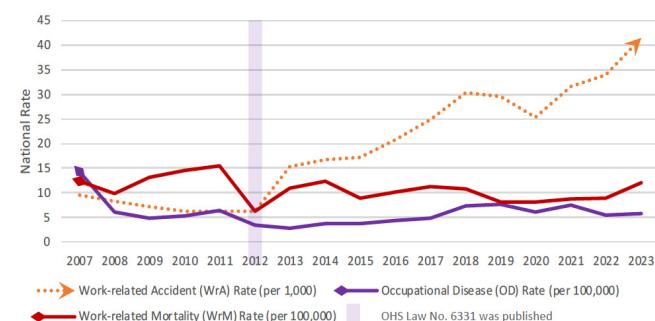
Figure 2. National Work-Related Incidence Rates in Türkiye (2007–2023).
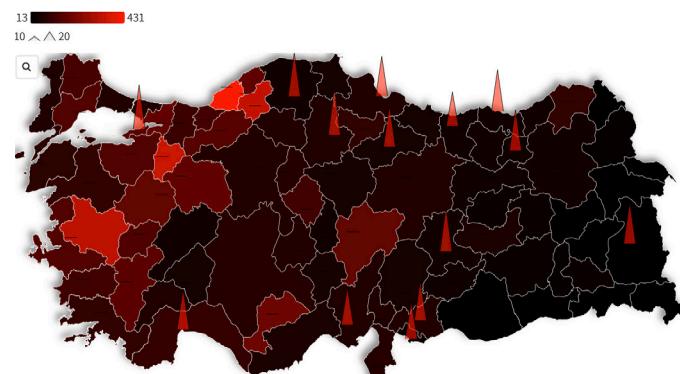
Figure 3: Heatmap of standardized work-related accident ($_s$WrA) ratios (%) by city (2007–2023).

Gazi Med J 2026;37(1):39-48

Bayramlar and İşsever. Impact of Law No. 6331 on Work-Related Incidents

City Level

The top seven cities with the highest overall ratios of sWrA, sOD, and sWrM were as follows: Zonguldak, Bilecik, Kütahya, Manisa, Bartın, Karabük, and Kocaeli. Notably, the top six cities consistently ranked at the forefront both before and after the implementation of Law No. 6331. When their locations on the map were examined, they were observed to be aligned nearly in a straight line along the north-south axis. In top-ranked cities, a noticeable decline in sWrA was observed following the implementation of Law No. 6331. While irregularities and wide fluctuations dominate sOD trends, a slight downward trend is evident in the maximum observed rates after the enactment of Law No. 6331. In contrast, sWrMs exhibit more frequent peaks and troughs and show no discernible pattern associated with Law No. 6331 (Figures 6–8).

Work-Related Accidents

Prior to the implementation of Law No. 6331, sWrA reached as high as 900% in some cities; however, no city subsequently recorded a rate exceeding 500% (Table 1, Figure 6). Specifically;

• Zonguldak: The sWrA ratio, which was 565% in 2007, decreased to 216% in 2023.
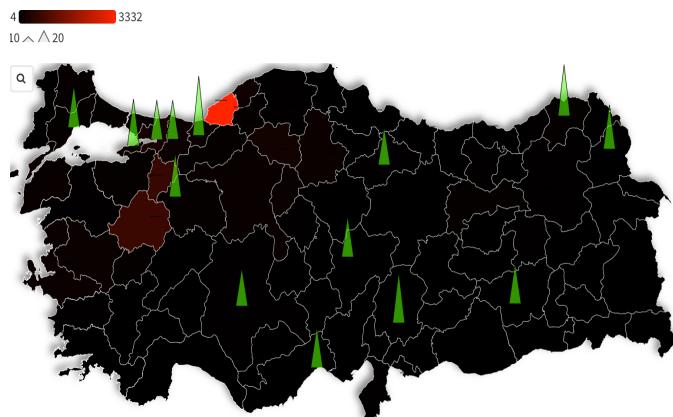
Figure 4. Heatmap of standardized occupational disease ($_s$OD) ratios (%) by city (2007–2023).
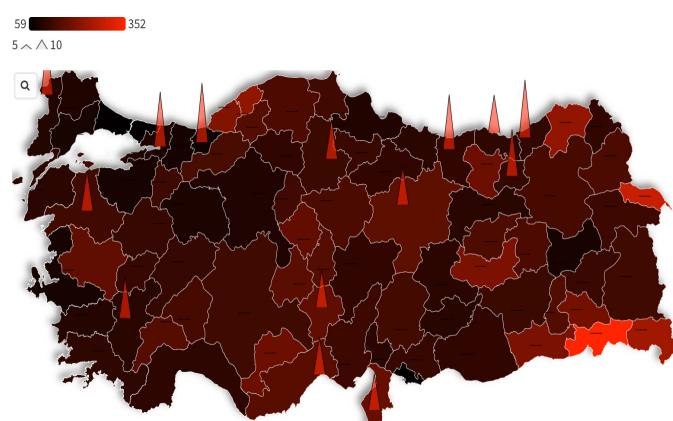
Figure 5. Heatmap of standardized work-related mortality ($_s$WrM) ratios (%) by city (2007–2023).
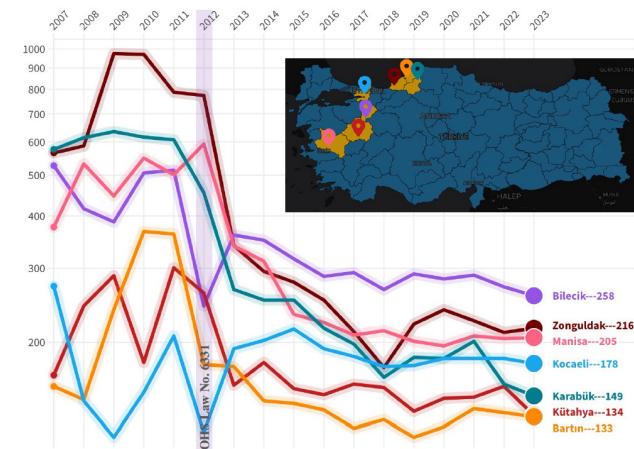
Figure 6. Trends in standardized ratios (%) of work-related accidents (WrA) in the top 7 cities (2007–2023).
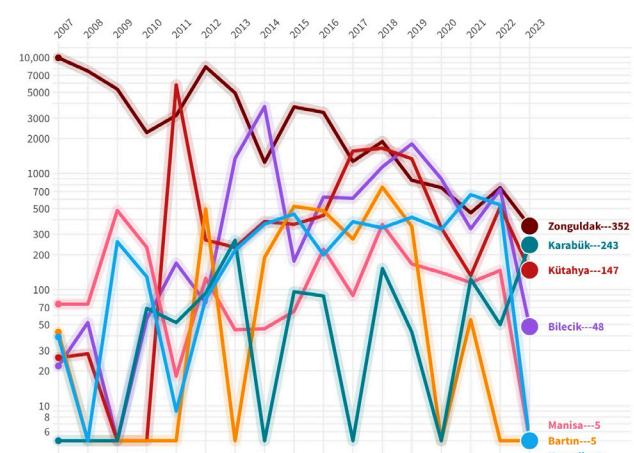
Figure 7. Trends in standardized ratios (%) of occupational diseases (OD) in the top 7 cities (2007–2023).
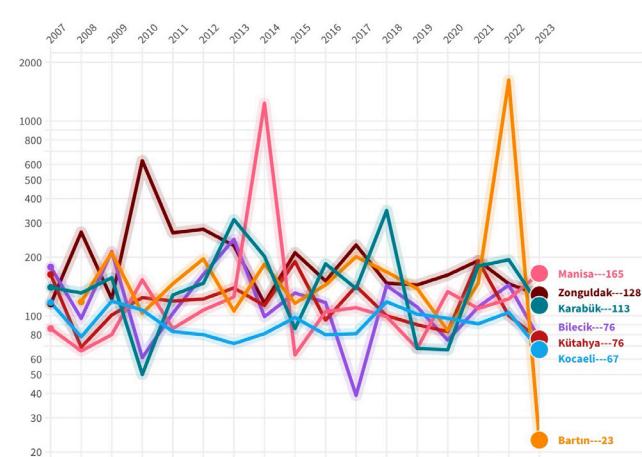
Figure 8. Trends in standardized ratios (%) of work-related mortality (WrM) in the top 7 cities (2007–2023).

Gazi Med J 2026;37(1):39-48

Bayramlar and İşsever. Impact of Law No. 6331 on Work-Related Incidents

• Bilecik and Karabük: In Bilecik, the ratio was 527% in 2007 and dropped to 258% in 2023, while in Karabük, the ratio decreased from 576% in 2007 to 149% in 2023.

• Manisa: The sWrA peaked at 593% in 2013 but showed a steady decline in subsequent years, reaching 205% in 2023.

• Bartın: In 2011, Bartın had a high sWrA ratio of 367%, which decreased to 133% in 2023.

Occupational Diseases

Prior to the implementation of Law No. 6331, excessively high sOD ratios were recorded in some cities, reaching 10,000%. In 2007, Zonguldak stood out with a ratio of 9,900%. Following the enactment of Law No. 6331, a significant decline in $_s$OD ratios was observed, with maximum rates decreasing to approximately 4,000% by 2016. For instance, Bilecik recorded a notable rate of 3,764% in 2013. During 2017–2019, sOD ratios further declined to approximately 1,000%, with cities such as Zonguldak (1,269%) and Kütahya (1,508%) maintaining relatively high ratios. From 2020 onwards, a trend toward lower sOD ratios was observed, with ratios above 500% becoming rare, and most cities reporting ratios in the range of 100–300%. However, the 2023 sOD ratio of 1,016% in Samsun is an exception to this general trend (Table 2, Figure 7). Specifically;

• Zonguldak had an exceptionally high $_s$OD ratio of 9,900% in 2007, which decreased to 302% in 2023.

• Bilecik experienced a notable spike in 2013 with a $_s$OD ratio of 3,764%, but this ratio dropped to 48% in 2023.

• Kütahya recorded one of the highest sOD ratios in 2011at 5,788%, which declined to 147% in 2023.

• Bartın had a high sOD ratio of 519% in 2015, but by 2023 the sOD ratio had dropped to zero.

Work-Related Mortalities

Regarding WrMs, no discernible pattern associated with Law No. 6331 is evident; the cities with the highest ratios vary significantly across years. Unlike the WrA and OD tables (Tables 1 and 2), where certain cities consistently rank at the top, the sWrM ratios exhibit sudden spikes in certain years. Cities experiencing spikes often have ratios exceeding the 200–300 level in multiple other years. However, cities such as Manisa (2014) and Bartın (2022) are exceptions to this generalization. In these cities, the rates typically remained low but then suddenly rose to very high levels. For example:

• Bartın exhibited a marked increase in 2022, with a sWrM ratio of 1,622%; however, this ratio declined to 23% in 2023.

• Manisa experienced a notable increase in 2014, reaching an sWrM ratio of 1,232%.

• Şırnak had one of the highest sWrM ratios in 2015, at 1,080%, but this ratio decreased to 131% in 2023.

• Zonguldak had a high $_s$WrM ratio of 626% in 2010, which dropped to 128% in 2023.

• Karabük reached an sWrM ratio of 312% in 2013, but this ratio fell to 113% in 2023.

These data indicate significant variations in sWrM ratios across cities and reveal sudden spikes in certain years (Table 3, Figure 8).

DISCUSSION

This study examined the effects of the OHS Law No. 6331, which came into force in Türkiye in 2013, through the standardization of data related to WrA, OD, and WrM. Analysis of data published by the SSI for all available years revealed a significant increase in sWrAs following the implementation of Law No. 6331, a slight increase in sOD ratios, and no significant change in sWrMs.reveals while has been observedhas occurred. Additionally, when examining the highest increases, all work-related incidences exhibited clustering in specific regions, and the highest standardized ratios declined over time.examined foralso.

The best indicators of occupational health are work-related incidence rates. Figure 1 provides a general overview by presenting the annual raw numbers of WrAs, ODs, and WrMs. Although the total number of WrMs appears largely stable in Figure 1, Figure 2 reveals a downward trend in WrM rates over time. Therefore, standardized incidence rates—as shown in Figure 2—provide a more reliable and meaningful basis for assessing actual risk levels and should be prioritized when interpreting the findings.

Typically, even in countries with the most advanced OHS systems, it is estimated that there are reporting deficiencies (including WrM) (16,17). Nevertheless, we believe that the most effective assessment can be achieved through a comparison with the official data of Germany, a country with a similar population and a strong OHS system.

Into provide a comparative general perspective, in terms of WrAs, while 870,000 WrAs were reported in Germany in 2019 (18), this number was below 430,000 in Türkiye (Figure 1). Normally, preventing WrA is an indicator of the effective functioning of OHS. However, Türkiye's significantly lower reporting of WrA compared to Germany indicates the opposite. This is because one of the main issues in Türkiye is the underreporting and lack of recording of WrAs (16).

This situation stemmed from the inadequacy of the OHS system prior to 2013. The ministry observed this situation and enacted Law No. 6331, which has had a positive impact on WrA reporting (Figure 2). Moreover, the effect of making OHS services compulsory in 2025 for public institutions and low-risk workplaces with fewer than 50 workers have yet to be seen, and it is anticipated that the situation will improve further. However, Despite the years that have passed since the law came into effect, our WrA counts were still half of those in Germany. The existing problem is likely due to the inadequate implementation of the OHS system and the lack of an established OHS culture in Türkiye. Therefore, any increase in WrAs in a specific location in Türkiye should be interpreted as an indication that the OHS system is beginning to take hold in that region. The concentration of cities in the black sea region that experienced the greatest increase in sOD diagnoses following the enactment of Law No. 6331 should be interpreted in this context (Figure 3).

The situation concerning OD in Türkiye is particularly striking. The expected increase in OD diagnoses began—perhaps unexpectedly—only in 2014, one year after Law No. 6331 was enacted. This rise showed a steady upward trend until fluctuations during the COVID-19 pandemic (Figure 2). As of 2022, the number of OD diagnoses in

Gazi Med J 2026;37(1):39-48

Bayramlar and İşsever. Impact of Law No. 6331 on Work-Related Incidents

Türkiye has only reached around 1,000 (Figure 1). In contrast, during the same period, the number in Germany was 200,000 (18,19). Part of this significant difference is due to Germany's recognition of COVID-19 cases as OD under certain circumstances. However, the situations in Türkiye and Germany did not differ substantially even before the pandemic. Moreover, the COVID-19 pandemic may provide a more accurate comparison, as the differing approaches to recognizing COVID-19 as an OD highlight the stark differences in the OHS culture (19). This disparity is not only present between Germany and Türkiye but also exists with many other countries (5).

The seriousness of missed diagnoses in OD is clearly observed in the complex trends depicted in the relevant graphs and the differences in the heat map (Figures 4 and 7). Authorities acknowledge that the number of OD diagnoses in Türkiye was quite low (6,8,20). Six hundred twenty following the enactment of Law No. 6331, the cities experiencing the highest increase in OD diagnoses were concentrated in the Marmara Region, the most developed area of Türkiye. This situation suggests that the infrastructure and awareness for identifying OD may be stronger in more industrialized and economically developed regions. In summary, a high reporting rate of OHS incidents in a region of Türkiye does not indicate poor workplace management; rather, it demonstrates that OHS systems are functioning effectively and that their existence is a positive aspect.

In 2014, the rate of WrM per 100,000 workers was recorded as 1.27 in EU countries (21), while in Türkiye, this rate was determined to be 12.2 (Figure 2) (21). Contrary to the issues of underreporting in WrAs and ODs, the problem concerning WrMs are the very high rates themselves, which is understandably concerning. Even if there is underreporting, it appears to be at much lower levels compared to WrA and OD. This is due to the fact that a concrete and extremely serious outcome, such as fatality, cannot be overlooked (22,23). It is evident that there are Significant deficiencies in OHS measures in Türkiye (3,24,27). The literature indicated that the prognosis of reported incidents in Türkiye is more severe compared to other countries (5,6). For all these reasons, we consider WrM data like a gold standard when evaluating the indicators of occupational health in Türkiye.

In our study, despite many developments following the enactment of Law No. 6331, the average WrM rate has not changed (Figure 2). This suggests that underreporting is not prevalent and that without fundamental changes and lasting cultural gains, this rate is unlikely to decrease. Additionally, we observed that the reporting ratios of sWrA were significantly lower in Türkiye's eastern regions compared to the west (Figure 3), whereas sWrM ratios were considerably higher (Figure 5). This indicates that the inadequacy of the OHS system in Türkiye is likely to be even more pronounced in the eastern regions.

Unfortunately, an ineffective OHS system can lead to disasters that result in the deaths of many workers. We have confirmed the effects of such incidents in our sWrM-specific outputs, allowing us to approach this data like a gold standard. In our study, we were able to observe the impacts of incidents that gained media attention and became public knowledge (25), such as the one in Kilimli (Zonguldak) in 2010, in our graphs, which underscores the consistency of the data.(25) According to the ILO accident hierarchy pyramid, expected fatalities can typically be predicted based on the quantity and

quality of WrA (26). However, in the Turkish context, it is clear that there is a lack of reporting regarding WrA; therefore, it is clear that strong predictions cannot be made. When we examine the 14 cities with the highest sWrM ratios, we find that, with the exception of two cities, these locations had already reached sWrMs of 200-300 prior to major incidents (Table 3, Figure 8). This indicates that these cities exhibited significant risks for major accidents and displayed clear warning signs even before such catastrophic events occurred. Consequently, in the case of Türkiye, this situation may suggest the potential for catastrophic events prevention if focused interventions are implemented in these high-risk cities.

Generally, the cities with the highest ratios of $_s$WrA, $_s$OD, and $_s$WrM included Zonguldak, Bilecik, Kütahya, Manisa, Bartın, Karabük, and Kocaeli (Tables 1–3). Mining activities were predominant in all of these cities except for Kocaeli, which was an industrial center. Furthermore, these mining cities consistently ranked at the top both before and after the enactment of Law No. 6331. This is also evident in Issever's research on industrial sectors (27). However, the pattern of decreasing peak values observed in previous years for sWrA and sOD was also evident in these cities over time (Figures 6, 7). The underlying reason for this may be the improvements in OHS practices in other cities following the enactment of Law No. 6331 and the resulting increase in work-related incidence rates, which has led to the growth of denominator in the standardization formula. Lastly, no direct or clear impact of COVID-19 had been observed in these cities.

Additionally, an analysis of $_s$WrMs in these cities revealed a direct association with specific catastrophic events. For instance, the 2010 Kilimli and 2013 Kozlu mining accidents in Zonguldak significantly increased the city's $_s$WrMs. Similarly, the 2014 Soma mining disaster in Manisa, which resulted in the fatalities of 301 workers, caused the city's sWrM ratio to spike to 1,232%. Another notable incident was the 2014 Ermenek mining accident in Karaman, which also contributed to elevated sWrM. More recently, the 2022 Amasra mining disaster in Bartın led to an extraordinary increase in the city's $_s$WrM, reaching 1,622% (Table 3, Figure 8).

Study Limitations

This study has several limitations that should be acknowledged. While the SSI presents work-related incidents by considering all individuals under the 4-1/a category collectively, our research specifically focused on compulsory insured individuals within the 4–1/a group, which we believe represents the primary risk group. This focus may have led to a slight overestimation of the rates during the standardization process. It would be beneficial for the annual statistical reports to provide detailed data on work-related incidents specifically for compulsory insured individuals under the 4–1/a category. Although expected incidents, standard deviations, errors, confidence intervals and inter-city/regional comparisons were calculated, they were excluded due to space constraints. standard thesenot included in the article Additionally, the study did not account for the severity of WrAs, which could have provided a more nuanced analysis (28). The absence of detailed sectoral data and international comparisons limits the broader applicability of the findings. Finally, the analysis could not consider the hazard levels of workplaces where the workers were employed.

Gazi Med J 2026;37(1):39-48

Bayramlar and İşsever. Impact of Law No. 6331 on Work-Related Incidents

CONCLUSION

This study provides critical insights into the state and deficiencies of the OHS system, particularly analyzing the period immediately preceding the expansion of the scope of Law No. 6331 in 2025. It elucidates the effects of the implementation of the law in 2013 on occupational health indicators. During this period, cities with the highest standardized ratios of WrA, OD, and WrM were predominantly those with intensive mining activities, including Zonguldak, Bilecik, Kütahya, Manisa, Bartın, Karabük, and Kocaeli.

Our findings reveal substantial disparities across regions, with eastern provinces showing lower reporting of WrAs and higher WrM rates, suggesting serious underreporting except in fatal cases. highlight systemic deficiencies in OHS practices, particularly in the regions. The combination of $_s$WrA$_s$WrM ratios in these areas suggests that WrAs are often underreported unless they result in severe outcomes. Nationwide, $_s$ODs remained notably low, with a relative increase observed in the Marmara Region, likely due to improved infrastructure and heightened awareness. Nevertheless, the declining peak values in $_s$WrAs and $_s$ODs over time indicate gradual improvements in reporting and compliance are evident from the decline in extreme peak values. The OHS system, as well as increased. The expansion of the scope of Law No. 6331 in 2025 is expected to play a crucial role in addressing these systemic deficiencies and fostering a safer, more sustainable working environment in Türkiye.

Ethics

Ethics Committee Approval: Ethical approval was not required, as the study utilized publicly available, anonymized data in compliance with the Declaration of Helsinki.

Informed Consent: Informed consent was obtained.

Footnotes

Authorship Contributions

Surgical and Medical Practices:O.F.B., H.İ.,Concept: O.F.B., H.İ., Design: O.F.B., H.İ., Data Collection or Processing: O.F.B., Analysis or Interpretation: O.F.B., Literature Search: O.F.B., Writing: O.F.B.

Conflict of Interest: No conflict of interest was declared by the authors.

Financial Disclosure: The authors have no relevant affiliations or financial involvement with any organization or entity with a financial interest in or financial conflict with the subject matter or materials discussed in the manuscript. This includes employment, consultancies, honoraria, stock ownership or options, expert testimony, grants or patents received or pending, or royalties. No financial, institutional, or in-kind support was received from Ziraat Bank. No writing assistance was utilized in the production of this manuscript.

References

1. Social Insurance and General Health Insurance Law (Law No. 5510) (2006).[cited:30.01.2025].Availablefrom:https://www.mevzuat.gov.tr/mevzuat?MevzuatNo=5510&MevzuatTur=1&MevzuatTertip=5.

2. Presidency of the Republic of Türkiye Social Security Institution (SSI). Annual Statistics Reports. Social Security Institution (SSI); 2007. [cited: 26.01.2025]. Available from: https://www.sgk.gov.tr/Istatistik/Yillik/fcd5e59b-6af9-4d90-a451-ee7500eb1cb4/

3. International Labour Organization (ILO). *Decent Work – Safe Work: Global Report on Work-Related Accidents and Illnesses.* Geneva, Switzerland: International Labour Organization; 2009. Available from: https://www.ilo.org/sites/default/files/wcmsp5/groups/public/@ed_norm/@relconf/documents/meetingdocument/wcms_103485.pdf

4. Occupational Health and Safety Law (Law No. 6331) (2012). [cited: 30.01.2025]. Available from: https://www.mevzuat.gov.tr/mevzuat?MevzuatNo=6331&MevzuatTur=1&MevzuatTertip=5.

5. Yuvka S, Zorlu E. The importance of statistics on occupational accidents and occupational diseases in the world and in Türkiye between 2000–2020. *Journal of Scientific Reports-A.* 2023; 53: 74–96.

6. Ucuncu K. *2014 SGK Analysis of Work Accidents and Occupational Diseases Statistics.* Ankara, Türkiye: Social Security Institution (SSI); 2014. Available from: http://www.isteguvenlik.tc/2014%20SGK%20Analiz.pdf

7. Presidency of the Republic of Türkiye Ministry of Labour and Social Security Directorate General of Occupational Health and Safety. Policy and Strategy. n.d. [cited: 26.01.2025]. Available from: https://www.csgb.gov.tr/isggm/ısg-hizmetleri/politika-ve-strateji/

8. Presidency of the Republic of Türkiye, Ministry of Labour and Social Security, Directorate General of Occupational Health and Safety. Policy and strategy [Internet]. Ankara: Ministry of Labour and Social Security; n.d. [cited 2025 Jan 26]. Available from: https://www.csgb.gov.tr/isggm/isg-hizmetleri/politika-ve-strateji/

9. Bayramlar OF, Ezirmik E, İşsever H, Bayramlar Z. Standardization of the numbers of work accidents, occupational diseases and mortality rates according to Social Security Institution's 2010–2015 years data based upon cities. *J Ist Faculty Med.* 2019; 82: 29–39.

10. Law on Amendments to Certain Laws and Decrees with the Force of Law (Law No. 7491), Article 71 (2023). [cited: 30.01.2025]. Available from: https://www.resmigazete.gov.tr/eskiler/2023/12/20231228-10.htm

11. Paneth N. *Introduction to Epidemiology (EPI 810).* Ankara, Türkiye: Ministry of Health, Republic of Türkiye; n.d. [cited: 26.01.2025]. Available from: https://ekutuphane.saglik.gov.tr/Home/GetDocument/411

12. Hayran O. *Sağlık Bilimlerinde Araştırma ve İstatistik Yöntemler.* 3. baskı. İstanbul, Türkiye: Nobel Yayıncılık; 2012.

13. Centers for Disease Control and Prevention (CDC). *Principles of Epidemiology in Public Health Practice: An Introduction to Applied Epidemiology and Biostatistics.* 3rd ed. Atlanta, GA: U.S. Department of Health and Human Services, Centers for Disease Control and Prevention, Office of Workforce and Career Development; 2006.

14. Lwanga SK, Cho-Yook T, Ayeni O. *Teaching Health Statistics: Lesson and Seminar Outlines.* 2nd ed. Geneva, Italy: World Health Organization; 1999: 230.

15. Akbulut T, Sabuncu H. *Epidemiyoloji: prensip ve uygulamalar.* 1. baskı. İstanbul: Sistem Yayıncılık; 1993. Available from: https://kutuphane.fisek.org.tr/kitap.php?book_id=601

16. Türkay M, Yıldız AN, İşsever H. Meslek hastalıkları ve işle ilgili hastalıklar. In: Yıldız AN, Sandal A, editors. *İş Sağlığı ve Güvenliği Meslek Hastalıkları* [Internet]. Ankara (Türkiye): Hacettepe Üniversitesi; 2020 [cited 2026 Jan 13]. Available from: http://hdl.handle.net/11655/23156

17. Hämäläinen P, Takala J, Kiat TB. *Global Estimates of Occupational Accidents and Work-related Illnesses 2017.* Finland: Ministry of Social Affairs and Health; 2017.

18. Deutsche Gesetzliche Unfallversicherung (DGUV). *Statistics on Accidents at Work and Occupational Diseases 2019.* 2019 [cited: 26.01.2025]. Available from: https://publikationen.dguv.de/widgets/pdf/download/article/3922

Gazi Med J 2026;37(1):39-48

Bayramlar and İşsever. Impact of Law No. 6331 on Work-Related Incidents

19. Nienhaus A, Stranzinger J, Kozak A. COVID-19 as an occupational disease—temporal trends in the number and severity of claims in Germany. *Int J Environ Res Public Health.* 2023; 20: 1182.

20. Keçeci S. Examination of Occupational Health Safety Strategies and Policies of Turkey and Some EU Countries. 2020; 3.

21. Eurostat. Accidents at Work Statistics. n.d. [cited: 26.01.2025]. Available from: https://ec.europa.eu/eurostat/statistics-explained/index.php?title=Accidents_at_work_statistics

22. Connor J, Norton R, Ameratunga S, Robinson E, Civil I, Dunn R, et al. The role of driver sleepiness in car crashes: a systematic review of epidemiological studies. *J Safety Res.* 2009; 40(4): 305–311. Available from: https://www.sciencedirect.com/journal/journal-of-safety-research/vol/40/issue/4

23. Şen M, Dursun S, Murat G. Work accidents in Turkey: an evaluation in the context of the European Union countries. *OPUS Int J Soc Res.* 2018; 9: 1167–90.

24. Ceylan H. Fatal occupational accidents in Turkey. *ISG Akademik.* 2021; 3(1): 1–13.

25. Vikipedi. Türkiye'deki madencilik kazaları listesi. 2025 [cited: 30.01.2025]. Available from: https://tr.wikipedia.org/wiki/Türkiye%27deki_madencilik_kazaları_listesi

26. Takala J. Introductory report: Decent work – safe work [Internet]. Paper presented at: XVIth World Congress on Safety and Health at Work; 2002 May 27; Vienna, Austria. Geneva: International Labour Office; 2002 [cited 2026 Jan 13]. Available from: https://webapps.ilo.org/public/libdoc/ilo/2002/463016.pdf

27. İşsever H, Ezirmik E, Öztan G, İşsever T. Standardization of work accidents and occupational diseases indicators of Social Security Institution between 2008–2017 years. *J Ist Faculty Med.* 2020; 83: 434–45.

28. Koçali K. Standardization of between 2012–2020 years work accidents indicators of Social Security Institution. *Journal of Academic Approaches.* 2021; 12: 302–27.

Supplementary Tables 1–4: https://d2v96fxpocvxx.cloudfront.net/8a9ff4da-541a-42fa-9980-1a9a3ab6d6c5/content-images/f2661266-6e82-4ead-9c73-100b9520b7b5.pdf

Stepwise Standardization of the Subperiosteal Pocket Technique in Cochlear Implantation: Effects on Surgical Efficiency and Consistency

Koklear İmplantasyonda Subperiostal Cep Tekniğinin Aşamalı Standardizasyonu: Cerrahi Verimlilik ve Tutarlılık Üzerine Etkileri

Said Sönmez[1], Mehmet Çelik[1], Beldan Polat[1], Demet Altun[2], Kadir Serkan Orhan[1], Yahya Güldiken[1]

[1]Department of Otolaryngology, İstanbul University-İstanbul Faculty of Medicine İstanbul, Türkiye
[2]Department of Anesthesiology, İstanbul University-İstanbul Faculty of Medicine İstanbul, Türkiye

ABSTRACT

Objective: The subperiosteal pocket technique (SPT) is widely used in cochlear implantation (CI) for its ability to reduce operative time and minimize complications. This study revisits the technique, focusing on surgical efficiency, stepwise analysis, and implications for training.

Methods: A retrospective analysis of 160 pediatric CI cases was conducted. The total surgery time and durations of eight defined steps were documented, and practical insights were integrated to optimize outcomes.

Results: The cumulative surgical step durations averaged 37.2 ± 6.2 minutes. The most time-intensive steps included suturing and skin closure (13.4 ± 3 minutes) and posterior tympanotomy (7.1 ± 2.7 minutes). These steps were critically analyzed for efficiency and educational value.

Conclusion: The SPT is comparable to conventional methods in safety and effectiveness , with the added benefits of reduced operative time and enhanced training potential. This study provides detailed guidance to improve surgical workflow and education in CI.

Keywords: Subperiosteal pocket, cochlear implantation, surgical training, operative efficiency, pediatric hearing loss

ÖZ

Amaç: Subperiostal cep tekniği (SPT), operasyon süresini kısaltma ve komplikasyonları azaltma potansiyeli nedeniyle koklear implantasyon (Kİ) cerrahisinde yaygın olarak kullanılmaktadır. Bu çalışma, tekniği yeniden ele alarak cerrahi verimlilik, basamaklı analiz ve eğitim açısından çıkarımlar üzerine odaklanmaktadır.

Yöntemler: Toplam 160 pediatrik Kİ olgusunun retrospektif analizi yapıldı. Toplam cerrahi süre ve tanımlanan sekiz cerrahi basamağın süreleri kaydedildi ve sonuçları optimize etmeye yönelik pratik çıkarımlar çalışmaya entegre edildi.

Bulgular: Cerrahi basamakların kümülatif süre ortalaması 37,2 ± 6,2 dakika olarak bulundu. En fazla zaman alan basamaklar sütür ve cilt kapatılması (13,4 ± 3 dakika) ile posterior timpanotomi (7,1 ± 2,7 dakika) idi. Bu basamaklar, verimlilik ve eğitsel değer açısından ayrıntılı olarak analiz edildi.

Sonuç: SPT, güvenlik ve etkinlik açısından konvansiyonel yöntemlerle karşılaştırılabilir olup, daha kısa operasyon süresi ve artmış eğitim potansiyeli gibi ek avantajlar sunmaktadır. Bu çalışma, Kİ cerrahisinde cerrahi iş akışını ve eğitimi geliştirmeye yönelik ayrıntılı rehberlik sağlamaktadır.

Anahtar Sözcükler: Subperiostal cep, koklear implantasyon, cerrahi eğitim, operatif verimlilik, pediatrik işitme kaybı

Address for Correspondence/Yazışma Adresi: Asst, Prof, Said Sönmez, MD, Department of Otolaryngology, İstanbul University-İstanbul Faculty of Medicine İstanbul, Türkiye
E-mail / E-posta: said.sonmez@istanbul.edu.tr
ORCID ID: orcid.org/0000-0003-1982-0386

Gazi Med J 2026;37(1):49-55

Sönmez et al. Stepwise analysis of the SPT in CI

INTRODUCTION

Cochlear implants (CIs) are sophisticated electronic devices surgically implanted to restore hearing in individuals with profound or severe hearing loss, for whom conventional sound amplification devices have proven ineffective.

Precision in surgical expertise is essential because of the potential for injury to critical structures, such as the facial nerve, chorda tympani, vestibular system, and cochlear structures, during CI. To ensure sufficient and minimally traumatic electrode insertion while preserving potential residual hearing, high-quality training and deliberate practice are indispensable (1,2).

The traditional gold-standard method for CI fixation involved drilling a bony recess and securing the device with sutures. Although effective, this approach is associated with longer operative time, increased risk of dural tears and cerebrospinal fluid leakage, and greater technical variability (3,4). These challenges have led to the development of alternative techniques such as the subperiosteal pocket method. Recent studies have compared fixation and non-fixation approaches, reporting no significant differences in implant stability (3,4). Furthermore, an international survey demonstrated variability in fixation preferences among CI surgeons (5), and prospective trials, such as the Cochlear Implant Fixation Techniques (COMFIT) study, are ongoing to further investigate these methods (6). In this study, we describe the application of the subperiosteal pocket technique (SPT) without fixation, focusing on a step-by-step description of the surgical timing and technical aspects of the workflow.

The SPT was initially described by Balkany et al. (7) as the temporal pocket technique. This technique has been validated by numerous comparative studies in subsequent years (8-10). It provides advantages in CI because it is easy to perform, shortens operating time, carries a minimal risk of postoperative complications, and does not require external part fixation (8-10).

A technical description serves to organize and standardize the conveyance of information and communication among surgical staff regarding procedural details, thereby potentially enhancing surgical safety (11). Widely adopted, efficacious, standardized, and structured approaches play a crucial role in enhancing surgical safety. A notable example is the integration of the surgical safety checklist, which has demonstrated a substantial decrease in postoperative complications and mortality rates (12,13).

At our tertiary institution, the SPT has been routinely performed in CI since 2008 (8). A growing body of literature on SPT addresses indications, alignment, outcomes, and complications (2,9,10,14). This study revisits the SPT in CI, providing a detailed examination of each surgical step while incorporating practical insights ("tips and tricks") derived from a single-center experience. Additionally, it evaluates the efficiency of each stage and its implications for surgical training. This study analyzes data from pediatric CI surgeries to contribute to the standardization of this technique, to offer actionable guidance for surgeons, and to address the growing need for optimized training methods in CI.

MATERIALS AND METHODS

Study Design and Setting

This retrospective study analyzed pediatric patients who underwent CI using the SPT at our institution between March 2017 and August 2023. Procedural timing and surgical steps were recorded and analyzed based on standardized operative protocols. To ensure methodological consistency and minimize variability, only surgeries performed by a single senior surgeon (Y.G.) with more than 10 years' experience in CI were included. The study was approved by the İstanbul University-İstanbul Faculty of Medicine Clinical Research Ethics Committee (approval number: 2024/940, reference number: 2572440, date: 24.05.2024).

Patient Selection

Patients with severe-to-profound hearing loss, including both prelingual and postlingual cases, were included in the study. Patients with temporal bone abnormalities, anatomical variations, or patients whose surgeries were extended due to abnormal surgical progress (such as instrument or device problems or anesthesia-related complications) were excluded.

Surgical Technique and Analysis

A standardized SPT procedure, divided into eight distinct surgical steps (Figures 1 and 2) was followed:

1. Retroauricular incision and Palva flap elevation.

2. Subperiosteal pocket creation.
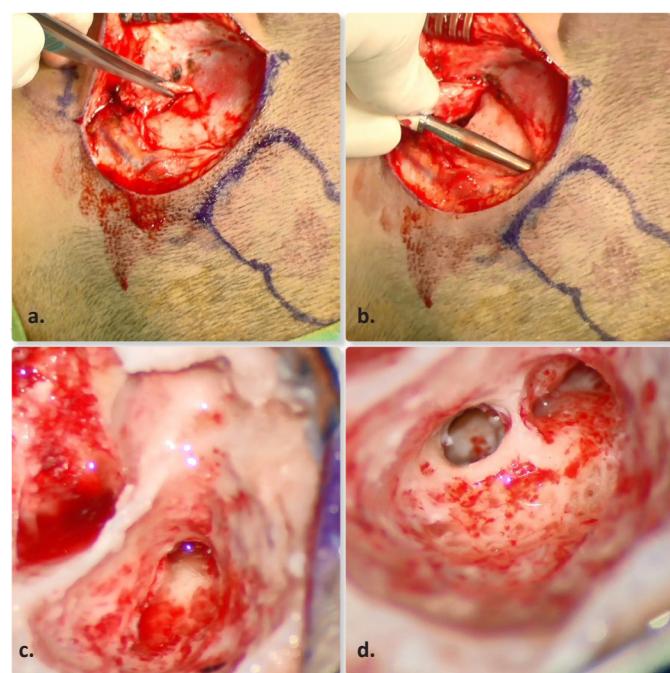
Figure 1. Key steps of the Subperiosteal pocket technique (a), Retroauricular incision with elevation anterior-based tailed Palva flap. (b) Subperiosteal pocket creation. (c) Cortical Mastoidectomy. (d) Posterior tympanotomy.

Gazi Med J 2026;37(1):49-55

Sönmez et al. Stepwise analysis of the SPT in CI
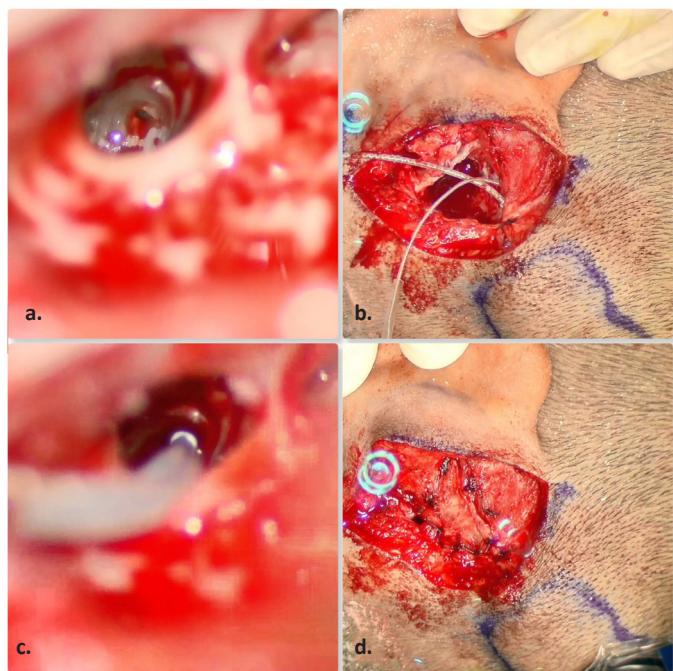
Figure 2. Key steps of the Subperiosteal Pocket Technique, with the subsequent stages continuing in the image. (a) Exposure of round window membrane. (b) Placement of the device in the pocket and suturing tail of Palva flap incision. (c) Electrode array insertion. (d) Suturing Palva flap and skin closure.

3. Cortical mastoidectomy.

4. Posterior tympanotomy.

5. Exposure of the round window (RW) membrane.

6. Placement of the device and suturing of the Palva flap.

7. Electrode array insertion.

8. Suturing of the Palva flap and skin closure.

Surgical technique was analyzed and quantified using surgical video recordings and operative notes. Total surgery time was defined as the duration from skin incision to skin closure. In contrast, cumulative surgical step durations included only the active phases of each of the eight defined steps. For this analysis, a timer was started at the beginning and stopped at the end of each step; short pauses between steps—such as material preparation, instrument handling, and brief workflow interruptions—were not included. Additionally, non–CI-specific intervals such as anesthesia preparation, patient positioning, surgical field preparation, hemostasis, and intraoperative testing were excluded from the cumulative analysis. This exclusion accounts for the difference between cumulative surgical duration and total surgery time.

Technique

Retroauricular Incision with Elevation Anterior-Based Tailed Palva Flap

This technique starts with standard positioning and a C-shaped retroauricular incision, typically placed 8-10 mm posterior to the postauricular skin crease. The incision is extended through the skin and into the subcutaneous tissue. After the posterior auricular muscle is dissected, the auricle is retracted anteriorly over the periosteum. The temporal lines were located through palpation. Following these lines, a 2-cm horizontal periosteal incision was made from the zygomatic root posteriorly using electrocautery. Another periosteal incision, parallel to the initial one, was made at the mastoid tip. These two periosteal incisions were then linked by a posterior vertical incision, creating an anteriorly based musculoperiosteal flap according to Palva's method. Moreover, a tailed Palva flap is created by making a 1–2-cm incision that includes the periosteum, extending from the posterosuperior corner of the flap toward the subperiosteal pocket where the internal receiver will be placed. This modification facilitates atraumatic implant placement and reduces skin tension without compromising the tightness of the subperiosteal pocket (15).

Subperiosteal Pocket Creation

Using the Freer elevator (Karl Storz, Tuttlingen, Germany), a subperiosteal pocket is made according to template of the IRS.

Cortical Mastoidectomy

In a RW approach, a complete mastoidectomy may not always be necessary, but exposing specific anatomical landmarks is crucial for success. These landmarks include the sigmoid sinus, dural plate, mastoid segment of the facial nerve, retrofacial recess, mastoid tip cell, and the thinned outer bony canal wall up to the origin of the chorda tympani at the facial nerve.

Posterior Tympanotomy

For safe access to the RW during CI surgery, the facial recess should be sufficiently widened, particularly inferiorly. The posterior tympanotomy should ideally begin at the origin of the chorda tympani on the facial nerve. It should be widened as much as possible along the chorda and the facial nerve while avoiding exposing the facial nerve sheath to prevent nerve damage and unnecessary bleeding. Opening the inferior facial recess is vital, as it aids in identifying the round window niche (RWN). The Incudal buttress should be protected to help prevent damage to the ossicles during drilling. Preservation of the buttress is necessary, particularly when significant residual hearing is present. In cases of incomplete exposure of the recess, anterior repositioning of the chorda tympani may resolve the issue. If the RW is not visible at this stage, the patient's position may be adjusted to facilitate better visualization, and the posteromedial bone overlying the facial canal may be drilled to expose the medial space of the posterior tympanum. Furthermore, if the visual field is obstructed by the funnel-shaped wall of the external auditory canal (EAC), lowering the EAC's outer margin can help provide a clearer visual field during the procedure.

Exposure of Round Window Membrane

When the RWN was identified after posterior tympanotomy, the anterior and posterosuperior bony overhangs of the RW were carefully removed using a low-speed drill or micro-curette until the annulus of the RW membrane became visible. The pseudomembrane covering the RW membrane was then delicately excised. Additionally, bone adjacent to the anterior-inferior RW annulus might be removed by 1 to 2 mm to facilitate the surgical approach. These meticulous

Gazi Med J 2026;37(1):49-55

Sönmez et al. Stepwise analysis of the SPT in CI

procedures were essential for optimizing the success and safety of RW CI.

Placement of the Device in the Pocket and Suturing Tail of Palva Flap Incision

The inner part of the implant was placed into the previously prepared pocket. The tail flap incision was then closed with absorbable sutures.

Electrode Array Insertion

A sharp, right-angled pick was used to make a vertical incision over the RW membrane, leaving the annulus intact to minimize perilymph leakage. To successfully preserve hearing, the electrode is placed in the anterior-inferior direction and slowly advanced in the posterior-superior direction. The crista semilunaris defines the space available for electrode insertion, primarily within the medial part of the scala tympani.

Suturing the Palva Flap and Skin Closure

Closure of the Palva flap incision and subcutaneous tissue was performed using separate absorbable sutures. For skin closure, intracutaneous absorbable sutures were used.

Statistical Analysis

Operative times were presented as mean ± standard deviation (SD). Differences in the duration of each surgical step were analyzed using one-way analysis of variance (ANOVA). Comparisons between the first and last quartiles of surgeries were performed using paired t-tests to evaluate procedural standardization. Statistical significance was set at $p < 0.05$. Furthermore, variability within steps was assessed using the coefficient of variation (CV).

RESULTS

A total of 160 pediatric patients underwent CI using the SPT. The mean age was 17.4 ± 7.3 months (range: 12–144 months [1–12 years]). Among the patients, 128 (80%) had prelingual hearing loss, while 32 (20%) had postlingual hearing loss. Right ear surgeries accounted for 96 cases (60%), and left ear surgeries for 64 cases (40%).

Operative Time Analysis

The average surgery time as interval skin incision to skin closure 58 ± 3.6 and the average cumulative surgical step durations was 37.2 ± 6.2 minutes. The mean duration, SD, and CV for each surgical step are summarized in Table 1.

Statistical Analysis Results

Stepwise Comparisons: Suturing of the Palva flap and skin closure took significantly longer than all other steps ($p < 0.01$, ANOVA).

• **Variability Across Surgical Steps:** The CV analysis showed that certain steps were performed more consistently than others. Retroauricular incision and Palva flap elevation (CV = 0.14), cortical mastoidectomy (CV = 0.17), device placement with flap suturing (CV = 0.21), and final skin closure (CV = 0.22) demonstrated the lowest variability, indicating a relatively high degree of standardization.

• **Learning Curve and Procedural Consistency:** A comparison of the first and last quartiles of surgeries revealed no significant difference in total operative time ($p = 0.6$), suggesting stable surgical performance over time. Furthermore, variability patterns across steps did not differ significantly between early and late cases ($p = 0.8$, t-test), supporting the overall standardization of the technique within this surgical series.

Complications

No intraoperative complications, including facial nerve injury, bleeding requiring additional intervention, or difficulties during electrode insertion, were observed. Similarly, no postoperative complications were noted; in particular, no device migration occurred, and all postoperative evaluations confirmed correct and stable positioning of the implants.

DISCUSSION

This study revisited the SPT in CI, providing a step-by-step analysis of surgical efficiency and its implications for training. By evaluating 160 pediatric cases, we identified critical areas for optimization and standardization.

The average cumulative surgical step duration was 37.2 ± 6.2 minutes, which aligns with the technique's reputation for reducing operative time. Among the eight procedural steps, suturing the Palva flap and closing the skin (13.4 ± 3 minutes) and posterior tympanotomy (7.1 ± 2.7 minutes) were the most time-intensive, accounting for a significant portion of the operative time. In contrast, steps such as subperiosteal pocket creation and electrode array insertion exhibited minimal variability and consistently shorter durations. This suggests that these steps are well standardized and less influenced

Table 1. Mean duration, standard deviation, and coefficient of variation for each of the eight surgical steps.

Surgical step	Mean duration (min)	SD (min)	Coefficient of variation
Retroauricular incision and Palva flap elevation	4.4	0.60	0.14
Subperiosteal pocket creation	1.2	0.37	0.31
Cortical mastoidectomy	5.2	0.90	0.17
Posterior tympanotomy	7.1	2.70	0.38
Round window membrane exposure	1.3	0.75	0.58
Device placement and Palva flap suturing	3.4	0.70	0.21
Electrode array insertion	1.2	0.50	0.42
Suturing of the Palva flap and skin closure	13.4	3.00	0.22

SD: Standard deviation, min: Minimum.

Gazi Med J 2026;37(1):49-55

Sönmez et al. Stepwise analysis of the SPT in CI

by surgeons' experience. In contrast, more complex steps such as posterior tympanotomy and suturing are affected by factors such as anatomical variations, surgeon experience, and the equipment used, which makes them more variable and challenging to standardize. Identifying these differences provides an opportunity to refine the more variable and time-consuming steps, thereby enhancing efficiency and reducing overall surgical duration, particularly in high-volume centers.

Numerous studies have demonstrated the reliability of SPT, showing an absence of device migration and, in some instances, spontaneous bone bed formation (15-18). Conventional methods for securing CIs typically include the creation of a bony bed and a channel within the calvarium, sometimes accompanied by tie-down sutures. However, the process of drilling through potentially thin calvarial bone carries the risk of rare but severe complications, such as epidural hematoma, cerebral infarction, and cerebrospinal fistulae (19-22). The shift towards the SPT can be attributed to its potential to mitigate these complications and reduce operation time. This trend underscores the growing recognition of the technique's advantages in enhancing patient safety and optimizing surgical efficiency (8-10,14,23).

A cross-sectional survey of the American Neurotology Society elucidated the collective preferences for internal device fixation in CI. Among the respondents, 65% expressed a predilection for a variation of the tight SPT, highlighting its prevalence in contemporary practice. The survey further revealed that 19% favored a bony bed and trough with tie-downs, 10% preferred a bony bed and trough without tie-downs, and 5% opted for a screw fixation system. Within the subset of respondents endorsing the SPT, 62% incorporated a bony trough, while 38% performed the SPT alone, underscoring the diversity of approaches within this specialized field (23).

Recent studies have highlighted the ongoing debate regarding COMFITs and their surgical implications (3-5,24). While multiple fixation methods, including bony bed preparation and tight subperiosteal pockets, have been proposed, systematic reviews have shown no significant differences in implant stability between these approaches (3,24,25). In line with these findings, the present study focused not on comparing fixation methods but rather on providing a detailed, step-by-step technical description of the SPT without fixation, and on analyzing surgical timing for each stage. Our results support the conclusion that the technique can be standardized with minimal variability across key surgical steps, thereby contributing to procedural reproducibility and educational frameworks. Moreover, recent international surveys emphasize the variability in surgeons' practices regarding fixation (5), reinforcing the need for clearly structured protocols rather than reliance on fixation type alone.

The simplicity and efficiency of the SPT make it highly suitable for surgical education and for reproducible clinical practice. In our series, total operative times did not differ significantly between the early and late surgical quartiles (p = 0.6), indicating consistent performance over time and suggesting that the procedure can be mastered without a prolonged learning curve. Variability analysis further supported this observation: steps such as retroauricular incision, cortical mastoidectomy, device placement, and final skin closure showed the lowest coefficients of variation, indicating a high degree of procedural standardization. In contrast, greater variability in steps such as posterior tympanotomy, RW exposure, subperiosteal pocket creation, and electrode insertion was observed, likely reflecting differences in anatomy, surgical complexity, and case-specific technical adjustments. This structured and stepwise breakdown of the procedure facilitates targeted learning by helping trainees focus on the more variable and technically demanding steps, while reliably executing the more standardized components. Historically, surgical skills have been transmitted through the master-apprentice model in which the apprentice begins by observing the master and gradually assumes more responsibility until capable of performing the procedure independently (26-28). However, changes in working-hour regulations and the increasing focus on operational efficiency have reduced instructional time, posing challenges for surgical education (29). In this context, a step-by-step framework like the one described in this study offers a standardized breakdown of procedures, enhancing education, communication, and evaluation for trainees. It ensures that critical skills are effectively imparted despite time constraints (28).

Our findings also highlight the relationship between the surgeon's experience and operative time. The SPT demonstrated a learning curve comparable to previous studies of stapedectomy, in which surgeons required 60–100 cases to achieve full proficiency (30-32). Adopting a standardized technique and surpassing this threshold resulted in significant reductions in operative time, which eventually plateaued as surgeons reached a high level of competence. This underscores the value of procedural standardization in optimizing both surgical efficiency and training outcomes.

The estimated cost for operating room time, encompassing both anesthesia and facility fees, is $42 per minute (33). Therefore, surgical duration is positively correlated with costs. In a different study using data from 2006–2007, the facility fee at another institution was $1,581 for the first 30 minutes of surgery and $1,265 for each subsequent half-hour. The facility fee alone has been reported as $6,641 for the standard unilateral CI procedure, which has a duration of 144 minutes. When Combined with the implant's list price of $28,900, the total bill reached $35,541. Additional fees, such as those for the recovery room, anesthesia, laboratory, pharmacy, surgeon, anesthesiologist, clinic, and other related costs, are not included in this calculation (34). We believe that our surgical description contributes to reducing surgical duration and, consequently, costs.

Study Limitations

One limitation of our study is its retrospective design, which may introduce biases in data collection and interpretation. Furthermore, our analysis focused exclusively on pediatric cases, limiting the generalizability of the findings to adult populations. At the time of the surgical interventions included in this study, the standard clinical practice at our institution typically resulted in implantation at a mean age of 17.4 months, which was influenced by national guidelines, referral patterns, and parental factors. We recognize the growing emphasis on implantation before 12 months of age in contemporary clinical practice. Moreover, this study did not assess functional or patient-reported outcome measures (PROMs), which are increasingly recognized as important indicators of surgical success and patient satisfaction (35). Prospective studies could expand on

Gazi Med J 2026;37(1):49-55

Sönmez et al. Stepwise analysis of the SPT in CI

these findings by incorporating long-term outcomes such as device stability, patient satisfaction, PROMs, and cost-effectiveness to further validate the advantages of the SPT.

CONCLUSION

This study concludes that the SPT is an efficient approach to CI, offering reduced operative time and a structured framework suitable for surgical training. By identifying time-intensive steps and analyzing procedural efficiency, this technique can be further optimized to enhance its clinical and educational utility. Future studies with diverse populations and long-term follow-up are recommended to expand on these findings.

Ethics

Ethics Committee Approval: The study was approved by the İstanbul Faculty of Medicine Clinical Research Ethics Committee (approval number: 2024/940, reference number: 2572440, date: 24.05.2024).

Informed Consent: Informed consent was not required due to the retrospective design of the study and the use of anonymized surgical records.

Footnotes

Authorship Contributions

Surgical and Medical Practices: S.S., M.Ç., B.P., D.A., K.S.O., Y.G., Concept: S.S., M.Ç., B.P., D.A., K.S.O., Y.G., Design: S.S., M.Ç., B.P., D.A., Data Collection or Processing: S.S., M.Ç., B.P., D.A., K.S.O., Y.G., Analysis or Interpretation: S.S., M.Ç., B.P., K.S.O., Y.G., Literature Search: S.S., M.Ç., B.P., K.S.O., Writing: S.S., M.Ç.

Conflict of Interest: No conflict of interest was declared by the authors.

Financial Disclosure: The authors declared that this study received no financial support.

REFERENCES

1. Ericsson KA: The scientific study of expert levels of performance: General implications for optimal learning and creativity. High Ability Studies. 1998; 9: 75–100.

2. Roland PS, Wright CG. Surgical aspects of cochlear implantation: mechanisms of insertional trauma. Adv Otorhinolaryngol. 2006; 64: 11–30.

3. Markodimitraki LM, Strijbos RM, Stegeman I, Thomeer HGXM. Cochlear implant fixation techniques: a systematic review of the literature. Otol Neurotol. 2021; 42: 959–66.

4. de Varebeke SP, Govaerts P, Cox T, Deben K, Ketelslagers K, Waelkens B. Fixation of cochlear implants: an evidence-based review of literature. B-ENT. 2012; 8: 85–94.

5. Kant E, Markodimitraki LM, Stegeman I, Thomeer HGXM. Variability in surgical techniques for cochlear implantation: an international survey study. Cochlear Implants Int. 2022; 23: 195–202.

6. Markodimitraki LM, Harkel TCT, Bennink E, Stegeman I, Thomeer HGXM. A monocenter, patient-blinded, randomized, parallel-group, non-inferiority study to compare cochlear implant receiver/stimulator device fixation techniques (COMFIT) with and without drilling in adults eligible for primary cochlear implantation. Trials. 2023; 24: 605.

7. Balkany TJ, Whitley M, Shapira Y, Angeli SI, Brown K, Eter E, et al. The temporalis pocket technique for cochlear implantation: an anatomic and clinical study. Otol Neurotol. 2009; 30: 903–7.

8. Güldiken Y, Orhan KS, Yiğit O, Başaran B, Polat B, Güneş S, et al. Subperiosteal temporal pocket versus standard technique in cochlear implantation: a comparative clinical study. Otol Neurotol. 2011; 32: 987–91.

9. Cohen MS, Ha AY, Kitsko DJ, Chi DH. Surgical outcomes with subperiosteal pocket technique for cochlear implantation in very young children. Int J Pediatr Otorhinolaryngol. 2014; 78: 1545–7.

10. Sweeney AD, Carlson ML, Valenzuela CV, Wanna GB, Rivas A, Bennett ML, et al. 228 cases of cochlear implant receiver-stimulator placement in a tight subperiosteal pocket without fixation. Otolaryngol Head Neck Surg. 2015; 152: 712–7.

11. Nagpal K, Vats A, Lamb B, Ashrafian H, Sevdalis N, Vincent C, et al. Information transfer and communication in surgery: a systematic review. Ann Surg. 2010; 252: 225–39.

12. de Vries EN, Prins HA, Crolla RM, den Outer AJ, van Andel G, van Helden SH, et al. Effect of a comprehensive surgical safety system on patient outcomes. N Engl J Med. 2010; 363: 1928–37.

13. Haynes AB, Weiser TG, Berry WR, Lipsitz SR, Breizat AH, Dellinger EP, et al. A surgical safety checklist to reduce morbidity and mortality in a global population. N Engl J Med. 2009; 360: 491–9.

14. Maxwell AK, Cass SP. Cochlear Implant receiver-stimulator migration using the subperiosteal pocket technique: objective measurements of early and late positioning. Otol Neurotol. 2019; 40: 328–34.

15. Orhan KS, Polat B, Enver N, Güldiken Y. Tailed Palva flap in the subperiosteal pocket technique for cochlear implantation. J Laryngol Otol. 2015; 129: 916–8.

16. Güldiken Y, Polat B, Enver N, Aydemir L, Çomoğlu Ş, Orhan KS. Evaluation of receiver-stimulator migration in cochlear implantation using the subperiosteal pocket technique: a prospective clinical study. J Laryngol Otol. 2017; 131: 487–91.

17. Orhan KS, Polat B, Enver N, Çelik M, Güldiken Y, Değer K. Spontaneous bone bed formation in cochlear implantation using the subperiosteal pocket technique. Otol Neurotol. 2014; 35: 1752–4.

18. Turanoglu AK, Yigit O, Acioglu E, Okbay AM. Radiologic evidence of cochlear implant bone bed formation following the subperiosteal temporal pocket technique. Otolaryngol Head Neck Surg. 2016; 154: 702–6.

19. Arnoldner C, Baumgartner WD, Gstoettner W, Hamzavi J. Surgical considerations in cochlear implantation in children and adults: a review of 342 cases in Vienna. Acta Otolaryngol. 2005; 125: 228–34.

20. Dodson KM, Maiberger PG, Sismanis A. Intracranial complications of cochlear implantation. Otol Neurotol. 2007; 28: 459–62.

21. Gosepath J, Maurer J, Mann WJ. Epidural hematoma after cochlear implantation in a 2.5-year-old boy. Otol Neurotol. 2005; 26: 202–4.

22. Proops DW, Stoddart RL, Donaldson I. Medical, surgical and audiological complications of the first 100 adult cochlear implant patients in Birmingham. J Laryngol Otol Suppl. 1999; 24: 14–7.

23. Carlson ML, O'Connell BP, Lohse CM, Driscoll CL, Sweeney AD. Survey of the American Neurotology Society on Cochlear Implantation: part 2, surgical and device-related practice patterns. Otol Neurotol. 2018; 39: e20–7.

24. Ceylan ME, Zorlu ME, Çorakçı O, Akı ES, Yıldırım GA, Dalgıç A. Comparison of conventional technique with suture fixation and subperiosteal tight pocket technique on revision cochlear implantation rate. J Int Adv Otol. 2024; 20: 301–5.

Gazi Med J 2026;37(1):49-55

Sönmez et al. Stepwise analysis of the SPT in CI

25. Stern Shavit S, Weinstein EP, Drusin MA, Elkin EB, Lustig LR, Alexiades G. Comparison of cochlear implant device fixation-well drilling versus subperiosteal pocket. A cost effectiveness, case-control study. Otol Neurotol. 2021; 42: 517–23.

26. Clark RE, Pugh CM, Yates KA, Inaba K, Green DJ, Sullivan ME. The use of cognitive task analysis to improve instructional descriptions of procedures. J Surg Res. 2012; 173: e37–42.

27. Halsted WS. The training of the surgeon. Bull Johns Hopkins Hosp. 1904;15:267-275. Available from: https://archive.org/details/b2246413x.

28. Nazari T, Vlieger EJ, Dankbaar MEW, van Merriënboer JJG, Lange JF, et al. Creation of a universal language for surgical procedures using the step-by-step framework. BJS Open. 2018; 2: 151–7.

29. Reznick RK, MacRae H. Teaching surgical skills--changes in the wind. N Engl J Med. 2006; 355: 2664–9.

30. Hughes GB. The learning curve in stapes surgery. Laryngoscope. 1991; 101: 1280–4.

31. Yung MW, Oates J. The learning curve in stapes surgery and its implication for training. Adv Otorhinolaryngol. 2007; 65: 361–9.

32. Yung MW, Oates J, Vowler SL. The learning curve in stapes surgery and its implication to training. Laryngoscope. 2006; 116: 67–71.

33. Pollei TR, Barrs DM, Hinni ML, Bansberg SF, Walter LC. Operative time and cost of resident surgical experience: effect of instituting an otolaryngology residency program. Otolaryngol Head Neck Surg. 2013; 148: 912–8.

34. Majdani O, Schuman TA, Haynes DS, Dietrich MS, Leinung M, Lenarz T, et al. Time of cochlear implant surgery in academic settings. Otolaryngol Head Neck Surg. 2010; 142: 254–9.

35. Markodimitraki LM, Stegeman I, Thomeer HGXM. Cochlear implant awareness: development and validation of a patient reported outcome measure. Front Neurosci. 2022; 16: 830768.

Clinical and Genetic Features of Gelatinous Drop-Like Corneal Dystrophy: First Cohort from Türkiye with a Novel *TACSTD2* Mutation

Gelatinöz Damla Benzeri Kornea Distrofisinin Klinik ve Genetik Özellikleri: Yeni Bir *TACSTD2* Mutasyonu ile Türkiye'den İlk Kohort

Fulya Yaylacıoğlu Tuncay[1], Hasan Diker[2], Ahmet Yücel Üçgül[2], Mehmet Cüneyt Özmen[2], Bahri Aydın[2]

[1]Department of Medical Biology, University of Health Sciences, Gülhane Faculty of Medicine, Ankara, Türkiye
[2]Department of Ophthalmology, Gazi University Faculty of Medicine, Ankara, Türkiye

ABSTRACT

Objective: To describe the clinical and genetic findings, as well as treatment outcomes, in patients with gelatinous drop-like corneal dystrophy (GDLD) from a single center in Türkiye.

Methods: In this retrospective study, 10 patients from five families who were clinically diagnosed with GDLD at the Ophthalmology Department of Gazi University Medical Faculty were included. Genetic analysis was performed using Sanger sequencing of the coding regions of the tumor-associated calcium signal transducer 2 (*TACSTD2*) gene and of exons 4 and 12 of the transforming growth factor-beta-induced (*TGFBI*) gene. Clinical findings, treatment modalities, and follow-up outcomes were documented.

Results: One novel *TACSTD2* mutation (c.779del, p.Tyr260SerfsTer11) and two previously reported *TACSTD2* mutations, c.355T>A (p.C119S) and c.341T>G (p.F114C), were identified in three families. In one family, no disease-associated variants were detected in either *TGFBI* or *TACSTD2*. The most common initial symptoms were photophobia, corneal pain, and blurred vision, and the mean age at onset was 11.3 years. The follow-up duration ranged from 2 to 21 years, and seven patients required repeated surgical interventions. Epithelial debridement followed by diamond burr polishing (ED-DBP) was performed in seven patients, resulting in symptomatic improvement and delaying the need for keratoplasty.

Conclusion: This is the first report of the clinical and genetic characteristics of GDLD patients from Central Anatolia, and it expands the *TACSTD2* mutational spectrum with a novel variant. ED-DBP is

ÖZ

Amaç: Bu çalışmanın amacı, Türkiye'de tek bir merkezden gelatinöz damla benzeri kornea distrofisi (GDLD) tanısı alan hastalarda klinik ve genetik bulgular ile tedavi sonuçlarını tanımlamaktır.

Yöntemler: Bu retrospektif çalışmaya, Gazi Üniversitesi Tıp Fakültesi Göz Hastalıkları Anabilim Dalı'nda klinik olarak GDLD tanısı konulan beş aileden 10 hasta dâhil edildi. Genetik analiz, tümörle ilişkili kalsiyum sinyal transdüseri 2 (*TACSTD2*) geninin kodlayıcı bölgeleri ile transforming growth factor-beta-induced (*TGFBI*) geninin 4. ve 12. ekzonlarının Sanger dizilemesi ile gerçekleştirildi. Klinik bulgular, uygulanan tedavi yöntemleri ve takip sonuçları kaydedildi.

Bulgular: Üç ailede, biri yeni (c.779del, p.Tyr260SerfsTer11) ve ikisi daha önce bildirilmiş c.355T>A (p.C119S) ve c.341T>G (p.F114C) üç *TACSTD2* mutasyonu saptandı. Bir ailede ise ne *TGFBI* ne de *TACSTD2* genlerinde hastalıkla ilişkili herhangi bir varyant tespit edilmedi. En sık görülen başlangıç semptomları fotofobi, kornea ağrısı ve bulanık görme olup, ortalama başlangıç yaşı 11,3 yıl idi. Takip süresi 2 ile 21 yıl arasında değişmekteydi ve yedi hastada tekrarlayan cerrahi girişimler gerekmişti. Yedi hastaya epitel debridmanı sonrası elmas freze ile polisaj (ED-DBP) uygulanmış; bu işlem semptomatik iyileşme sağlamış ve keratoplasti gereksinimini geciktirmiştir.

Sonuç: Bu çalışma, Orta Anadolu'dan bildirilen GDLD hastalarının klinik ve genetik özelliklerine ilişkin ilk rapor olup, *TACSTD2* mutasyon spektrumunu yeni bir varyant ile genişletmektedir. ED-DBP, GDLD için bir tedavi seçeneği olarak önerilmektedir; hastalığın ilerlemesini

Address for Correspondence/Yazışma Adresi: Fulya Yaylacıoğlu Tuncay, MD, PhD, FEBO, Department of Medical Biology, University of Health Sciences, Gülhane Faculty of Medicine, Ankara, Türkiye
E-mail / E-posta: drfulyatuncay@gmail.com
ORCID ID: orcid.org/0000-0002-2088-3416

Gazi Med J 2026;37(1):56-64

Yaylacıoğlu Tuncay et al. Gelatinous Drop-Like Corneal Dystrophy in Türkiye

ABSTRACT

proposed as a treatment modality for GDLD; it may not halt disease progression but can alleviate corneal discomfort, temporarily improve vision, and postpone corneal transplantation.

Keywords: Gelatinous drop-like corneal dystrophy, Epithelial debridement with diamond burr polishing, *TACSTD2*, Sanger sequencing, keratoplasty

ÖZ

durdurmasa da korneal rahatsızlığı azaltabilir, görmeyi geçici olarak iyileştirebilir ve kornea transplantasyonunu erteleyebilir.

Anahtar Sözcükler: Gelatinöz damla benzeri kornea distrofisi, elmas freze ile epitel debridmanı, *TACSTD2*, Sanger dizileme, keratoplasti

INTRODUCTION

Gelatinous drop-like corneal dystrophy (GDLD) is a rare inherited corneal disorder (OMIM 2014870) characterized by subepithelial and stromal deposition of amyloid. GDLD has been most frequently reported in Japan, where its prevalence is estimated at 1 in 33,000 (1,2). However, cases have also been described in other countries (3-10). Because the disease follows an autosomal recessive inheritance pattern, consanguineous marriages are more common among families affected by GDLD (11).

GDLD typically presents during the first or second decade of life and affects both sexes equally. The most common initial symptoms include foreign body sensation, photophobia, and visual impairment, depending on the location and severity of the corneal deposits (12). In the early stages, deposits usually appear in the subepithelial central cornea. As the disease progresses, these deposits increase in number and depth, extend peripherally, and coalesce (13). In advanced stages, superficial and deep corneal vascularization often accompany the corneal deposits (13). Four clinical subtypes of GDLD have been described based on the appearance of corneal deposits: 1. Typical mulberry type: observed in early stages, characterized by white-grayish gelatinous deposits; 2. Band-keratopathy type: also seen in early stages, featuring band-shaped amyloid deposits in the subepithelial space; 3. Stromal opacity type: found in advanced stages, in which deposits extend into the deeper stromal layers; 4. Kumquat-like type: an advanced form characterized by yellow-white, widespread deposits with neovascularization (14). Treatment strategies for GDLD include removal of the superficial corneal layer via photoablation or keratectomy in early stages, and corneal transplantation using DALK or penetrating keratoplasty (PKP) in advanced cases (12). In addition, limbal stem cell transplantation (LSCT) and the Boston keratoprosthesis have been reported as treatment options for patients with GDLD (15-17). Recurrence of amyloid deposits remains the main challenge during follow-up, and repeated interventions are often required (12).

Mutations in the tumor-associated calcium signal transducer 2 (*TACSTD2*) gene are responsible for the majority of GDLD cases (18,19). *TACSTD2*, located on chromosome 1p32, encodes a transmembrane glycoprotein consisting of 323 amino acids. The non-sense variant p.Gln118Ter (Q118X) has been reported in up to 90% of Japanese GDLD cases (18). Nevertheless, the Human Genome Mutation Database (HGMD) lists more than 30 distinct *TACSTD2* mutations across different populations. Loss-of-function mutations in *TACSTD2* alter the expression of key cell-junction proteins, disrupting cell-to-cell and cell-to-substrate adhesion in the corneal epithelium, thereby increasing epithelial permeability (20, 21). This abnormal permeability facilitates protein leakage—such as lactoferrin—into the cornea, resulting in amyloid deposition (22). In the early stages of disease, the basal lamina, Bowman's membrane (BM), and stroma remain intact in corneas with GDLD (23). However, with disease progression, BM destruction occurs, and amyloid deposits extend into the deeper stromal layers (23,24). Corneal vascularization and mechanical stress have also been shown to exacerbate deposit formation (25).

To date, two siblings from a Turkish family have been clinically and genetically characterized by Uhlig et al. (25) no additional cases have been reported from Türkiye (26). Furthermore, there are few studies describing long-term follow-up of GDLD patients, and none have reported the use of epithelial debridement with diamond burr polishing (ED-DBP) as a treatment modality (25,27). In this study, we present the clinical characteristics, treatment modalities, and long-term outcomes of 10 patients with GDLD from five Turkish families and identify three disease-causing *TACSTD2* variants in three of those families, one of which is novel.

MATERIALS AND METHODS

Ethical Approval

This retrospective study was approved by the Institutional Ethics Review Board of Gazi University (approval number: 2025–405/04, date: 11.03.2025) and conducted in accordance with the principles of the Declaration of Helsinki. Written informed consent was obtained from all participants and/or their legal guardians.

Participants and Clinical Evaluation

Patients clinically diagnosed with GDLD and followed at the Department of Ophthalmology Gazi University Faculty of Medicine between January 2004 and January 2025 were included in the study. A detailed medical history was obtained from all patients, including information on ethnicity, family history, parental consanguinity, history of ocular trauma, exposure to chemicals, drug use, systemic diseases, and previous treatments.

Comprehensive ophthalmic evaluations were performed, including best-corrected visual acuity (BCVA), intraocular pressure measurement, slit-lamp biomicroscopy, and, when feasible depending on the degree of corneal opacity or photophobia, fundus examination. In cases where fundus visualization was limited, ultrasonography was performed. Treatment modalities, treatment outcomes, and follow-up durations were also recorded. Interocular asymmetry in BCVA was evaluated in patients and defined as a difference of more than two lines between the eyes.

Gazi Med J 2026;37(1):56-64

Yaylacıoğlu Tuncay et al. Gelatinous Drop-Like Corneal Dystrophy in Türkiye

Genetic Analyses

Peripheral blood samples (5 mL) were collected from patients, when available, their parents for DNA extraction and molecular analysis. DNA isolation was performed using a spin-column-based nucleic acid purification method (MN Macherey-Nagel, Düren, Germany). The coding regions and exon–intron boundaries of *TACSTD2*, as well as exons 4 and 12 of *TGFBI*, were amplified by polymerase chain reaction using primers designed with Primer3 (Table 1).

Bidirectional Sanger sequencing was conducted using the BigDye Terminator Mix v3.1 (Applied Biosystems, Foster City, CA, USA) and analyzed on an ABI-3100 Genetic Analyzer (Applied Biosystems). Chromatograms were reviewed using ChromasPro v1.7.7 (Technelysium, South Brisbane, Australia), and obtained sequences were compared with reference gene sequences in the National Center for Biotechnology Information database. Familial segregation of the novel variant was confirmed by sequencing the parents of the probands.

Identified variants were classified according to the 2015 ACMG/AMP guidelines for sequence variant interpretation. Population allele frequencies were obtained from the Genome Aggregation Database (gnomAD v4.1.0; https://gnomad.broadinstitute.org/). Variant pathogenicity was evaluated using the Ensembl Variant Effect Predictor (VEP; https://useast.ensembl.org/Tools/VEP) and Franklin (https://franklin.genoox.com/). Additional data on variant function and associated phenotypes were retrieved from the Human Gene Mutation Database (Professional 2025.1), ClinVar (https://www.ncbi.nlm.nih.gov/clinvar/), and the relevant published literature.

RESULTS

Demographic and Clinical Findings

Ten patients from five unrelated families were included in the present study. All families consisted of sibling groups. The demographic and clinical characteristics of the patients are summarized in Table 2. The mean age at the first ophthalmological examination (AE) at our center was 28.3 years (range, 8–42 years). The sex distribution was equal for males and females. The mean age of onset (AO) of the first ocular symptoms or signs was 11.3 years (range, 6–17 years). All participants self-identified as Turkish and originated from the Central Anatolia region. Parental consanguinity was present in all families, with marriages between first cousins reported in three of them. Participants with Systemic diseases, a history of drug use, or ocular trauma that could lead to corneal amyloid deposition were

excluded based on detailed medical history. The most common presenting symptoms were photophobia, corneal pain, and blurred vision (Table 2).

At the first examination, the BCVA ranged from hand motion (HM) to 0.8. Slit-lamp examination revealed central and paracentral mulberry-like, transparent or whitish nodular corneal elevations; band keratopathy; corneal scarring; widespread yellow-white deposits; recurrent nodular lesions in the graft; and opaque corneal grafts (Figure 1). Corneal neovascularization was present in four patients at baseline and was subsequently observed in five patients during follow-up (Table 2, Figure 1).

Patients from the same family exhibited similar phenotypes, including anterior segment findings, BCVA, and AO. Notable interocular asymmetry was observed only in patient 8, particularly in BCVA and anterior segment findings (Tables 2 and 3).

Treatment Modalities and Outcomes

The mean follow-up duration of the patients was 9.4 years, ranging from 2 to 21 years (Table 3). Surgical interventions performed during follow-up included ED-DBP photorefractive keratectomy (PRK), deep anterior lamellar keratoplasty (DALK), and PKP (Table 3). In addition to surgical procedures, bandage contact lenses and medical therapy were administered as needed for symptomatic relief. Between the first and last visits, BCVA increased in 7 eyes, remained stable in 5 eyes, and decreased in 8 eyes (Table 3). In the better-seeing eye, BCVA was at least 0.1 in seven of 10 patients and at least 0.5 in four (Table 3).

To remove the superficial corneal layer, ED-DBP or PRK was performed. During ED-DBP, the corneal epithelium surrounding the lesions was removed to Bowman's layer, followed by diamond-burr polishing of the entire corneal surface. A handheld, battery-powered ophthalmic burr with a 3.3-mm diamond-dusted spherical tip was used to polish the corneal surface for approximately 10–15 seconds (Figure 2a). At the end of the procedure, a soft bandage contact lens was applied. Postoperatively, patients received topical corticosteroids, antibiotics, and artificial tears, each administered four times daily for one month. The bandage lens was removed on the fifth postoperative day. ED-DBP was performed as the initial surgical step in 7 eyes (5 patients) and as a secondary procedure following keratoplasty in 2 eyes (2 patients) (Table 3). Recurrent ED-DBP was applied to 3 eyes of 2 patients during follow-up; in one eye, a stromal anti-VEGF injection was co-administered. All patients reported significant symptomatic relief following ED-DBP, with

Table 1. Primer List of *TACSTD2* and *TGFBI* genes.

TACSTD2	Sequences of primers (5'-3')	Tm (°C)	PCR product (bp)
Primer_1	F: CCTGCAGACCATCCCAGAC	59	1140
	R: CAGGAAGCGTGACTCACTTG		
TGFBI	Sequences of primers (5'-3')	Tm (°C)	PCR product (bp)
Exon 4	F: TCGTCCTCTCCACCTGTAGA	59.0	548
	R: AACATGTTCTCAGCCCTCGT		
Exon 12	F: AACCAAGGTGTGTGCATTCC	59.0	415
	R: TTTAGTCCCGCCCACTCTTT		

TACSTD2: Tumor-associated calcium signal transducer 2, *TGFBI*: Transforming growth factor-beta-induced, PCR: Polymerase chain reaction.

Gazi Med J 2026;37(1):56-64

Yaylacıoğlu Tuncay et al. Gelatinous Drop-Like Corneal Dystrophy in Türkiye

Table 2. Demographic, clinical and genetic findings of Turkish GDLD patients.

Patient no	Sex	AE	AO	Initial symptom	Anterior segment findings	Genetic test	Gene	Nucleotide change	Amino acid change	Zygosity
1[1]	M	33	10	Vision loss	OD: typical yellow-white nodules, vascularization OS: corneal scar, vascularization	Yes	TACSTD2	c.355T>A	p.C119S	Homozygous
2[1]	M	32	8	Vision loss	OD: corneal scar, vascularization OS: typical yellow-white nodules, vascularization	Yes	*TACSTD2*	c.355T>A	p.C119S	Homozygous
3[2]	M	26	12	Corneal pain	OD: yellow-white nodules OS: yellow-white nodules, band keratopathy	Yes	TACSTD2	c.341T>G	p.F114C	Homozygous
4[2]	M	33	16	Corneal pain	OD: typical yellow-white nodules OS: typical yellow-white nodules	No	NA	NA	NA	NA
5[3]	F	42	15	Vision loss	OD: opaque graft with vascularization OS: opaque graft with vascularization	Yes	TACSTD2	c.779delT*	p.Tyr260SerfsTer11	Homozygous
6[3]	F	32	10	Vision loss	OD: widespread nodules OS: widespread nodules, vascularization	Yes	TACSTD2	c.779delT*	p.Tyr260SerfsTer11	Homozygous
7[4]	F	42	17	Vision loss	OD: corneal scar with vascularization OS: widespread nodules	No	NA	NA	NA	NA
8[4]	F	18	6	Vision loss	OD: few corneal deposits OS: corneal scar	No	NA	NA	NA	NA
9[5]	F	8	8	Photophobia	OD: typical yellow-white nodules OS: typical yellow-white nodules	Yes	Negative	NA	NA	NA
10[5]	M	17	11	Corneal pain	OD: typical yellow-white nodules OS: typical yellow-white nodules	Yes	Negative	NA	NA	NA

*Denotes novel variant, [1, 2, 3, 4, 5]denotes family numbers.
M: Male; F: Female; AO: Age of onset, AE: Age at exam, OD: Right eye; OS: Left eye, NA: Non-available, GDLD: Gelatinous drop-like corneal dystrophy

improvement lasting for at least 12 months during follow-up (Figure 2b). Three eyes of three patients underwent PRK, including one eye that received intraoperative mitomycin-C. In two patients, PRK was performed as a secondary procedure following ED-DBP.

For corneal transplantation, either DALK or PKP was performed. Six eyes in four patients underwent PKP as a second-step procedure following ED-DBP during the follow-up period; one patient received PKP as the primary surgical treatment. Two eyes of one patient initially underwent DALK; however, one of these later required PKP as a second surgery (Figure 2c). The interval between ED-DBP and keratoplasty ranged from 12 to 38 months (Table 3). Following DALK or PKP, BCVA improved further in treated eyes. However, Patient

1 developed retinal detachment in the left eye during follow-up, resulting in permanent vision loss. Additionally, recurrence of corneal deposits within the graft led to a decrease in BCVA during late postoperative visits and necessitated repeated keratoplasties in six eyes of six patients, as shown in Table 3.

Variants in TACSTD2 and TGFBI

Sanger sequencing was successfully performed in seven patients from four families (Table 1). In two families, previously reported disease-associated homozygous missense variants were detected: c.355T>A (p.C119S) and c.341T>G (p.F114C) (Table 2). Both variants were classified as likely pathogenic according to the ACMG

Gazi Med J 2026;37(1):56-64

Yaylacıoğlu Tuncay et al. Gelatinous Drop-Like Corneal Dystrophy in Türkiye

Figure 1. Anterior segment images of representative Gelatinous drop-like corneal dystrophy patients at first visit. (a) Youngest patient in the cohort (Patient 9) with few corneal deposits; (b) Patient 4 with yellow-white nodules and band keratopathy; (c) One of the sibling pair, Patient 1, with typical central whitish mulberry-like nodular corneal elevations; (d) The other sibling, Patient 2, with a similar pattern of corneal deposits with his brother; (e) Opaque corneal graft with corneal vascularization in Patient 5; (f) Central severe corneal deposits and vascularization in Patient 6.

guidelines. In one family, no disease-associated variant was detected in *TACSTD2*. No disease-associated variants were identified in exons 4 or 12 of the *TGFBI* gene in any of the patients.

In Family 3, a novel biallelic frameshift variant was identified: c.779del (p.Tyr260SerfsTer11) (Figure 3). The allele frequency of this variant has been reported as 8.477×10^{-7} in populations of European ancestry, and this variant has not been reported in the homozygous state in any database. This variant has not been described in HGMD, LOVD, or ClinVar, nor has it been reported in association with GDLD in the literature or in the Turkish Genome Project Data Sharing Portal. Given its predicted loss-of-function effect and extremely low frequency in population databases, this variant was classified as likely pathogenic under ACMG criteria (Pathogenic very strong 1_PVS1, Pathogenic moderate 2_PM2). Segregation analysis revealed heterozygosity in both parents, who were second-degree cousins and exhibited no corneal abnormalities. Family 3 included two affected female siblings diagnosed at ages 10 and 15 years. Their initial symptom was visual loss. Patient 5 underwent PKP in both eyes in her twenties at another hospital. At her first visit to our center, both corneal grafts were opaque and vascularized, and ultrasonography detected chronic retinal detachment in the left eye (Table 2, Figure 1e). Slit-lamp examination of patient 6 revealed central, severe, yellowish corneal deposits in both eyes, with peripheral corneal vascularization in the left eye. In both siblings, BCVA at diagnosis was HM in the right eye and 0.05 in the left eye. Patient 5 underwent recurrent PKP on the right eye at our center

in 2016 and 2025. The right eye of patient 6 underwent ED-DBP as the first intervention, followed by PKP on subsequent follow-up, whereas the left eye underwent PRK as the first intervention, followed by DALK on subsequent follow-up.

The clinical findings of patients with the frameshift variant regarding AO, BCVA, anterior segment findings, and the need for and timing of corneal transplantation tended to be more severe than those in patients with missense variants (Tables 2 and 3).

DISCUSSION

In this study, we investigated the clinical findings of five pairs of siblings with GDLD from Türkiye. Three disease-associated *TACSTD2* variants were identified in three families; one variant was novel. A follow-up period of up to 21 years was documented, including treatment modalities and patient outcomes.

The novel *TACSTD2* variant identified in our cohort, c.779del (p.Tyr260SerfsTer11), is a frameshift variant predicted to cause premature truncation of the protein, resulting in the loss of the transmembrane and PIP$_2$-binding domains. A previously reported truncating mutation located near this site, c.798del (p.Lys267SerfsTer4), has been shown to be deleterious in HeLa cells, leading to loss of function and impaired trafficking of claudin-1 and claudin-7 from the cytoplasm to the plasma membrane (28). In our cohort, patients carrying this truncating variant (Patients 5 and 6) exhibited a more severe phenotype than those with missense variants (Tables 2 and 3). However, previous studies have reported conflicting results regarding the relationship between mutation type and disease severity 6,14,29.

Previously reported *TACSTD2* missense variants, c.355T>A (p.C119S) and c.341T>G (p.F114C), were identified in two families in our study. Both p.C119S and p.F114C affect the thyroglobulin-like repeat domain, a region crucial for protein stability and epithelial cell adhesion, and have been described in patients from Tunisia, Saudi Arabia, and Iran 6,10,30. A Sudanese patient carrying the p.C119S variant experienced recurrent keratoplasties, similar to patient 1 in our cohort (30). In contrast, the Iranian patient with the p.F114C variant exhibited earlier disease onset and a more severe phenotype than patient 3 in our series (6). Although previous reports from Japan and Iran have highlighted phenotypic heterogeneity both within families and among patients carrying the same *TACSTD2* variant, the siblings in our cohort exhibited remarkably similar clinical findings (Tables 2 and 3) 6,31. Nevertheless, interocular differences were evident in patients 1, 7, and 8. Interocular asymmetry and even unilateral cases have previously been reported in GDLD (6,32). These observations support the concept that loss of *TACSTD2* function is essential for GDLD development; however, it is unlikely to be the sole determinant of disease severity. The variability in clinical expression may depend on factors such as tear film composition, epithelial microtrauma, eyelid structure, glandular function, systemic conditions, and other genetic or epigenetic modifiers (8,10).

The only previously reported Turkish GDLD family in the literature consisted of two siblings who carried a different *TACSTD2* truncating mutation, c.653delA, which was not detected in our cohort (9). The 15-year follow-up of that family showed a clinical course comparable to that of our patients with truncating *TACSTD2* variants, as repeated PKP were required because of recurrent corneal deposits (25).

Gazi Med J 2026;37(1):56-64

Yaylacıoğlu Tuncay et al. Gelatinous Drop-Like Corneal Dystrophy in Türkiye

Table 3. Treatment modalities and treatment outcomes of patients of GDLD patients.

Patient no/eye	Tx_1/Year	Tx_2/Year	Tx_3/Year	Tx_4/Year	BCVA at first visit/year	BCVA at last visit/year
1/OD	ED-DBP+anti-VEGF/2015	ED-DBP/2019	ED-DBP/2023	PRK/2025	0.2/2004	0.1/2025
1/OS	PPK/2004	PPK+PPV/2013	_	_	0.05/2004	HM/2025
2/OD	PPK/2004	ED-DBP/2018	PRK+MMC/2022	_	HM/2004	0.05/2022
2/OS	ED-DBP/2015	_	_	_	0.05/2004	0.05/2022
3/OD	ED-DBP/2013	_	_	_	0.4/2013	0.6/2020
3/OS	ED-DBP/2014	_	_	_	0.3/2013	0.5/2020
4/OD	ED-DBP/2014	ED-DBP/2021	ED-DBP/2023	ED-DBP+/2025	0.4/2014	0.2/2025
4/OS	ED-DBP/2014	ED-DBP/2021	ED-DBP/2023	_	0.6/2014	0.2/2025
5/OD	PPK/1996*	PPK/2016	PPK/2025	_	HM/2016	0.05/2025
5/OS	PPK/2000*	_	_	_	0.05/2016	HM/2025
6/OD	ED-DBP/2016	PPK/2017	PPK/2025	_	HM/2016	0.05/2025
6/OS	PRK/2020	DALK/2025	_	_	0.05/2016	0.05/2025
7/OD	DALK/2023	Cataract surgery/2024	_	_	HM/2017	0.5/2024
7/OS	DALK/2017	Cataract surgery /2020	ED-DBP/2023	PPK/2024	0.2/2017	0.1/2024
8/OD	_	_	_	_	0.8/2017	0.8/2024
8/OS	PPK/2007	PPK/2017	_	_	HM/2017	0.2/2024
9/OD	_	_	_	_	0.7/2021	0.7/2023
9/OS	_	_	_	_	0.5/2021	0.4/2023
10/OD	_	_	_	_	0.4/2020	0.3/2023
10/OS	_	_	_	_	0.3/2020	0.3/2023

*Denotes treatment applied in another center.

OD: Right eye, OS: Left eye, ED-DBP: Epithelial debridement with diamond burr polishing, PPV: Pars plana vitrectomy, PRK: Photorefractive keratectomy, DALK: Deep anterior lamellar keratoplasty, PPK: Partial penetrating keratoplasty, BCVA: Best-corrected visual acuity, HM: Hand motion, MMC: Mitomycin-C, Anti-VEGF: Anti-vascular endothelial growth factor, BCVA: Best-corrected visual acuity.

Figure 2. Anterior segment images of representative Gelatinous drop-like corneal dystrophy patients during follow-up regarding treatment modalities and outcomes. (a) Intraoperative image of Epithelial debridement with diamond burr polishing in the left eye of Patient 2; (b) Preoperative image of the left eye of Patient 2; (c) Postoperative image of the left eye of Patient 2; (d) Right eye of Patient 7 in 2018 after deep anterior lamellar keratoplasty; (e) Right eye of Patient 7 in 2024 showing recurrence of deposits in the graft; (f) Right eye of Patient 7 in 2025 after partial penetrating keratoplasty.

There was one family without any disease-associated *TACSTD2* variants in our cohort. Sequencing of exons 4 and 12 of *TGFBI* also did not reveal any variants. In the literature, GDLD patients without variants in the *TACSTD2* gene have been reported (10,33,34). A detailed investigation, by next-generation sequencing, of the non-coding regions of the *TACSTD2* gene or of other genes may reveal the responsible genetic variant in these patients.

The surgical management of GDLD primarily aims to remove the superficial corneal layers during the early stages of deposit formation, thereby improving vision, alleviating discomfort, and delaying the need for corneal transplantation. Among these procedures, phototherapeutic keratectomy (PTK) is one of the most frequently performed treatments in reported cases. In our cohort, ED-DBP was applied as the first surgical intervention to seven eyes of five patients and found to improve visual acuity, reduce corneal discomfort, and effectively postpone corneal transplantation, as anticipated. To the best of our knowledge, this is the first report describing the use of ED-DBP in patients with GDLD. ED-DBP has been demonstrated to be an effective treatment modality for recurrent corneal erosion and epithelial basement membrane dystrophy and is considered a safe, convenient, and cost-effective approach for managing

Gazi Med J 2026;37(1):56-64

Yaylacıoğlu Tuncay et al. Gelatinous Drop-Like Corneal Dystrophy in Türkiye
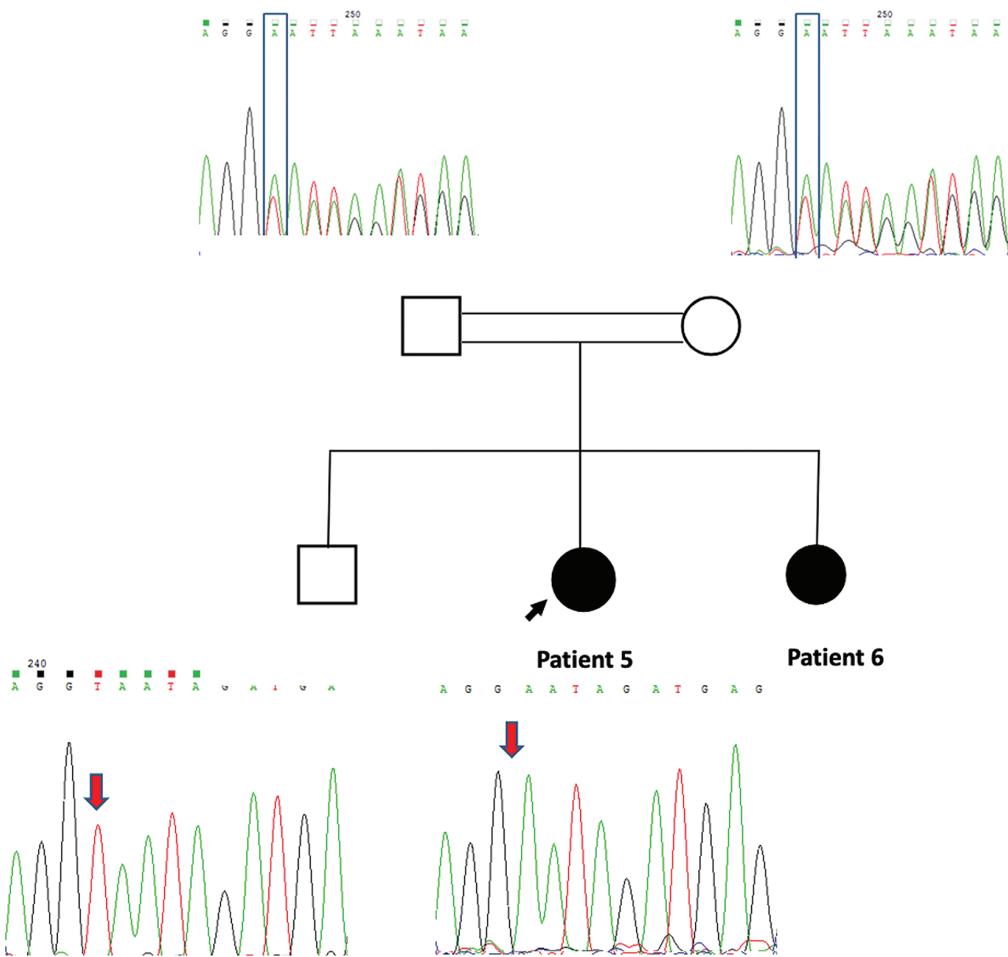
Figure 3. Pedigree of family 3 including Patient 5 and Patient 6 with homozygous novel frameshift variant, c.779del, p.Tyr260SerfsTer11, father and mother is heterozygous for this variant and the brother does not carry this variant and does not have any corneal signs or symptoms.

these pathologies (35-37). Furthermore, ED-DBP is reported to be technically simpler and less expensive than excimer laser PTK (38). Hieda et al. (39) reported that, after PTK combined with soft contact lens wear, the mean time to significant recurrence of GDLD was approximately 10 years. In contrast, Ozbek et al. (40) observed recurrence as early as two years after PTK without contact lens use, a recurrence interval comparable to that observed after ED-DBP in our cohort (Table 3).

Reports on long-term follow-up of GDLD patients are limited in the literature, and generally describe recurrent surgical interventions during the disease course. In our cohort, the longest follow-up period was 21 years, observed in patient 1, who underwent multiple ED-DBP procedures in the right eye and repeated PKPs in the left eye and had a BCVA of 0.1 in the better-seeing eye at the last visit. The longest follow-up reported in the literature is that of a Turkish patient, lasting 15 years, who required repeated PKPs and achieved a BCVA of 0.2 at the final examination (25). During follow-up, several of our GDLD patients required repeated keratoplasties, consistent with previous reports (Table 3). Recurrence rates after keratoplasty in GDLD have been reported as high as 50–70% within two years, and up to 97% within four years (1,12). To reduce recurrence, LSCT

combined with keratoplasty has been reported to maintain corneal clarity and improve vision for up to two years 41,42. However, this technique has not gained routine clinical use due to complications such as severe glaucoma, the requirement for aggressive immunosuppression, and the need for repeat LSCT in failed cases (41,42). In the present study, LSCT was not performed on any of our GDLD patients.

Study Limitations

This study has several limitations. First, genetic testing could not be performed on all patients, and additional genetic analyses for those with negative Sanger sequencing results were unavailable. Second, histopathological evaluation of corneal specimens could not be performed on any patient. Third, statistical comparisons could not be performed due to the limited sample size. Finally, the pathogenicity of the novel variant was assessed only by *in silico* prediction methods.

CONCLUSION

In conclusion, this study represents the first report of GDLD patients from Central Anatolia and provides the most comprehensive clinical

Gazi Med J 2026;37(1):56-64

Yaylacıoğlu Tuncay et al. Gelatinous Drop-Like Corneal Dystrophy in Türkiye

and genetic characterization of Turkish GDLD patients to date. Our findings expand the mutational spectrum of *TACSTD2* in GDLD by identifying a novel variant and underscore the importance of genetic analyses of patients from diverse populations to better understand allelic and phenotypic heterogeneity. Furthermore, ED-DBP is proposed as a potential treatment modality for GDLD, particularly for cases with superficial deposits in both native corneas and grafts.

Ethics

Ethics Committee Approval: This retrospective study was approved by the Institutional Ethics Review Board of Gazi University (approval number: 2025–405/04, date: 11.03.2025) and conducted in accordance with the principles of the Declaration of Helsinki.

Informed Consent: Retrospective study.

Footnotes

Authorship Contributions

Surgical and Medical Practices: A.Y.Ü., M.C.Ö., B.A., Concept: F.Y.T., H.D., A.Y.Ü., M.C.Ö., B.A., Design: F.Y.T., H.D., A.Y.Ü., M.C.Ö., B.A., Data Collection or Processing: F.Y.T., H.D., A.Y.Ü., Analysis or Interpretation: F.Y.T., A.Y.Ü., M.C.Ö., B.A., Literature Search: F.Y.T., Writing: F.Y.T.

Conflict of Interest: No conflict of interest was declared by the authors.

Financial Disclosure: The authors declared that this study received no financial support.

REFERENCES

1. Fujiki K, Nakayasu K, Kanai A. Corneal dystrophies in Japan. J Hum Genet. 2001; 46: 431–5.

2. Santo RM, Yamaguchi T, Kanai A, Okisaka S, Nakajima A. Clinical and histopathologic features of corneal dystrophies in Japan. Ophthalmology. 1995 Apr;102(4):557-67. doi:10.1016/S0161-6420(95)30982-7. Available from: https://pubmed.ncbi.nlm.nih.gov/7724173/

3. Paliwal P, Gupta J, Tandon R, Sharma N, Titiyal JS, Kashyap S, et al. Identification and characterization of a novel TACSTD2 mutation in gelatinous drop-like corneal dystrophy. Mol Vis. 2010; 16: 729–39.

4. Maimaitiming R, Zhao R, Ding L, Ailimu M, Qin Y, Yasin G, et al. A Novel homozygous non-sense mutation in TACSTD2 gene causes gelatinous drop-like corneal dystrophy in a chinese consanguineous family: a case report and literature review. Cornea. 2025; 44: 1026–32.

5. Masmali A, Alkanaan A, Alkatan HM, Kirat O, Almutairi AA, Almubrad T, et al. Clinical and ultrastructural studies of gelatinous drop-like corneal dystrophy (GDLD) of a patient with TACSTD2 gene mutation. J Ophthalmol. 2019; 2019: 5069765.

6. Alavi A, Elahi E, Tehrani MH, Amoli FA, Javadi MA, Rafati N, et al. Four mutations (three novel, one founder) in TACSTD2 among Iranian GDLD patients. Invest Ophthalmol Vis Sci. 2007; 48: 4490–7.

7. Cabral-Macias J, Zenteno JC, Ramirez-Miranda A, Navas A, Bermudez-Magner JA, Boullosa-Graña VM, et al. Familial gelatinous drop-like corneal dystrophy caused by a novel non-sense TACSTD2 mutation. Cornea. 2016; 35: 987–90.

8. Morantes S, Evans CJ, Valencia AV, Davidson AE, Hardcastle AJ, Ruiz Linares A, et al. Spectrum of clinical signs and genetic characterization of gelatinous drop-like corneal dystrophy in a colombian family. Cornea. 2016; 35: 1141–6.

9. Markoff A, Bogdanova N, Uhlig CE, Groppe M, Horst J, Kennerknecht I. A novel TACSTD2 gene mutation in a Turkish family with a gelatinous drop-like corneal dystrophy. Mol Vis. 2006; 12: 1473–6.

10. Ren Z, Lin PY, Klintworth GK, Iwata F, Munier FL, Schorderet DF, et al. Allelic and locus heterogeneity in autosomal recessive gelatinous drop-like corneal dystrophy. Hum Genet. 2002; 110: 568–77.

11. Kawasaki S, Kinoshita S. Clinical and basic aspects of gelatinous drop-like corneal dystrophy. Dev Ophthalmol. 2011; 48: 97–115.

12. Kaza H, Barik MR, Reddy MM, Mittal R, Das S. Gelatinous drop-like corneal dystrophy: a review. Br J Ophthalmol. 2017; 101: 10–5.

13. Weber FL, Babel J. Gelatinous drop-like dystrophy. A form of primary corneal amyloidosis. Arch Ophthalmol. 1980; 98: 144–8.

14. Ide T, Nishida K, Maeda N, Tsujikawa M, Yamamoto S, Watanabe H, et al. A spectrum of clinical manifestations of gelatinous drop-like corneal dystrophy in japan. Am J Ophthalmol. 2004; 137: 1081–4.

15. Azher TN, Maltry AC, Hou JH. Staged limbal stem cell transplantation and keratoplasty surgeries as a treatment for gelatinous drop-like corneal dystrophy. GMS Ophthalmol Cases. 2023; 13: Doc02.

16. Movahedan H, Anvari-Ardekani HR, Nowroozzadeh MH. Limbal stem cell transplantation for gelatinous drop-like corneal dystrophy. J Ophthalmic Vis Res. 2013; 8: 107–12.

17. Lekhanont K, Jongkhajornpong P, Chuephanich P, Inatomi T, Kinoshita S. Boston type 1 keratoprosthesis for gelatinous drop-like corneal dystrophy. Optom Vis Sci. 2016; 93: 640–6.

18. Tsujikawa M, Kurahashi H, Tanaka T, Nishida K, Shimomura Y, Tano Y, et al. Identification of the gene responsible for gelatinous drop-like corneal dystrophy. Nat Genet. 1999; 21: 420–3.

19. Ren Z, Lin PY, Klintworth GK, Iwata F, Munier FL, Schorderet DF, et al. Allelic and locus heterogeneity in autosomal recessive gelatinous drop-like corneal dystrophy. Hum Genet. 2002; 110: 568–77.

20. Takaoka M, Nakamura T, Ban Y, Kinoshita S. Phenotypic investigation of cell junction-related proteins in gelatinous drop-like corneal dystrophy. Invest Ophthalmol Vis Sci. 2007; 48: 1095–101.

21. Nakatsukasa M, Kawasaki S, Yamasaki K, Fukuoka H, Matsuda A, Tsujikawa M, et al. Tumor-associated calcium signal transducer 2 is required for the proper subcellular localization of claudin 1 and 7: implications in the pathogenesis of gelatinous drop-like corneal dystrophy. Am J Pathol. 2010; 177: 1344–55.

22. Tasaki M, Ueda M, Matsumoto K, Kawaji T, Misumi Y, Eiki D, et al. Clinico-histopathological and biochemical analyses of corneal amyloidosis in gelatinous drop-like corneal dystrophy. Amyloid. 2015; 22: 67–9.

23. Ohnishi Y, Shinoda Y, Ishibashi T, Taniguchi Y. The origin of amyloid in gelatinous drop-like corneal dystrophy. Curr Eye Res. 1982-1983; 2: 225–31.

24. Küchlin S, Maier PC, Reinhard T, Auw-Hädrich C. Gelatinous Drop-Like Corneal Dystrophy - 2 Clinical Cases. Klin Monbl Augenheilkd. 2020; 237: 841–5.

25. Uhlig CE, Groppe M, Busse H, Saeger W. Morphological and histopathological changes in gelatinous drop-like corneal dystrophy during a 15-year follow-up. Acta Ophthalmol. 2010; 88: e273–4.

26. Markoff A, Bogdanova N, Uhlig CE, Groppe M, Horst J, Kennerknecht I. A novel TACSTD2 gene mutation in a Turkish family with a gelatinous drop-like corneal dystrophy. Mol Vis. 2006; 12: 1473–6.

27. Büchi ER, Daicker B, Uffer S, Gudat F. Primary gelatinous drop-like corneal dystrophy in a white woman. A pathologic, ultrastructural, and immunohistochemical study. Cornea. 1994; 13: 190–4.

28. Nagahara Y, Tsujikawa M, Takigawa T, Xu P, Kai C, Kawasaki S, et al. A novel mutation in gelatinous drop-like corneal dystrophy and functional analysis. Hum Genome Var. 2019; 6: 33.

Gazi Med J 2026;37(1):56-64

Yaylacıoğlu Tuncay et al. Gelatinous Drop-Like Corneal Dystrophy in Türkiye

29. Alehabib E, Jamshidi J, Ghaedi H, Emamalizadeh B, Andarva M, Daftarian N, et al. Novel mutations in TACSTD2 gene in families with gelatinous drop-like corneal dystrophy (GDLD). Int J Mol Cell Med. 2017; 6: 204–11.

30. Masmali A, Alkanaan A, Alkatan HM, Kirat O, Almutairi AA, Almubrad T, et al. Clinical and ultrastructural studies of gelatinous drop-like corneal dystrophy (GDLD) of a patient with TACSTD2 gene mutation. J Ophthalmol. 2019; 2019: 5069765.

31. Tsujikawa M, Maeda N, Tsujikawa K, Hori Y, Inoue T, Nishida K. Chromosomal sharing in atypical cases of gelatinous drop-like corneal dystrophy. Jpn J Ophthalmol. 2010; 54: 494–8.

32. Akiya S, Nagaya K, Fukui A, Hamada T, Takahashi H, Furukawa H. Inherited corneal amyloidosis predominantly manifested in one eye. Ophthalmologica. 1991; 203: 204–7.

33. Yajima T, Fujiki K, Murakami A, Nakayasu K. [Gelatinous drop-like corneal dystrophy: mutation analysis of membrane component, chromosome 1, surface marker 1]. Nippon Ganka Gakkai Zasshi. 2002; 106: 265–72.

34. Alavi A, Elahi E, Amoli FA, Tehrani MH. Exclusion of TACSTD2 in an Iranian GDLD pedigree. Mol Vis. 2007; 13: 1441–5.

35. Yang Y, Mimouni M, Trinh T, Sorkin N, Cohen E, Santaella G, et al. Phototherapeutic keratectomy versus epithelial debridement combined with anterior stromal puncture or diamond burr for recurrent corneal erosions. Can J Ophthalmol. 2023; 58: 198–203.

36. Vo RC, Chen JL, Sanchez PJ, Yu F, Aldave AJ. Long-term outcomes of epithelial debridement and diamond burr polishing for corneal epithelial irregularity and recurrent corneal erosion. Cornea. 2015; 34: 1259–65.

37. Suri K, Kosker M, Duman F, Rapuano CJ, Nagra PK, Hammersmith KM. Demographic patterns and treatment outcomes of patients with recurrent corneal erosions related to trauma and epithelial and Bowman layer disorders. Am J Ophthalmol. 2013; 156: 1082-7.e2.

38. Tzelikis PF, Rapuano CJ, Hammersmith KM, Laibson PR, Cohen EJ. Diamond burr treatment of poor vision from anterior basement membrane dystrophy. Am J Ophthalmol. 2005; 140: 308–10.

39. Hieda O, Kawasaki S, Yamamura K, Nakatsukasa M, Kinoshita S, Sotozono C. Clinical outcomes and time to recurrence of phototherapeutic keratectomy in Japan. Medicine (Baltimore). 2019; 98: e16216.

40. Ozbek Z, Akbulut Yagci B, Yuksel B, Durak I. Long-term management of gelatinous droplet dystrophy with phototherapeutic keratectomy and toric soft contact lenses. Eur Eye Res. 2023; 3: 32–5.

41. Shimazaki J, Shimmura S, Tsubota K. Limbal stem cell transplantation for the treatment of subepithelial amyloidosis of the cornea (gelatinous drop-like dystrophy). Cornea. 2002; 21: 177–80.

42. Movahedan H, Anvari-Ardekani HR, Nowroozzadeh MH. Limbal stem cell transplantation for gelatinous drop-like corneal dystrophy. J Ophthalmic Vis Res. 2013; 8: 107–12.

Effects of Lavender Oil on Wound Healing in an Experimental Diabetes Model in Rats: A Randomized Controlled Trial

Deneysel Diyabet Modeli Oluşturulmuş Ratlarda Lavanta Yağının Yara İyileşmesine Etkisi: Randomize Kontrollü Bir Çalışma

Ⓘ Merve Gülpak[1], Ⓘ Özlem Ovayolu[2], Ⓘ Atila Yoldaş[3], Ⓘ Aslı Yaylalı[4]

[1]Department of Nursing and Internal Medicine Nursing, Kahramanmaraş Sütçü İmam University Faculty of Health Sciences, Kahramanmaraş, Türkiye
[2]Department of Nursing and Internal Medicine Nursing, Gaziantep University Faculty of Health Sciences, Gaziantep, Türkiye
[3]Department of Anatomy, Kahramanmaraş Sütçü İmam University Faculty of Medicine, Kahramanmaraş, Türkiye
[4]Department of Histology and Embryology, Kahramanmaraş Sütçü İmam University Faculty of Medicine, Kahramanmaraş, Türkiye

ABSTRACT

Objective: Lavender oil has antimicrobial, anti-inflammatory, analgesic properties as well as beneficial activities on wound healing. This study aims to determine the effect of lavender oil on wound healing in an experimental diabetes model in rats.

Methods: This randomized controlled experiment included three diabetic and three non-diabetic groups of 42 male Wistar albino rats. A 12-mm-diameter, full-thickness wound was created on the backs of the rats. Lavender oil, Madecassol, and 0.9% sodium chloride [normal saline (NS)] were applied as wound dressings. During macroscopic evaluation of wound healing, wound-healing percentage was calculated using the Walker formula, and wound area was determined using the ImageJ image analysis program. For microscopic evaluation, the tissue samples were taken from the rats on days 1, 7, and 14. Hematoxylin-Eosin staining findings and the distributions of vascular endothelial growth factor-A (VEGFA), collagen-I, and collagen-III were determined.

Results: In all groups, the highest wound-healing percentage and the lowest wound-area measurements were observed in those treated with lavender oil. Lavender oil increased inflammatory cell infiltration and angiogenesis, and accelerated granulation tissue formation and re-epithelialization. The VEGFA and collagen-III levels on day 7, and the collagen-I levels on day 14, were highest in those treated with lavender oil. Although rats treated with lavender oil differed significantly from those treated with NS in wound healing, there was no difference between rats treated with Madecassol and those treated with lavender oil.

ÖZ

Amaç: Lavanta yağı, antimikrobiyal, antiinflamatuar, analjezik özelliklerinin yanı sıra yara iyileşmesi üzerinde de yararlı etkilere sahiptir. Bu çalışmanın amacı deneysel diyabet modeli oluşturulmuş ratlarda lavanta yağının yara iyileşmesi üzerine etkisini belirlemektir.

Yöntemler: Bu randomize kontrollü deneysel çalışmada, 42 erkek Wistar albino sıçandan oluşan üç diyabetik ve üç diyabetik olmayan grup yer almaktadır Sıçanların sırtlarına 12 mm çapında, tam kalınlıkta yara oluşturuldu. Lavanta yağı, Madecassol ve %0,9 sodyum klorür [serum fizyolojik (SF)] yaralara uygulandı. Yara iyileşmesinin makroskobik değerlendirilmesinde; Walker formülüyle yara iyileşme yüzdesi ve ImageJ görüntü analizi programıyla yara alanları hesaplandı. Mikroskobik değerlendirmede; 1., 7., 14. günlerde sıçanlardan doku örnekleri alındı. Hematoksilen-Eozin boyama bulguları ve vascular endothelial growth factor-A (VEGFA), kollajen-I, kollajen-III dağılımları belirlendi.

Bulgular: Tüm gruplarda en yüksek yara iyileşme yüzdesi ve Image J ölçümlerinde en düşük yara alanının, lavanta yağıyla pansumanı yapılan gruplarda olduğu saptandı. Lavanta yağının; inflamatuar hücre infiltrasyonunu ve anjiyogenezisi arttırdığı, granülasyon doku oluşumunu ve reepitelizasyonu hızlandırdığı belirlendi. 7. günde VEGFA, kollajen-III, 14.günde ise kollajen-I düzeyinin en yüksek lavanta yağı uygulanan gruplarda olduğu saptandı. Yara iyileşmesi açısından lavanta yağı-SF grupları arasında anlamlı farklılık saptanırken, madecassol-lavanta arasında fark olmadığı belirlenmiştir.

Address for Correspondence/Yazışma Adresi: Merve Gülpak, Department of Nursing and Internal Medicine Nursing, Kahramanmaraş Sütçü İmam University Faculty of Health Sciences, Kahramanmaraş, Türkiye
E-mail / E-posta: mervegulpak@ksu.edu.tr
ORCID ID: orcid.org/0000-0003-0585-3160

Gazi Med J 2026;37(1):65-77

Gülpak et al. Lavender Oil and Diabetic Wound Healing

ABSTRACT

Conclusions: On both macroscopic and microscopic examination, dressing with lavender oil was effective in promoting wound healing in all groups.

Keywords: Diabetic foot, lavender oil, rats, wound care, nursing

ÖZ

Sonuç: Lavanta yağıyla pansumanın tüm gruplarda makroskopik ve mikroskobik olarak yara iyileşmesinde etkili olduğu belirlendi.

Anahtar Sözcükler: Diyabetik ayak, lavanta yağı, sıçanlar, yara bakımı, hemşirelik

INTRODUCTION

Diabetes mellitus (DM) is a chronic disease characterized by major abnormalities in carbohydrate, fat, and protein metabolism, resulting from the hormone insulin (1,2). DM is a progressive disease, and uncontrolled DM can lead to acute and chronic complications (3). One of these complications is the diabetic foot, which can develop in association with neuropathy, peripheral arterial disease, infection, and immune system disorders (4,5). Although the negative effects of diabetes on wound healing cannot be fully explained, hyperglycemia is thought to affect this process due to factors such as impaired collagen synthesis; decreased fibroblast proliferation and reduced growth factor production; increased apoptosis of cells within scar tissue; impaired angiogenesis; defective granulation tissue formation; and increased risk of infection due to decreased chemotaxis and phagocytosis (3,6,7). To prevent pathogen proliferation and to enable debridement of necrotic tissue, treatments currently used for wound healing include application of antimicrobial agents. Although applied simultaneously, the effects of both treatments are not permanent (6). Topical application of compounds containing antioxidants will be beneficial, especially for wound healing and protection of tissues against oxidative damage. Furthermore, certain plant species can be used to treat both acute and chronic wounds (8). Lavender is one of these medicinal plants, and its oil is known to have antimicrobial, anti-inflammatory, and analgesic properties, as well as beneficial biological activities in wound healing. Studies have concluded that the chemical components in lavender oil, such as α-borneol, α-terpinene, terpinen-4-ol, α-terpineol, linalyl acetate, and linalool, are effective in wound healing (9–11). A review of the evidence on the effects of lavender oil on wound healing found that wounds treated with lavender oil exhibited an increased healing rate, elevated collagen expression, and enhanced activity of proteins involved in tissue remodeling (12). Additionally, lavender oil has the potential to accelerate the formation of granulation tissue, remodel the tissue through collagen replacement, and support wound healing by promoting early wound contractions mediated by transforming growth factor beta (TGF-β) (13). This study aimed to assess the effect of lavender oil on the healing of diabetic wounds. Teamwork is essential to the healing of diabetic wounds. Among the team members, nurses play a central role as the primary providers of care (14). Currently, the discipline of nursing is producing new high-quality evidence on care through rigorous research. In this context, the use of experimental animals in nursing constitutes research that strengthens evidence-based nursing knowledge, advances the development of nursing practices, and fosters innovation in nursing (15). Because wound care is one of the primary responsibilities of nurses, it is considered a basic research topic. For this reason, it is essential to conduct various studies in nursing science, including animal (preclinical) and clinical research. This study aimed to evaluate the effects of lavender oil on wound healing in an experimental rat model of diabetes.

MATERIALS AND METHODS

Animal Experimentation and Study Groups

In this study, Wistar albino male rats aged 4–5 months, with an average weight of 250–350 g, were used. These rats were obtained from the Kahramanmaraş Sütçü İmam University, Faculty of Medicine, Experimental Research Laboratory. During the experiment, the rats were housed in rooms with a 12-h light/dark cycle, at a room temperature of 22°C±2°C and a humidity level of 45%–50%, and were provided with tap water and a standard portion of pellet food. With the alpha level (type I error) set at 0.05 and the power set at 0.80 in the statistical power analysis, the required sample size was 48. The effect size was interpreted using Cohen's criteria (17). The study consisted of three diabetic and three non-diabetic groups. The rats were randomly assigned to the groups using the Research Randomizer software (https://www.randomizer.org/) (16). Due to anesthesia complications, six rats died: some during wound dehiscence and others after tissue removal on the seventh day. The study included 42 rats.

Non-DM-normal saline (NS), (n = 7): The dressing was applied daily with 0.9% sodium chloride (NaCl) solution.

Non-DM-lavender oil (n = 7): The dressing was applied with 0.5 mL of lavender oil daily.

Non-DM-madecassol, (n = 7): For the positive control, the dressing was treated with 0.5 g of Madecassol ointment daily.

DM-NS, n = 7: The dressing was applied daily using 0.9% NaCl solution.

DM-lavender oil, (n = 7): The dressing was applied with 0.5ml lavender oil every day

DM-madecassol (n = 7): The dressing was applied using 0.5 g of Madecassol ointment daily.

Development of Experimental Diabetes Model and Incisional Wound Model

To develop the diabetes model, streptozotocin (Sigma-Aldrich, Germany) was administered intraperitoneally to rats at a dose of 60 mg/kg after 18 h of food deprivation. Rats with blood glucose levels > 250 mg/dL, measured from the tail vein 48 h after induction, were considered diabetic (18). The rats were weighed sequentially, and, after determining the appropriate doses from their weights, they were induced. Plasma glucose levels were measured from the tail vein 24 hours after induction, and rats with levels of 250 mg/dL or higher were considered diabetic. No action was taken in the non-DM groups. To develop the wound model, rats were anesthetized intraperitoneally with xylazine (10 mg/kg) and ketamine (50 mg/kg). The rats' dorsal hair was shaved without damaging the skin, which was then cleaned with a povidone-iodine solution.

Gazi Med J 2026;37(1):65-77

Gülpak et al. Lavender Oil and Diabetic Wound Healing

Three full-thickness skin-defect wounds, each 12 mm in diameter and containing the panniculus carnosus muscle, were created by punch biopsy; the dorsal midline wounds were separated by at least 15 mm. To avoid impairing the evaluation of wound healing when tissue was taken on days 1, 7, and 14, three wounds were opened in each rat. The day the wounds were created was considered day 0, and wound care was provided for 14 days.

Wound Care Materials and Dressing Application

Lavender oil (Lavandula angustifolia L., natural), with a density of 0.879 g/mL at 25°C, was obtained from Sigma-Aldrich (Germany). This natural lavender oil, whose stability and quantification tests were performed by the company, was applied locally to the wounds. Prior to application of lavender oil to the wounds, potential irritant effects were evaluated, and no allergic or irritant reactions were detected. As a positive control and consistent with the literature, Madecassol pomade (Bayer, Germany) was used as a reference drug (19,20). Madecassol is an ointment derived from the extract of Centella asiatica, a medicinal plant that accelerates connective tissue and prevents scars formation (21). The NS solution provided by Eczacıbaşı/Baxter (Türkiye) was used as a negative control. The rats were dressed at the same time each day for 14 days. In the DM and non-DM groups, 0.5 mL lavender oil and 0.5 g Madecassol pomade were applied topically to the wounds with a sterile sponge, and the NS was applied dropwise to the wounds. The wounds were left open after the application. At the end of the study, the rats were euthanized by an overdose of anesthetic.

Data Collection Method

Research data were obtained from day 0 (wound creation) to day 14 (study completion). In this study, wound healing data were collected macroscopically and microscopically. For macroscopic examination, after the rats' wounds were identified, wound measurements were obtained using a digital caliper on days 3, 5, 7, 11, and the percentage of healing was calculated using the Walker formula given below.

Walker Formula

% wound area = (Wound area on day X/Wound area on day 0) × 100.

Wound area closure percentage on day X = 100%–% unclosed wound area.

Additionally, the wound was photographed on days 3, 5, 7, 11, and 14 using a digital camera, and the wound area was measured using the ImageJ image analysis program. ImageJ is a Java-based image-processing program available free of charge for public use at https://imagej.nih.gov/ij/download.html. The calculations and results of the program are internationally recognized and may be used in scientific studies (22–24).

For the microscopic examination, one-fourth of the tissue samples were taken from the wounds of the rats in all groups on days 1,7 and 14. Some tissue samples taken for light microscopic examination were stained with Hematoxylin–eosin (H&E), while other sections were stained for vascular endothelial growth factor A (VEGFA) (Abcam, England), collagen-I (Abcam, England), and collagen-III (Abcam, England) by the indirect immunoperoxidase method to determine their distribution.

H&E Staining

The tissues taken from the wound sites were subjected to routine tissue processing after 48 h of fixation in a 10% neutral-buffered formalin solution. The tissues were blocked, sectioned at 5 μm, and stained with H&E for examination by light microscopy. Parameters used to evaluate wound healing on histopathological examination were scored using the method of Galeano et al. (25,26).

Indirect Immunoperoxidase Staining

Tissue sections 5-μm thick taken from the wound areas were placed on polylysine-coated slides and incubated at 60 °C for 1 h for immunohistochemical staining. Then two changes of xylene clearing, 30 min each, were performed. They were further rehydrated through a graded alcohol series and then held in distilled water for 10 min. To inhibit endogenous tissue peroxidase, the sections incubated in Dakopen solution for 15 min at room temperature were treated with 3% H_2O_2 for 5 min. The sections were washed three times for 5 min each with phosphate-buffered saline and then treated with a blocking solution for 10 min. After the blocking solution was removed from the tissue, the sections were incubated overnight with primary antibodies against VEGFA, collagen-I, and collagen-III. The following day, the sections were washed three times with phosphate-buffered saline and then stained with secondary antibodies against VEGFA, collagen-I, and collagen-III for 30 min each. To detect the visibility of the immunohistochemical reaction, the sections that were washed three times with phosphate-buffered saline for 5 min each wash were also stained with 3-Amino-9-ethylcarbazolefor 5min. After the background staining was completed with Mayer's hematoxylin, the sections were washed with distilled water for 10 min and covered with a mounting medium. After indirect immunohistochemistry, the samples are evaluated by the histology technician and scored as following; no findings of immunoreactivities "0", partial/slight "1", complete but immature or mild "2", complete and mature/moderately rated"3", and severe "4" (25,26).

Ethical Dimensions of the Research

Consistent with the Declaration of Helsinki, developed by the World Medical Association and with the Regulation on the Working Procedures and Principles of Animal Experiments Ethics Committees (dated: 07.06.2006, number: 26220), the researcher received the Certification of Experimental Animal Usage following training of the personnel involved in the use of animals for experimental research. Prior to conducting the research, approval was obtained from Kahramanmaraş Sütçü İmam University Experimental Animals Ethics Committee on June 6, 2018 (session number: 2018/08; decision number: 05). Informed consent was not applicable, as this study did not involve human participants and was conducted using experimental animals.

Statistical Analysis

The data obtained from the study were entered into SPSS version 22.0 (SPSS Inc, Chicago, IL, USA) for statistical analyses. Data were analyzed with parametric tests when assumptions of normality were met, and with non-parametric tests when those assumptions were not met. Student's t-test and the Mann-Whitney U test were used to examine differences between the two groups, depending on the results of the normality test. For comparisons among multiple groups,

Gazi Med J 2026;37(1):65-77

Gülpak et al. Lavender Oil and Diabetic Wound Healing

the Kruskal–Wallis test was used when the data were not normally distributed; post hoc tests were used for pairwise comparisons. In the statistical analysis, the level of significance was set at p < 0.05.

RESULTS

Macroscopic Results

During macroscopic examination on days 3, 5, 7, 11, and 14, the healing percentage was calculated using the Walker formula, and the wound area was measured with the ImageJ image-analysis program. By day 14, among the groups, rats whose wounds were dressed with lavender oil had the highest wound-healing percentage. A significant difference between the NS and Lavender groups was observed in the diabetic group on days 5, 7, 11, and 14, and in the non-DM group on days 5, 11, and 14 (p < 0.05). Similar wound-healing percentages were observed in the control groups treated with Madecassol and Lavender. On all days, as measured using the ImageJ program, the lowest wound area was observed in the lavender oil group, and the highest average wound area was observed in the groups dressed with NS. Significant differences were observed between the DM and non-DM groups on day 7, between the NS and Lavender groups on days 11 and 14, and between the Lavender group and the other groups. ImageJ measurements showed significant differences between the NS and Lavender groups on day 7 within both the DM and non-DM groups, and between the Lavender group and the other groups on days 11 and 14 (Figure 1; p <0.05). There were no complications or infections in the wounds (Figure 2).

Microscopic Results

Microscopic examination for the study was performed by the histology technician. The parameters for each tissue on H&E staining, including inflammatory cell infiltration, increase in granulation tissue, angiogenesis, and levels of re-epithelialization, were considered. On the first day, the highest level of inflammatory cell infiltration was measured in the DM and non-DM groups treated with lavender oil. Formation of granulation tissue, angiogenesis, and re-epithelialization were not observed on day 1 in any group(s). For Granulation tissue formation on day 14, the highest mean score was observed in the DM-Madecassol, DM-Lavender, and non-DM-Lavender groups. The highest mean angiogenesis score was observed in the groups treated with lavender oil on days 7 and 14. The highest mean level of re-epithelialization was observed in the groups dressed with lavender oil on day 7, and in the DM-Madecassol, DM-Lavender, and non-DM-Lavender groups on day 14 (Table 1, Figure 3). VEGFA, collagen-I, and collagen-III levels were evaluated in tissues stained with indirect immunoperoxidase. On days 7 and 14, the highest mean VEGFA level was observed in the groups dressed with lavender oil. When collagen-I levels were evaluated, the highest mean across all days was observed in the DM-Lavender and non-DM-Lavender groups. The highest mean collagen-III level was observed in the groups dressed with lavender oil on day 7. The lowest mean score was observed in the NS groups on day 14 (Table 2; Figures 4–6).

DISCUSSION

Previous studies evaluated the effects of lavender oil on wound healing, but the effects on diabetic wounds were not examined

(3,10,12,13,27,28). Studies have shown that lavender oil stimulates wound contraction and skin regeneration by increasing activities of antioxidant enzymes; accelerates the development of granulation tissue, collagen replacement, and wound closure; and may support wound repair by promoting early wound contraction via TGF-β (10,12,13). Given these characteristics, lavender oil is thought to accelerate wound healing. In this study, rats treated with lavender oil had the highest wound-healing percentages and the lowest wound-area measurements at 14 days compared with other groups (Figure 1).

Reduction of inflammatory cells in diabetic individuals increases susceptibility to wound infection, and prolongation of the inflammatory phase further delays wound healing (3,6). Mori et al. (13) reported that topical application of lavender oil induced inflammation in wound lesions. In a study by Koca Kutlu et al. (27) on wound healing in rats, the authors found no signs of local infection in groups treated with lavender oil. However, to our knowledge, no study in the available literature has examined the effects of lavender oil on diabetic wounds. In this study, lavender oil showed the highest level of inflammatory cell infiltration on day 1 across all groups, whereas on day 7 the highest level was observed in groups dressed with Madecassol. Nevertheless, there was no significant difference between the groups on day 7. On day 14, the lowest mean scores were measured in the DM-Lavender and non-DM-Madecassol groups. These findings show that lavender oil produces results consistent with the positive control and with the literature, and that it affects inflammatory cell infiltration.
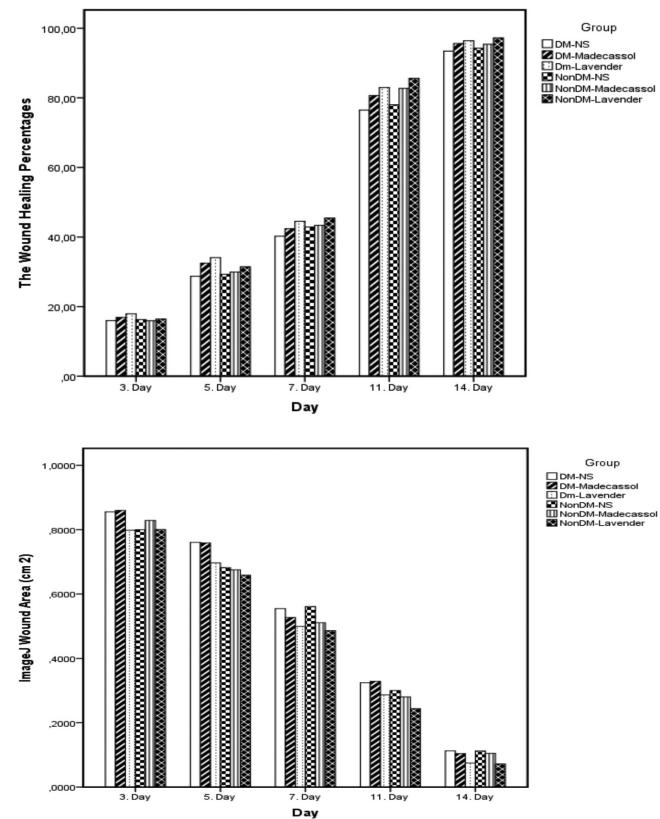

Figure 1. Walker formula, The Wound Healing Percentages and ImageJ Wound Area (cm²)

Gazi Med J 2026;37(1):65-77

Gülpak et al. Lavender Oil and Diabetic Wound Healing

Table 1. Hematoxylin-eosin staining results.

	Group	1 day	7 day	14 day
İnflammatory cell infiltration	DM-NS (n = 7)	0.86 ± 0.69	1.71 ± 0.76	1.86 ± 0.69d
	DM-Madecassol (n = 7)	0.86 ± 0.69	2.43 ± 0.98	1.57 ± 0.53d
	DM-lavender (n = 7)	1.14 ± 0.69	1.86 ± 0.69	0.43 ± 0.53
	Non-DM-NS (n = 7)	1.57 ± 0.53	2.71 ± 1.11	1.71 ± 0.49
	Non-DM-Madecassol (n = 7)	2.29 ± 1.11[a]	2.86 ± 0.69	0.29 ± 0.49[a,c]
	Non-DM-lavender (n = 7)	2.43 ± 0.98[a]	2.71 ± 0.76	0.43 ± 0.53[a,c]
Granulation tissue increase	DM-NS (n = 7)	0.0 ± 0.0	1.57 ± 0.98	1.57 ± 0.53
	DM-Madecassol (n = 7)	0.0 ± 0.0	3.00 ± 0.82[b]	2.86 ± 0.90[b]
	DM-lavender (n = 7)	0.0 ± 0.0	3.00 ± 0.82[b]	2.86 ± 0.90[b]
	Non-DM-NS (n = 7)	0.0 ± 0.0	2.57 ± 1.13	2.71 ± 1.11[a]
	Non-DM-Madecassol (n = 7)	0.0 ± 0.0	3.71 ± 0.49[a]	2.86 ± 0.69[a]
	Non-DM-lavender (n = 7)	0.0 ± 0.0	3.71 ± 0.49[a]	3.14 ± 0.69[a]
Angiogenesis	DM-NS (n = 7)	0.0 ± 0.0	0.71 ± 0.49[d]	0.71 ± 0.49
	DM-Madecassol (n = 7)	0.0 ± 0.0	0.86 ± 0.69[d]	2.29 ± 1.11[b]
	DM-lavender (n = 7)	0.0 ± 0.0	1.57 ± 0.53	2.43 ± 0.98[b]
	Non-DM-NS (n = 7)	0.0 ± 0.0	1.57 ± 0.53[a]	2.14 ± 0.69[a]
	Non-DM-Madecassol (n = 7)	0.0 ± 0.0	1.57 ± 0.53[a]	3.29 ± 0.76[a,c]
	Non-DM-lavender (n = 7)	0.0 ± 0.0	1.71 ± 0.49[a]	3.29 ± 0.95[a,c]
Re-epithelialization	DM-NS (n = 7)	0.0 ± 0.0	0.14 ± 0.38	1.57 ± 0.79
	DM-Madecassol (n = 7)	0.0 ± 0.0	0.86 ± 0.69	3.29 ± 0.76[b]
	DM-lavender (n = 7)	0.0 ± 0.0	1.29 ± 0.76[b]	3.29 ± 0.76[b]
	Non-DM-NS (n = 7)	0.0 ± 0.0	0.86 ± 0.69[a]	2.43 ± 0.53
	Non-DM-Madecassol (n = 7)	0.0 ± 0.0	0.86 ± 0.69[a]	3.43 ± 0.53[a,c]
	Non-DM-lavender (n = 7)	0.0 ± 0.0	1.43 ± 0.53[a]	3.71 ± 0.49[a,c]

[a]: The difference between the DM-NS group and the non-DM group on the specified days was p < 0.05.

[b]: The difference between the DM-NS group and the other diabetic groups on the specified days was p < 0.05.

[c]: The difference between the non-DM-NS group and the other non-DM groups on the specified days was p < 0.05.

[d]: The difference between the DM-Lavender and diabetic groups on the specified days was p < 0.05.

Granulation tissue begins to form during the proliferation phase of wound healing, approximately 4 days after the lesion, providing the basis for the remodeling and maturation phase (29,30). In this study, because granulation tissue development began during the proliferative phase, no granulation tissue was observed on the first day. High blood glucose levels impair fibroblast formation and collagen synthesis, causing impaired development of granulation tissue. Therefore, in diabetic individuals, wound healing is impaired and the wound closure time is prolonged (3,6,31). Lavender oil accelerates the development of granulation tissue in the early stages and promotes tissue remodeling through collagen replacement (13). In dogs with wounds dressed with lavender oil, the proliferative phase had an earlier onset, and the development of granulation tissue and collagen deposition were increased (28). In this study, on day 7, when development had increased, the highest mean granulation tissue was measured in the lavender oil and Madecassol groups. A significant difference was observed between the DM-NS group and the other DM groups on days 7 and 14 (Table 1; p < 0.05). The fact that lavender oil gave similar results to Madecassol led to positive results in our study. Consistent with these results, lavender oil appears to accelerate the development of granulation tissue.

Angiogenesis is a coordinated process that occurs during the proliferation phase (29,32). In this study, angiogenesis did not occur on day 1. The angiogenesis process started to occur on day 7 and reached its peak level on day 14. Hyperglycemia in individuals with diabetes impairs angiogenesis and delays wound healing. This situation plays an important role in the development of the diabetic foot (31,33,34) . An *in vivo* study demonstrated that high glucose concentrations impair angiogenesis by causing loss of endothelial integrity, endothelial cell detachment, and increased sensitivity of endothelial cells (35). Angiogenesis was decreased in diabetic groups compared with the non-DM groups. A significant difference between the DM-NS and non-DM groups was observed on days 7 and 14 (p < 0.05). The angiogenesis phase is crucial to wound healing. Therefore, it is necessary to prevent diabetes-induced impairment of angiogenesis, which contributes to diabetic skin ulcers, particularly diabetic foot ulcers. In this study, in the DM and non-DM groups, the highest level of angiogenesis was evaluated in the groups dressed

Gazi Med J 2026;37(1):65-77

Gülpak et al. Lavender Oil and Diabetic Wound Healing

with lavender oil on days 7 and 14 (Table 1). This suggests that lavender oil is effective at promoting angiogenesis.

Re-epithelialization, which occurs in the proliferative phase of wound healing, begins 24h after the injury with migration of keratinocytes to the wound site (32,36). Re-epithelialization was not observed in all groups on day 1 of the study. Moreover, re-epithelialization was lower in diabetic rats than in non-diabetic rats, and a significant difference was observed between the DM-NS group and the non-DM groups on days 7 and 14 (Table 1; p < 0.05). The findings of this study indicate that diabetes delays re-epithelialization by inhibiting keratinocyte migration on the extracellular matrix, thereby delaying re-epithelialization during the proliferative phase (31,37). The re-epithelialization process is stimulated by growth factors such as epidermal growth factor (EGF), TGF-β, and fibroblast growth factor; this stimulation is important for rapid closure of the wound area (33). In a study of wound healing in rats, lavender oil accelerated re-epithelialization and wound closure by increasing EGF secretion (27). In this study, re-epithelialization levels were high in the lavender
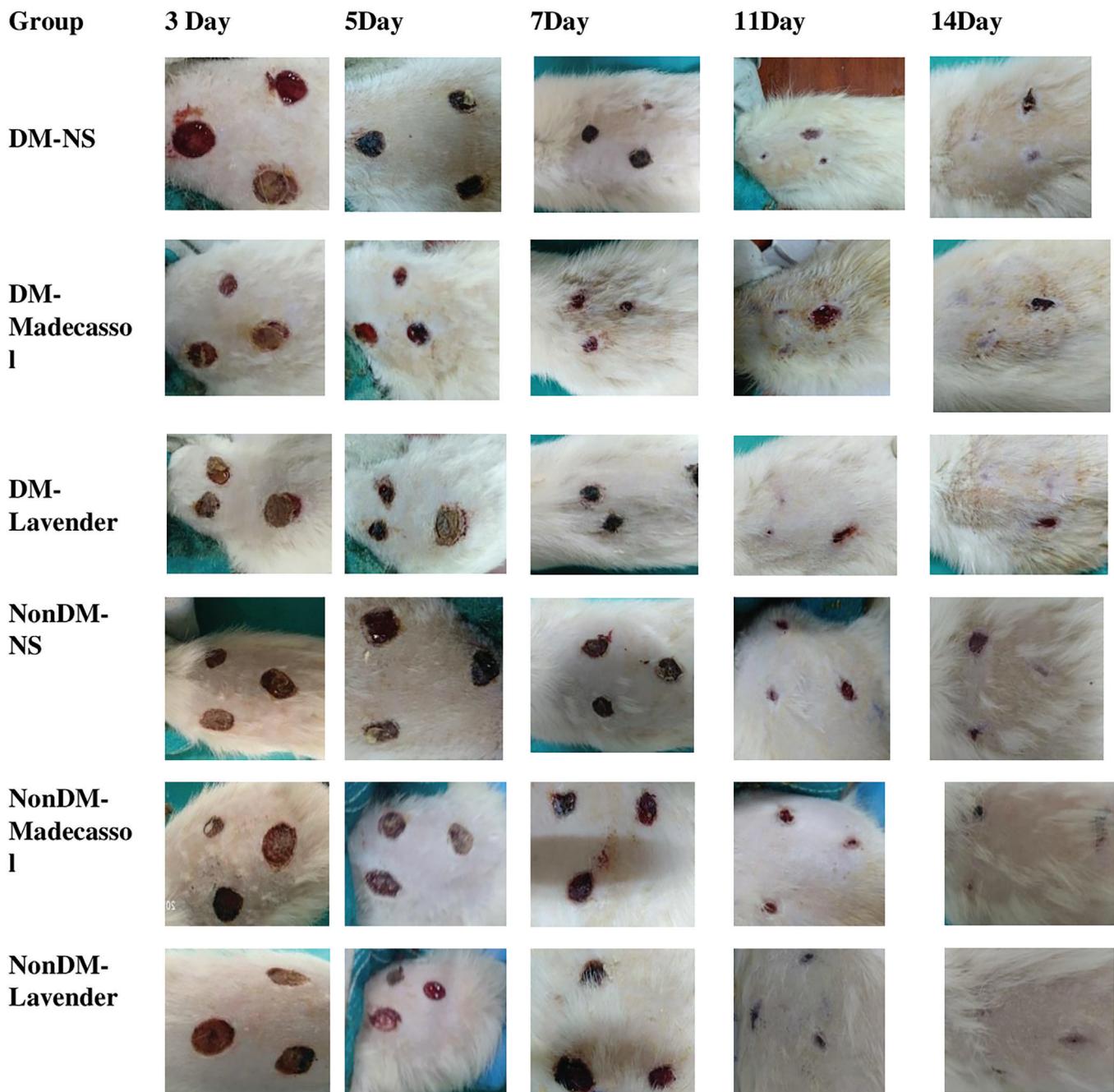

Figure 2. Examples of the wound healing process in groups based on time.

Gazi Med J 2026;37(1):65-77

Gülpak et al. Lavender Oil and Diabetic Wound Healing

Table 2. Immunohistochemistry VEGFA, collagen-I, and collagen-III levels in groups based on days.

	Group	1 day	7 day	14 day
VEGFA	DM-NS (n = 7)	0.0 ± 0.0	0.14 ± 0.38	0.14 ± 0.38
	DM-Madecassol (n = 7)	0.14 ± 0.38	2.29 ± 1.11[b]	2.00 ± 0.82[b]
	DM-lavender (n = 7)	0.29 ± 0.49	2.43 ± 0.98[b]	2.43 ± 0.53[b]
	Non-DM-NS (n = 7)	0.14 ± 0.38	3.57 ± 0.53[a]	2.71 ± 0.76[a]
	Non-DM-Madecassol (n = 7)	0.29 ± 0.49	3.71 ± 0.49[a]	3.00 ± 0.82[a]
	Non-DM-lavender (n = 7)	0.0 ± 0.0	4.00 ± 0.0[a]	3.14 ± 0.90[a]
Collagen-I	DM-NS (n =7)	0.14 ± 0.38	0.43 ± 0.53	1.00 ± 0.58
	DM-Madecassol (n = 7)	0.71 ± 0.76	1.57 ± 0.53[b]	2.29 ± 0.49[b]
	DM-lavender (n = 7)	0.86 ± 0.69	1.71 ± 0.76[b]	2.71 ± 0.49[b]
	Non-DM-NS (n = 7)	1.14 ± 0.38[a]	1.43 ± 0.53[a]	2.14 ± 0.69
	Non-DM-Madecassol (n = 7)	1.14 ± 0.69[a]	1.71 ± 0.76[a]	2.86 ± 0.90[a]
	Non-DM-lavender (n = 7)	1.43 ± 0.53[a]	1.86 ± 0.69[a]	3.71 ± 0.49[a]
Collagen-III	DM-NS (n = 7)	0.29 ± 0.49	0.71 ± 0.76	0.43 ± 0.53
	DM-Madecassol (n = 7)	0.29 ± 0.49	2.57 ± 0.79[b]	1.71 ± 0.76[b]
	DM-lavender (n = 7)	0.43 ± 0.79	3.00 ± 0.58[b]	1.57 ± 0.53[b]
	Non-DM-NS (n = 7)	0.43 ± 0.53	2.14 ± 0.69	1.43 ± 0.53[a]
	Non-DM-Madecassol (n = 7)	1.00 ± 0.82	3.00 ± 0.82[a]	1.71 ± 0.76[a]
	Non-DM-lavender (n = 7)	1.14 ± 0.69	3.71 ± 0.49[a]	1.86 ± 0.69[a]

[a]: The difference between the DM-NS group and the non-DM group on the specified days was $p < 0.05$.
[b]: The difference between the DM-NS group and the other diabetic groups on the specified days was $p < 0.05$.
[c]: The difference between the non-DM-NS group and the other non-DM groups on the specified days was $p < 0.05$.
[d]: The difference between the DM-Lavender and diabetic groups on the specified days was $p < 0.05$.

groups on days 7 and 14. By day 14 of the study, a significant difference was found between the NS group and the lavender and Madecassol groups in both the DM and non-DM groups. No difference was observed between the positive-control groups for lavender oil and Madecassol. This shows that lavender oil yields results consistent with the positive control and accelerates wound healing by promoting re-epithelialization.

VEGF is an important angiogenic growth factor that regulates vascular permeability in the wound-healing process; it also contributes to the revascularization of the wound site, development of new granulation tissue, and epithelialization (38,39). Errors in VEGFA release cause delays in wound healing (40–42). In this study, the VEGFA levels were evaluated in tissues obtained from the wound area. Studies have shown that the synthesis of various growth factors, including VEGF, is decreased in wounds of streptozotocin-induced diabetic mice (43). Reduced expression of VEGF in non-obese diabetic mice decreased angiogenesis, whereas increased VEGF expression could increase it (42). In this study, average VEGFA levels were lower in the diabetic groups than in the non-DM groups, and a significant difference in VEGFA levels between the DM-NS and non-DM groups was observed on days 7 and 14. Previous studies have reported that an increase in VEGF levels in the wound area can promote healing in diabetic wounds by improving angiogenesis and increasing perfusion. Many different factors also contribute to wound healing through multiple activities, including collagen deposition and re-epithelialization (44,45). In this study, the highest VEGFA levels in the

DM and non-DM groups were observed in rats treated with lavender oil. Additionally, a significant difference was observed between the DM-NS group and the other diabetic groups on days 7 and 14 (Table 2; $p < 0.05$). Dressing with lavender oil increased VEGFA levels and showed a positive effect on wound healing.

İn the early stages of wound healing, collagen-III is first to occur, as the scar formation progresses, collagen-I increases as it is better regulated against mechanical stress in the remodeling phase (46-48). In the results of this study, collagen-III levels were found to be higher on day 7 than on other days in all groups, whereas the collagen-I levels were found to be higher on day 14. In addition, the mean scores of collagen-I and collagen-III were found to be lower in the diabetic groups. The results of this study indicate that diabetes affects collagen synthesis. In the study of Mori et al. (13) on wound healing in rats, it has been stated that, compared with the control groups, the number of fibroblasts synthesizing collagen increased in wounds treated with lavender oil. Furthermore, 4 days after injury, the collagen-III and collagen-I level, significantly increased in wounds treated with lavender oil compared with those treated with a control solution. In this study, the collagen levels in the DM and non-DM groups were found to be higher in those dressed with lavender oil on all days. Although dressing with lavender oil in diabetic rats increased the collagen-I and III levels, since there is no study on the use of lavender oil in diabetic wound healing in the literature, a comparison could not be made. It was determined that there was a significant difference between the NS and lavender

Gazi Med J 2026;37(1):65-77

Gülpak et al. Lavender Oil and Diabetic Wound Healing
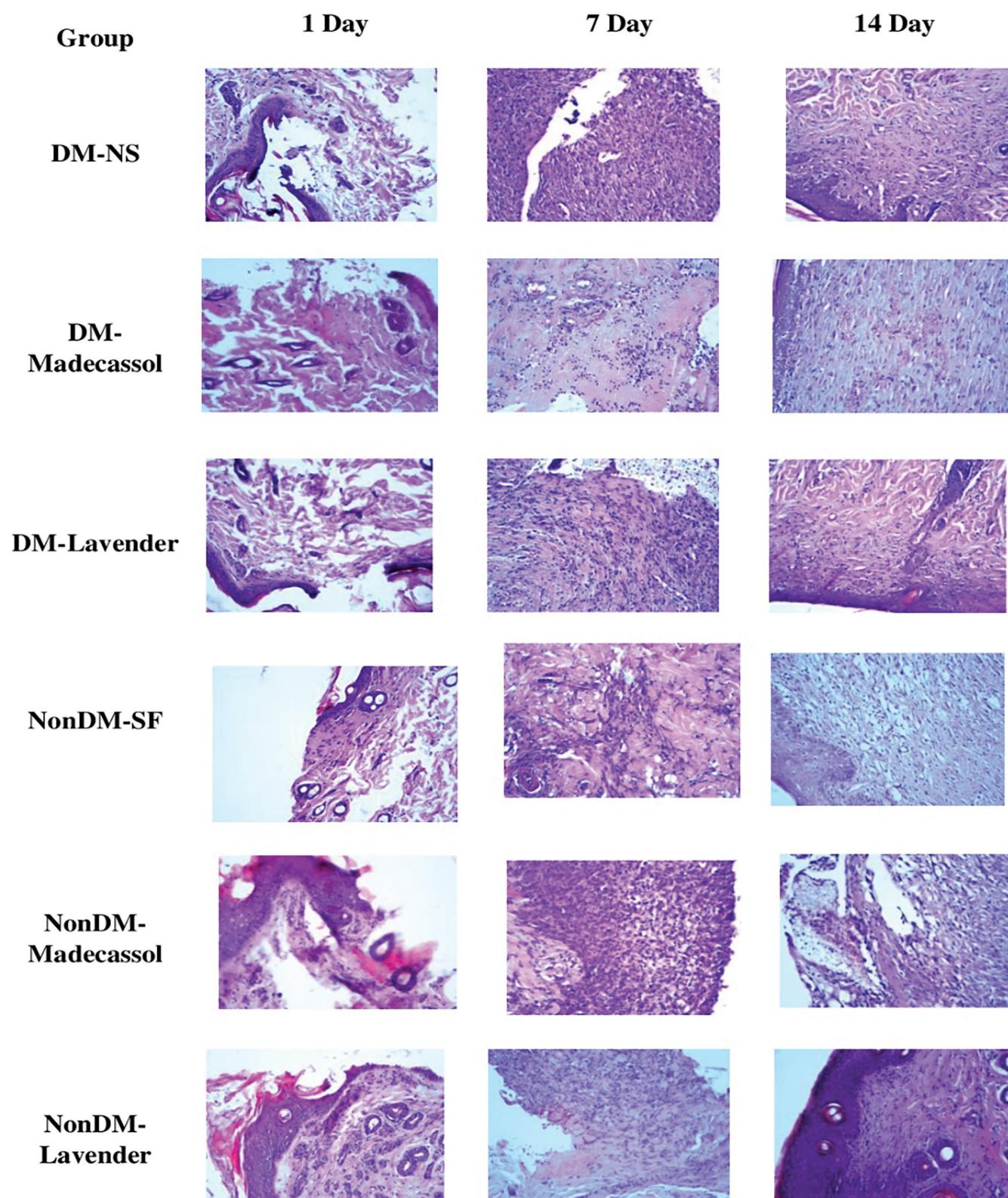
Figure 3. Examples of the Hematoxylin–Eosin staining process in groups based on time.

Gazi Med J 2026;37(1):65-77

Gülpak et al. Lavender Oil and Diabetic Wound Healing
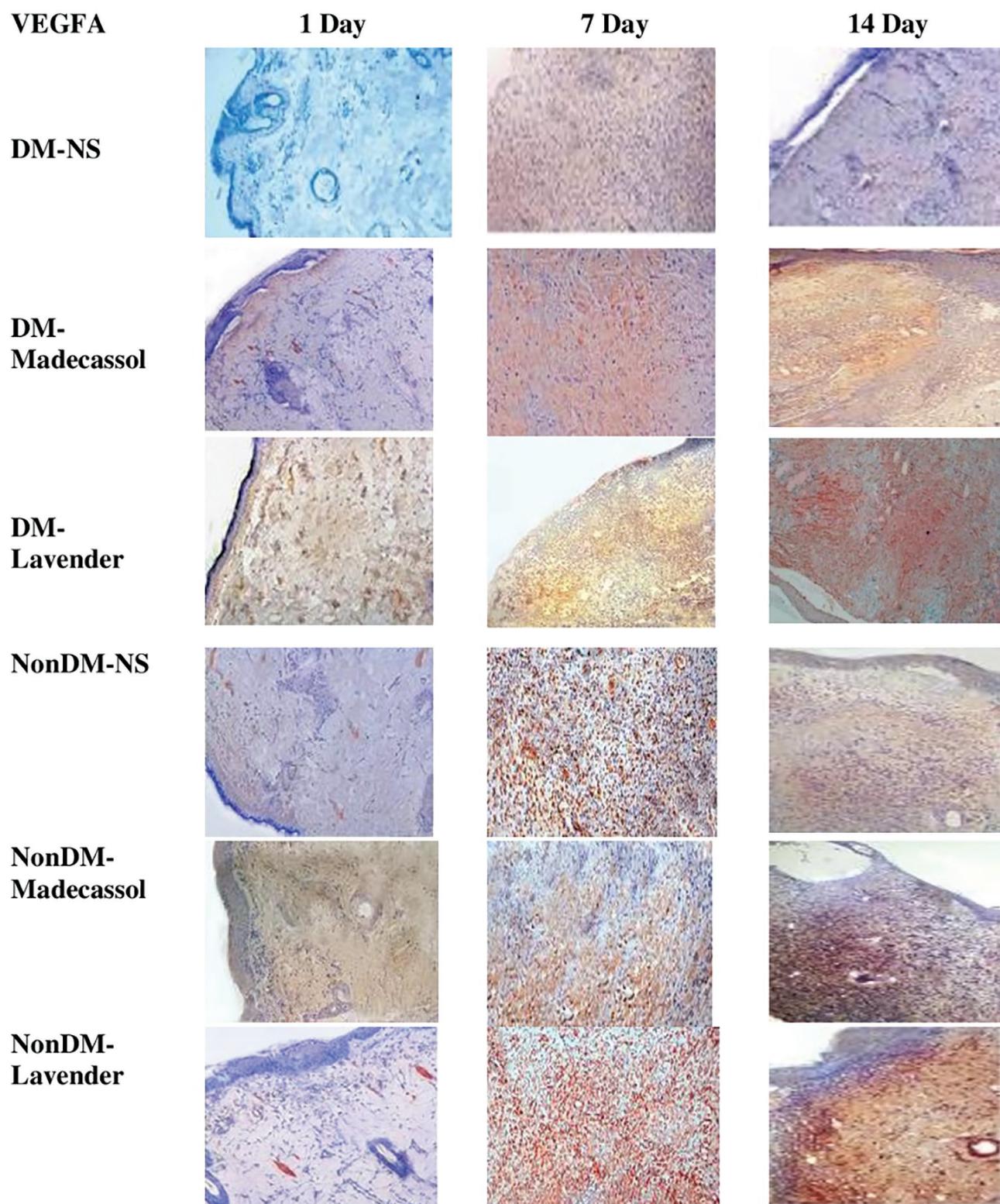
Figure 4. VEGFA immunohistochemistry staining samples in groups based on time.

Gazi Med J 2026;37(1):65-77

Gülpak et al. Lavender Oil and Diabetic Wound Healing
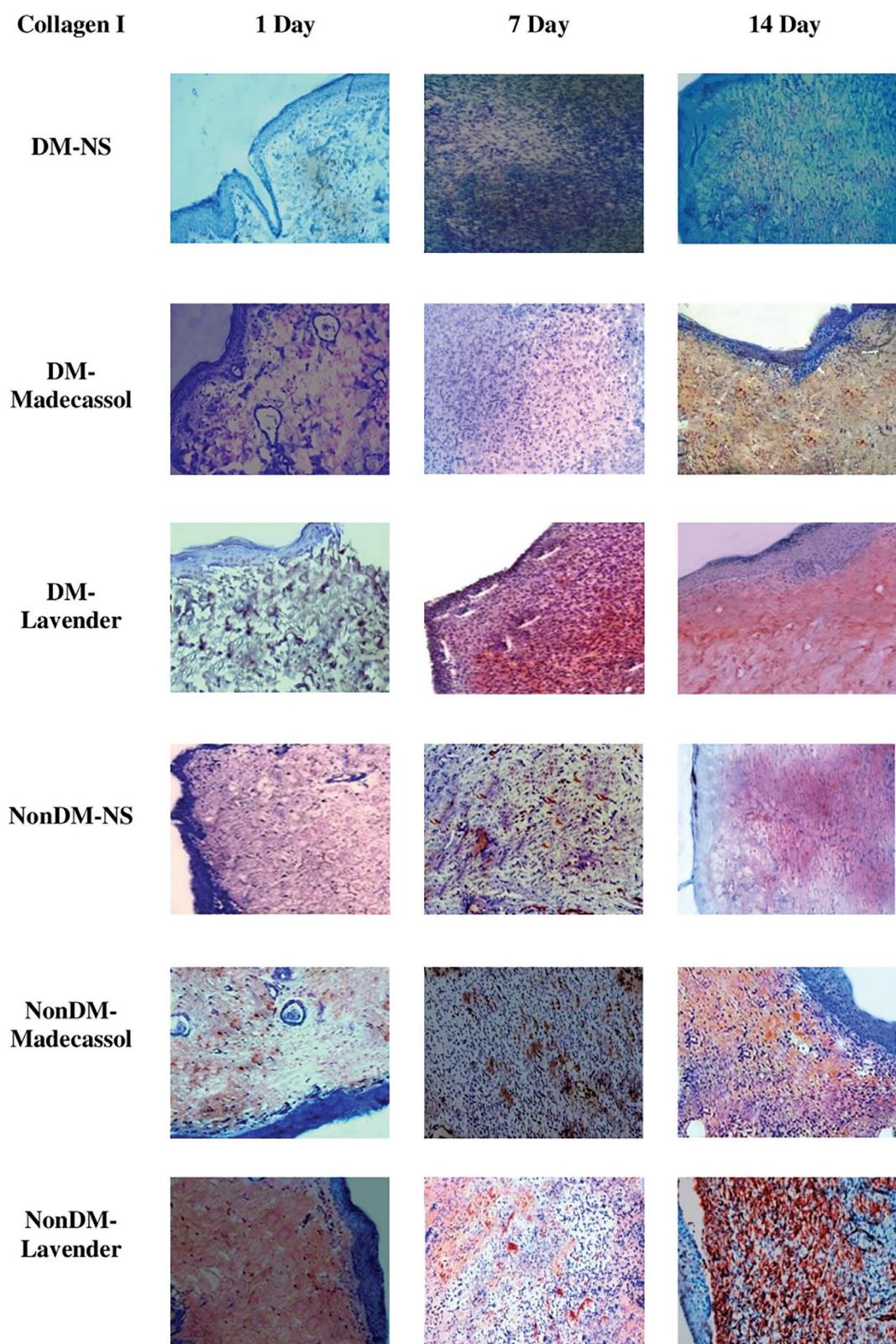
Figure 5. Collagen-I immunohistochemistry staining samples in groups based on time.

Gazi Med J 2026;37(1):65-77

Gülpak et al. Lavender Oil and Diabetic Wound Healing

| Collagen III | 1 Day | 7 Day | 14 Day |
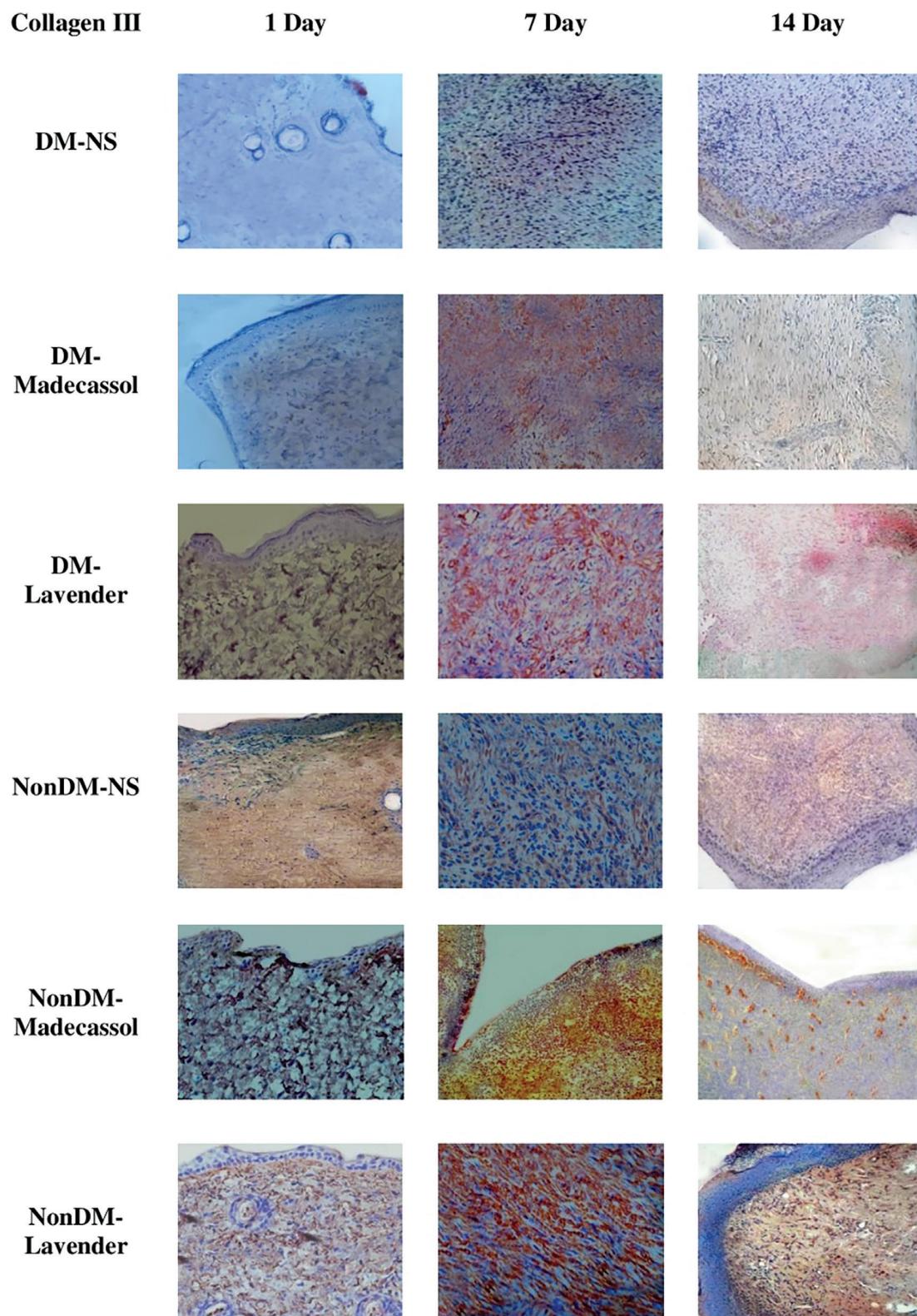
Figure 6. Collagen-III immunohistochemistry staining samples in groups based on time.

DM: Diabetes mellitus, NS: Normal saline

Gazi Med J 2026;37(1):65-77

Gülpak et al. Lavender Oil and Diabetic Wound Healing

groups. However, no significant difference was found between the Madecassol and lavender groups. This indicates that lavender oil gives results that are consistent with those of the positive control and that it is effective on collagen synthesis.

Study Limitations

The present study is situated within the preclinical stage of research. While the findings obtained from experimental animal models provide significant insights and predictive value regarding the efficacy of lavender oil in wound healing, they do not directly represent clinical outcomes in humans. To establish the clinical utility of these findings for human subjects, further investigations based on these results must be designed as clinical trials. Additionally, as this research was conducted on acute wounds created via full-thickness skin defects in diabetic rats, the results are representative of diabetic acute wounds specifically. Consequently, the scope of the study findings is limited to the context of acute wound healing.

CONCLUSION

Lavender oil dressing was found to be effective in wound healing, both macroscopically and microscopically, in all groups. The results of this study suggest that the positive effects of lavender oil on wound healing may increase the likelihood of using it as a novel dressing material in combination with conventional treatment. It's recommended to plan randomized, controlled clinical trials to evaluate the application of lavender oil in the treatment of diabetic wounds and to identify the active constituent(s) responsible for its healing effect.

The results:

• Wounds dressed with lavender oil healed faster than those dressed with NS or Madecassol.

• On day 14, groups dressed with lavender oil showed the highest wound-healing percentage and the smallest wound area.

• Lavender oil produced results consistent with those of the positive control, Madecassol.

Ethics

Ethics Committee Approval: Consistent with the Declaration of Helsinki, developed by the World Medical Association and with the Regulation on the Working Procedures and Principles of Animal Experiments Ethics Committees (dated: 07.06.2006, number: 26220), the researcher received the Certification of Experimental Animal Usage following training of the personnel involved in the use of animals for experimental research. Prior to conducting the research, approval was obtained from Kahramanmaraş Sütçü İmam University Experimental Animals Ethics Committee on June 6, 2018 (session number: 2018/08; decision number: 05).

Informed Consent: Informed consent was not applicable, as this study did not involve human participants and was conducted using experimental animals.

Footnotes

Authorship Contributions

Surgical and Medical Practices: M.G., A.Y., Concept: M.G., Ö.O., A.Y., A.Y., Design: M.G., Ö.O., A.Y., A.Y., Data Collection or Processing: M.G., A.Y., A.Y., Analysis or Interpretation: M.G., Ö.O., A.Y., A.Y., Literature Search: M.G., Ö.O., A.Y., A.Y., Writing: M.G., Ö.O.

REFERENCES

1. Samancioglu S. Endocrine system diseases and nursing management. In: Ovayolu N, Ovayolu O, editors. Basic internal medicine nursing and chronic diseases with different dimensions. 2nd ed. Adana (Turkey): Cukurova Nobel Tip Kitabevi; 2017. p. 189-213. Available from: https://www.nobelkitabevi.com.tr/hemsirelik-ve-ebelik-kitaplari/20809-temel-ic-hastaliklari-hemsireligi-ve-farkli-boyutlariyla-kronik-hastaliklar-9786052369012.html

2. American Diabetes Association. 2. Classification and diagnosis of diabetes: standards of medical care in diabetes-2019. Diabetes Care. 2019; 42: S13–28.

3. Berk A, Dokumaci AH, Kaymaz MB. Yara iyileşmesi ve diyabetik yara tedavisinde kullanılan tıbbi bitkiler (Wound healing and medicinal plants used in the treatment of diabetic wounds). Sağlık Bilimleri Dergisi (Journal of Health Sciences). 2015;24(3):185-192. Available from: https://search.trdizin.gov.tr/en/yayin/detay/263476/yara-iyilesmesi-ve-diyabetik-yara-tedaviside-kullanilan-tibbi-bitkiler

4. Papatheodorou K, Banach M, Bekiari E, Rizzo M, Edmonds M. Complications of Diabetes 2017. J Diabetes Res. 2018; 2018: 3086167.

5. Rewers A. Acute metabolic complications in diabetes. In: Cowie CC, Casagrande SS, Menke A, et al., editors. Diabetes in America. 3rd ed. Bethesda (MD): National Institute of Diabetes and Digestive and Kidney Diseases (US); 2018 Aug [cited 2026 Jan 7]. Chapter 17. Available from: https://www.ncbi.nlm.nih.gov/books/NBK567993/

6. Lai JC, Lai HY, Nalamolu KR, Ng SF. Treatment for diabetic ulcer wounds using a fern tannin optimized hydrogel formulation with antibacterial and antioxidative properties. J Ethnopharmacol. 2016; 189: 277–89.

7. Baltzis D, Eleftheriadou I, Veves A. Pathogenesis and treatment of impaired wound healing in diabetes mellitus: new insights. Adv Ther. 2014; 31: 817–36.

8. Faydaoğlu E, Sürücüoğlu MS. Medical and aromatic plants' antimicrobial, antioxidant activities and use opportunities. Fen Bilimleri Enstitüsü Dergisi 2013; 6: 233–65.

9. Cavanagh HMA, Wilkinson JM. Lavender essential oil: a review. Aust Infect Control. 2005 Mar;10(1):35-7. Available from: https://www.sciencedirect.com/science/article/pii/S1329936016300888.

10. Ben Djemaa FG, Bellassoued K, Zouari S, El Feki A, Ammar E. Antioxidant and wound healing activity of Lavandula aspic L. ointment. J Tissue Viability. 2016; 25: 193–200.

11. Silva GL, Luft C, Lunardelli A, Amaral RH, Melo DA, Donadio MV, et al. Antioxidant, analgesic and anti-inflammatory effects of lavender essential oil. An Acad Bras Cienc. 2015; 87: 1397–408.

12. Samuelson R, Lobl M, Higgins S, Clarey D, Wysong A. The effects of lavender essential oil on wound healing: a review of the current evidence. J Altern Complement Med. 2020; 26: 680–90.

13. Mori HM, Kawanami H, Kawahata H, Aoki M. Wound healing potential of lavender oil by acceleration of granulation and wound contraction through induction of TGF-β in a rat model. BMC Complement Altern Med. 2016; 16: 144.

14. Olgun N, Eti Aslan F. Diyabetes mellitus. In: Karadakovan A, Eti Aslan F, editörler. Dahiliye ve cerrahi hastalıklarda bakım. Adana: Nobel Kitabevi;2010.s.829-864. Available from: https://scholar.google.com/scholar?q=Dahiliye+ve+cerra hi+hastal%C4%B1klarda+bak%C4%B1 m+Karadak ovan+Eti+Aslan+Diyabetes +mellitus.

Gazi Med J 2026;37(1):65-77

Gülpak et al. Lavender Oil and Diabetic Wound Healing

15. *Özsoy S, Yıldırım JG. Hemşirelikte hayvan araştırmaları.* Hemşirelikte Araştırma Geliştirme Dergisi. 2012; 1: 56–69.

16. Randomizer.org. Random number generator [Internet]. Available from: https://www.randomizer.org. Accessed March 2021.

17. Akbulut Ö. Hayvan Deneylerinde Örneklem Büyüklüğünün Kaynak Eşitlik Yöntemi ile Belirlenmesi ve Güç Analizi. KSÜ Tıp Fak Der. 2023; 18: 117–25.

18. Erbaş O. Deneysel diyabet modelleri. İstanbul Bilim Üniversitesi Florence Nightingale Tıp Dergisi. 2015; 1.

19. Uyar A, Akyol T, Yaman T, Keleş ÖF. A histopathological and biochemical ınvestigation of the wound healing and oxidative stress effect on the wound model of the achillea millefolium in rats. Van Veterinary Journal. 2017; 28: 157–63.

20. Ayla S, Okur ME, Günal MY, Özdemir EM, Çiçek Polat D, Yoltaş A, et al. Wound healing effects of methanol extract of Laurocerasus officinalis roem. Biotech Histochem. 2019; 94: 180–8.

21. Bayer Türk Kimya San. Ltd. Şti. MADECASSOL® merhem: instructions for use (Kullanma Talimatı) [Internet]. Available from: https://pdf.ilacprospektusu.com/14373-madecassol-merhem-kt.pdf. Accessed April 2020.

22. Bayırlı M. "ImageJ" yazılımı kullanarak morfolojik görüntülerin tanımlanması. Akademik Bilişim. 2013.

23. Ferreira T, Rasband W. ImageJ User Guide [Internet]. Last updated 2012 Oct 2. Available from: https://imagej.net/ij/docs/guide/user-guide.pdf.Accessed March 2020.

24. ImageJ. Image processing and analysis in Java (IMAGEJ) [Internet]. Available from: https://imagej.net/ij/download.html. Accessed March 2020.

25. Galeano M, Altavilla D, Bitto A, Minutoli L, Calò M, Lo Cascio P, et al. Recombinant human erythropoietin improves angiogenesis and wound healing in experimental burn wounds. Crit Care Med. 2006; 34: 1139–46.

26. Galeano M, Altavilla D, Cucinotta D, Russo GT, Calò M, Bitto A, et al. Recombinant human erythropoietin stimulates angiogenesis and wound healing in the genetically diabetic mouse. Diabetes. 2004; 53: 2509–17.

27. Koca Kutlu A, Ceçen D, Gürgen SG, Sayın O, Cetin F. A comparison study of growth factor expression following treatment with transcutaneous electrical nerve stimulation, saline solution, povidone-iodine, and lavender oil in wounds healing. Evid Based Complement Alternat Med. 2013; 2013: 361832.

28. Nada AM, Abu-Ahmed HM, Khafaga AF, El-Kammar MH. Clinical and histopathological evaluation of the effectiveness of lavender oil compared with black seed oil, ostrich oil and cod liver oil on the second intention wound healing in dogs. Alexandria Journal for Veterinary Sciences. 2015; 46: 57–67.

29. Gonzalez AC, Costa TF, Andrade ZA, Medrado AR. Wound healing - a literature review. An Bras Dermatol. 2016; 91: 614–20.

30. Dekoninck S, Blanpain C. Stem cell dynamics, migration and plasticity during wound healing. Nat Cell Biol. 2019; 21: 18–24.

31. Anderson K, Hamm RL. Factors that impair wound healing. J Am Coll Clin Wound Spec. 2014; 4: 84–91.

32. Janis JE, Harrison B. Wound healing: part I. basic science. Plast Reconstr Surg. 2016; 138: 9S-17S.

33. Kolluru GK, Bir SC, Kevil CG. Endothelial dysfunction and diabetes: effects on angiogenesis, vascular remodeling, and wound healing. Int J Vasc Med. 2012; 2012: 918267.

34. Piconi L, Quagliaro L, Assaloni R, Da Ros R, Maier A, Zuodar G, et al. Constant and intermittent high glucose enhances endothelial cell apoptosis through mitochondrial superoxide overproduction. Diabetes Metab Res Rev. 2006; 22: 198–203.

35. Takeo M, Lee W, Ito M. Wound healing and skin regeneration. Cold Spring Harb Perspect Med. 2015; 5: a023267.

36. Pastar I, Stojadinovic O, Yin NC, Ramirez H, Nusbaum AG, Sawaya A, et al. Epithelialization in wound healing: a comprehensive review. Adv Wound Care (New Rochelle). 2014; 3: 445–64.

37. Powers JG, Higham C, Broussard K, Phillips TJ. Wound healing and treating wounds: chronic wound care and management. J Am Acad Dermatol. 2016; 74: 607–25.

38. Khalaf AA, Hassanen EI, Zaki AR, Tohamy AF, Ibrahim MA. Histopathological, immunohistochemical, and molecular studies for determination of wound age and vitality in rats. Int Wound J. 2019; 16: 1416–25.

39. Johnson KE, Wilgus TA. Vascular endothelial growth factor and angiogenesis in the regulation of cutaneous wound repair. Adv Wound Care (New Rochelle). 2014; 3: 647–61.

40. Ong HT, Dilley RJ. Novel non-angiogenic role for mesenchymal stem cell-derived vascular endothelial growth factor on keratinocytes during wound healing. Cytokine Growth Factor Rev. 2018; 44: 69–79.

41. Pikuła M, Langa P, Kosikowska P, Trzonkowski P. Komórki macierzyste i czynniki wzrostuw gojeniu ran [Stem cells and growth factors in wound healing]. Postepy Hig Med Dosw (Online). 2015; 69: 874–85.

42. Zhou K, Ma Y, Brogan MS. Chronic and non-healing wounds: the story of vascular endothelial growth factor. Med Hypotheses. 2015; 85: 399–404.

43. Tsui HY, Liu YC, Yan X, Lin Y, Xu Y, Tan Q. Combined effects of artificial dermis and vascular endothelial growth factor concentration gradient on wound healing in diabetic porcine model. Growth Factors. 2017; 35: 216–24.

44. Onodera H, Ikeuchi D, Nagayama S, Imamura M. Weakness of anastomotic site in diabetic rats is caused by changes in the integrity of newly formed collagen. Dig Surg. 2004; 21: 146–51.

45. Yan X, Chen B, Lin Y, Li Y, Xiao Z, Hou X, et al. Acceleration of diabetic wound healing by collagen-binding vascular endothelial growth factor in diabetic rat model. Diabetes Res Clin Pract. 2010; 90: 66–72.

46. Xue M, Jackson CJ. Extracellular matrix reorganization during wound healing and its impact on abnormal scarring. Adv Wound Care (New Rochelle). 2015; 4: 119–36.

47. Adams DH, Shou Q, Wohlmuth H, Cowin AJ. Native Australian plant extracts differentially induce Collagen I and Collagen III in vitro and could be important targets for the development of new wound healing therapies. Fitoterapia. 2016; 109: 45–51.

48. Wang T, Gu Q, Zhao J, Mei J, Shao M, Pan Y, et al. Calcium alginate enhances wound healing by up-regulating the ratio of collagen types I/III in diabetic rats. Int J Clin Exp Pathol. 2015; 8: 6636–45.

Evaluation of the Characteristics of Hand and Wrist Ganglion Cysts and Their Relationship with Ligamentous Injury

El ve El Bileği Ganglion Kistlerinin Özellikleri ve Ligament Hasarıyla İlişkilerinin Değerlendirilmesi

Ⓘ Toygun Kağan Eren[1], Ⓘ Yusufhan Arslan[2]

[1]Department of Orthopedics and Traumatology, Gazi University Faculty of Medicine Ankara, Türkiye
[2]Department of Orthopedics and Traumatology, University of Health Sciences Türkiye, Ankara Training and Research Hospital, Ankara, Türkiye

ABSTRACT

Objective: The present study aimed to examine the characteristics of ganglion cysts in the hand and wrist region using magnetic resonance imaging (MRI) and to evaluate the relationship between these cyst existence and ligamentous injuries.

Methods: Patients who were diagnosed with ganglion cysts after being evaluated with wrist MRI due to chronic wrist pain between January 2018 and December 2022 were retrospectively reviewed. Patients with a history of hand or wrist trauma in the last 3 months or previous hand and wrist surgeries were excluded from the study. The ganglion cysts were assessed in terms of location, size, and accompanying to the triangular fibrocartilage complex (TFCC) and intercarpal ligament (ICL) injuries.

Results: A total of 156 patients were included in the study The average age of the patients was 37.53 (± 15.02) years. The ganglion cyst was located dorsally in 85 patients (54.5%), volarly in 68 patients (43.6%), and both dorsally and volarly in 3 patients (1.9%). TFCC injury was detected in 33 patients (21.1%). There was no statistically significant relationship between TFCC injury and cyst location (dorsal, volar) (p = 0.187). ICL injury was present in 2 patients (1.2%). Dorsal cysts were more frequent in patients younger than 40 years old.

Conclusion: The majority of patients with ganglion cysts did not have accompanying ligament injuries this finding raises doubts about the role of ligament injuries in the formation of ganglion cysts. While dorsal ganglion cysts were slightly more common overall, the frequency of volar localization increased with age.

Keywords: Ganglion cyts, ligament injury, TFCC, intercarpal ligament

ÖZ

Amaç: Bu çalışmanın amacı, el ve el bileği bölgesindeki ganglion kistlerinin manyetik rezonans görüntüleme (MRG) ile özelliklerini incelemek ve bu kistlerin varlığı ile ligaman yaralanmaları arasındaki ilişkiyi değerlendirmektir.

Yöntemler: Ocak 2018 ile Aralık 2022 tarihleri arasında kronik el bileği ağrısı nedeniyle el bileği MRG ile değerlendirilen ve ganglion kisti tanısı alan hastalar retrospektif olarak incelendi. Son 3 ay içinde el veya el bileği travma öyküsü bulunanlar ile daha önce el veya el bileği cerrahisi geçirmiş hastalar çalışma dışı bırakıldı. Ganglion kistleri; lokalizasyon, boyut ve eşlik eden triangular fibrokartilaj kompleks (TFCC) ve interkarpal ligaman (ICL) yaralanmaları açısından değerlendirildi.

Bulgular: Çalışmaya toplam 156 hasta dahil edildi. Hastaların ortalama yaşı 37,53 (±15,02) yıldı. Ganglion kistleri 85 hastada (%54,5) dorsal, 68 hastada (%43,6) volar yerleşimliydi; 3 hastada (%1,9) ise hem dorsal hem volar yerleşim mevcuttu. Otuz üç hastada (%21,1) TFCC yaralanması saptandı. TFCC yaralanması ile kist lokalizasyonu (dorsal, volar) arasında istatistiksel olarak anlamlı bir ilişki bulunmadı (p = 0,187). İki hastada (%1,2) ICL yaralanması tespit edildi. Dorsal yerleşimli kistler 40 yaş altındaki hastalarda daha sık izlendi.

Sonuç: Ganglion kisti olan hastaların büyük çoğunluğunda eşlik eden ligaman yaralanması bulunmamaktadır. Bu bulgu, ganglion kistlerinin oluşumunda ligaman yaralanmalarının rolü konusunda şüphe uyandırmaktadır. Genel olarak dorsal ganglion kistleri biraz daha sık görülmekle birlikte, yaş ilerledikçe volar yerleşim sıklığının arttığı izlenmiştir.

Anahtar Sözcükler: Ganglion kisti, bağ yaralanmaları, TFCC, interkarpal bağlar

INTRODUCTION

Ganglion cysts are the most common tumor-like condition of the hand and wrist region, reportedly accounting for 70% of lesions in this area (1,2). Studies have shown that they are more frequently located on the wrist, particularly on the dorsal side (3, 4). Additionally, they are more commonly observed in women than in men (5).

A meta-analysis by Head et al. (6) reported recurrence rates after treatment for ganglion cysts of 21% for open excision, 6% for arthroscopic excision, and 59% for aspiration. One possible reason for these high recurrence rates is the unclear etiology and pathogenesis of ganglion cysts. Several theories regarding the pathogenesis of ganglion cysts exist, but no consensus has been reached (7).

Some theories suggest that repetitive wrist stress, as seen in gymnasts, weakens the joint capsule, leading to the formation of ganglion cysts (8,9). It has been proposed that myxoid degeneration of peri-articular tissue may cause cyst formation, or that cysts arise primarily from herniation of the joint capsule (10). However, the absence of a synovial lining, which is typically present in normal cystic lesions, raises questions about this theory. Moreover, the inflammatory theory, which posits that cyst formation is related to inflammation, has been discounted due to the lack of expected peri-cystic inflammatory changes in ganglion cysts (9, 11). Recent studies involving patients who underwent arthroscopic excision of ganglion cysts have linked these cysts to ligamentous injuries (5,12). It has also been suggested that ganglion cysts might arise from intercarpal ligament (ICL) injuries (5,12-14). While the dorsal cysts commonly arise from the scapholunate joint, volar ganglion cysts mostly originate from the scaphotrapeziotrapezoid and radiocarpal joints. the other major ligament of the wrist and hand is the (TFCC), which may also contribute to the etiology of ganglion cysts (12,15-17).

The aim of this study was to examine the characteristics of ganglion cysts of the hand and wrist using magnetic resonance imaging (MRI) and to evaluate the relationship between these cysts and non-acute ligamentous injuries of the hand and wrist.

MATERIALS AND METHODS

Patients diagnosed with ganglion cysts who underwent wrist imaging MRI for chronic hand and wrist pain lasting more than 6 weeks between January 2018 and December 2022 were retrospectively evaluated. Patients with a history of hand and wrist trauma within the last 3 months (n = 11) or previous hand and wrist surgeries (n = 5) were excluded from the study. The ganglion cysts in the patients were examined using MRI. The presence of solitary or multiple ganglion cysts was assessed. The patients were grouped based on the location of the ganglion cysts (volar or dorsal), the anatomic level (wrist, intercarpal, carpometacarpal, metacarpal, and metacarpophalangeal), and the presence of associated ligament injuries, such as injury to the triangular fibrocartilage complex (TFCC) or the ICL. Additionally, the patients were grouped by age (< 40 and ≥ 40 years). These groups were compared statistically to evaluate their association with the frequency of ganglion cysts.

Statistical Analysis

The statistical analyses were performed using SPSS version 21.0 (Statistical Package for Social Sciences, Chicago, IL, USA). All tests were conducted at a 95% confidence level, with a margin of error set at 0.05. A p-value of less than 0.05 was considered statistically significant. The normality of the distributions was assessed using the Shapiro-Wilk test. Variables that failed the normality test (Shapiro–Wilk test p < 0.05) were analyzed with non-parametric tests. For inter-group comparisons, Mann-Whitney U test, Kruskal-Wallis test, and chi-square tests were used.

This study was performed in line with the principles of the Declaration of Helsinki. Approval was granted by the Ethics Committee of University of Health Sciences Türkiye, Ankara Training and Research Hospital (decision number: 135/2024, date: 24/07/2024), and informed consent was obtained from each patient.

RESULTS

A total of 156 patients were included in the study. Among the patients, 43 (27.6%) were male and 113 (72.4%) were female. The mean age of the participants was 37.53 ± 15.02 years. Sixty patients (38.4%) were under 40 years of age, while 96 patients (61.6%) were 40 years or older (Table 1).

The mean size of the ganglion cysts identified in the patients was 8.72 ± 6.87 mm. The smallest ganglion cyst measured 2 mm in length, while the largest measured 40 mm in length. Solitary ganglion cysts were found in 151 patients (96.7%), whereas multiple cysts were present in only 5 patients (3.3%). The ganglion cyst was located on the dorsal side in 85 patients (54.5%), on the volar side in 68 patients (43.6%), and on both the dorsal and volar sides in 3 patients (1.9%). In 136 patients (87.2%), the cyst was located at the wrist; in 19 patients (12.2%), at the hand; and in 1 patient (0.6%) at both the hand and wrist (Table 1). 75% (51/68) of the volar ganglion cysts were located at the radiocarpal joint; however, only 23.5% (20/85) of the dorsal cysts originated from the radiocarpal joint. 40% (34/85) of the dorsal cysts originated from the scapholunate joint, whereas only 2.9% (2/85) of volar cysts did.

The majority of patients with ganglion cysts (61.6%) were under 40 years of age. Dorsal cysts were more frequent in patients younger than 40 years, at a rate of 64.5%; however, volar cysts were more frequent in patients aged 40 years or older, at a rate of 60%. (p = 0.001) The side of the affected extremity was comparable between groups (p = 0.739) (Table 2).

TFCC injuries were identified in 33 patients (21.1%). There was no statistically significant association between TFCC injury and cyst location (dorsal vs. volar; p = 0.187) (Table 3). An ICL injury was present in two patients (1.2%). The injured ligaments were the scapholunate ligaments.

When the relationship between TFCC injury and patient age (under or over 40 years), cyst location (p = 0.187), cyst level (p = 0.355), and multiplicity (p = 0.535) was examined, no significant associations were found (p = 0.901) (Table 3).

DISCUSSION

The most important finding of the present study was that only 22% of patients with ganglion cysts and chronic wrist pain had associated ligament injuries. Among those with ligament injuries, only 3% had a complete rupture. The majority of ligament injuries were TFCC injuries, and only 1.2% of patients had ICL (Scapholunate ligament) injuries, which have been reported as the most common

Table 1. Patient and lesion characteristics

		n	%
Gender	Male	43	27.6
	Female	113	72.4
Age	< 40 years	60	38.4
	> 40 years	96	61.6
Multiplicity	Solitary	151	96.8
	Multiple	5	3.2
Cyst level	Hand	19	12.1
	Wrist	136	87.1
	Hand + wrist	1	0.8
Cyst location	Dorsal	85	54.4
	Volar	68	43.6
	Dorsal + volar	3	2

Table 2. The relationship between the side and location of the ganglion cyst and patient age groups

		< 40 years	≥ 40 years	p
Side	Right	55	36	0.739
	Left	41	24	
Cyst location	Dorsal	62	23	0.001*
	Volar	32	36	
	Dorsal + volar	2	1	

Table 3. The relationship between the incidence of ligament injury and ganglion cyst localization,level and multiplicity

		TFCC injury			
		No	Yes		
			Partial injury	Total injury (rupture)	p
		n	n	n	
Age	< 40 years	76	19	1	0.901
	≥ 40 years	47	10	3	
Cyst location	Dorsal	70	13	2	0.187
	Volar	50	16	2	
	Dorsal + volar	3	0	0	
Cyst level	Wrist	105	27	4	0.355
	Hand	17	2	0	
	Wrist + hand	1	0	0	
Multiplicity	Solitary	118	29	4	0.535
	Multiple	5	0	0	

TFCC: Triangular fibrocartilage complex

origin of ganglion cysts. Ganglion cysts are commonly reported, as they are often related to ICLs and most commonly arise from the scapholunate joint (18). Several studies have examined the relationship between ganglion cysts and TFCC injuries (5,13,14). Langner et al. (15) hypothised that TFCC injuries can also cause ganglion cysts, similar to meniscal tears in the knee. They evaluated the patients arthroscopically and concluded that recurrent radiopalmar ganglions are also associated with TFCC pathologies (19). In a study of arthroscopic findings in painful ganglion cysts, ICL injury was reported in 75% of patients (13). The authors proposed that joint anomalies, such as ligament injuries, may cause cysts similar to popliteal cysts of the knee. They also noted that wrist pain could persist even after ganglion excision, without recurrence of the cyst. This conflict may be attributable to the patient group in the referenced study consisted primarily of individuals with instability. In another study, Watson et al. (8) suggested that ganglion cysts might be a secondary manifestation of peri-scaphoid ligamentous injury and recommended that patients with persistent symptoms after excision be investigated for instability. McKeon and colleaguess (20), in a prospective study, suggested the presence of ligamentous hyperlaxity in patients with symptomatic ganglion cysts. El-Noueam et al. (21) reported associated ligament injuries in approximately 30% of symptomatic ganglion cyst cases. On the other hand, there are also studies in the literature that do not support this claim. Rizzo et al. (22) indicated that none of the patients treated for dorsal wrist ganglion cysts had scapholunate ligament instability. Similarly, Lowden et al. (23) found no evidence of ligament injury on MRI in patients with ganglion cysts, aligning with the present study's findings. Moreover, in a recent study that compared dynamic wrist radiographs of patients with or without ganglion cysts, the authors concluded that there were no differences in scapholunate gap and radiocarpal angles between the groups, and these findings do not support the instability hypothesis. With respect to the TFCC, the percentage of patients with ICL injuries was particularly low. Although TFCC injuries were commonly observed, a previous study using MRI to evaluate patients reported that TFCC injuries were present in up to 50% of the population, regardless of age. This suggests that while TFCC damage is frequently present, it may not always be directly related to the presence of ganglion cysts. In the present study, the absence of ligament injury in most patients suggests that ligament injury may not be a major factor in the etiology of ganglion cysts. Notably, the fact that symptomatic ganglion cysts often become asymptomatic with conservative treatment calls into question the role of ligamentous hyperlaxity in their etiology.

The risk of developing ganglion cysts is three times higher in women than in men. A previous study reported that 60% of patients diagnosed with ganglion cysts were women (24). In our study, 72.4% of the patients diagnosed with ganglion cysts were female, consistent with the literature.

The mean age in the present study was 37.53 years, consistent with many previous studies. Kulinski et al. (25) reported an average age of 41.3 years in their retrospective study, while Dermon and colleagues (3) reported an average age of 37.2 years. Other studies of surgically treated patients found an average age of 43 years, while a study with a broader patient population reported an average age of 35.6 years (26). These findings indicate that ganglion cysts tend to be more frequent from the late 30s to the early 40s.

In a previous study of ganglion cysts, 76% of cases were reported to occur at the wrist (25). Similarly, in the present study, 87% of cysts were located at the wrist level. Regarding cyst localization, it has been suggested that 70% of ganglion cysts are found dorsally, 20% volarly, and 10% at other body sites (24). While the dorsal cysts commonly arise from scapholunate joint, volar ganglion cysts mostly originate from the scaphotrapeziotrapeziodal and radiocarpal joints. In contrast, several studies have reported that ganglion cysts are more common on the volar side (12,16,23,27). In the present study, ganglion cysts were located dorsally in 54.4% of patients and volarly in 43.6%. Also, the majority of the volar ganglion cysts originated from the radiocarpal joint while dorsal wrist ganglions commonly originated from the scapholunate joint, which is similar to previous studies' findings. Analysis of the relationship between cyst formation and age revealed that, among patients older than 40 years, 60% of ganglion cysts were located on the volar side. No significant difference was observed in the incidence of ligament injury between patients younger than 40 years and those 40 years or older. Previous studies have provided limited data on the relationship between age and cyst location. Kuliński et al. (25) also noted that patients with volar wrist ganglion cysts tended to be older than those with dorsal cysts. Degeneration has previously been suggested as a potential factor in cyst formation (28). The increased occurrence of volar ganglion cysts with advancing age may be related to their degenerative nature, warranting further histopathological studies.

In the current study, the mean ganglion cyst size was 8.72 ± 6.87 mm. A similar study examining wrist ganglion cysts on MRI found a mean diameter of 8 mm, with many studies reporting comparable findings (23,29,30). Despite recent research indicating that wrist ganglion cysts do not typically favor one side, the present study found that right-sided cysts were more frequent than left-sided cysts, at 58.3% and 41.7%, respectively (25,31,32).

Study Limitations

The study has several limitations. First, it was a single-center retrospective study. Diagnosis is based on MRI findings; however, the sensitivity of MRI for subtle TFCC or ligamentous pathologies may result in missed diagnoses. A further limitation is the lack of a control group without signs of ganglion cysts. However, the results of the present study were carefully discussed in relation to the findings in the literature to minimize the limitation arising from the absence of a control group.

CONCLUSION

The present study found that most patients with ganglion cysts did not have associated ligament injuries, raising questions about the role of ligament injuries in the formation of ganglion cysts. Additionally, most ganglion cysts were located at the wrist. Although dorsal ganglion cysts were slightly more common, volar cysts were more frequent in patients aged 40 years or older.

Ethics

Informed Consent: Informed consent was obtained from each patient.

Footnotes

Authorship Contributions

Surgical and Medical Practices: T.K.E., Y.A., Concept: T.K.E., Design: T.K.E., Data Collection or Processing: Y.A., Analysis or Interpretation: T.K.E., Literature Search: T.K.E., Y.A., Writing: T.K.E., Y.A.

Conflict of Interest: No conflict of interest was declared by the authors.

Financial Disclosure: The authors declared that this study received no financial support.

REFERENCES

1. Bain GI, Munt J, Turner PC. New advances in wrist arthroscopy. Arthroscopy. 2008; 24: 355–67.

2. Nahra ME, Bucchieri JS. Ganglion cysts and other tumor related conditions of the hand and wrist. Hand Clin. 2004; 20: 249–60.

3. Dermon A, Kapetanakis S, Fiska A, Alpantaki K, Kazakos K. Ganglionectomy without repairing the bursal defect: long-term results in a series of 124 wrist ganglia. Clin Orthop Surg. 2011; 3: 152–6.

4. McEVEDY BV. The simple ganglion: a review of modes of treatment and an explanation of the frequent failures of surgery. Lancet. 1954; 266: 135–6.

5. Osterman AL, Raphael J. Arthroscopic resection of dorsal ganglion of the wrist. Hand Clin. 1995; 11: 7–12.

6. Head L, Gencarelli JR, Allen M, Boyd KU. Wrist ganglion treatment: systematic review and meta-analysis. J Hand Surg Am. 2015; 40: 546–53.

7. Graham JG, McAlpine L, Medina J, Jawahier PA, Beredjiklian PK, Rivlin M. Recurrence of Ganglion Cysts Following Re-excision. Arch Bone Jt Surg. 2021; 9: 387–90.

8. Watson HK, Rogers WD, Ashmead D 4th. Reevaluation of the cause of the wrist ganglion. J Hand Surg Am. 1989; 14: 812–7.

9. Linscheid RL, Dobyns JH. Athletic injuries of the wrist. Clin Orthop Relat Res. 1985: 141–51.

10. Zoller SD, Benner NR, Iannuzzi NP. Ganglions in the hand and wrist: advances in 2 decades. JAAOS - Journal of the American Academy of Orthopaedic Surgeons. 2023; 31.

11. Psaila JV, Mansel RE. The surface ultrastructure of ganglia. J Bone Joint Surg Br. 1978; 60-b: 228–33.

12. Edwards SG, Johansen JA. Prospective outcomes and associations of wrist ganglion cysts resected arthroscopically. J Hand Surg Am. 2009; 34: 395–400.

13. Povlsen B, Peckett WR. Arthroscopic findings in patients with painful wrist ganglia. Scand J Plast Reconstr Surg Hand Surg. 2001; 35: 323–8.

14. P Povlsen B, Tavakkolizadeh A. Outcome of surgery in patients with painful dorsal wrist ganglia and arthroscopic confirmed ligament injury: a five-year follow-up. Hand Surg. 2004; 9: 171–3.

15. Langner I, Krueger PC, Merk HR, Ekkernkamp A, Zach A. Ganglions of the wrist and associated triangular fibrocartilage lesions: a prospective study in arthroscopically-treated patients. J Hand Surg Am. 2012; 37: 1561–7.

16. Mathoulin C, Hoyos A, Pelaez J. Arthroscopic resection of wrist ganglia. Hand Surg. 2004; 9: 159–64.

17. Ho PC, Griffiths J, Lo WN, Yen CH, Hung LK. Current treatment of ganglion of the wrist. Hand Surg. 2001; 6: 49–58.

18. Angelides AC, Wallace PF. The dorsal ganglion of the wrist: its pathogenesis, gross and microscopic anatomy, and surgical treatment. J Hand Surg Am. 1976; 1: 228–35.

19. Beuckelaers E, Hollevoet N. Dynamic wrist radiographs in patients with and without a ganglion cyst. J Wrist Surg. 2020; 9: 470–4.

20. McKeon KE, London DA, Osei DA, Gelberman RH, Goldfarb CA, Boyer MI, et al. Ligamentous hyperlaxity and dorsal wrist ganglions. J Hand Surg Am. 2013; 38: 2138–43.

21. el-Noueam KI, Schweitzer ME, Blasbalg R, Farahat AA, Culp RW, Osterman LA, et al. Is a subset of wrist ganglia the sequela of internal derangements of the wrist joint? MR imaging findings. Radiology. 1999; 212: 537–40.

22. Rizzo M, Berger RA, Steinmann SP, Bishop AT. Arthroscopic resection in the management of dorsal wrist ganglions: results with a minimum 2-year follow-up period. J Hand Surg Am. 2004; 29: 59–62.

23. Lowden CM, Attiah M, Garvin G, Macdermid JC, Osman S, Faber KJ. The prevalence of wrist ganglia in an asymptomatic population: magnetic resonance evaluation. J Hand Surg Br. 2005; 30: 302–6.

24. Gregush RE, Habusta SF. Ganglion Cyst. 2023 Jul 17. In: StatPearls [Internet]. Treasure Island (FL): StatPearls Publishing; 2025.

25. Kuliński S, Gutkowska O, Mizia S, Gosk J. Ganglions of the hand and wrist: Retrospective statistical analysis of 520 cases. Adv Clin Exp Med. 2017; 26: 95–100.

26. Jebson PJ, Spencer EE Jr. Flexor tendon sheath ganglions: results of surgical excision. Hand (N Y). 2007; 2: 94–100.

27. Zhang A, Falkowski AL, Jacobson JA, Kim SM, Koh SH, Gaetke-Udager K. Sonography of wrist ganglion cysts: which location is most common? J Ultrasound Med. 2019; 38: 2155–60.

28. Colman MW, Lozano-Calderon S, Raskin KA, Hornicek FJ, Gebhardt M. Non-neoplastic soft tissue masses that mimic sarcoma. Orthop Clin North Am. 2014; 45: 245–55.

29. Binkovitz LA, Berquist TH, McLeod RA. Masses of the hand and wrist: detection and characterization with MR imaging. AJR Am J Roentgenol. 1990; 154: 323–6.

30. Cardinal E, Buckwalter KA, Braunstein EM, Mih AD. Occult dorsal carpal ganglion: comparison of US and MR imaging. Radiology. 1994; 193: 259–62.

31. Singhal R, Angmo N, Gupta S, Kumar V, Mehtani A. Ganglion cysts of the wrist : a prospective study of a simple outpatient management. Acta Orthop Belg. 2005; 71: 528–34.

32. Shoaib A, Clay NR. Ganglions. Current Orthopaedics. 2002; 16: 451–61.

miR-99b-5p as a Modulator of KLF4 Expression and Drug Response in Luminal B Breast Cancer via a Ubiquitin-Mediated Mechanism

miR-99b-5p'nin Ubikütin-Aracılı Mekanizma ile Luminal B Meme Kanserinde KLF4 Ekspresyonunu Düzenlemesi

◉ Senem Noyan, ◉ Bala Gür Dedeoğlu

Biotechnology Institute, Ankara University, Ankara, Türkiye

ABSTRACT

Objective: Luminal B breast cancer (BC) exhibits aggressive behavior and distinct molecular features, often leading to resistance to therapies such as trastuzumab and tamoxifen. MicroRNAs have emerged as key regulators of cancer progression and drug response. This study explores the role of miR-99b-5p in modulating treatment resistance in Luminal B BC.

Methods: Both trastuzumab-sensitive BT-474 cells and trastuzumab-resistant BT-474 cells were employed to evaluate the functional role of miR-99b-5p through mimic and inhibitor transfections. Gene and protein expression levels were measured using qRT-PCR and Western blotting, respectively. Bioinformatic analyses were performed using the ENCORI, UALCAN, GeneMiner, ROCplot, and UbiBrowser databases.

Results: Our results demonstrated that miR-99b-5p expression was initially downregulated following tamoxifen or trastuzumab treatment, but was subsequently elevated in trastuzumab-resistant cells, suggesting a dynamic regulatory role in therapeutic adaptation. Bioinformatic analyses identified an association between miR-99b-5p and Kruppel-like factor 4 (KLF4), a zinc-finger transcription factor implicated in BC progression and therapy sensitivity. Biological assays provided evidence that miR-99b-5p positively regulates KLF4 and BCL2 protein levels, potentially promoting cell survival and contributing to drug resistance. Mechanistically, we identified TRAF7 as a downstream target of miR-99b-5p, and TRAF7 modulates KLF4 protein stability through ubiquitin-mediated degradation. Suppression of TRAF7 by miR-99b-5p reduces KLF4 ubiquitination, enhancing its stability and downstream signaling.

ÖZ

Amaç: Luminal B tipi meme kanseri, artmış tümör agresifliği ve özgün moleküler özellikleriyle karakterize olup, trastuzumab ve tamoksifen gibi hedefe yönelik tedavilere karşı direnç gelişimiyle sıklıkla ilişkilidir. MikroRNA'lar (miRNA), kanser progresyonu ve tedavi yanıtının temel düzenleyicileri olarak öne çıkmaktadır. Bu çalışmada, miR-99b-5p'nin Luminal B meme kanserinde tedavi direncini düzenleyici rolü araştırılmıştır.

Yöntemler: Trastuzumab'a duyarlı ve trastuzumab dirençli BT-474 meme kanseri hücrelerinde, miR-99b-5p'nin fonksiyonu, özgül mimik ve inhibitörler kullanılarak değerlendirilmiştir. Gen ve protein ekspresyon düzeyleri sırasıyla qRT-PCR ve Western blot yöntemleriyle analiz edilmiştir. Ayrıca, ENCORI, UALCAN, GeneMiner, ROCplot ve UbiBrowser gibi biyoinformatik veri tabanları aracılığıyla hedef genlerin ekspresyon profilleri ve tedavi cevabı ile ilişkisi incelenmiştir.

Bulgular: miR-99b-5p ekspresyonu, tamoksifen veya trastuzumab uygulaması sonrasında ilaca duyarlı BT-474 hücrelerinde azalırken, trastuzumab dirençli hücrelerde artış göstermiştir; bu durum, terapötik adaptasyonda dinamik bir düzenleyici rolüne işaret etmektedir. Biyoinformatik ve deneysel analizler, miR-99b-5p'nin çinko parmak transkripsiyon faktörü (KLF4) ile ilişkili olduğunu ortaya koymuştur. Hücre temelli analizlerde miR-99b-5p'nin KLF4 ve BCL2 protein düzeylerini artırarak hücre sağkalımını desteklediği ve ilaç direncine katkıda bulunduğu gözlemlenmiştir. Mekanistik olarak, miR-99b-5p'nin hedeflediği TRAF7 olarak bilinen E3 ubikütin ligazın KLF4'ün ubikütinasyonu aracılı yıkımını düzenlediği; TRAF7'nin baskılanmasıyla KLF4 ubikütinasyonunun azaldığı ve protein stabilitesinin arttığı belirlenmiştir.

Address for Correspondence/Yazışma Adresi: Senem Noyan, Biotechnology Institute, Ankara University, Ankara, Türkiye

E-mail / E-posta: senemnoyan@gmail.com/snoyan@ankara.edu.tr
ORCID ID: orcid.org/0000-0001-6455-3702

Gazi Med J 2026;37(1):83-91

Noyan and Gür Dedeoğlu. Ubiquitin-Mediated KLF4 Regulation by miR-99b-5p

ABSTRACT

Conclusion: These findings reveal a novel miR-99b-5p/TRAF7/KLF4 axis that promotes drug resistance in Luminal B BC through post-transcriptional and ubiquitin-mediated mechanisms. Targeting this regulatory pathway may represent a promising strategy to overcome therapy resistance and may warrant further investigation in biomarker development and targeted treatment design.

Keywords: Luminal breast cancer, miR-99b-5p, post-transcriptional regulation and drug response

ÖZ

Sonuç: miR-99b-5p/TRAF7/KLF4 ekseni, Luminal B meme kanserinde post-transkripsiyonel ve ubikütin aracılı mekanizmalarla tedavi direncinin gelişiminde rol oynamaktadır. Bu düzenleyici ağın hedeflenmesi, tedaviye direnç gelişimini engellemeye yönelik yeni terapötik stratejilerin geliştirilmesine katkı sağlayabilir. Bulgular, bu eksenin daha kapsamlı fonksiyonel ve çoklu omik yaklaşımlarla incelenmesini gerekli kılmaktadır.

Anahtar Sözcükler: Luminal meme kanseri, miR-99b-5p, transkripsiyon sonrası regülasyon ve ilaç yanıtı

INTRODUCTION

Given the heterogeneity of breast cancer (BC), targeted therapeutic approaches have become essential in enhancing treatment efficacy (1). The routine assessment of biomarkers, including progesterone receptor, estrogen receptor (ER), HER2, and Ki-67, is essential for accurate diagnosis and to inform adjuvant treatment strategies in BC management (2). Molecular analytical techniques have significantly refined the identification of prognostic and predictive biomarkers, enabling more accurate patient stratification (3). The molecular classification system introduced by Sorlie et al. (4), based on gene expression profiling, established a framework for distinguishing biologically distinct subtypes of BC. Among these, the Luminal subtypes, typically distinguished by the expression of ER/PR and the absence of HER2 amplification, are routinely classified by immunohistochemistry and further subclassified into Luminal A and Luminal B based on molecular profiling, with each subtype carrying distinct prognostic significance. Additionally, multigene expression assays such as Oncotype DX, PAM50, MammaPrint, and EndoPredict offer improved risk stratification and inform decisions regarding the potential benefit of adjuvant chemotherapy when used alongside endocrine therapy, thereby advancing the paradigm of personalized BC management (5,6).

For hormone-receptor-positive Luminal A and Luminal B BC, adjuvant endocrine therapy is the cornerstone of treatment. These tumors are generally responsive to anti-estrogen therapies, including tamoxifen and aromatase inhibitors, and, when applicable, to HER2-directed therapies (7). Tamoxifen inhibits ER signaling, thereby reducing tumor proliferation, and is typically given long-term to lower recurrence risk (7). Trastuzumab, a monoclonal antibody targeting HER2, is primarily used to treat HER2-positive Luminal B tumors, where it inhibits HER2 signaling (8). It also helps overcome resistance to endocrine therapy by modulating the interplay between HER2 and ER signaling pathways (9). Nevertheless, prolonged anti-estrogen and HER2-targeted therapies often lead to intrinsic or acquired drug resistance, limiting treatment effectiveness and promoting disease progression.

MicroRNAs (miRNAs) are small, non-coding RNAs that control gene expression post-transcriptionally (10) and, in BC, influence major oncogenic and tumor-suppressive pathways by regulating processes such as proliferation, apoptosis, and metastasis (11). Epigenetic regulation mediated by miRNAs has emerged as a central focus of recent research aimed at developing prognostic and predictive models (12). Numerous miRNAs are significantly upregulated or downregulated depending on the BC stage, the risk of tumor recurrence, and the overall survival, underscoring their potential

as valuable biomarkers and therapeutic targets (13). Dysregulated miRNA expression is closely linked to various malignancies, including BC (14,15); altered expression profiles not only distinguish cancerous from healthy tissues but also enable classification of distinct molecular subtypes (16). This underscores the significance of miRNA profiling as a promising tool in personalized medicine, particularly for the early detection and accurate classification of BC subtypes (17). Specifically, in Luminal BC, miRNA profiling provides significant prognostic and predictive value beyond that provided by traditional endocrine therapies (18). Distinct miRNA expression patterns have been shown to differentiate between Luminal A and Luminal B subtypes, with certain profiles correlating with tumor grade, proliferation rate, and clinical outcomes (19). These findings indicate that miRNAs acting both as molecular biomarkers for disease detection and prognostic assessment, and as valuable surrogates for guiding and personalizing therapeutic interventions.

Kruppel-like factor 4 (KLF4) plays a fundamental role in BC, integrating multiple signaling pathways that regulate cell proliferation, differentiation, apoptosis, and maintenance of cancer stem cells (20). Due to its dual and context-dependent roles, acting either as a tumor suppressor or as an oncogene, tight regulation of KLF4 expression and activity is essential (21). Recent studies have highlighted the importance of post-transcriptional regulatory mechanisms in modulating KLF4 protein levels, particularly in BC (22). These mechanisms include miRNAs, non-coding RNAs, RNA-binding proteins, mRNA modifications, and alternative splicing events. This study presents a comprehensive overview of the post-transcriptional regulation of miR-99b-5p, which is downregulated in response to drug treatment in Luminal BC. It explores the underlying molecular mechanisms driving this regulation and examines the impact of miR-99b-5p on tumor behavior and therapeutic response. We hypothesize that therapeutic pressure from tamoxifen or trastuzumab in Luminal B BC dynamically modulates miR-99b-5p levels, which, in turn, regulate KLF4 expression through an ubiquitin-mediated mechanism, thereby influencing the drug response. Recent evidence suggests that post-transcriptional regulation of key transcription factors, including KLF4, plays a pivotal role in BC progression and therapy response (23). However, the mechanisms controlling KLF4 protein stability remain incompletely understood. Emerging data implicate E3 ubiquitin ligases such as TRAF7 in modulating protein degradation pathways in cancer. Yet, the interplay between miRNAs and ubiquitin ligases in regulating KLF4 stability in Luminal B BC has not been elucidated. Here, we investigate the role of miR-99b-5p in modulating KLF4 expression through targeting TRAF7, unveiling a novel miR-99b-5p/TRAF7/KLF4 regulatory axis that may contribute to therapy resistance and BC progression.

Gazi Med J 2026;37(1):83-91

Noyan and Gür Dedeoğlu. Ubiquitin-Mediated KLF4 Regulation by miR-99b-5p

MATERIALS AND METHODS

Cell Culture and Drug Treatment

BT-474 BC cells, either trastuzumab-sensitive or -resistant, were grown in RPMI-1640 supplemented with 10% fetal bovine serum and 1% penicillin under standard culture conditions at 37 °C with 5% CO_2 in a humidified incubator. In addition to the BT-474 BC cell line, the SK-BR-3 and MCF7 cell lines were used. SKBR3 cells were cultured in McCoy's medium, and MCF7 cells were cultured in DMEM high glucose medium. Tamoxifen (Tocris) and trastuzumab (Roche) were used in this study; their IC_{50} values were determined in our previous research (24). BT-474 (trastuzumab-resistant) cells were continuously treated with 6 µg/mL trastuzumab to maintain the resistant phenotype (25,26).

As this study involves *in vitro* cell culture experiments, ethics committee approval is not required according to the guidelines of the Scientific and Technological Research Council of Turkey (TUBITAK) for such studies.

miRNA Transfection

Overexpression of miR-99b-5p was induced using a miR-99b-5p mimic (Qiagen, Cat. No. MSY0000689), with a scrambled negative control (Qiagen, Cat. No. SI03650318); downregulation was achieved using a miR-99b-5p inhibitor (Dharmacon, Cat. No. IH-300658-05) and its corresponding scrambled control (Dharmacon, Cat. No. IN-001005-01). Cells were plated in 6-well plates (3×10^5 cells/well) and cultured overnight under standard conditions (37 °C, 5% CO_2, humidified atmosphere). Transfection was carried out the following day using 25 nM of the mimic or 100 nM of the inhibitor. Cell pellets were collected 48 and 72 hours after transfection for RNA isolation and protein extraction, respectively.

Quantitative Real-Time PCR (qRT-PCR)

Total RNA was isolated from the harvested cell pellets using TRIzol reagent (Invitrogen), and complementary DNA (cDNA) was synthesized from 1 µg of RNA using the iScript™ cDNA Synthesis Kit (Bio-Rad). qRT-PCR analysis was then performed on a LightCycler® 480 system (Roche) using a SYBR Green-based master mix. Primer sequences and corresponding reference IDs are listed in Table 1. The expression of miR-99b-5p in BC cells was evaluated by reverse-transcribing total RNA using the miScript II RT Kit (Qiagen, Cat. No. 218160) according to the manufacturer's instructions. Quantification of miR-99b-5p was performed by qRT-PCR using a specific miScript Primer Assay (Qiagen, Cat. No. MS00032165) and the miScript SYBR®

Table 1. Primer sequences.

Gene name	Sequences 5'---3'	RefSeq ID
KLF4	F: ACCCACACAGGTGAGAAACC	NM_004235.6
	R: ATGTGTAAGGCGAGGTGGTC	
BCL2	F: CTTTGAGTTCGGTGGGGTCA	NM_000633.3
	R: GCCGGTTCAGGTACTCAGTC	
TRAF7	F: ACCACAGGGACCAGAATGGA	NM_032271.3
	R: GTCCTGCAGTGCTGCTTGTA	
GAPDH	F: TTCGACAGTCAGCCGCAT	NM_002046.7
	R: TGAAGGGGTCATTGATGGCA	

Green PCR Kit (Qiagen, Cat. No. 218075) on the LightCycler® 480 system (Roche). Each reaction was conducted in duplicate using 5 ng of cDNA. The endogenous control RNU6 (Qiagen, Cat. No. MS00033740) was used for normalization, and relative expression was quantified via the $2^{-\Delta CT}$ approach.

Western Blot

Total protein was extracted from cell pellets using RIPA buffer (Cell Signaling Technology, Cat. No. 9806) and quantified by the Bradford assay (Thermo Scientific). Equal amounts (15 µg per sample) were separated by SDS-PAGE at 100 V for 2 hours. Proteins were transferred to membranes by wet transfer, and subjected to immunoblotting with specific primary antibodies, and then incubated with corresponding secondary antibodies. The following primary antibodies were used: KLF4 (Invitrogen, Cat. No. MA5-41214, 1:1000), BCL2 (Cell Signaling Technology, D17C4, 1:1000), and β-actin (ACTB, BioLegend, Cat. No. 643801, 1:1000). S The secondary antibodies used were HRP-conjugated anti-mouse IgG (Cell Signaling Technology, Cat. No. 7076) and HRP-conjugated anti-rabbit IgG (Cell Signaling Technology, Cat. No. 7074). Immunoreactive bands were visualized using the WesternBright Sirius Kit (Advansta, Cat. No. K12043-D20) and imaged with the LI-COR Odyssey Imaging System.

Bioinformatic Analysis

The expression of miR-99b-5p in BC was analyzed using the ENCORI and UALCAN databases. KLF4 expression was evaluated separately in tumor versus normal tissues, as well as across PAM50 molecular subtypes, utilizing GTEx and The Cancer Genome Atlas (TCGA) datasets through the GeneMiner platform. Additionally, the association between miR-99b-5p expression and drug response was investigated using ROCplot analysis. The substrate proteins of E3s were predicted using UbiBrowser.

Statistical Analysis

Statistical significance for pairwise comparisons was assessed using Student's t-test, with p-values below 0.05 deemed statistically significant. Statistical analyses were conducted using SPSS software (IBM Corporation, New York, USA).

RESULTS

miR-99b-5p Expression Dynamics in Drug Response and Resistance

Our previous research analyzed miRNA expression profiles that were altered in response to therapeutic regimens, including tamoxifen and trastuzumab. We observed that miR-99b-5p expression was significantly downregulated following exposure to either drug (24). Supporting these findings, an independent study reported that the overexpression of miR-99b-5p promotes proliferation of BT-474 BC cells (27). In this study, we aimed to elucidate the regulatory role of miR-99b-5p, which is consistently suppressed following drug exposure (Figure 1a). miR-99b-5p expression was markedly upregulated in trastuzumab-resistant BT-474 cells (Figure 1c), suggesting a potential role in acquired resistance mechanisms. Consequently, its predictive value for trastuzumab response in patients with luminal BC was assessed by receiver operating characteristic (ROC) curve analysis (n = 47). The analysis revealed a 1.1-fold change that was statistically

Gazi Med J 2026;37(1):83-91

Noyan and Gür Dedeoğlu. Ubiquitin-Mediated KLF4 Regulation by miR-99b-5p

significant (p=0.005). The ROC analysis yielded an area under the curve of 0.833, demonstrating robust discriminative performance; sensitivity (true positive rate) was 0.71, specificity (true negative rate) was 1.0, and the optimal threshold was 14.74 (Figure 1b). Collectively, these results demonstrate that miR-99b-5p expression is acutely downregulated in response to tamoxifen and trastuzumab, but is significantly elevated in resistant cell populations, highlighting its potential dual role in drug sensitivity and resistance.

Bioinformatic Evidence for the Regulatory Role of miR-99b-5p on KLF4 in Breast Cancer

KLF4 expression was analyzed in BC using datasets from GTEx and TCGA. The analysis revealed that KLF4 expression was significantly downregulated in breast tumor tissue compared with both normal breast tissue and adjacent non-tumorous tissue samples. PAM50-based subtype-specific analysis further demonstrated that the Luminal B subtype exhibits the lowest KLF4 expression levels (Figure 2a). In contrast, data from the ENCORI database indicated that miR-99b-5p is significantly upregulated in BC tissues. Consistently, analysis of the BRCA dataset showed elevated miR-99b-5p expression across all PAM50 subtypes relative to normal tissue (Figure 2b). Bioinformatic analyses identified a potential correlation between miR-99b-5p and KLF4 expression, suggesting a post-transcriptional regulatory interaction. Collectively, these findings imply that miR-99b-5p may modulate KLF4 expression in BC, particularly within the Luminal B subtype.

Regulatory Effects of miR-99b-5p on KLF4 and BCL2 Expression in Luminal Breast Cancer Cells

Expanding upon our previous research that suggests a regulatory interaction between miRNA and KLF4, and considering the observed downregulation of miR-99b-5p following drug treatment, we investigated the effects of miR-99b-5p modulation on KLF4 expression in BT-474 cells, a representative model of the Luminal B BC subtype. qRT-PCR (Figure 3a) and protein expression analyses (Figure 3b) revealed that miR-99b-5p inhibition led to a significant reduction in KLF4 levels, while its overexpression did not elicit a notable change. In parallel, suppression of miR-99b-5p resulted in decreased BCL2 protein levels, supporting a positive correlation between KLF4 and BCL2 expression. Notably, tamoxifen-treated BT-474 cells exhibited increased miR-99b-5p expression, and this increase was accompanied by significant upregulation of both KLF4 and BCL2 relative to the scrambled control. A similar pattern of miR-99b-5p induction and associated protein upregulation was observed following trastuzumab treatment (Figure 3c). Collectively, these findings suggest a context-dependent positive regulatory relationship between miR-99b-5p and expression of KLF4, potentially contributing to tumor cell proliferation.

KLF4 Expression is Downregulated by miRNA Inhibition Through an Indirect Ubiquitination Mechanism

The observed decrease in KLF4 expression following miR-99b-5p inhibition was hypothesized to result from enhanced KLF4 degradation mediated by a ubiquitination-related gene targeted by miR-99b-5p. We propose that miR-99b-5p indirectly regulates KLF4 protein levels by suppressing a gene involved in KLF4 ubiquitination. Inhibition
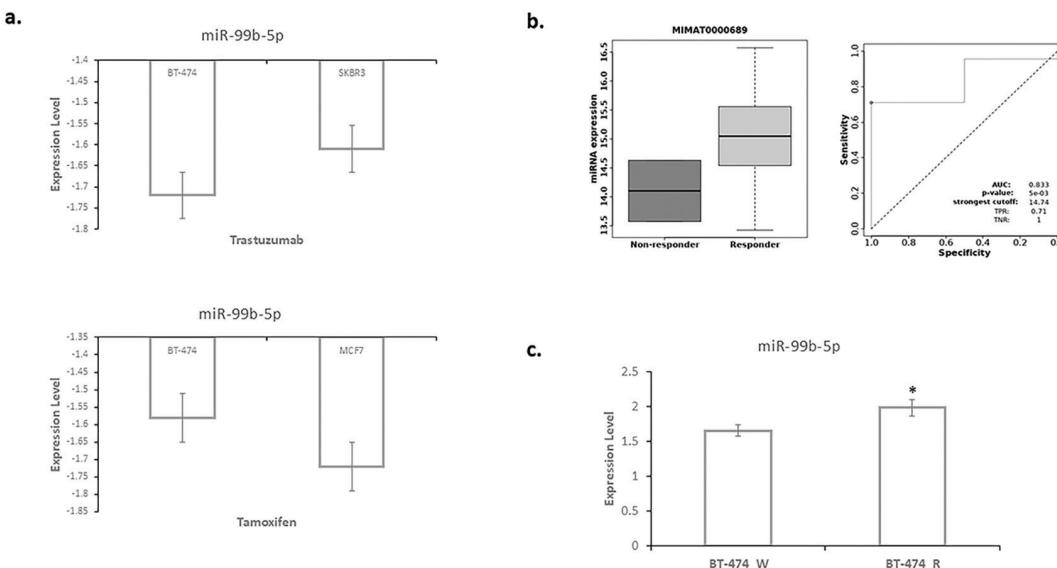

Figure 1. Expression levels of miR-99b-5p in Luminal breast cancer cells. (a) Luminal breast cancer cell lines were treated with tamoxifen (10 µM) or trastuzumab (6 µg/mL) for 48 hours, and miR-99b-5p expression levels were assessed by qPCR-array. (b) Predictive performance of miR-99b-5p expression in response to trastuzumab was evaluated using receiver operating characteristic curve analysis in Luminal breast cancer patients (n =47), stratified by median follow-up time. The area under the curve was 0.833, with a statistically significant p-value (p=0.005). The optimal cut-off value for miR-99b-5p expression was 14.74, yielding a true positive rate of 0.71 and a true negative rate of 1.0. (c) miR-99b-5p expression levels were measured in parental (BT-474_W) and trastuzumab-resistant BT-474 (BT-474_R) cells using qRT-PCR, normalized to U6 snRNA. Data are presented as mean ± standard deviation from two independent experiments. Statistical significance was determined using the Student's t-test (*p<0.01).

KLF4: Kruppel-like factor 4, AUC: Area under the curve, TPR: True positive rate, TNR: True negative rate, miRNA: MicroRNA.

Gazi Med J 2026;37(1):83-91

Noyan and Gür Dedeoğlu. Ubiquitin-Mediated KLF4 Regulation by miR-99b-5p

of miR-99b-5p leads to upregulation of this target gene, thereby promoting KLF4 ubiquitination and reducing its protein stability. To investigate this post-transcriptional regulatory mechanism, predicted miR-99b-5p target genes were intersected with known E3 ubiquitin ligases implicated in KLF4 degradation. This analysis yielded *FBXO22*, *FBXO32*, *FZR1*, and *TRAF7* as common candidates (Figure 4a). Subsequent evaluation based on expression levels, presence of a miR-99b-5p binding site within the 3'-untranslated region (3'-UTR), and literature evidence led to the selection of TRAF7 for further analysis. Comprehensive bioinformatic interrogation of the

TCGA BC cohort identified a statistically significant overexpression of TRAF7 in tumor specimens compared to matched normal tissues. In contrast, KLF4 expression was lower in tumors than in normal samples (Figure 4b). Based on this inverse correlation (Figure 4c), we evaluated TRAF7 expression in BT-474 cells after transfection with a miR-99b-5p mimic. Overexpression of miR-99b-5p led to a marked decrease in *TRAF7* expression (Figure 4d). Furthermore, target prediction analysis revealed a putative miR-99b-5p binding site within the 3'-UTR of *TRAF7*, supporting the notion that miR-99b-5p directly interacts with *TRAF7* mRNA. Collectively, these data
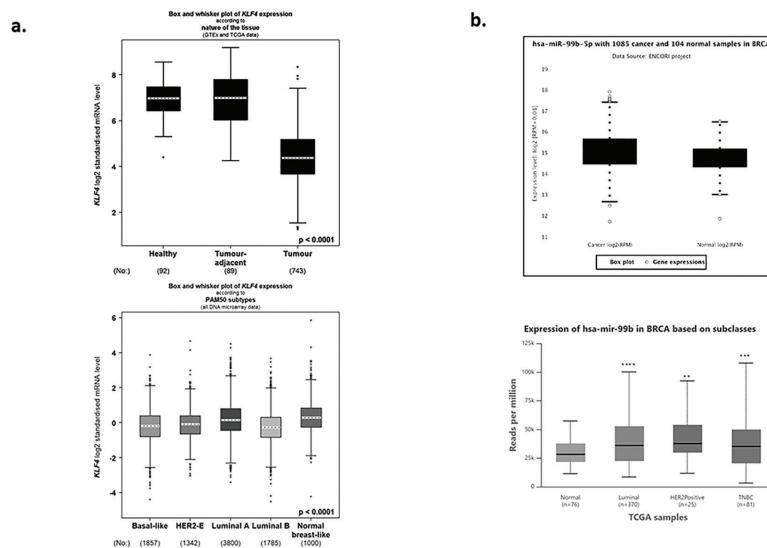

Figure 2. Bioinformatic analysis of miR-99b-5p and KLF4 expression in breast cancer. (a) KLF4 expression was analyzed using transcriptomic datasets from GTEx and TCGA, showing significant downregulation in breast tumor tissues compared to both normal breast tissue and adjacent non-tumorous samples (healthy, n =92; tumor adjacent, n =89; tumor, n =743; p<0.0001). Subtype-specific analysis based on PAM50 classification revealed that the Luminal B subtype exhibits the lowest KLF4 expression levels among subtypes (basal-like, n =1857; HER2-enriched, n =1342; Luminal A, n =3800; Luminal B, n =1785; normal-like, n =1000; p<0.0001). (b) Conversely, miR-99b-5p expression was significantly upregulated in breast cancer tissues compared to normal samples, as assessed via the ENCORI database (tumor, n =1085; normal, n =104; p<0.001). Furthermore, analysis of PAM50 subtypes in the UALCAN BRCA dataset showed that all breast cancer subtypes exhibit elevated miR-99b-5p levels compared to normal tissue (normal, n =76; Luminal A, n =370; HER2-enriched, n =25; TNBC, n =81) Differences between normal and breast cancer subtypes were evaluated using the two-sided Wilcoxon rank-sum test. Bars represent median expression values. Statistical significance is indicated as follows: ****p<0.0001, ***p<0.001, **p<0.01.

KLF4: Kruppel-like factor 4.
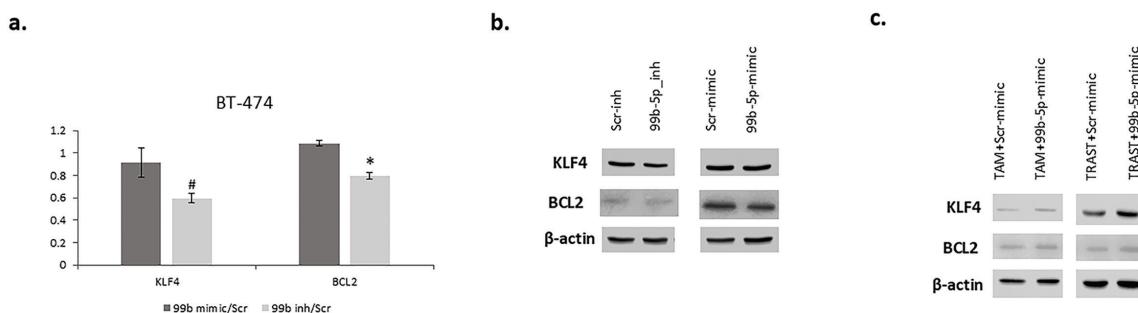
Figure 3. miR-99b-5p regulates KLF4 and BCL2 expression in BT-474 Luminal breast cancer. Modulation of miR-99b-5p in BT-474 cells, a model of Luminal B breast cancer, was performed to investigate its impact on KLF4 and BCL2 expression. qRT-PCR (a) and protein analyses (b) demonstrated that inhibition of miR-99b-5p significantly reduced KLF4 expression, whereas miR-99b-5p overexpression did not cause notable changes (two biological replicates, #p<0.01, *p<0.05). Concurrently, suppression of miR-99b-5p led to decreased BCL2 protein levels, suggesting a positive correlation between KLF4 and BCL2 expression. (c) Upon treatment with tamoxifen, BT-474 cells showed increased miR-99b-5p expression accompanied by significant upregulation of both KLF4 and BCL2 proteins compared to scrambled controls. A similar induction of miR-99b-5p and associated protein upregulation was observed following trastuzumab treatment.

KLF4: Kruppel-like factor 4, Scr: Scrambled control, TAM: Tamoxifen, TRAST: Trastuzumab.

Gazi Med J 2026;37(1):83-91

Noyan and Gür Dedeoğlu. Ubiquitin-Mediated KLF4 Regulation by miR-99b-5p
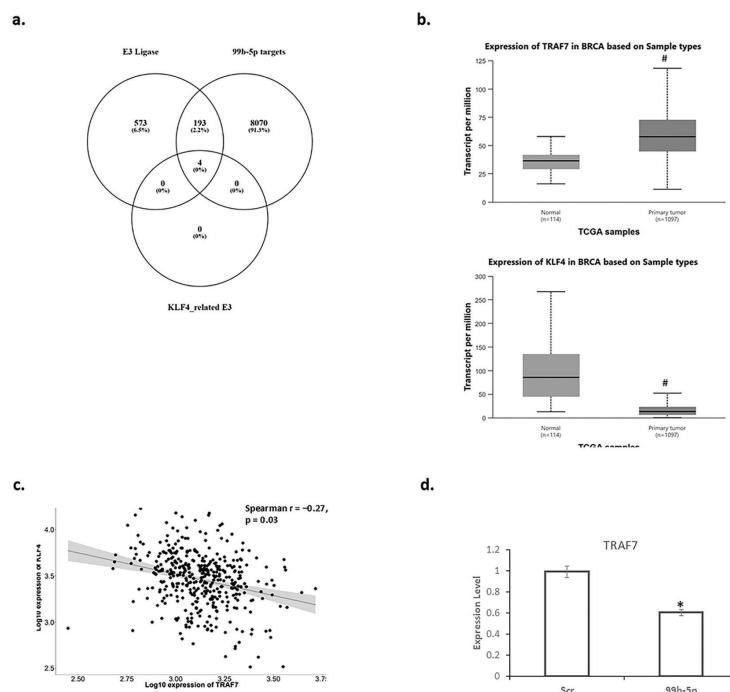
Figure 4. Indirect regulation of KLF4 by miR-99b-5p through targeting the E3 Ligase TRAF7. (a) Venn diagram showing the intersection between predicted miR-99b-5p target genes and known E3 ubiquitin ligases associated with KLF4 degradation. Four common candidates, *FBXO22, FBXO32, FZR1*, and *TRAF7*, were identified for further analysis. (b) Expression analysis of TRAF7 and KLF4 in breast cancer tissues using UALCAN database. Box plots illustrating *TRAF7* and *KLF4* mRNA expression levels in breast tumor tissues compared to normal breast tissues. TRAF7 expression is significantly elevated in tumor samples, whereas KLF4 expression is decreased, indicating an inverse expression pattern between the two genes in breast cancer (#p<0.001). (c) Negative correlation between *TRAF7* and *KLF4* expression in breast cancer. Scatter plot showing a significant inverse correlation between *TRAF7* and *KLF4* mRNA expression levels in breast cancer samples, as determined by Spearman correlation analysis (r= −0.27, p=0.03; n =403). (d) Relative *TRAF7* mRNA expression levels in BT-474 cells transfected with scrambled control or miR-99b-5p mimic. Overexpression of miR-99b-5p significantly reduced *TRAF7* expression compared to scrambled controls (two biological replicates, *p<0.05), indicating that *TRAF7* is negatively regulated by miR-99b-5p in Luminal breast cancer cells.

KLF4: Kruppel-like factor 4, Scr: Scrambled control.

imply that miR-99b-5p modulates KLF4 protein levels indirectly by targeting TRAF7, which in turn regulates KLF4 degradation via the ubiquitin–proteasome system.

DISCUSSION

Features of Luminal B BC include distinct profiles of somatic point mutations, DNA methylation patterns, and gene copy-number alterations (28) and are associated with aggressive clinical behavior. Its prognosis parallels those of HER2-enriched and basal-like subtypes, whereas Luminal A BC generally exhibits a more favorable outcome. Notably, Luminal B tumors demonstrate higher relapse rates within the first five-years post-diagnosis, which decline over time, alongside a metastatic dissemination pattern similar to that observed in basal-like and HER2-enriched cancers (29).

miRNAs serve as master regulators of BC development and drug response by integrating signals from diverse cellular pathways (30). Their capacity to target multiple genes simultaneously not only drives tumor progression and metastasis but also modulates chemotherapeutic efficacy, making them promising biomarkers and therapeutic targets for overcoming drug resistance in BC (31). Both

tamoxifen and trastuzumab, key therapeutic agents for hormone receptor-expressing and HER2-overexpressing BCs, respectively, exhibit variable clinical responses that may be modulated by miRNAs (24,32,33). In line with these findings, our study revealed that miR-99b-5p expression decreased following treatment with tamoxifen and trastuzumab, regardless of cell line or drug, suggesting that miR-99b-5p may be downregulated in response to therapeutic pressure in luminal BC. Moreover, we observed increased miR-99b-5p levels in trastuzumab-resistant cells, further supporting the hypothesis that this miRNA is dynamically regulated by drug exposure and may play a role in acquired resistance mechanisms.

KLF4, a zinc-finger transcription factor, exhibits a context-dependent dual role in BC, acting either as an oncogene or as a tumor suppressor, and is regulated by a complex post-transcriptional network (34). miRNAs represent one of the principal mechanisms regulating KLF4 via post-transcriptional control (35). By binding to the 3' untranslated region of KLF4 mRNA, these small non-coding RNAs induce either degradation of the target mRNA or inhibition of its translation. A previous study revealed that KLF4 mediates estrogen signaling in BC by promoting estrogen-induced transactivation and cell proliferation (23). Mechanistically, estrogen downregulates pVHL, a key regulator

Gazi Med J 2026;37(1):83-91

Noyan and Gür Dedeoğlu. Ubiquitin-Mediated KLF4 Regulation by miR-99b-5p

of KLF4 degradation, leading to KLF4 accumulation, which in turn drives BC progression (23). Moreover, another study demonstrated that KLF4 enhances sensitivity to tamoxifen in BC by suppressing the MAPK/ERK and p38 signaling pathways. High KLF4 expression is associated with an improved therapeutic response and a favorable prognosis, suggesting that targeting the KLF4/MAPK regulatory axis may constitute a novel therapeutic approach to overcome tamoxifen resistance in BC (36). Our study, building upon this evidence, reveals that upregulation of miR-99b-5p in the presence of tamoxifen leads to increased expression of both KLF4 and BCL2. This suggests that elevated levels of miR-99b-5p may compromise therapeutic efficacy by modulating the expression of key regulators of drug response, including KLF4. These findings indicate a potentially oncogenic role for miR-99b-5p in the context of endocrine resistance and underscore the complexity of KLF4 regulation in tamoxifen-treated luminal BC.

E3 ubiquitin ligases, which control protein turnover by targeting substrates for ubiquitin-dependent proteasomal degradation, play critical roles in signal transduction, cellular homeostasis, and cancer development (37); their dysregulation has been implicated in BC progression, metastasis, and therapy resistance (38). Among E3 ligases, members of the TRAF family, particularly TRAF7, have emerged as context-dependent regulators of tumorigenesis (39). TRAF7, which also functions as an adaptor protein in TNF signaling pathways, promotes or suppresses KLF4 expression, the depending on tumor type. In hepatocellular carcinoma, TRAF7 facilitates KLF4 degradation via ubiquitination, while in meningiomas, TRAF7 loss leads to increased KLF4 expression (40). Our findings suggest that in Luminal B BC cells, miR-99b-5p positively regulates KLF4 protein levels by targeting *TRAF7*. An inverse correlation between miR-99b-5p and *TRAF7* expression was observed by bioinformatic analysis and was further supported by the identification of a putative miR-99b-5p binding site within *TRAF7* 3' UTR, suggesting a direct post-transcriptional regulatory interaction. Functional suppression of *TRAF7* by miR-99b-5p is postulated to attenuate KLF4 ubiquitination, thereby promoting its stabilization by preventing proteasomal degradation. Taken together, this miR-99b-5p/TRAF7/KLF4 axis may contribute to BC cell survival and drug response, highlighting the context-dependent role of ubiquitin-mediated regulation in BC.

Collectively, these post-transcriptional regulatory mechanisms constitute a highly adaptable and evolutionarily conserved network, enabling BC cells to dynamically modulate KLF4 expression in response to microenvironmental cues, therapeutic pressure, and intrinsic genomic alterations. A comprehensive understanding of this regulatory landscape not only deepens our insight into BC pathophysiology but also reveals promising therapeutic opportunities aimed at correcting dysregulated KLF4 signaling and re-establishing cellular homeostasis. In this context, our findings support the existence of a miR-99b-5p/TRAF7/KLF4 regulatory axis that governs KLF4 protein stability through a ubiquitin-dependent mechanism, potentially contributing to therapy resistance in Luminal B BC. These data demonstrate the central importance of post-transcriptional and ubiquitin-mediated modulation in BC progression and drug responsiveness. Targeting specific components of this axis, particularly miRNA–E3 ligase interactions, may represent a novel and effective strategy to restore tumor suppressor activity and overcome resistance in hormone receptor–positive BCs.

Study Limitations

Although this study provides important insights into the role of miR-99b-5p in modulating KLF4 expression and drug resistance mechanisms in Luminal B BC through *in vitro* models, further validation in in vivo systems, such as animal models, is essential to substantiate the mechanistic findings. The translation of these results into a clinical context presents additional challenges, as the complex interactions within the tumor microenvironment and the variability in patient-specific factors may influence the regulation and functional activity of the key molecules involved. Consequently, it is crucial that future studies incorporate in vivo validation and clinical cohort analysis to confirm the clinical relevance of targeting the miR-99b-5p/TRAF7/KLF4 axis and to assess its therapeutic potential in patient populations.

CONCLUSION

Our findings delineate a novel post-transcriptional regulatory axis whereby miR-99b-5p indirectly enhances KLF4 protein stability through the targeted suppression of the E3 ubiquitin ligase TRAF7. This regulatory pathway appears to modulate therapeutic response in Luminal B BC cells, particularly by influencing sensitivity to tamoxifen and trastuzumab. This evidence supports the notion that miR-99b-5p may function as a positive regulator of KLF4 and BCL2, contributing to therapy response dynamics and potentially to resistance mechanisms. Hormone-dependent BCs represent the predominant subtype, rendering acquired or intrinsic resistance to endocrine therapies a significant clinical obstacle. Consequently, extensive research efforts have focused on characterizing the molecular mechanisms underlying hormone resistance, identifying robust biomarkers indicative of the resistant phenotype, and investigating alternative molecular targets to overcome these resistance mechanisms. One promising strategy is the use of epigenetic drugs that target reversible epigenetic modifications and, when combined with chemotherapy or endocrine therapy, may help restore therapeutic responsiveness. Moving forward, integrating multi-omics approaches, including transcriptomics, epitranscriptomics, proteomics, and functional genomics, will be essential to achieving a more comprehensive understanding of how post-transcriptional regulation of key factors, such as KLF4, contributes to BC progression and therapy resistance. In particular, investigations into the temporal dynamics of miRNA expression and the interplay between lncRNAs and circRNAs under different treatment conditions will be critical for the development of next-generation therapeutic strategies capable of effectively modulating these complex regulatory networks.

Ethics

Gazi Med J 2026;37(1):83-91

Noyan and Gür Dedeoğlu. Ubiquitin-Mediated KLF4 Regulation by miR-99b-5p

REFERENCES

1. Liang Y, Zhang H, Song X, Yang Q. Metastatic heterogeneity of breast cancer: molecular mechanism and potential therapeutic targets. Semin Cancer Biol. 2020; 60: 14–27.

2. Korde LA, Somerfield MR, Carey LA, Crews JR, Denduluri N, Hwang ES, et al. Neoadjuvant chemotherapy, endocrine therapy, and targeted therapy for breast cancer: ASCO Guideline. J Clin Oncol Off J Am Soc Clin Oncol. 2021; 39: 1485–505.

3. Bischoff H, Espié M, Petit T. Neoadjuvant therapy: current landscape and future horizons for ER-positive/HER2-negative and triple-negative early breast cancer. Curr Treat Options Oncol. 2024; 25: 1210–24.

4. Sorlie T, Perou CM, Tibshirani R, Aas T, Geisler S, Johnsen H, et al. Gene expression patterns of breast carcinomas distinguish tumor subclasses with clinical implications. Proc Natl Acad Sci U S A. 2001; 98: 10869–74.

5. Jia Z, Yue F, Chen X, Narayanan N, Qiu J, Syed SA, et al. Protein arginine methyltransferase PRMT5 regulates fatty acid metabolism and lipid droplet biogenesis in white adipose tissues. Adv Sci (Weinh). 2020; 7: 2002602.

6. Mondal S, Preetam S, Deshwal RK, Thapliyal S, Rustagi S, Alghamdi S, et al. Advances in prognostic and predictive biomarkers for breast cancer: integrating multigene assays, hormone receptors, and emerging circulating biomarkers. Clin Chim Acta. 2025; 578: 120513.

7. Shien T, Iwata H. Adjuvant and neoadjuvant therapy for breast cancer. Jpn J Clin Oncol. 2020; 50: 225–9.

8. Giordano SH, Temin S, Kirshner JJ, Chandarlapaty S, Crews JR, Davidson NE, et al. Systemic therapy for patients with advanced human epidermal growth factor receptor 2-positive breast cancer: American Society of Clinical Oncology clinical practice guideline. J Clin Oncol Off J Am Soc Clin Oncol. 2014; 32: 2078–99.

9. Sharaf BM, Giddey AD, Alniss H, Al-Hroub HM, El-Awady R, Mousa M, et al. Untargeted metabolomics of breast cancer cells MCF-7 and SkBr3 treated with tamoxifen/trastuzumab. Cancer Genomics Proteomics. 2022; 19: 79–93.

10. Saliminejad K, Khorram Khorshid HR, Soleymani Fard S, Ghaffari SH. An overview of microRNAs: biology, functions, therapeutics, and analysis methods. J Cell Physiol. 2019; 234: 5451–65.

11. Weidle UH, Dickopf S, Hintermair C, Kollmorgen G, Birzele F, Brinkmann U. The role of micro RNAs in breast cancer metastasis: preclinical validation and potential therapeutic targets. Cancer Genomics Proteomics. 2018; 15: 17–39.

12. Diener C, Keller A, Meese E. Emerging concepts of miRNA therapeutics: from cells to clinic. Trends Genet. 2022; 38: 613–26.

13. Tarighati E, Keivan H, Mahani H. A review of prognostic and predictive biomarkers in breast cancer. Clin Exp Med. 2023; 23: 1–16.

14. Quiat D, Olson EN. MicroRNAs in cardiovascular disease: from pathogenesis to prevention and treatment. J Clin Invest. 2013; 123: 11–8.

15. Dehwah MAS, Xu A, Huang Q. MicroRNAs and type 2 diabetes/obesity. J Genet Genomics. 2012; 39: 11–8.

16. Cantini L, Bertoli G, Cava C, Dubois T, Zinovyev A, Caselle M, et al. Identification of microRNA clusters cooperatively acting on epithelial to mesenchymal transition in triple negative breast cancer. Nucleic Acids Res. 2019; 47: 2205–15.

17. Zubor P, Kubatka P, Dankova Z, Gondova A, Kajo K, Hatok J, et al. miRNA in a multiomic context for diagnosis, treatment monitoring and personalized management of metastatic breast cancer. Future Oncol. 2018; 14: 1847–67.

18. Kudela E, Samec M, Koklesova L, Liskova A, Kubatka P, Kozubik E, et al. miRNA Expression profiles in luminal a breast cancer-implications in biology, prognosis, and prediction of response to hormonal treatment. Int J Mol Sci. 2020; 21.

19. Lowery AJ, Miller N, Devaney A, McNeill RE, Davoren PA, Lemetre C, et al. MicroRNA signatures predict oestrogen receptor, progesterone receptor and HER2/neu receptor status in breast cancer. Breast Cancer Res. 2009; 11: R27.

20. Yu F, Li J, Chen H, Fu J, Ray S, Huang S, et al. Kruppel-like factor 4 (KLF4) is required for maintenance of breast cancer stem cells and for cell migration and invasion. Oncogene. 2011; 30: 2161–72.

21. He Z, He J, Xie K. KLF4 transcription factor in tumorigenesis. Cell death Discov. 2023; 9: 118.

22. Zhou Z, Song X, Chi JJ, Gius DR, Huang Y, Cristofanilli M, et al. Regulation of KLF4 by posttranslational modification circuitry in endocrine resistance. Cell Signal. 2020; 70: 109574.

23. Hu D, Zhou Z, Davidson NE, Huang Y, Wan Y. Novel insight into KLF4 proteolytic regulation in estrogen receptor signaling and breast carcinogenesis. J Biol Chem. 2012; 287: 13584–97.

24. Noyan S, Gurdal H, Dedeoglu BG. Involvement of miR-770-5p in trastuzumab response in HER2 positive breast cancer cells. PLoS One. 2019; 14.

25. Noyan S, Gür Dedeoğlu B. miR-770-5p-induced cellular switch to sensitize trastuzumab resistant breast cancer cells targeting HER2/EGFR/IGF1R bidirectional crosstalk. Turkish J Biol = Turk Biyol Derg. 2024; 48: 153–62.

26. Dolapçi İB, Noyan S, Polat AY, Gürdal H, Dedeoğlu BG. miR-216b-5p promotes late apoptosis/necroptosis in trastuzumab-resistant SK-BR-3 cells. Turkish J Biol. 2023; 47: 199–207.

27. Noyan S, Gür Dedeoğlu B. Upregulation of miR-99b-5p Modulates ESR1 expression as an adaptive mechanism to circumvent drug response via facilitating ER/HER2 crosstalk. Balkan Med J. 2025; 42: 150–6.

28. Weinstein JN, Collisson EA, Mills GB, Shaw KRM, Ozenberger BA, Ellrott K, et al. The Cancer Genome Atlas Pan-Cancer analysis project. Nat Genet. 2013; 45: 1113–20.

29. Li ZH, Hu PH, Tu JH, Yu NS. Luminal B breast cancer: patterns of recurrence and clinical outcome. Oncotarget. 2016; 7: 65024–33.

30. An X, Sarmiento C, Tan T, Zhu H. Regulation of multidrug resistance by microRNAs in anti-cancer therapy. Acta Pharm Sin B. 2017; 7: 38–51.

31. Bhatia A, Upadhyay AK, Sharma S. miRNAs are now starring in "no time to die: overcoming the chemoresistance in cancer". IUBMB Life. 2023; 75: 238–56.

32. Zhang W, Xu J, Shi Y, Sun Q, Zhang Q, Guan X. The novel role of miRNAs for tamoxifen resistance in human breast cancer. Cell Mol Life Sci. 2015; 72: 2575–84.

33. Rezaei Z, Sebzari A, Kordi-Tamandani DM, Dastjerdi K. Involvement of the dysregulation of miR-23b-3p, miR-195-5p, miR-656-5p, and miR-340-5p in trastuzumab resistance of HER2-positive breast

Gazi Med J 2026;37(1):83-91

Noyan and Gür Dedeoğlu. Ubiquitin-Mediated KLF4 Regulation by miR-99b-5p

cancer cells and system biology approach to predict their targets involved in resistance. DNA Cell Biol. 2019; 38: 184–92.

34. Frazzi R. KLF4 is an epigenetically modulated, context-dependent tumor suppressor. Front cell Dev Biol. 2024; 12: 1392391.

35. Frazzi R, Farnetti E, Nicoli D. circRNA/miRNA networks regulate KLF4 in tumor development. Non-coding RNA. 2025; 11.

36. Jia Y, Zhou J, Luo X, Chen M, Chen Y, Wang J, et al. KLF4 overcomes tamoxifen resistance by suppressing MAPK signaling pathway and predicts good prognosis in breast cancer. Cell Signal. 2018; 42: 165–75.

37. Sampson C, Wang Q, Otkur W, Zhao H, Lu Y, Liu X, et al. The roles of E3 ubiquitin ligases in cancer progression and targeted therapy. Clin Transl Med. 2023; 13: e1204.

38. Qi J, Ronai ZA. Dysregulation of ubiquitin ligases in cancer. Drug Resist Updat Rev Comment Antimicrob Anticancer Chemother. 2015; 23: 1–11.

39. Zotti T, Scudiero I, Vito P, Stilo R. The emerging role of TRAF7 in tumor development. J Cell Physiol. 2017; 232: 1233–8.

40. He H, Wu Z, Li S, Chen K, Wang D, Zou H, et al. TRAF7 enhances ubiquitin-degradation of KLF4 to promote hepatocellular carcinoma progression. Cancer Lett. 2020; 469: 380–9.

Retrospective Analysis of Multi-Method Sequencing Results in Patients with Skeletal Dysplasia

İskelet Displazisi Olan Hastalarda Çok Metotlu Dizileme Sonuçlarının Retrospektif Analizi

● Ezgi Urtekin[1], ● Ferda Perçin[2], ● Aysun Bideci[2], ● Hasan Hüseyin Kazan[3], ● Yusuf Bahap[1], ● Gülsüm Kayhan[1]

[1]Department of Medical Genetics, Gazi University Faculty of Medicine, Ankara, Türkiye
[2]Department of Child Health and Diseases, Gazi University Faculty of Medicine, Ankara, Türkiye
[3]Department of Medical Biology, University of Health Sciences Gülhane Faculty of Medicine, Ankara, Türkiye

ABSTRACT

Objective: Skeletal dysplasia is a heterogeneous disease affecting the development of the skeletal system. Due to its complexity, clinical or radiological examinations can be informative; therefore, molecular approaches may be more effective for differential diagnosis and may assist in clarifying subtypes. Although studies in cohorts have identified associated genes and variants, further research is needed. This study aims to investigate the genotype-phenotype relationship in a Turkish cohort.

Methods: Thirty-six patients were involved in the study. Patients were classified according to the 2023 revision of the Nosology of Genetic Diseases of the Skeletal System. Following the genetic diagnostic algorithm, Sanger sequencing, targeted gene panels, clinical exome sequencing, or whole exome sequencing were performed. The existing literature was reviewed for some of the identified variants.

Results: The proportion of females (63.9%) was higher than that of males (36.1%). Notably, the parents of 16 patients (45.7%) were consanguineous. Pathogenic or likely pathogenic variants were identified in 29 of 36 patients, while variants of uncertain significance were identified in 6 patients. The diagnostic yield was 80% based on sequencing methods. The groups with the highest number of molecular diagnoses were group 2, type II collagen disorders (5 patients with COL2A1 variants), and group 34, syndromes with craniosynostosis (5 patients with FGFR2, FGFR3, TWIST1, or SMO variants), according to nosology.

ÖZ

Amaç: İskelet displazisi, iskelet sisteminin gelişimini etkileyen heterojen hastalık gurubudur. Kompleks doğası nedeniyle, klinik ya da radyolojik değerlendirmeler bilgi verici olabilir; ancak moleküler yaklaşımlar ayırıcı tanı ve alt tiplerin belirlenmesi açısından daha etkilidir. Kohort çalışmaları ilişkili genleri ve varyantları aydınlatmış olsa da bu konuda halen çalışmaya ihtiyaç duyulmaktadır. Sunulan çalışma bir Türk kohortunda genotip-fenotip ilişkisini araştırmayı amaçlamaktadır.

Yöntemler: Sunulan çalışmaya 36 hasta dahil edilmiştir. Hastalar, Genetik İskelet Hastalıklarının Nozolojisi, 2023'e göre gruplandırılmıştır. Genetik tanı algoritmasına uygun olarak hastalara Sanger dizileme, hedefli gen paneli, klinik ekzom dizileme ya da tüm ekzom dizileme çalışılmıştır. Tespit edilen spesifik varyantlar için mevcut literatür derlenmiştir.

Bulgular: Katılımcılar arasında kadın sayısı (%63,9), erken sayısından (%36,1) daha fazladır. Kritik olarak, 16 hastanın (%45,7) ebeveynleri akrabadır. Otuz altı hastanın 29'unda patojenik ya da olası patojenik varyant tespit edilmiştir. Dizileme metoduna bağlı olarak tanı verimi %80'dir. Nozolojiye göre moleküler tanısı en yüksek olan gruplar, grup 2, tip II kolajen hastalıkları (5 hastada COL2A1 varyantları) ve grup 34, kraniosinostozlu sendromlar (5 hastada FGFR2, FGFR3, TWIST1 ya da SMO varyantları) şeklindedir.

Gazi Med J 2026;37(1):92-99

Urtekin et al. Multi-Method Sequencing in Skeletal Dysplasia

ABSTRACT

Conclusion: This study emphasizes the genetic and phenotypic variation in skeletal dysplasia within a Turkish cohort. We expect these findings to contribute to the current literature and help clinicians in patient follow-up and assessment.

Keywords: Skeletal dysplasia, molecular diagnosis, sequencing

ÖZ

Sonuç: Sunulan çalışma, bir Türk kohortunda, iskelet displazisinde genetik ve fenotipik varyasyonları vurgulamıştır. Elde edilen bulguların mevcut literatüre katkı sunması ve hasta takibi ve değerlendirmesi açısından klinisyenleri yönlendirmesi beklenmektedir.

Anahtar Sözcükler: İskelet displazisi, moleküler tanı, dizileme

INTRODUCTION

Skeletal dysplasia encompasses a wide range of genetic disorders involving abnormalities in bone and cartilage resulting from defects in skeletal development and maintenance (1). It is highly heterogeneous, with more than 450 diseases or syndromes affecting bone growth. In addition to bones and cartilage, skeletal dysplasia can negatively affect muscles, tendons, and ligaments (2,3). Although isolated cases are rare, the overall occurrence of skeletal dysplasia is approximately one in 5,000 people worldwide (2-4).

At the molecular level, various pathways involved in regulating structural proteins, metabolic processes, and the epiphysis play critical roles in the development of skeletal dysplasia (3,5). According to the 2023 revision of the Nosology of Genetic Skeletal Disorders, these conditions are classified into 41 categories, with 552 genes associated with them. Therefore, beyond standard clinical and radiological diagnostic methods, molecular testing can be a valuable tool for differential and definitive diagnosis of skeletal dysplasia. Among these testing methods, gene panels and exome sequencing (ES) are important not only for diagnosing but also for identifying new genes or pathways related to skeletal dysplasia (6,7).

Given the rise of next-generation sequencing (NGS) for disease diagnosis, numerous studies in diverse populations have documented variant frequencies and identified novel or potentially disease-related genes (8-10). However, these efforts still need to confirm variant classifications, especially for those of unknown significance, and to discover new variants in the associated genes by screening diverse cohorts. Therefore, this study analyzed data from Sanger sequencing, gene panels, and ES from 36 patients with skeletal dysplasia. Our results show the usefulness of these methods within a genetic algorithm for the molecular and differential diagnosis of skeletal dysplasia.

MATERIALS AND METHODS

Ethics

The present study was approved by the Ethics Committee of Gazi University (approval number 403; dated 30 May 2022). Both verbal and written consent was obtained from patients or their guardians before the study was initiated.

Participants

The present study involved 36 patients with skeletal dysplasia who were enrolled at the Department of Medical Genetics, Faculty of Medicine, Gazi University in Ankara, between July 2017 and January 2022. Patients were classified according to the 2023 revision of the Nosology of Genetic Skeletal Disorders. Patients with mild phenotypes, including isolated short stature, were excluded from the study.

Genetic Analyses

The disease-related genes were sequenced, and a genetic algorithm-based diagnostic approach was applied. Accordingly, patients with specific skeletal dysplasias who had known genetic mutations in siblings and/or parents were screened using Sanger sequencing. In other cases, NGS using gene panels, clinical ES (CES), or whole-ES (WES) was performed to comprehensively analyze genes associated with skeletal dysplasia phenotypes. All sequencing procedures were carried out after isolating genomic DNA from peripheral venous blood samples using the Qiagen EZ1 Advanced XL automated system (Qiagen Inc., Switzerland), following the manufacturer's standard protocol. The integrity of the isolated DNA was verified by 1% agarose gel electrophoresis, and concentrations were measured using a NanoDrop (NanoDrop 1000; Thermo Scientific, USA) or a Qubit 4.0 (Thermo Scientific, USA).

Sanger sequencing was performed after amplification of specific gene regions containing the relevant variants and further processing using the BigDye™ Terminator v3.1 Cycle Sequencing Kit (Thermo Scientific, USA). All amplicons were run on the Applied Biosystems 3130 Genetic Analyzer (Thermo Scientific, USA). Finally, chromatogram files were visualized using Chromas 2.6.6 (Technelysium Pty Ltd, Australia), and relevant variants were manually screened.

For the NGS gene-panel application, amplification-based custom panels were used. After single or multiplex amplification of target genes, the amplicons were processed with the Nextera XT DNA Library Preparation Kit and sequenced on the MiSeq System (Illumina Inc., USA). For CES and WES, target regions, including intron–exon boundaries and entire exons, were identified using hybridization-based methods: the SOPHiA Clinical Exome Solution (Sophia Genetics, France) for CES and the Whole Exome Sequencing Panel—Exome 2.0 (Twist Biosciences, USA) for WES. All amplicons were sequenced on either an MGISEQ-2000 (BGI Inc., China) or a NovaSeq 6000 (Illumina Inc., USA) platform.

NGS data were processed using either the Variant Annotation and Filter Tool (VarAft) v2.17.1 (11) or Genomize-SEQ (Genomize, Türkiye). Using these programs, raw FASTQ files were aligned to the human reference genome (hg19) and a binary alignment map file was generated. Next, variant call format files were produced. Using the same tools, variants were filtered based on minor allele frequencies of less than 0.001 in common genome databases and on genes listed in the Human Phenotype Ontology (https://hpo.jax.org/) related to disease. Finally, variants were prioritized and classified using VarSome (https://varsome.com/) or Franklin by Genoox (https://franklin.genoox.com/clinical-db/home), in accordance with the American College of Medical Genetics (ACMG) Guidelines (12).

Gazi Med J 2026;37(1):92-99

Urtekin et al. Multi-Method Sequencing in Skeletal Dysplasia

RESULTS

Clinical Findings

The current study involved 36 patients with skeletal dysplasia. The patients were classified according to the 2023 revision of the Nosology of Genetic Diseases of the Skeletal System and assigned to 16 groups (Table 1). Participants' ages ranged from newborn to 69 years. The proportion of females (23, 63.9%) was higher than that of males (13, 36.1%). The parents of 16 of 36 patients (44.4%) were consanguineous, and 16 of 36 patients (44.4%) had family members with similar clinical features.

Analysis of height measurements in patients within the pathogenic/likely pathogenic (LP) group showed that six individuals had heights above the 3rd percentile at the time of evaluation. These patients were diagnosed with conditions such as Stickler syndrome, Keutel syndrome, osteopetrosis, Shwachman-Diamond syndrome, and craniosynostosis, for which short stature is not typically expected. Although short stature can occur in Shwachman-Diamond syndrome, the height of patient P15 was recorded at the 14th percentile, and data on other indicators, such as growth velocity and bone age, were

unavailable. Among five patients with craniosynostosis syndromes, primarily characterized by craniofacial features, two had heights below -3 SD. One of the remaining 25 patients lacked height data; this patient was diagnosed with osteogenesis imperfecta primarily on the basis of recurrent fractures. Among the 18 patients with skeletal dysplasia, in whom short stature was a key feature, 12 had heights below -3 SD and 8 had heights between -3 and -2 SD. A summary of the clinical findings of these patients is shown in Supplementary Table 1.

Molecular Findings

Sequencing results showed that all patients except one (P30, 35/36, 97.2%) had a variant associated with skeletal dysplasia. Of these 35 variants, 28 were classified as pathogenic or LP, indicating a diagnostic yield of 80%, while the remaining 7 (20%) were of unknown significance. Among the 29 patients with pathogenic or LP variants, 24 distinct variants were identified in 20 genes. The number of patients with variants, categorized by nosological groups, is shown in Table 1. Ten of these variants (detected in P6, P9, P11-15, P17, P19, P24, and P28) were novel, and ACMG classifications and in silico predictions of those variants were provided in Supplementary Table 2.

Table 1. Number of patients in groups of nosology.

Nosology group no	Nosology group name	Gene	Patient number	
			P/ LP variant	VUS
1	FGFR3 chondrodysplasias	FGFR3	3	1
2	Type 2 collagen disorders	COL2A1	5	
3	Type 11 collagen disorders	COL11A1		1
4	Sulfation disorders	PAPSS2	1	
5	Dysplasias with multiple joint dislocations	SLC10A7	1	
7	Proteoglycan core proteins disorders	HSPG2	1	
9	Pseudoachondroplasia and the multiple epiphyseal dysplasias	COL9A1	1	
11	Metaphyseal dysplasias	COL10A1	1	
		EFL1	2	
15	Mesomelic and rhizo-mesomelic dysplasias	ROR2	1	
		SHOX		2
17	Acromelic dysplasias	FBN1	1	
		GNAS	1	2
21	Primordial dwarfism and slender bones group	CCDC8	1	
23	Chondrodysplasia punctata (CDP) group	MGP	1	
24	Osteopetrosis and related osteoclast disorders	CLCN7	1	
26	Osteogenesis Imperfecta and bone fragility group	COL1A1	1	
		SERPINF1	1	
		TMEM38B	1	
34	Syndromes featuring craniosynostosis	FGFR2	2	
		FGFR3	1	
		TWIST1	1	
		SMO	1	
38	Limb hypoplasia – reduction defects group	-	1	

P: Pathogenic, LP: Likely pathogenic, VUS: Variant of unknown significance.

Gazi Med J 2026;37(1):92-99

Urtekin et al. Multi-Method Sequencing in Skeletal Dysplasia

Fifteen patients with these variants exhibited an autosomal dominant inheritance pattern, four of whom inherited the disease from an affected parent. All 13 patients with an autosomal recessive disease had consanguineous parents. Additionally, one patient was found to have a somatic mosaic variant in the *SMO* gene, consistent with Curry-Jones syndrome (CRJS). In a patient initially diagnosed with fibular aplasia, tibial campomelia, and oligosyndactyly (FATCO) syndrome, no variants were identified in genes associated with these clinical features. The *COL2A1* gene, which encodes the collagen type II alpha 1 chain, was the most commonly affected gene in this group. Five patients were assigned to cluster 2 (type II collagen) and five to cluster 34 (syndromes with craniosynostosis) based on nosological classification. Within the FGFR3 chondroplasia group, the second nosology category, one patient exhibited a variant of uncertain clinical significance, while three patients carried pathogenic variants associated with achondroplasia. Variants identified in the patients are listed in Table 2.

Table 2. Variants detected in the participants in the presence of zygosity, pathogenicity, associated disease and familial segregation information.

Patient	Method	Variant	Zygosity	Variant classification (ACMG criteria)	Diagnosis (#OMIM; inheritance pattern)	Familial segregation
P1	Sanger Sequencing	*FGFR3*:NM_000142.4:c.1138G>A (p.Gly380Arg)	Het	Pathogenic	Achondroplasia (100800), AD	Father: Het Mother: Wt
P2	Sanger Sequencing	*FGFR3*:NM_000142.4:c.1138G>A (p.Gly380Arg)	Het	Pathogenic	Achondroplasia (100800), AD	NA
P3	Sanger Sequencing	*FGFR3*:NM_000142.4:c.1138G>A (p.Gly380Arg)	Het	Pathogenic	Achondroplasia (100800), AD	NA
P4	WES	*COL2A1*:NM_001844.5:c.1510G>A (p.Gly504Ser)	Het	Pathogenic	*COL2A1*-associated skeletal dysplasia (120280), AD	Father: Het Mother: NA
P5	WES	*COL2A1*:NM_001844.5:c.2059G>A (p.Gly687Ser)	Het	LP	*COL2A1*-associated skeletal dysplasia (120280), AD	Father: Wt Mother: Wt
P6	WES	*COL2A1*:NM_001844.5:c.2095G>A (p.Gly699Ser)	Het	LP	*COL2A1*-associated skeletal dysplasia (120280), AD	Father: Wt Mother: Wt
P7	CES	*COL2A1*:NM_001844.5:c.1510G>A (p.Gly504Ser)	Het	Pathogenic	*COL2A1*-associated skeletal dysplasia (120280), AD	Father: NA Mother: NA
P8	CES	*COL2A1*:NM_001844.5:c.1699G>A (p.Gly567Ser)	Het	Pathogenic	*COL2A1*-associated skeletal dysplasia (120280), AD	Father: NA Mother: NA
P9	CES	*PAPSS2*:NM_001015880.1:c.520+2T>A	Hom	LP	Brachyolmia 4 with mild epiphyseal and metaphyseal changes (612847), AR	Father: NA Mother: NA
P10	WES	*SLC10A7*:NM_001029998.6:c.335G>A (p.Gly112Asp)	Hom	LP	Short stature, amelogenesis imperfecta, and skeletal dysplasia with scoliosis (618363), AR	Father: NA Mother: NA
P11	WES	*HSPG2*:NM_005529.7:c.4948T>G (p.Cys1650Gly)	Hom	LP	Schwartz-Jampel syndrome, type 1 (255800), AR	Father: NA Mother: NA
P12	WES	*COL9A1*:NM_001851.4:c.1852C>T (p.Arg618Ter)	Hom	Pathogenic	Stickler syndrome, type IV (614134), AR	Father: NA Mother: Het
P13	CES	*COL10A1*: NM_000493.4:c.1766T>C (p.Phe589Ser)	Het	LP	Metaphyseal chondrodysplasia, Schmid type (156500), AD	Father: NA Mother: NA
P14	WES	*EFL1*:NM_024580:c.277T>C (p.Ser93Pro)	Hom	LP	Shwachman-Diamond syndrome 2 (617941), AR	Father: Het Mother: Het
P15	Sanger Sequencing	*EFL1*:NM_024580:c.277T>C (p.Ser93Pro)	Hom	LP	Shwachman-Diamond syndrome 2 (617941), AR	Father: NA Mother: NA
P16	WES	*ROR2*:NM_004560.4:c.355C>T (p.Arg119Ter)	Hom	Pathogenic	Robinow syndrome (268310), AR	Father: NA Mother: NA
P17	CES	*FBN1*:NM_000138.4:c.5285G>A p.(Gly1762Asp)	Het	LP	*FBN1*-associated skeletal dysplasia (134797), AD	Father: Het Mother: NA Affected sibling: Het

Gazi Med J 2026;37(1):92-99

Urtekin et al. Multi-Method Sequencing in Skeletal Dysplasia

Table 2. Continued

Patient	Method	Variant	Zygosity	Variant classification (ACMG criteria)	Diagnosis (#OMIM; inheritance pattern)	Familial segregation
P18	CES	*GNAS*:NM_000516.5:c.125G>T (p.Arg42Leu)	Het	LP	Pseudopseudohypoparathyroidism (612463), AD	Father: NA Mother: NA
P19	CES	*CCDC8*:NM_032040.5:c.84_85delTA (p.Lys29AlafsTer118)	Hom	LP	3-M syndrome 3 (614205), AR	Father: NA Mother: NA
P20	Gene Panel	*MGP:*NM_000900.5:c.43del (p.Val15Ter)	Hom	LP	Keutel syndrome (245150), AR	Father: NA Mother: NA
P21	Gene Panel	*CLCN7*:NM_001287.6:c.1576C>T (p.Arg526Trp)	Hom	LP	Osteopetrosis, autosomal recessive 4 (611490), AR	Father: NA Mother: NA
P22	Gene Panel	*COL1A2*:NM_000089.4:c.2521G>A (p.Gly841Ser)	Het	LP	*COL1A2*-associated osteogenesis imperfect (120160), AD	Father: NA Mother: NA
P23	Gene Panel	*SERPINF1*:NM_002615.7:c.271_279dup (p.Ala91_Ser93dup)	Hom	LP	Osteogenesis imperfecta, type VI (613982), AR	Father: NA Mother: NA
P24	WES	*TMEM38B*:NM_018112.3:c.240_247dup (p.Ile83ThrfsTer21)	Hom	Pathogenic	Osteogenesis imperfecta, type XIV (615066), AR	Father: Het Mother: Het
P25	CES	*FGFR2:*NM_000141.4:c.1021A>C (p.Thr341Pro)	Het	Pathogenic	Crouzon syndrome (123500), AD	Father: NA Mother: NA
P26	WES	*FGFR2*:NM_000141.4:c.983A>G (p.Tyr328Cys)	Het	Pathogenic	Crouzon syndrome (123500), AD	Father: NA Mother: NA Siblings: NA
P27	CES	*FGFR3*:NM_000142.5:c.749C>G (p.Pro250Arg)	Het	Pathogenic	Muenke syndrome (602849), AD	Father: NA Mother: NA
P28	WES	*TWIST1*:NM_000474.4:c.464A>C (p.Tyr155Ser)	Het	LP	Saethre-Chotzen syndrome with or without eyelid anomalies (101400), AD	Father: Het Mother: Wt Affected twin: Het
P29	Sanger Sequencing	*SMO*:NM_005631.5:c.1234C>T (p.Leu412Phe)	Het (somatic; skin biopsy)	Pathogenic	Curry-Jones syndrome, somatic mosaic (601707)	Father: NA Mother: NA
P30	WES	-			FATCO syndrome (246570)	
P31	CES	*FGFR3:*NM_000142.5:c.1748A>T (p.Lys583Met)	Het	VUS	-	Father: NA Mother: NA
P32	WES	*COL11A1*:NM_001854.4:c.206G>C (p.Gly69Ala)	Het	VUS	-	Father: NA Mother: NA
P33	CES	*SHOX:*NM_000451.3c.847del (p.Ala283ArgfsTer124?)	Het	VUS	-	Father: NA Mother: NA
P34	CES	*SHOX:*NM_000451.3c.847del (p.Ala283ArgfsTer124?)	Het	VUS	-	Father: NA Mother: NA
P35	CES	*GNAS:*NM_080425.3:c.2968-3C>G	Het	VUS	-	Father: Wt Mother: Het
P36	CES	*GNAS:*NM_080425.3:c.2968-3C>G	Het	VUS	-	Father: Wt Mother: Het

LP: Likely pathogenic, VUS: Variant of unknown significance, Wt: Wildtype, Het: Heterozygous, Hom: Homozygous, AD: Autosomal dominant, AR: Autosomal recessive, WES: Whole exome sequencing, CES: Clinical exome sequencing, NA: Not applicable, ACMG: American College of Medical Genetics.

Gazi Med J 2026;37(1):92-99

Urtekin et al. Multi-Method Sequencing in Skeletal Dysplasia

DISCUSSION

Skeletal dysplasia encompasses a highly heterogeneous group of genetic disorders, and its differential diagnosis can be difficult based on radiographic and clinical evaluation. Therefore, molecular techniques are valuable for precise diagnosis, thereby influencing disease management (13). Although the genetic basis of skeletal dysplasia has been described in various populations (14-18) and even in the Turkish population (19,20), further studies are needed to identify novel associated genes and variants.

This study presents molecular genetic findings in 36 Turkish patients with skeletal dysplasia. Using various sequencing methods for genetic diagnosis, the researchers successfully identified all but one patient at the molecular and diagnostic levels. Including Sanger sequencing, the diagnostic success rate reaches 80%. The *COL2A1* gene was the most affected in this group. Ages at diagnosis ranged from 1 month to 69 years, showing that skeletal dysplasia can have a wide range of severity. Patients were grouped into nosological categories based on their specific or probable diagnoses. The largest groups were group 2 (type II collagen disorders, 5 patients) and group 34 (syndromes with craniosynostosis, 5 patients). Variants of unknown significance in the *FGFR3, COL11A1, SHOX*, and *GNAS* genes, potentially associated with clinical features, were identified in six patients.

Type II collagen disorders are characterized by skeletal dysplasia, ocular manifestations (such as cataracts, myopia, lens subluxation, vitreous abnormalities, and retinal detachment), hearing loss, and orofacial features. They cause a wide range of diseases, from fatal conditions in the perinatal period to mild symptoms in adulthood (21). This study included five patients with pathogenic or LP variants in the *COL2A1* gene. All patients carried missense variants (Gly504Ser, Gly687Ser, p.Gly567Ser, and Gly699Ser) that lead to the substitution of glycine, a neutral, non-polar amino acid that is small enough to occupy the center of the collagen triple helix, with serine, a neutral, polar amino acid. Due to the unique structural role of glycine residues in the collagen triple helix, missense substitutions have a greater impact than truncating variants, making them the most common pathogenic variants (22). Aside from Gly699Ser, the other variants had been identified previously. The Gly504Ser variant has frequently been associated with the spondyloepiphyseal dysplasia congenita (SEDC) phenotype (23,24). In a cohort study of 93 patients with SEDC or related phenotypes, glycine substitutions in the triple-helical domain were identified in 68 (73%) patients. Additionally, in 28 of these patients, glycine was replaced by serine (25).

In group 34 of the nosological classification, which includes syndromes with craniosynostosis, pathogenic variants were identified in FGFR2 (two patients) and in FGFR3, TWIST1, and SMO (one patient each). A somatic mosaic c.1234C>T (p.Leu412Phe) variant in the SMO gene was identified in P29, who had macrocephaly, facial and cranial asymmetry, frontal bossing, microphthalmia of the left eye, low-set ears, and bilateral polysyndactyly (Figures 1a and 1b). This variant causes CRJS, which is a skeletal dysplasia characterized by polysyndactyly, craniosynostosis, microphthalmia, and patchy skin lesions. Within this group, a small number of cases of CRJS have been reported in the literature (26). While most findings in P29


Figure 1. Clinical images of the selected patients. a) Dysmorphic facial features of the P29; macrocephaly, facial and cranial asymmetry, frontal bossing, microphthalmia of the left eye, low-set ears. b) Polysyndactyly of the right hand of the P29. c) X-ray image of P9's right hand showing short metacarpals (2nd–5th), with the 5th metacarpal being the most prominent.

Gazi Med J 2026;37(1):92-99

Urtekin et al. Multi-Method Sequencing in Skeletal Dysplasia

match those of other patients described in the literature, this patient also exhibited bilateral sensorineural hearing loss.

Patient 9, with short stature (-3.27 SD), short neck, pectus carinatum, short metacarpals of the right hand (Figure 1c), and mild epiphyseal and vertebral changes, carried a homozygous LP variant in the 3-*prime-phosphoadenosine 5-prime-phosphosulfate synthase 2 (PAPSS2)* gene, classified as group 4 in the nosology. *PAPSS2* has been associated with brachyolmia type 4, characterized by a short trunk, mild shortening of the metacarpal bones, mild epiphyseal and metaphyseal changes in the tubular bones, a short femoral neck, and vertebral changes (rectangular vertebral bodies with irregular end plates and narrow intervertebral discs; OMIM #612847). *PAPSS2*-related brachyolmia results from a loss-of-function mechanism (27). The c.520+2T>A variant detected at P9 is located in intron 4. This variant is predicted to cause nonsense-mediated mRNA decay. Alternatively, if exon skipping occurs, exon 5, which constitutes part of the adenylyl-sulfate kinase domain, is also predicted to be affected. This variant has been reported as homozygous in two patients with disproportionate short stature and platyspondyly and as compound heterozygous in another case (27). Compared with other patients reported in the literature, whether or not they had the same variant, P9 lacked a short trunk, scoliosis, and platyspondyly. Since P9 is only 4.5 years old, further findings may emerge. Variable expressivity should also be considered. A summary of clinical findings for patients with biallelic *PAPSS2* variants is available in Supplementary Table 3.

In P10, a homozygous LP variant was found in the *SLC10A7* gene; this variant is linked to a group of dysplasias involving multiple joint dislocations. The gene is associated with autosomal recessive short stature, amelogenesis imperfecta, and skeletal dysplasia with scoliosis (OMIM #611459). The c.335G>A (p.Gly112Asp) variant in transmembrane domain 4, present in P10, was previously identified as part of compound heterozygosity with a splicing variant in siblings (28). Another report described this variant paired with p.Gly130Arg, also in exon 4 of the same gene (29). As detailed in Supplementary Table 4., all patients with biallelic pathogenic variants in *SLC10A7* exhibited amelogenesis imperfecta, with nearly all showing kyphoscoliosis. Unlike other patients, P10 did not have intellectual disability or hearing loss, but had pectus deformity and a narrow thorax—features absent in other patients. These differences may result from compound heterozygosity. Additionally, azoospermia was observed in P10, representing a novel finding. His hormonal profile and scrotal ultrasound results were normal. A previous report described azoospermia in an SLC10A7-associated case that also exhibited a structural chromosomal abnormality ([nv ins(2;4)] involving SLC10A7 at the breakpoint (30). However, further studies are needed to elucidate the relationship between this finding and *SLC10A7*.

P16, carrying an LP *FBN1* variant, was classified within the 17th nosology group, known as acromelic dysplasias. This group includes *FBN1*-associated geleophysic dysplasia (GD), acromicric dysplasia, and Weill-Marchesani syndrome. The c.5285G>A p.(Gly1762Asp) variant detected in P16 has not been previously reported, although similar variants, such as Gly1762Val and Gly1762Ser, have been linked to GD (31,32). Considering the features observed in P16—disproportionate short stature, short limbs, and brachydactyly—the diagnosis was deemed consistent with GD.

P30, diagnosed with FATCO syndrome, was categorized in group 38 (limb hypoplasia–reduction defects). FATCO syndrome involves fibular aplasia, tibial campomelia, and oligosyndactyly, although its genetic basis remains unknown. The WES test for P30 did not detect any variants linked to the observed features.

This study was limited because some patients had limited skeletal imaging or limited physical exam findings, which hindered full identification of disease-related features. Furthermore, in the group with variants of uncertain clinical significance, there remains a possibility of a different genetic cause—either not detected by the CES analysis or attributable to mechanisms outside the scope of CES/WES methods.

CONCLUSION

In genetic disorders, such as skeletal dysplasias, where molecular diagnostics may not always specify subtypes, discovering new variants and characterizing clinical features that resemble or differ from those of known variants are essential for accurate diagnosis and treatment. We believe that this study will enhance the understanding of genotype-phenotype relationships by presenting clinical data from patients with genetic skeletal diseases.

Authorship Contributions

Ethics

Acknowledgements

Footnotes

Authorship Contributions

References

1. Cui Y, Zhao H, Liu Z, Liu C, Luan J, Zhou X, et al. A systematic review of genetic skeletal disorders reported in Chinese biomedical journals between 1978 and 2012. Orphanet J Rare Dis. 2012; 7: 55.

2. Krakow D. Skeletal dysplasias. Clin Perinatol. 2015; 42: 301-19.

3. Jurcă MC, Jurcă SI, Mirodot F, Bercea B, Severin EM, Bembea M, et al. Changes in skeletal dysplasia nosology. Rom J Morphol Embryol. 2021; 62: 689–96.

Gazi Med J 2026;37(1):92-99

Urtekin et al. Multi-Method Sequencing in Skeletal Dysplasia

4. Handa A, Nishimura G, Zhan MX, Bennett DL, El-Khoury GY. A primer on skeletal dysplasias. Jpn J Radiol. 2022; 40: 245–61.

5. Guasto A, Cormier-Daire V. Signaling pathways in bone development and their related skeletal dysplasia. Int J Mol Sci. 2021; 22: 4321.

6. Mortier GR, Cohn DH, Cormier-Daire V, Hall C, Krakow D, Mundlos S, et al. Nosology and classification of genetic skeletal disorders: 2019 revision. Am J Med Genet A. 2019; 179: 2393–419.

7. Unger S, Ferreira CR, Mortier GR, Ali H, Bertola DR, Calder A, et al. Nosology of genetic skeletal disorders: 2023 revision. Am J Med Genet A. 2023; 191: 1164–209.

8. Lazarus S, Zankl A, Duncan EL. Next-generation sequencing: a frameshift in skeletal dysplasia gene discovery. Osteoporos Int. 2014; 25: 407–22.

9. Geister KA, Camper SA. Advances in Skeletal Dysplasia Genetics. Annu Rev Genomics Hum Genet. 2015; 16: 199–227.

10. Bae JS, Kim NK, Lee C, Kim SC, Lee HR, Song HR, et al. Comprehensive genetic exploration of skeletal dysplasia using targeted exome sequencing. Genet Med. 2016; 18: 563–9.

11. Desvignes JP, Bartoli M, Delague V, Krahn M, Miltgen M, Béroud C, et al. VarAFT: a variant annotation and filtration system for human next generation sequencing data. Nucleic Acids Res. 2018; 46: W545-W553.

12. Richards S, Aziz N, Bale S, Bick D, Das S, Gastier-Foster J, et al. Standards and guidelines for the interpretation of sequence variants: a joint consensus recommendation of the American College of Medical Genetics and Genomics and the Association for Molecular Pathology. Genet Med. 2015; 17: 405–24.

13. Najjar D, Maver A, Peterlin A, Jaklič H, Peterlin B. Unraveling the complexity of skeletal dysplasias in the national health system. Front Endocrinol (Lausanne). 2025; 16: 1523737.

14. Uttarilli A, Shah H, Bhavani GS, Upadhyai P, Shukla A, Girisha KM. Phenotyping and genotyping of skeletal dysplasias: Evolution of a center and a decade of experience in India. Bone. 2019; 120: 204–11.

15. Kim SJ, Lee SM, Choi JM, Jang JH, Kim HG, Kim JT, et al. Genetic analysis using a next generation sequencing-based gene panel in patients with skeletal dysplasia: a single-center experience. Front Genet. 2021; 12: 670608.

16. Sentchordi-Montané L, Benito-Sanz S, Aza-Carmona M, Díaz-González F, Modamio-Høybjør S, de la Torre C, et al. High prevalence of variants in skeletal dysplasia associated genes in individuals with short stature and minor skeletal anomalies. Eur J Endocrinol. 2021; 185: 691–705.

17. Scocchia A, Kangas-Kontio T, Irving M, Hero M, Saarinen I, Pelttari L, et al. Diagnostic utility of next-generation sequencing-based panel testing in 543 patients with suspected skeletal dysplasia. Orphanet J Rare Dis. 2021; 16: 412.

18. Silveira KC, Kanazawa TY, Silveira C, Lacarrubba-Flores MDJ, Carvalho BS, Cavalcanti DP. Molecular diagnosis in a cohort of 114 patients with rare skeletal dysplasias. Am J Med Genet C Semin Med Genet. 2021; 187: 396–408.

19. Tüysüz B, Kasap B, Sarıtaş M, Alkaya DU, Bozlak S, Kıykım A, et al. Natural history and genetic spectrum of the Turkish metaphyseal dysplasia cohort, including rare types caused by biallelic COL10A1, COL2A1, and LBR variants. Bone. 2023; 167: 116614.

20. Taşdemir Ü, Eyisoy ÖG, Gezer M, Karaman A, Demirci O. Molecular analysis of 31 cases with fetal skeletal dysplasia. J Perinat Med. 2024; 52: 886–95.

21. Gregersen PA, Savarirayan R. Type II Collagen Disorders Overview. 2019 Apr 25 [updated 2024 Oct 24]. In: Adam MP, Bick S, Mirzaa GM, Pagon RA, Wallace SE, Amemiya A, editors. GeneReviews® [Internet]. Seattle (WA): University of Washington, Seattle; 1993–2025.

22. Richards AJ, Snead MP. Molecular basis of pathogenic variants in the fibrillar collagens. Genes (Basel). 2022; 13: 1199.

23. Nishimura G, Haga N, Kitoh H, Tanaka Y, Sonoda T, Kitamura M, et al. The phenotypic spectrum of COL2A1 mutations. Hum Mutat. 2005; 26: 36–43.

24. Wu K, Li Z, Zhu Y, Wang X, Chen G, Hou Z, et al. Discovery of sensorineural hearing loss and ossicle deformity in a Chinese Li nationality family with spondyloepiphyseal dysplasia congenita caused by p.G504S mutation of COL2A1. BMC Med Genomics. 2021; 14: 170.

25. Terhal PA, Nievelstein RJ, Verver EJ, Topsakal V, van Dommelen P, Hoornaert K, et al. A study of the clinical and radiological features in a cohort of 93 patients with a COL2A1 mutation causing spondyloepiphyseal dysplasia congenita or a related phenotype. Am J Med Genet A. 2015; 167A: 461–75.

26. Twigg SRF, Hufnagel RB, Miller KA, Zhou Y, McGowan SJ, Taylor J, et al. A recurrent mosaic mutation in SMO, encoding the hedgehog signal transducer smoothened, is the major cause of curry-jones syndrome. Am J Hum Genet. 2016; 98: 1256–65.

27. Iida A, Simsek-Kiper PÖ, Mizumoto S, Hoshino T, Elcioglu N, Horemuzova E, et al. Clinical and radiographic features of the autosomal recessive form of brachyolmia caused by PAPSS2 mutations. Hum Mutat. 2013; 34: 1381–6.

28. Ashikov A, Abu Bakar N, Wen XY, Niemeijer M, Rodrigues Pinto Osorio G, Brand-Arzamendi K, et al. Integrating glycomics and genomics uncovers SLC10A7 as essential factor for bone mineralization by regulating post-Golgi protein transport and glycosylation. Hum Mol Genet. 2018; 27: 3029–45.

29. Dubail J, Huber C, Chantepie S, Sonntag S, Tüysüz B, Mihci E, et al. SLC10A7 mutations cause a skeletal dysplasia with amelogenesis imperfecta mediated by GAG biosynthesis defects. Nat Commun. 2018; 9: 3087.

30. Tzschach A, Ramel C, Kron A, Seipel B, Wüster C, Cordes U, et al. Hypergonadotropic hypogonadism in a patient with inv ins (2;4). Int J Androl. 2009; 32: 226–30.

31. Le Goff C, Mahaut C, Wang LW, Allali S, Abhyankar A, Jensen S, et al. Mutations in the TGFβ binding-protein-like domain 5 of FBN1 are responsible for acromicric and geleophysic dysplasias. Am J Hum Genet. 2011; 89: 7–14.

32. Hasegawa K, Numakura C, Tanaka H, Furujo M, Kubo T, Higuchi Y, et al. Three cases of Japanese acromicric/geleophysic dysplasia with FBN1 mutations: a comparison of clinical and radiological features. J Pediatr Endocrinol Metab. 2017; 30: 117–21.

Does Endoscopic Adenoidectomy Really Make a Difference? A Retrospective Comparison with Conventional Adenoidectomy

Endoskopik Adenoidektomi Gerçekten Fark Yaratıyor mu? Konvansiyonel Adenoidektomi ile Retrospektif Karşılaştırma

◉ Banu Tijen Ceylan, ◉ Emirhan Akyol, ◉ Berkan Uygun

Department of Otorhinolaryngology, Gazi University Faculty of Medicine, Ankara, Türkiye

ABSTRACT

Objective: To compare endoscopic and conventional curettage adenoidectomy in terms of operative time, postoperative pain, complications, and recurrence.

Methods: This retrospective, observational comparative study screened 532 adenoidectomy cases performed between December 2015 and December 2024. After applying the inclusion and exclusion criteria, 143 patients were included in the final analysis: 73 in the endoscopic group and 70 in the conventional group, all of whom had a follow-up period of at least 12 months. Postoperative pain was assessed using visual analogue scale (VAS) at 6 and 12 hours. Recurrence at 1 year was defined as recurrence of symptoms accompanied by endoscopic evidence of adenoid hypertrophy of grade ≥ 2.

Results: Groups were comparable in sex, age, and preoperative adenoid grade. Postoperative VAS pain (4.84 ± 1.31 vs. 4.34 ± 1.34; p = 0.033) and operative time (30.75 ± 8.11 vs. 15.64 ± 5.03 minutes; p < 0.001) were significantly greater in the endoscopic group. No perioperative complications occurred in the endoscopic group, whereas one patient (1.4%) in the conventional group experienced postoperative bleeding (p = 0.490). No recurrence was observed in the endoscopic group. Recurrence occurred in two patients (2.9%) in the conventional group at the 1-year follow-up (p = 0.238).

Conclusion: Endoscopic adenoidectomy was associated with longer operative time and higher early postoperative pain. Complication and recurrence rates were lower in the endoscopic group; however, these differences did not reach statistical significance.

Keywords: Adenoidectomy, endoscopic adenoidectomy, conventional curettage adenoidectomy, postoperative pain, operative time, complication

ÖZ

Amaç: Endoskopik ve konvansiyonel küretaj adenoidektomiyi cerrahi süre, postoperatif ağrı, komplikasyon ve nüks açısından karşılaştırmak.

Yöntemler: Retrospektif, gözlemsel karşılaştırmalı bu çalışmada Aralık 2015–Aralık 2024 döneminde yapılan 532 adenoidektomi olgusu tarandı. Dâhil edilme/dışlama kriterleri uygulandıktan sonra en az 12 aylık takibi olan 143 hasta analize alındı: endoskopik grup 73, konvansiyonel grup 70. Postoperatif ağrı 6. ve 12. saatte görsel analog skala (VAS) ile değerlendirildi. Nüks, 1. yılda şikâyetlerin tekrarıyla birlikte endoskopide grade ≥ 2 adenoid hipertrofisi saptanması olarak tanımlandı.

Bulgular: Gruplar cinsiyet, yaş ve preoperatif adenoid boyutu açısından benzerdi. Postoperatif VAS ağrı skoru endoskopik grupta anlamlı olarak daha yüksekti (4,84 ± 1,31 vs. 4,34 ± 1,34; p = 0,033) ve cerrahi süre endoskopik grupta belirgin daha uzundu (30,75 ± 8,11 vs. 15,64 ± 5,03 dk; p < 0,001). Endoskopik grupta komplikasyon izlenmezken, konvansiyonel grupta 1 hastada (%1,4) kanama görüldü (p = 0,490). Endoskopik grupta nüks saptanmazken, konvansiyonel grupta 1. yıl kontrolünde 2 hastada (%2,9) nüks izlendi (p = 0,238).

Sonuç: Endoskopik adenoidektomi, daha uzun cerrahi süre ve daha yüksek erken postoperatif ağrı ile ilişkili bulundu. Komplikasyon ve nüks oranları endoskopik grupta daha düşük olmakla birlikte, bu farklar istatistiksel olarak anlamlı değildi.

Anahtar Sözcükler: Adenoidektomi, endoskopik adenoidektomi, konvansiyonel küretaj adenoidektomi, postoperatif ağrı, cerrahi süre, komplikasyon

Address for Correspondence/Yazışma Adresi: Emirhan Akyol, Department of Otorhinolaryngology, Gazi University Faculty of Medicine, Ankara, Türkiye
E-mail / E-posta: dremirhanakyol@gmail.com
ORCID ID: orcid.org/0000-0001-9233-6123

INTRODUCTION

The adenoid is a pharyngeal lymphoid tissue located in the midline of the nasopharynx, forming part of Waldeyer's ring and contributing to immune defense. It begins to develop in early embryogenesis, continues to enlarge until approximately six years of age, and then undergoes involution, typically regressing during adolescence (1,2). Adenoid hypertrophy is common in children and may result in upper airway obstruction and recurrent infections, particularly during the early school-age period. Typical clinical manifestations include nasal obstruction, mouth breathing, snoring, obstructive sleep apnoea, recurrent sinusitis, Eustachian tube dysfunction, otitis media, speech problems, and impaired maxillofacial development (3). When symptoms persist despite medical therapy, adenoidectomy is considered. Conventional curettage adenoidectomy remains the most commonly performed technique because of its low cost and technical simplicity. However, the limited surgical field may lead to residual adenoid tissue, which can increase the risk of symptom recurrence. In addition, complications such as bleeding and soft palate injury may occur with this technique.

Endoscopic adenoidectomy, by contrast, involves the removal of adenoid tissue under direct visualisation with a nasal endoscope. This technique was first described by Uçar (4) and has been reported as a safe alternative. Performing the procedure under direct visualisation facilitates more complete adenoid removal and may reduce symptomatic recurrence (5). Nevertheless, the endoscopic approach requires additional equipment and may prolong operative time.

The present study aimed to compare conventional and endoscopic adenoidectomy with respect to operative time, postoperative pain, complications, and recurrence, and to contribute to clinical decision-making regarding technique selection.

MATERIALS AND METHODS

Study Design and Ethical Approval

This retrospective, observational, comparative review was approved by the Ethics Committee of Gazi University Faculty of Medicine (decision number: 2025-223, date: 28.01.2025).

Study Population

Between December 2015 and December 2024, 532 patients who underwent adenoidectomy at the Department of Otorhinolaryngology of Gazi University Hospital were screened. Patients aged 5–14 years who underwent endoscopic or conventional adenoidectomy and had Grade III (50–75%) or Grade IV (>75%) adenoid hypertrophy on flexible nasopharyngoscopy were considered eligible. Patients were excluded if they had craniofacial anomalies; a history of cleft lip and/or palate (even if surgically corrected), velopharyngeal insufficiency, or nasal polyposis; prior adenoidectomy or adenotonsillectomy; concomitant tonsillectomy and/or ventilation tube insertion; malignancy involving the adenoid/nasopharynx; or incomplete postoperative follow-up data. After applying these criteria (Figure 1), 143 patients remained and were included in the final analysis, comprising 73 patients in the endoscopic adenoidectomy group and 70 patients in the conventional curettage adenoidectomy group; all with at least 12 months of follow-up.

Surgical Technique

All procedures were performed under general anaesthesia with orotracheal intubation by a single experienced otolaryngologist with at least 10 years' experience. Operative time was defined as the interval from initiation of adenoid excision to achievement of final haemostasis.

For endoscopic adenoidectomy, the nasopharynx was visualised via the nasal route using a 3-mm, 0° endoscope. Adenoid tissue was excised transorally using an adenotome under endoscopic guidance, and haemostasis was achieved by endoscopic identification and cauterisation of bleeding foci.

For conventional curettage adenoidectomy, the adenoid tissue was assessed transorally by digital palpation, and curettage was then performed. Residual tissue was then re-assessed by digital palpation, and curettage was repeated until the surgeon was satisfied that no residual tissue remained. Haemostasis was subsequently achieved, and the procedure was concluded.
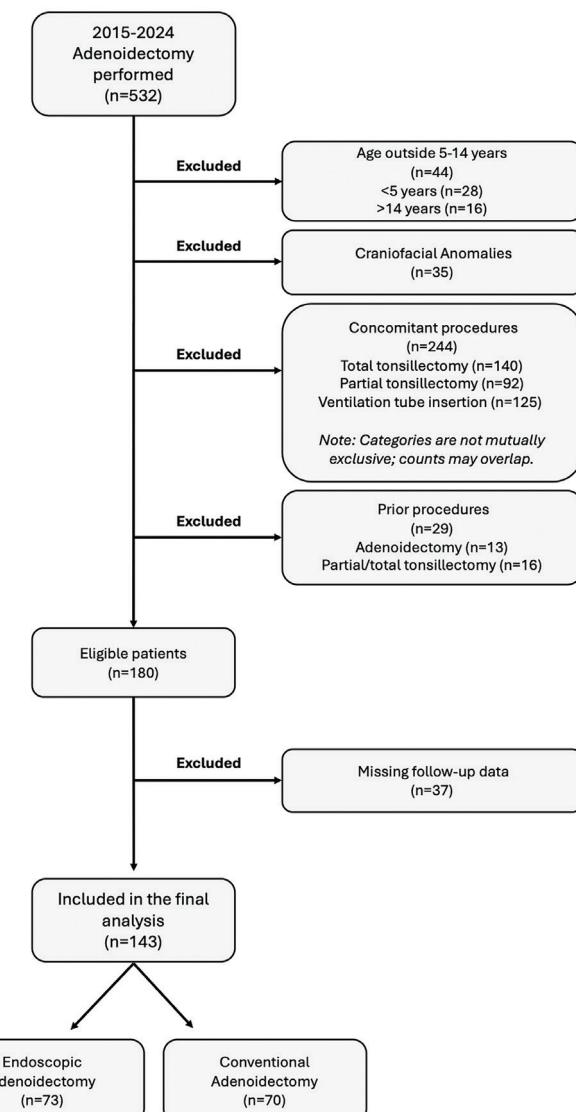

Figure 1. Flow diagram of patient selection.

Postoperative Follow-Up

Postoperative pain was assessed in all patients using the visual analogue scale (VAS) at 6 and 12 hours after surgery; the higher of the two scores was used for analysis. Patients underwent endoscopic follow-up on postoperative day 7, at 3 months, and at 1 year. Recurrence was defined as the return of symptoms at the 1-year follow-up and endoscopic evidence of grade ≥ 2 adenoid hypertrophy.

Statistical Analysis

All statistical analyses were performed using IBM SPSS Statistics (version 26.0; USA). Continuous and ordinal variables were summarised as mean ± standard deviation and median (minimum–maximum), and categorical variables were summarised as number and percentage [n (%)]. The Shapiro–Wilk test was used to assess normality. Because variables were non-normally distributed or ordinal, comparisons between the two independent groups (endoscopic vs. conventional adenoidectomy) were conducted using the Mann–Whitney U test for age, pain VAS score, operative time, and adenoid grade. Categorical variables were compared using Pearson's chi-square test when appropriate (e.g., sex) and Fisher's exact test when expected cell counts were fewer than 5 (e.g., recurrence and complications). A two-sided p-value < 0.05 was considered statistically significant.

RESULTS

A total of 143 patients were included in the study: 73 underwent endoscopic adenoidectomy, and 70 underwent conventional adenoidectomy. The demographic and clinical characteristics of the study groups are summarised in Table 1. The two groups were comparable in terms of sex distribution (endoscopic: 63.0% male, 37.0% female; conventional: 65.7% male, 34.3% female; p = 0.598). The groups were similar in age (endoscopic: 85.07 ± 21.88 months; conventional: 90.30 ± 22.88 months; p = 0.115). Preoperative adenoid size was similarly high in both groups; the mean adenoid grade was 3.75 ± 0.43 in the endoscopic group and 3.86 ± 0.35 in the conventional group (p = 0.120). Postoperative pain, assessed using the VAS, was significantly higher in the endoscopic group than in the conventional group (endoscopic: 4.84 ± 1.31; conventional: 4.34 ± 1.34; p = 0.033). Operative time also differed markedly between groups: it was longer in the endoscopic group (30.75 ± 8.11 min) than the conventional group (15.64 ± 5.03 min; p < 0.001). No perioperative complications were observed in the endoscopic group, whereas one patient (1.4%) in the conventional group experienced bleeding. This difference was not statistically significant (p = 0.490). Similarly, no recurrence was detected in the endoscopic group, whereas recurrence occurred in two patients (2.9%) in the conventional group at the 1-year follow-up; this difference was not statistically significant (p = 0.238).

DISCUSSION

In this retrospective study, we compared the two most commonly used techniques—conventional adenoidectomy and endoscopic adenoidectomy—in terms of operative time, complications, postoperative pain, and symptom recurrence. Our findings indicate that endoscopic adenoidectomy significantly prolongs operative time and is associated with slightly higher postoperative pain, whereas complication and recurrence rates are comparable to those observed with the conventional technique.

Operative Time

According to our findings, operative time was significantly longer in the endoscopic group (mean, 30.75 ± 8.11 minutes) than in the conventional group (mean, 15.64 ± 5.03 minutes) (p < 0.001). Previous studies have reported variable results regarding operative time in endoscopic adenoidectomy. In the 2023 systematic review and meta-analysis by Malas et al. (6), no significant difference in operative time was reported between conventional curettage and other surgical techniques; however, our results are consistent with those reported by Beemrote et al. (5), Manhas et al. (7), and the systematic review by Saibene et al. (8), indicating longer operative times with the endoscopic approach. This increase in operative time may be explained by the time required for endoscopic equipment setup, detailed visualisation of the nasopharynx, and meticulous, piecemeal resection in relatively difficult-to-access areas such as the torus tubarius and the nasopharyngeal roof. In addition, achieving haemostasis under direct visualisation may prolong the procedure. Given the aim of achieving more complete excision and minimising residual tissue, the longer operative time associated with the endoscopic technique may be considered acceptable.

Residual Adenoid Tissue and Recurrence

The primary goal of adenoidectomy is complete removal of adenoid tissue to minimise the risk of symptom recurrence. Conventional

Table 1. Comparison of demographic and clinical variables between endoscopic and conventional adenoidectomy groups

Parameter	Endoscopic adenoidectomy (n = 73)	Conventional adenoidectomy (n = 70)	p-value
Gender[a], n (%)			0.598
Male	46 (63)	46 (65.7)	
Female	27 (37)	24 (34.3)	
Age (months)[b]			0.115
Mean ± SD	85.07 ± 21.88	90.30 ± 22.88	
Median (min–max)	78 (60–142)	84 (60–156)	
Pain VAS score[b]			**0.033***
Mean ± SD	4.84 ± 1.31	4.34 ± 1.34	
Median (min–max)	5 (2–8)	4 (1–7)	
Operative time (min)[b]			**<0.001***
Mean ± SD	30.75 ± 8.11	15.64 ± 5.03	
Median (min–max)	30 (15–55)	15 (10–30)	
Adenoid grade[b]	3.75 ± 0.43	3.86 ± 0.35	0.120
Mean ± SD	4 (3–4)	4 (3–4)	
Median (min–max)			
Complication[c], n (%)	-	1 (1.4)	0.490
Recurrence[c], n (%)	-	2 (2.9)	0.238

[a]Pearson chi-square test, [b]Mann–Whitney U test, [c]Fisher's exact test, *p < 0.05
SD: Standard deviation, min: Minimum, max: Maximum, VAS: Visual analogue scale

curettage is often regarded as an "blind" procedure because surgical exposure is limited. In addition, after curettage, residual tissue is typically assessed by digital palpation, and the procedure is terminated once the surgeon is satisfied. These factors may contribute to residual adenoid tissue and subsequent symptom recurrence (9,10). Postoperative adenoid regrowth has been reported in up to 31.3% of cases, particularly in children younger than 5 years (11). Residual tissue has also been reported more frequently in the choanal and tubal regions, which are relatively difficult to address with the conventional technique (9,12,13)

In our study, no recurrence attributable to residual tissue was observed in the endoscopic group, whereas recurrence occurred in two patients (2.9%) in the conventional group. While this finding supports the potential advantage of the endoscopic approach in reducing residual tissue, the lack of statistical significance may be related to the relatively small sample size and a limited one-year follow-up period. Consistent with this interpretation, the literature generally emphasises the superiority of endoscopic techniques over conventional curettage with respect to residual adenoid tissue. In a systematic review and meta-analysis, Malas et al. (6) reported that the likelihood of residual adenoid tissue was 97% lower in patients treated with alternative techniques (including endoscopic methods) than in those treated with conventional curettage. Similarly, Songu et al. (14), using adenoid/nasopharyngeal measurements derived from temporal bone CT, reported that the endoscopic technique was more effective than curettage in reducing postoperative adenoid size. Another study found 23.3% of patients in the curettage group, whereas no residual adenoid tissue was observed in the endoscopic group (7). Overall, removal under direct endoscopic visualisation facilitates more complete excision and may reduce the likelihood of residual tissue.

Complications

With regard to perioperative complications, none were observed in the endoscopic adenoidectomy group, whereas one patient (1.4%) in the conventional adenoidectomy group developed early postoperative bleeding within the first 24 hours. Overall, there was no statistically significant difference between groups in terms of postoperative complications. Although uncommon, adenoidectomy may be associated with complications such as infection, bleeding, pain, dehydration, and velopharyngeal insufficiency, with bleeding generally considered the most concerning event. In a large multicentre study reviewing 10 years of data, the most frequently reported complications within the first month were pain (3.1%), postoperative bleeding (2.3%), dehydration (2.1%), infection (0.26%), and acute respiratory complications (0.21%) (15).

The available literature suggests broadly similar complication profiles across adenoidectomy techniques. In a comparative study by Wadia and Dabholkar (16), no significant differences were found between endoscopic adenoidectomy and conventional adenoidectomy with respect to postoperative pain or bleeding. Likewise, Malas et al.(6), in a systematic review and meta-analysis comparing conventional curettage with other techniques, reported no significant differences in postoperative bleeding or in overall complication rates.

Findings regarding blood loss vary across studies. Manhas et al. (7) reported a higher mean blood loss in the endoscopic group (29.15 mL) than in the conventional adenoidectomy group (15.2 mL); this

difference was statistically significant. Juneja et al. (17) reported a similar trend, although it did not reach statistical significance. In contrast, Kumar et al. (18) found higher rates of intraoperative and early postoperative primary bleeding using the conventional technique. In a meta-analysis, Yang et al. (19) reported greater blood loss with conventional curettage compared with endoscopic-assisted adenoidectomy, attributing this to the advantages of direct visualisation and more effective control of bleeding sources with endoscopic techniques. In the present study, no significant between-group difference in postoperative infection was observed. Consistent with findings from large-scale studies, overall complication rates after adenoidectomy appear to be low and serious complications are rare; this supports the view that isolated adenoidectomy is generally associated with low morbidity (20,21).

Postoperative Pain

In our cohort, postoperative pain assessed by VAS was significantly higher in the endoscopic group (4.84 ± 1.31) than in the conventional group (4.34 ± 1.34) (p = 0.033). The higher pain scores observed after endoscopic adenoidectomy may be related to the need for targeted cauterisation of residual adenoid tissue and bleeding foci performed under direct endoscopic visualisation. Previous reports on postoperative pain following endoscopic techniques are heterogeneous. Juneja et al. (17) reported significantly lower pain scores in the endoscopic group. In another study comparing standard and microdebrider adenoidectomy, postoperative pain was lower in the microdebrider group, although the difference between techniques was not statistically significant (22). Conversely, in a randomised controlled trial comparing cold dissection and coblation techniques for adenotonsillectomy, Shapiro and Bhattacharyya (23) found no significant difference in daily postoperative pain scores between the groups. These discrepancies may reflect differences in pain assessment methods and the influence of concomitant procedures, such as tonsillectomy.

A primary strength of this study is that both techniques were evaluated by a single surgeon, enabling a consistent comparison between the two approaches. The main limitations include the retrospective design, the relatively small sample size, and the follow-up period limited to one year. Larger prospective studies with longer follow-up, ideally including randomised comparisons, are needed to better define long-term outcomes associated with each technique.

CONCLUSION

Endoscopic adenoidectomy allows direct visualisation of the surgical field, enabling more controlled resection and prompt management of bleeding. However, longer operative time, the need for additional equipment, and higher cost are important disadvantages. In our study, no significant differences were observed between endoscopic and conventional adenoidectomy in terms of clinical outcomes and postoperative complications. Therefore, the selection of the adenoidectomy technique should consider the surgeon's experience, available technical resources, and operative conditions.

Ethics

Ethics Committee Approval: This retrospective, observational, comparative review was approved by the Ethics Committee of Gazi University Faculty of Medicine (decision number: 2025-223, date:

28.01.2025).

Informed Consent: Retrospective study.

Footnotes

Authorship Contributions

Concept: B.T.C., Design: B.T.C., B.U., Data Collection or Processing: E.A., B.U., Analysis or Interpretation: E.A., Literature Search: B.T.C., E.A., Writing: B.T.C., E.A.

Conflict of Interest: No conflict of interest was declared by the authors.

Financial Disclosure: The authors declared that this study received no financial support.

REFERENCES

1. Havas T, Lowinger D. Obstructive adenoid tissue: an indication for powered-shaver adenoidectomy. Arch Otolaryngol Head Neck Surg. 2002; 128: 789–91.

2. Rout MR, Mohanty D, Vijaylaxmi Y, Bobba K, Metta C. Adenoid hypertrophy in adults: a case series. Indian J Otolaryngol Head Neck Surg. 2013; 65: 269–74.

3. Brambilla I, Pusateri A, Pagella F, Caimmi D, Caimmi S, Licari A, et al. Adenoids in children: advances in immunology, diagnosis, and surgery. Clin Anat. 2014; 27: 346–52.

4. Uçar C. Endoskopik adenoidektomi [Endoscopic adenoidectomy]. Kulak Burun Bogaz Ihtis Derg. 2008; 18: 66–8.

5. Beemrote DS, Aseri Y, Rawat DS, Mahich S, Verma PC. A Comparative study of endoscopic assisted powered adenoidectomy versus conventional adenoidectomy. Indian J Otolaryngol Head Neck Surg. 2023; 75: 1598–603.

6. Malas M, Althobaiti AA, Sindi A, Bukhari AF, Zawawi F. Comparison of the efficacy and safety of conventional curettage adenoidectomy with those of other adenoidectomy surgical techniques: a systematic review and network meta-analysis. J Otolaryngol Head Neck Surg. 2023; 52: 21.

7. Manhas M, Deva FAL, Sharma S, Koul D, Gul N, Jamwal PS, et al. Endoscopic adenoidectomy replacing the outdated curette adenoidectomy: comparison of the two methods at a tertiary care centre. Indian J Otolaryngol Head Neck Surg. 2022; 74: 4788–94.

8. Saibene AM, Rosso C, Pipolo C, Lozza P, Scotti A, Ghelma F, et al. Endoscopic adenoidectomy: a systematic analysis of outcomes and complications in 1006 patients. Acta Otorhinolaryngol Ital. 2020; 40: 79–86.

9. Ark N, Kurtaran H, Ugur KS, Yilmaz T, Ozboduroglu AA, Mutlu C. Comparison of adenoidectomy methods: examining with digital palpation vs. visualizing the placement of the curette. Int J Pediatr Otorhinolaryngol. 2010; 74: 649–51.

10. Saxby AJ, Chappel CA. Residual adenoid tissue post-curettage: role of nasopharyngoscopy in adenoidectomy. ANZ J Surg. 2009; 79: 809–11.

11. Lesinskas E, Drigotas M. The incidence of adenoidal regrowth after adenoidectomy and its effect on persistent nasal symptoms. Eur Arch Otorhinolaryngol. 2009; 266: 469–73.

12. Owens D, Jaramillo M, Saunders M. Suction diathermy adenoid ablation. J Laryngol Otol. 2005; 119: 34–5.

13. Pearl AJ, Manoukian JJ. Adenoidectomy: indirect visualization of choanal adenoids. J Otolaryngol. 1994; 23: 221–4.

14. Songu M, Altay C, Adibelli ZH, Adibelli H. Endoscopic-assisted versus curettage adenoidectomy: a prospective, randomized, double-blind study with objective outcome measures. Laryngoscope. 2010; 120: 1895–9.

15. Anwaegbu OS, Clark DES, Iyamah SO, Ezenwukwa C, Etufugh UL, McKinnon BJ. Trends in postoperative complications following pediatric tonsillectomy & adenoidectomy: A 10-year analysis. Am J Otolaryngol. 2025; 46: 104712.

16. Wadia J, Dabholkar Y. Comparison of conventional curettage adenoidectomy versus endoscopic powered adenoidectomy: a randomised single-blind study. Indian J Otolaryngol Head Neck Surg. 2022; 74: 1044–9.

17. Juneja R, Meher R, Raj A, Rathore P, Wadhwa V, Arora N. Endoscopic assisted powered adenoidectomy versus conventional adenoidectomy - a randomised controlled trial. J Laryngol Otol. 2019; 133: 289–93.

18. Kumar A, Narayan P, Narain P, Singh J, Porwal PK, Sharma S. A comparative study of endoscopic assisted curettage adenoidectomy with conventional adenoidectomy. Int J Otorhinolaryngol Head Neck Surg. 2018; 4: 1053.

19. Yang L, Shan Y, Wang S, Cai C, Zhang H. Endoscopic assisted adenoidectomy versus conventional curettage adenoidectomy: a meta-analysis of randomized controlled trials. Springerplus. 2016; 5: 426.

20. Gerhardsson H, Stalfors J, Sunnergren O. Postoperative morbidity and mortality after adenoidectomy: A national population-based study of 51 746 surgeries. Int J Pediatr Otorhinolaryngol. 2022; 163: 111335.

21. Losgar H, Boeger D, Buentzel J, Hoffmann K, Podzimek J, Kaftan H, et al. Pediatric adenoidectomy is safe surgery with a low complication rate: a population-based study. Sci Rep. 2025; 15: 27967.

22. Abo Elmagd EA, Khalifa MS, Abeskharoon BK, El Tahan AA. Comparative study between conventional adenoidectomy and adenoidectomy using micro-debrider. The Egyptian Journal of Otolaryngology. 2021; 37: 56.

23. Shapiro NL, Bhattacharyya N. Cold dissection versus coblation-assisted adenotonsillectomy in children. The Laryngoscope. 2007; 117: 406–10.

The Neck Arteriovenous Malformations that May Rupture Anytime

Her An Yırtılabilen Boyun Arteriovenöz Malformasyonları

Hwee Chin Ong[1], Marcella Dorainne Mansah[1], Hui Ying Chio[1], Yoon Chin Yap[1], Zhen Zhen Lo[2]

[1]Department of Emergency and Trauma, Queen Elizabeth Hospital, Ministry of Health Malaysia, Sabah, Malaysia
[2]Department of Emergency Medicine, Universiti Malaysia Sabah Faculty of Medicine and Health Sciences, Sabah, Malaysia

ABSTRACT

This case illustrates the rare incidence of arteriovenous malformations (AVMs) of the head and neck in an adult male, possibly caused by the preceding trauma. A 30-year-old male with a chief complaint of headache worsened over the past day a sudden expansion of swelling over the back of the neck. The swelling was preceded by trauma to the neck two years ago. The contrast-enhanced computed tomography scan and computed tomography angiography of the head and neck concluded right neck AVM with aneurysms and contained hematoma. He was suggested for digital subtraction angiography and embolisation. Preceding trauma over the region was believed to have caused the neck swelling, and the ruptured aneurysm presented with a sudden onset of severe pain. It may progress to devastating complications if it is not treated in a timely manner.

Keywords: Arteriovenous malformations, trauma, head and neck

ÖZ

Bu olgu, yetişkin bir erkekte baş ve boyun arteriovenöz malformasyonlarının (AVM) nadir görülen bir insidansını göstermektedir; bu durum muhtemelen önceki travmadan kaynaklanmaktadır. Baş ağrısı şikâyeti olan 30 yaşında bir erkek hastanın, son bir günde boynunun arkasında aniden büyüyen şişlik kötüleşti. Şişlik, iki yıl önce boyun travmasından önce oluşmuştur. Kontrastlı bilgisayarlı tomografi taraması ve baş ve boyun bilgisayarlı tomografi anjiyografisi, sağ boyun AVM'sinin anevrizmalı olduğu ve hematom içerdiği sonucuna varmıştır. Hastaya dijital subtraksiyon anjiyografisi ve embolizasyon önerilmiştir. Boyun şişmesine, bölgedeki önceki travmanın neden olduğu düşünülmüş ve yırtılmış anevrizma, ani başlayan şiddetli bir ağrı ile ortaya çıkmıştır. Zamanında tedavi edilmezse yıkıcı komplikasyonlara ilerleyebilir.

Anahtar Sözcükler: Arteriovenöz malformasyonlar, travma, baş ve boyun

INTRODUCTION

Arteriovenous malformation (AVM) is a vascular malformation with direct communications of feeding arteries and draining veins without intervening normal capillaries. AVM is usually congenital, but trauma is also a frequent cause. AVM of the head and neck is a rare vascular anomaly, and extracranial AVM is particularly aggressive in a localised manner, which progresses to an expansive mass. AVM would further progress to complications such as pain, ulceration, severe disfigurement, rupture, and cardiac volume overload.

CASE REPORT

A 30-year-old male presented with a chief complaint of a headache which worsened over the past day. He also complained of swelling over the back of the neck (Figure 1) for the past two years, which has remained the size of an apple but suddenly enlarged significantly over the course of a day. The swelling was preceded by trauma to the neck two years ago. He described the mechanism of the fall as a direct hit to his neck while he was in a supine position. However, over the past day, he noted a sudden enlargement of the mass, which was not provoked by any repeating or new trauma. Clinically,

Address for Correspondence/Yazışma Adresi: Yoon Chin Yap, MD, MMED (EM), Department of Emergency and Trauma, Queen Elizabeth Hospital, Ministry of Health Malaysia, Sabah, Malaysia
Address for Correspondence/Yazışma Adresi: Zhen Zhen Lo, MBBS, MMED (EM), Department of Emergency Medicine, Universiti Malaysia Sabah Faculty of Medicine and Health Sciences, Sabah, Malaysia
E-mail / E-posta: angelineyap7@gmail.com, lozhenzhen@ums.edu.my
ORCID ID: orcid.org/0000-0002-4419-8413, orcid.org/0000-0001-7960-1412

the patient was in pain and distress. His blood pressure (BP) upon arrival was 178/109 mmHg, with a pulse rate of 98 beats/min. He was not hypoxic. There was swelling over the right posterior region of the neck that expanded to the occipital region and crossed the midline, measuring 13 x 15 cm with a smooth surface. The mass was non-mobile, firm on palpation, and pulsating. There were bruits. No neurological deficit was noted on his physical examination. Bedside ultrasound revealed a heterogeneous mass with turbulent blood flow. The contrast-enhanced computed tomography scan (Figure 2) and computed tomography angiography (CTA) (Figure 3) of the head and neck showed a large right posterior cervical lesion measuring

Figure 1. The mass arises from the posterior neck and extends to the occipital region.

10 x 9 x 11 cm (AP x W x CC)—revealing the presence of mass effect on the adjacent right parotid gland, right carotid, and perivertebral space. Multiple nidi with a dilated feeding artery are seen arising from the right external carotid artery and, to a lesser extent, from the right vertebral artery and the occipital branches of the left external carotid artery. Three aneurysms were seen within, with the largest measuring 4.6 x 8.2 cm, and contained hematoma was noted, along with bony erosion of the right occipital, petrous, and mastoid part of the right temporal bone. The scan concluded he had a right neck AVM with aneurysms and containing hematoma. He was suggested for digital subtraction angiography and embolisation. However, the patient was not agreeable to treatment.

DISCUSSION

Abnormal connections between arteries and veins form an AVM. The prevalence of AVM is 1 in 100,000 people (1). Most AVMs are congenital. However, up to 20% present with a history of trauma (2). AVMs are commonly located in the central nervous system. Extracranial AVMs are rare and mainly located in the head and neck (3). The most common cause of arteriovenous communications between cervical region blood vessels is trauma, as seen in this patient (4).

Most of the AVMs are asymptomatic, and only 12% of them are symptomatic (5). AVMs might become more symptomatic over the years (6).

The International Society for the Study of Vascular Anomalies has divided vascular malformations into high-flow and low-flow lesions. High-flow lesions are defined as an abnormal connection between artery and vein without an intervening capillary bed, whereas low-flow lesions consist of a dilated vein and lymphatic vessels (7-9). Sudden enlargement of AVMs may happen in response to trauma, extremely high BP or hormonal changes during puberty, or pregnancy (7,8). The patient had developed an AVM after a fall, and the AVM rapidly increased in size for a day without sustaining any new trauma. His BP was noted to be high upon arrival. Therefore, we suspected, the aneurysm rupture was mainly precipitated by the high BP.

The natural course of AVM can be divided into four stages (I-IV)
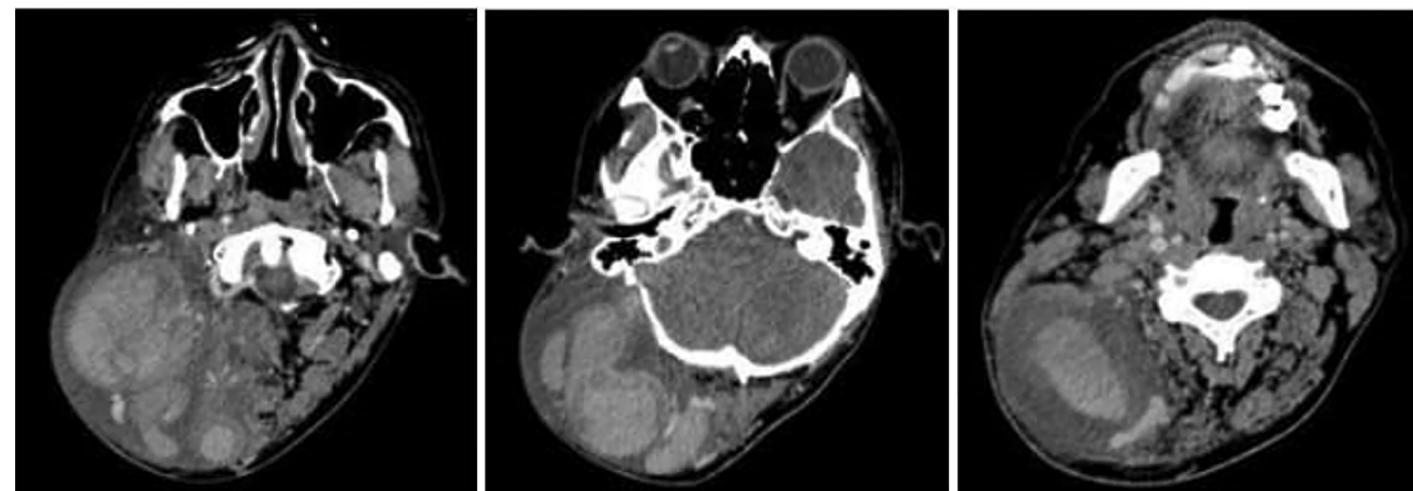
Figure 2. CECT shows right neck AVM with aneurysm containing hematoma.

*CECT: Contrast-enhanced computed tomography, AVM: Arteriovenous malformation.*
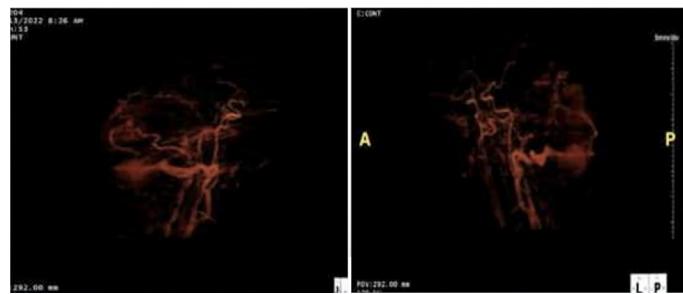
Figure 3. Shows CT angiography with the 3D reconstruction of the right neck AVM.

CT: Computed tomography, AVM: Arteriovenous malformation, 3D: Three-dimensional.

based on the Schobinger system, which includes quiescence, expansion, destruction, and decompensation (10). The four stages of AVM progression are well demonstrated in this patient based on his history and clinical findings.

Clinical examination can suggest the diagnosis of AVMs, but vascular imaging is necessary to confirm the clinical diagnosis. Magnetic resonance imaging is the imaging modality for diagnosing AVMs. It helps visualise the central nidus and feeder arteries, thereby aiding in planning the management of malformations (11). The patient underwent CTA, which showed multiple dilated feeding arteries from the right external carotid artery to a lesser extent, from the right vertebral and occipital branches of the left external carotid artery. Three aneurysms were seen with hematoma—bony erosion of the right occipital, and the petrous and mastoid parts of the right temporal bone. Most of the time, the high-flow lesion showed destructive skeletal changes, and changes in bone density were found in his CTA (7).

The treatment options for AVM are affected by specific flow characteristics. High-flow lesions are often treated with complete embolisation, excision, or a mixture of both (9).

On the other hand, untreated AVM lesions, as illustrated in this case, may cause devastating complications and significant morbidity due to rapid expansile growth. The mortality rate can be up to 15% (5).

Preceding trauma over the region was believed to have caused the neck swelling, and the ruptured aneurysm was presented as a sudden onset of severe pain. It may progress to devastating complications if it is not treated in time.

CONCLUSION

The case illustrates the rare occurrence of AVM of the head and neck in an adult male, possibly caused by the preceding trauma.

Ethics

Informed Consent: Verbal informed consent was obtained from the patient after a full explanation of the study and its purpose. Due to logistical constraints, written consent could not be obtained despite multiple attempts. The authors affirm that the patient understood and agreed to the publication of anonymized information, and that all procedures adhered to the ethical standards of the Declaration of Helsinki and relevant institutional guidelines.

REFERENCES

1. Arteriovenous malformation brain imaging: practice essentials, ultrasonography, computed tomography. Medscape. 2022. Available from: https://emedicine.medscape.com/article/337220-overview

2. Tisetso Morare NM, Baloyi ERJ. Post-traumatic arteriovenous malformation of the superficial temporal artery. J Vasc Surg Cases Innov Tech. 2020; 6: 50–4.

3. Mulliken JB, Fishman SJ, Burrows PE. Vascular anomalies. Curr Probl Surg. 2000; 37: 517–84.

4. Dieng PA, Ba PS, Gaye M, Diatta S, Diop MS, Sene E, et al. Giant arteriovenous malformation of the neck. Case Rep Vasc Med. 2015; 2015: 124010.

5. Bokhari MR, Bokhari SRA. Arteriovenous malformation of the brain. StatPearls [Internet]. Treasure Island (FL): StatPearls Publishing; 2023. Available from: https://www.ncbi.nlm.nih.gov/books/NBK430744/

6. Azis KA, Koh KL, Wan Sulaiman WA, Al-Chalabi MMM. Extracranial arteriovenous malformations rupture in pregnancy. Cureus. 2022; 14: e22798.

7. Jackson IT, Carreño R, Potparic Z, Hussain K. Hemangiomas, vascular malformations, and lymphovenous malformations: classification and methods of treatment. Plast Reconstr Surg. 1993; 91: 1216–30.

8. National Institute of Neurological Disorders and Stroke. Arteriovenous malformations (AVMs). Bethesda (MD): NINDS; [Accessed on January 2023]. Available from: https://www.ninds.nih.gov/health-information/disorders/arteriovenous-malformations-avms

9. Funaki B, Funaki C. Embolization of high-flow arteriovenous malformation. Semin Intervent Radiol. 2016; 33: 157–60.

10. Rayasam S, Mitchell RB, Liu C. A neck mass in a 9-year-old child. Ear Nose Throat J. 2022; 101: NP80–2.

11. Rosenberg TL, Suen JY, Richter GT. Arteriovenous malformations of the head and neck. Otolaryngol Clin North Am. 2018; 51: 185–95.

Cutaneous Mucormycosis in an Immunosuppressed Patient: A Case Report

İmmünsüpresif Hastada Kutanöz Mukormikoz: Olgu Sunumu

Ⓘ Elif Afacan Yıldırım[1], Ⓘ Esra Adışen[2], Ⓘ Özlem Erdem[3]

[1]Department of Dermatology, Demiroğlu Bilim University Faculty of Medicine, İstanbul, Türkiye
[2]Department of Dermatology, Gazi University Faculty of Medicine, Ankara, Türkiye
[3]Department of Pathology, Gazi University Faculty of Medicine, Ankara, Türkiye

ABSTRACT

Cutaneous mucormycosis is a rare, invasive fungal infection with high morbidity and mortality, particularly in immunocompromised individuals. This report presents the case of a 30-year-old male with acute myeloid leukemia who developed cutaneous mucormycosis, manifesting as necrotic nodules on the arms and a hemorrhagic papule on the tongue. Despite negative fungal culture results, histopathological examination revealed broad, non-septated hyphae, confirming the diagnosis. The patient was treated with intravenous amphotericin B. This case underscores the critical need for early clinical suspicion, prompt histopathological evaluation, and timely initiation of empirical antifungal therapy to improve patient outcomes in high-risk populations.

Keywords: Mucormycosis, skin diseases, fungal, immunosuppression, leukemia, myeloid, acute, antifungal agents, amphotericin B, histopathological diagnosis

ÖZ

Kutanöz mukormikoz, özellikle immünsüprese bireylerde yüksek morbidite ve mortaliteyle seyreden nadir görülen invaziv bir mantar enfeksiyonudur. Bu olgu sunumunda, akut miyeloid lösemi tanılı 30 yaşında bir erkek hastada kollarda nekrotik nodüller ve dilde hemorajik bir papül şeklinde kendini gösteren kutanöz mukormikoz vakası sunulmaktadır. Mantar kültürü negatif sonuçlanmasına rağmen histopatolojik inceleme geniş, septasız hiflerin varlığını ortaya koymuş ve tanı doğrulanmıştır. Hasta intravenöz amfoterisin B ile tedavi edilmiştir. Bu olgu, yüksek riskli popülasyonlarda erken klinik şüphe, hızlı histopatolojik değerlendirme ve ampirik antifungal tedavinin zamanında başlatılmasının hasta sonuçlarını iyileştirmede kritik önemini vurgulamaktadır.

Anahtar Sözcükler: Mukormikoz, deri hastalıkları, fungal, immunsupresyon, akut miyeloid lösemi, antifungal ajanlar, amfoterisin B, histopatolojik tanı

INTRODUCTION

Cutaneous mucormycosis is an opportunistic deep fungal infection with diverse clinical presentations, particularly affecting immunosuppressed and diabetic patients (1). It is an invasive fungal infection caused by fungi within the phylum Glomeromycota, the subphylum mucormycotina (2). Organisms of the order Mucorales are ubiquitous in nature and are commonly found in soil, decaying vegetation, and animal excreta (3). Cutaneous mucormycosis is rare and typically results from direct inoculation into traumatized skin (4). Beyond cutaneous involvement, mucormycosis frequently manifests in rhinocerebral and pulmonary forms and less commonly in gastrointestinal, disseminated, and miscellaneous forms (1). Given its invasive and potentially life-threatening nature, timely diagnosis and multidisciplinary management are crticial for improving patient survival. This report describes a rare case of cutaneous mucormycosis in a patient with hematological malignancy, highlighting diagnostic challenges and histopathological findings.

CASE REPORT

A 30-year-old male patient, admitted to the hematology clinic for neutropenic fever, was referred to our department because of mucosal and cutaneous lesions. Dermatological examination revealed a black hemorrhagic papule on the tongue and two erythematous-purple, indurated nodules on both arms, one of which was necrotic (Figure 1).

His medical history included acute myeloid leukemia diagnosed 2 years earlier, followed by allogeneic stem cell transplantation and, 1 year later, the development of cutaneous graft-versus-host disease. The patient, who was neutropenic and immunosuppressed, had received multiple chemotherapy regimens over the past two years. Given his medical background, a fungal culture of the necrotic lesion on his arm was performed, and a biopsy was obtained for histopathological examination. The fungal culture was reported negative.

During the same period, high-resolution computed tomography revealed new pulmonary nodular infiltrates. Because of the suspicion of fungal infection, empiric treatment with amphotericin B was initiated. Histopathological examination of the punch biopsy from the patient's arm demonstrated a predominantly neutrophilic infiltrate in the reticular dermis, without epidermal involvement. Hematoxylin and eosin (H&E) staining revealed hyphae-like structures within the dermis (Figure 2). Subsequently, gomori methenamine silver staining confirmed the presence of widespread, non-septate hyphae predominantly in the dermis (Figure 3). Based on these findings, cutaneous mucormycosis was diagnosed.

DISCUSSION

The clinical manifestations of cutaneous mucormycosis are non-specific, making rapid identification of the fungus crucial for the timely initiation of antifungal therapy [1]. The most commonly affected skin areas, as observed in our patient, are the arms and legs [3]. Cutaneous mucormycosis is frequently associated with skin trauma, and in this case, it was linked to an intravenous catheter.

Diagnosis is generally established through potassium hydroxide examination, fungal culture, and histopathological evaluation. Since fungal cultures may yield no growth, the characteristic morphology of Mucorales in histopathology specimens serves as a key diagnostic indicator. Although fungal cultures are positive in approximately 50% of cases, recent studies report an increased positivity rate in skin lesions, ranging from 72% to 89% [1,5].

Histopathological findings typically include edema, thrombosis, infarction, necrosis, and a predominantly polymorphonuclear inflammatory infiltrate. The characteristic thick, hyaline, non-septate hyphae are visible on H&E-stained sections but are more distinctly identified with special fungal stains.
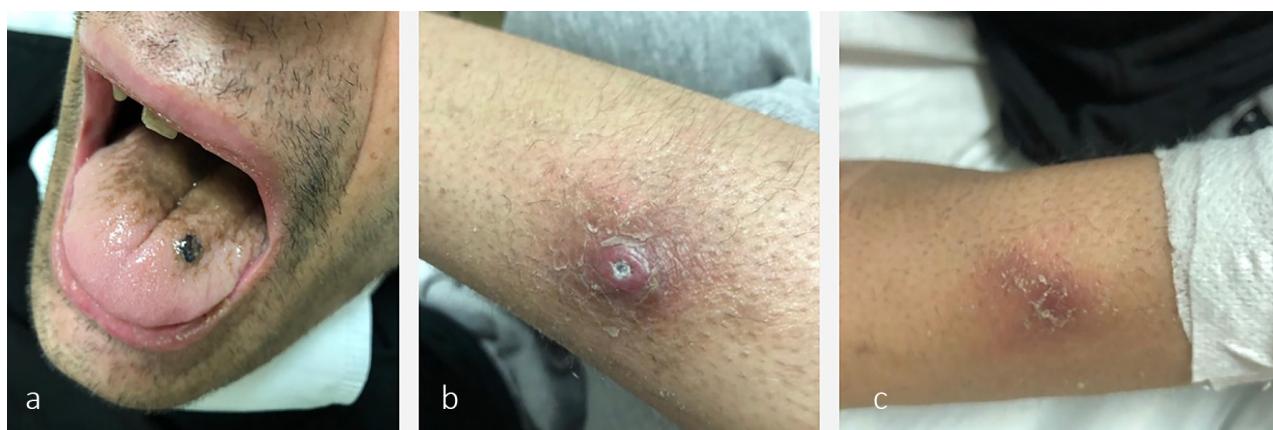

Figure 1. (a) Necrotic-hemorrhagic papule on tongue, (b, c) erythematous-purple, indurated, nectoric nodules on arms.
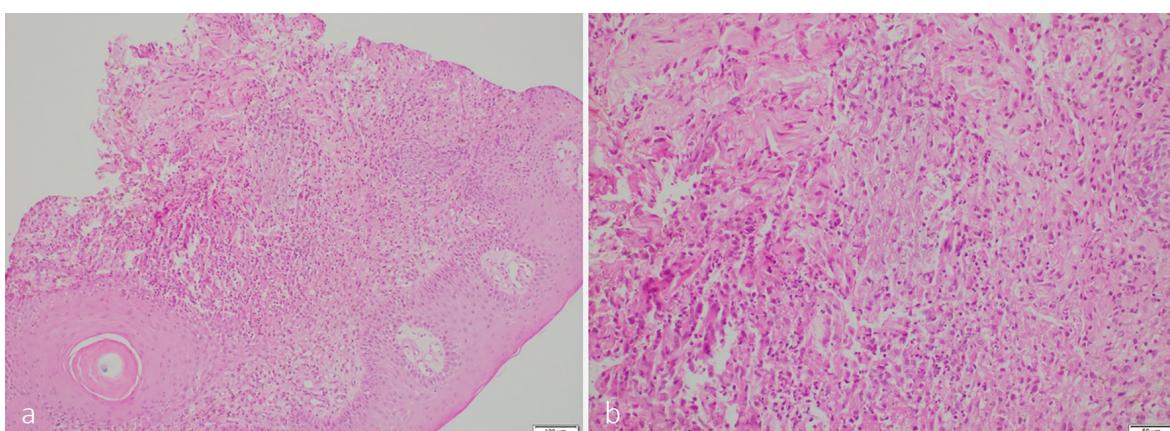

Figure 2. Skin biopsy, haematoxylin-eosin stain, (a) preserved epidermal integrity with predominantly neutrophilic infiltrates in reticular dermis. (× 10 original magnification), (b) hyphae-like structures in the dermis (× 20 original magnification).
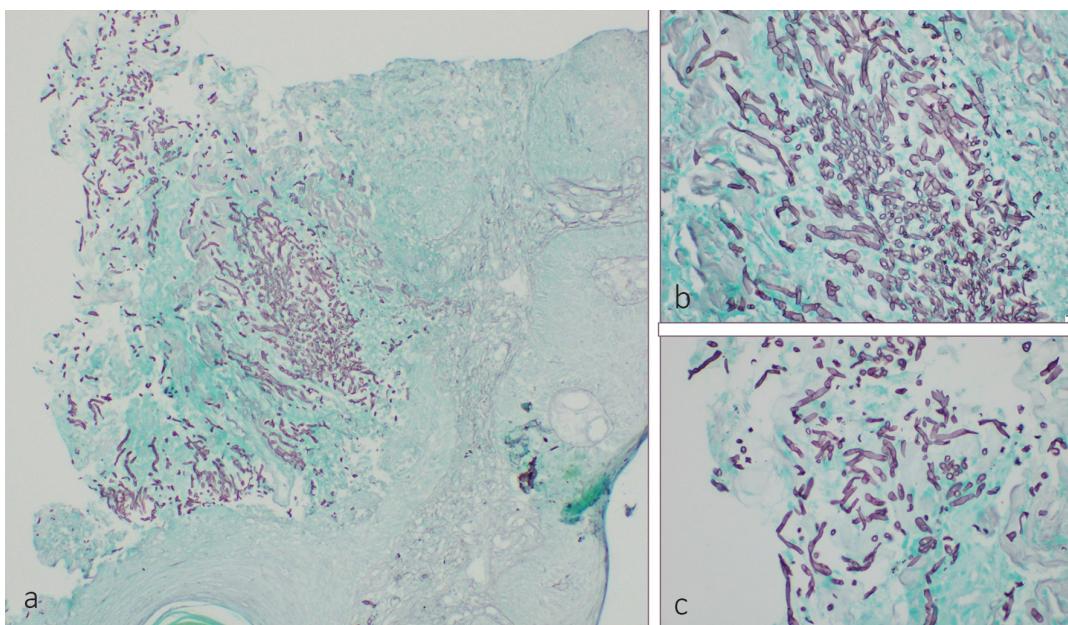
Figure 3. Skin biopsy, Gomori Methenamine-Silver stain, (a) widespread hyphae in reticular dermis (× 10 original magnification), (b, c) thick, hyaline, non-septated hyphae predominantly in dermis (× 40 original magnification).

Differential diagnoses should exclude other infectious etiologies, such as aspergillosis and gangrenous bacterial infections. Non-infectious differentials include drug reactions, neoplastic conditions, and infiltrative disorders (6). In our patient, the differential diagnosis included aspergillosis, leukemia cutis, ecthyma, leishmaniasis, Sweet syndrome, and keratoacanthoma, all of which were out through histopathological examination. Management of cutaneous mucormycosis involves systemic antifungal therapy and surgical debridement. Intravenous amphotericin B remains the first-line treatment, administered at a standard dose of 5 mg/kg/day, a dose that can be increased to 10 mg/kg/day as needed. Additionally, newer azoles such as posaconazole and isavuconazole serve as step-down or salvage therapies (7).

CONCLUSION

This case highlights the need for heightened clinical vigilance in the evaluation of immunosuppressed patients presenting with erythematous, necrotic nodules, as early recognition of opportunistic fungal infections is crucial for improving outcomes. Given the high morbidity and mortality associated with cutaneous mucormycosis, timely biopsy and histopathological evaluation are essential for definitive diagnosis. Empirical antifungal therapy should be promptly initiated in suspected cases, as delayed treatment significantly worsens prognosis. Increased awareness, coupled with a multidisciplinary approach, can lead to earlier diagnosis, more effective management, and improved survival rates in high-risk patients.

Ethics

Informed Consent: Written informed consent was obtained from the patient.

REFERENCES

1. Castrejón-Pérez AD, Welsh EC, Miranda I, Ocampo-Candiani J, Welsh O. Cutaneous mucormycosis. An Bras Dermatol. 2017; 92: 304–11.

2. Kwon-Chung KJ. Taxonomy of fungi causing mucormycosis and entomophthoramycosis (zygomycosis) and nomenclature of the disease: molecular mycologic perspectives. Clin Infect Dis. 2012; 54 Suppl 1: S8–15.

3. Skiada A, Rigopoulos D, Larios G, Petrikkos G, Katsambas A. Global epidemiology of cutaneous zygomycosis. Clin Dermatol. 2012; 30: 628–32.

4. Roden MM, Zaoutis TE, Buchanan WL, Knudsen TA, Sarkisova TA, Schaufele RL, et al. Epidemiology and outcome of zygomycosis: a review of 929 reported cases. Clin Infect Dis. 2005; 41: 634–53.

5. Skiada A, Petrikkos G. Cutaneous zygomycosis. Clin Microbiol Infect. 2009; 15 Suppl 5: 41–5.

6. Bonifaz A, Vázquez-González D, Tirado-Sánchez A, Ponce-Olivera RM. Cutaneous zygomycosis. Clin Dermatol. 2012; 30: 413–9.

7. Chowdhary A, Kathuria S, Singh PK, Sharma B, Dolatabadi S, Hagen F, et al. Molecular characterization and in vitro antifungal susceptibility of 80 clinical isolates of mucormycetes in Delhi, India. Mycoses. 2014; 57 Suppl 3: 97–107.

Nasopharyngeal Carcinoma with Generalized Lymphadenopathy and Hematological Abnormalities Masquerade as Lymphoma: A Case Series of Atypical Presentations and Prognostic Significant

Jeneralize Lenfadenopati ve Hematolojik Anormalliklerle Seyreden Nazofarengeal Karsinomun Lenfomayı Taklit Etmesi: Atipik Sunumlar ve Prognostik Önemi Olan Bir Olgu Serisi

Ⓘ V Sha Kri Eh Dam

Department of Otorhinolaryngology–Head and Neck Surgery, Hospital Lahad Datu, Sabah, Malaysia

ABSTRACT

Nasopharyngeal carcinoma (NPC) is a unique type of head and neck squamous cell carcinoma, characterized by distinct etiology, epidemiology, and biological characteristics. Neck swelling is the most common presenting symptom, but generalized lymphadenopathy involving other parts of the body is rarely reported. Severe anemia, leukocytosis, and thrombocytopenia are rare but may occur at an advanced stage. The combination of these atypical presentations leads to the more common diagnosis of lymphoma instead of NPC. In addition, the hematological derangements are indicators of a poor prognosis. The clinician should be aware of these atypical presentations to avoid delays in management and worsening of overall survival.

Keywords: Nasopharyngeal carcinoma, generalized lymphadenopathy, severe anemia, leukocytosis, thrombocytopenia

ÖZ

Nazofarengeal karsinom (NFK), kendine özgü etiyoloji, epidemiyoloji ve biyolojik özelliklerle karakterize, benzersiz bir baş ve boyun skuamöz hücreli karsinom türüdür. Boyunda şişlik en sık görülen başvuru belirtisidir; ancak vücudun diğer bölgelerini içeren jeneralize lenfadenopati nadiren bildirilmiştir. Şiddetli anemi, lökositoz ve trombositopeni de nadir olmakla birlikte ileri evrede ortaya çıkabilir. Bu atipik klinik bulguların bir arada görülmesi, NFK yerine daha sık görülen bir hastalık olan lenfoma tanısının konulmasına yol açabilmektedir. Ayrıca, hematolojik bozukluklar kötü prognoz göstergeleridir. Klinisyenlerin, tedavide gecikmelerin ve genel sağkalımın kötüleşmesinin önlenmesi için bu atipik bulguların farkında olması gerekmektedir.

Anahtar Sözcükler: Nazofarengeal karsinom, jeneralize lenfadenopati, şiddetli anemi, lökositoz, trombositopeni

Address for Correspondence/Yazışma Adresi: V Sha Kri Eh Dam, Department of Otorhinolaryngology–Head and Neck Surgery, Hospital Lahad Datu, Sabah, Malaysia
E-mail / E-posta: kridamrong@gmail.com
ORCID ID: orcid.org/0000-0003-4802-2260

INTRODUCTION

Nasopharyngeal carcinoma (NPC) is a distinct subtype of head and neck squamous cell carcinoma arising in the nasopharynx. It has distinct etiology, epidemiology, and biological characteristics (1). The World Health Organization has classified it into three histopathological types, namely keratinizing, non-keratinizing, and basaloid squamous cell carcinoma (2). It is a rare tumor globally, accounting for only 0.7% of all cancers diagnosed in 2018, but is relatively common in Asia, as 85% of all cases are from this region, especially in East and Southeast Asia (1,3,4).

Neck swelling is the most common presenting symptom, affecting up to 80% of patients (5,6). In contrast, generalized involvement of the lymph node (LN) in other parts of the body, such as the axilla, inguinal region, mediastinum, and abdomen, is rarely reported. The majority of patients with NPC have normal hematological profiles; however, abnormalities may be observed in patients with advanced-stage disease (7). In addition to the extent of the disease, as defined by the tumor node metastasis staging system, anemia, leukocytosis, thrombocytosis, and thrombocytopenia are found to be additional prognostic indicators of an unfavorable prognosis (7).

The combination of generalized lymphadenopathy, severe anemia, leukocytosis, and thrombocytopenia has led to the more common diagnosis of lymphoma rather than NPC. These atypical presentations of NPC may delay diagnosis and treatment and lead to poor overall survival. We present a case series of advanced NPC (stage 4B) presenting with generalized LN enlargement, severe anemia, leukocytosis, and thrombocytopenia, without an obvious mass in the nasopharynx, masquerading as lymphoma at initial presentation, with 100% mortality within 4 months of diagnosis.

CASE REPORTS

Case 1

A 44-year-old male without underlying medical illness presented with painless bilateral neck swellings for 6 months and bilateral axillary and inguinal swellings for 2 months. It was associated with loss of appetite, weight loss, intermittent fever, and lethargy. He has had lower back pain for the past month, which has limited his ability to work and perform daily activities. There were no nasal or otological symptoms. A full blood picture obtained at another center showed normochromic, normocytic anemia (hemoglobin: 6.7 g/dL), leukocytosis with neutrophilia (white blood cell count: 30.4×10^9/L, absolute neutrophil count: 22.1×10^9/L), and thrombocytopenia (platelet count: 92×10^9/L). In view of the presentations that were more suggestive of lymphoma, with generalized lymphadenopathy and the presence of B symptoms, computed tomography (CT) scans of the neck, thorax, abdomen, and pelvis were performed for staging. The CT scan showed no enhancing lesion in the nasopharynx, oropharynx, or laryngopharynx (Figure 1A). There were multiple enlarged LNs in the cervical, mediastinal, and abdominal regions (Figures 1B, 1C and 1D). Hepatomegaly with multiple ill-defined hypodense lesions was present, and lytic lesions were present in the lumbar spine. He was admitted to the hematology ward and referred to the otorhinolaryngology (ORL) team for an excisional biopsy to obtain a definitive tissue diagnosis. Upon examination, multiple enlarged LNs were present bilaterally in the neck (Figure 2A) and in the axillary and inguinal regions, and hepatomegaly was noted. No obvious mass at nasopharynx or Fossa of Rosenmüller (FOR) on naso-endoscopy examination (Figure 2B). Other head and neck examinations were unremarkable. An excisional biopsy of the left level V cervical LN was performed. Histopathology examination (HPE) and immunohistochemistry (IHC) studies showed metastatic squamous cell carcinoma but unable to determine the primary site of origin. Bone marrow trephine biopsy also demonstrated metastasis from the primary tumor to the marrow. Pan-endoscopy, esophagoscopy, and biopsy were performed due to the unavailability of magnetic resonance imaging (MRI) or positron emission tomography scans at our center. A biopsy of the left FOR confirmed non-keratinizing NPC. The patient was planned to receive palliative chemotherapy for advanced disease (stage IVB) but had a poor Eastern Cooperative Oncology Group (ECOG) performance status and died 3 months after diagnosis from hospital-acquired pneumonia.
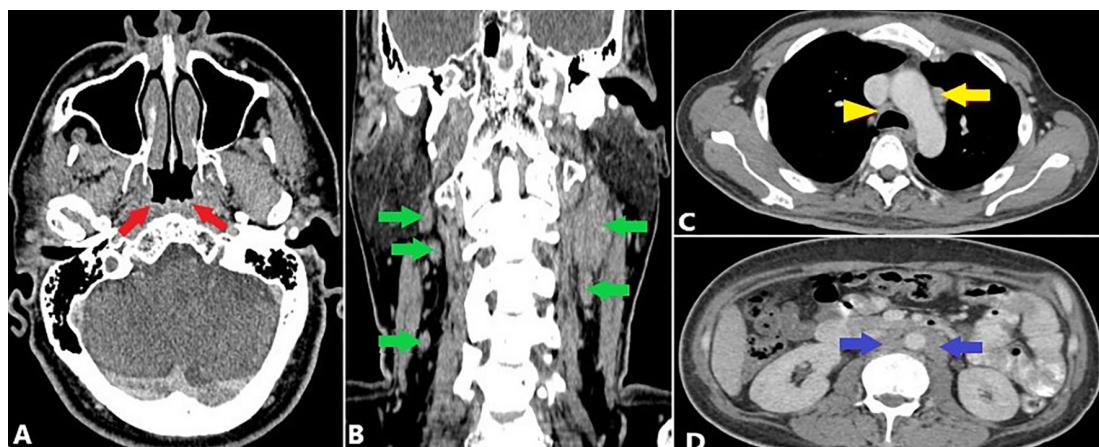
Figure 1. Contrast-enhanced CT scan of neck, thorax, and abdomen. Axial image at the level of the nasopharynx shows no enhancing lesion in the nasopharynx or the FOR (red arrow) (A). Coronal image of the neck shows bilateral cervical nodes at levels II, III, and IV (green arrow; B). An axial thoracic image depicts the right paratracheal LN (yellow arrowhead) and para-aortic LN (yellow arrow) (C). An Axial image of the abdomen shows para-aortic LN enlargement (blue arrow) (D).

CT: Computed tomography, LN: Lymph node, FOR: Fossa of Rosenmüller

Case 2

A 40-year-old man with no underlying medical illness presented with a 3-month history of painless bilateral neck swellings and a 1-month history of bilateral axillary and inguinal swellings. It was associated with symptoms of anemia, loss of appetite and weight loss, intermittent fever, and night sweats for one month. There was no nasal or otological symptoms. The full blood picture showed hypochromic, microcytic anemia (hemoglobin 6.2 g/dL), leukocytosis with neutrophilia (white blood cell count of 55.9 × 10^9/L, absolute neutrophil count of 52.1 × 10^9/L), and thrombocytopenia (platelet count of 90 × 10^9/L). The patient was admitted to the hematology ward with an impression of lymphoma and was referred to the ORL team for an excisional biopsy. Upon examination, there were multiple enlarged LN bilaterally in the neck (Figure 3A), axillae, and inguinal regions. The right torus tubarius was bulky compared with the left side; however, no obvious mass was identified in the nasopharynx or FOR on naso-endoscopy (Figure 3B). Other head neck examinations were unremarkable. Excision biopsy of the left level V cervical LN

was performed. HPE and IHC studies showed metastatic squamous cell carcinoma. CT scans of the brain, neck, thorax, abdomen, and pelvis were performed to identify the primary tumor. The CT scan showed mild thickening of the right torus tubarius compared with the left side, effacement of the right FOR, and no enhancing lesion (Figure 4A). Multiple enlarged LN were present in the cervical, axillary, mediastinal, abdominal, and inguinal regions (Figures 4B, 4C, 4D, 4E). In addition, there were multiple hypodense lesions in the liver and widespread lytic lesions in the pelvis, bilateral femora, spine, sternum, ribs, and bilateral humeri. A biopsy taken from the right FOR confirmed non-keratinizing NPC. Palliative chemotherapy was planned, but he developed sepsis secondary to pneumonia and died before initiation of chemotherapy.

Case 3

A 55-year-old woman, with no underlying medical illness, presented with painless left-sided neck swellings of 4 months' duration and bilateral axillary and inguinal swellings of 1 month's duration. It was

Figure 2. Multiple enlarged lymph node at left level II, III, and IV (A). No obvious mass in the nasopharynx (yellow star) or the Fossa of Rosenmüller (yellow arrow, left; yellow arrowhead, right) on naso-endoscopic examination (B).

LN: Lymph node
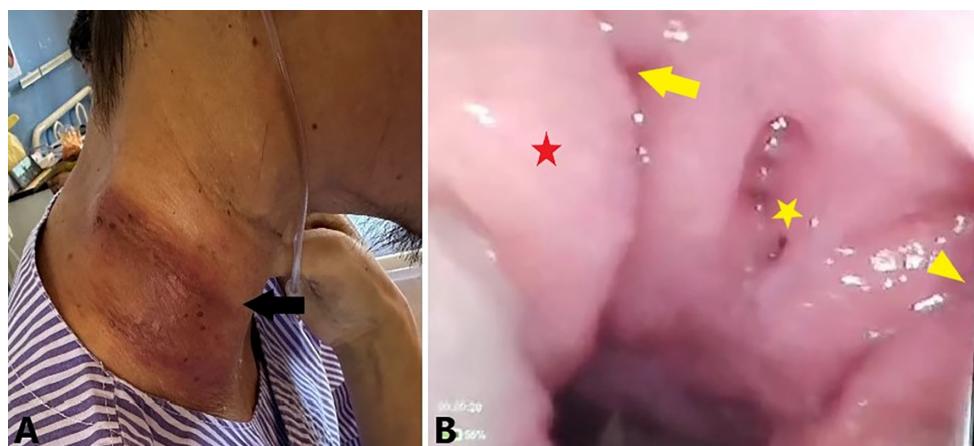
Figure 3. Huge right neck swelling with inflamed overlying skin (A). The right torus tubarius (red star) is bulky compared with the left side; however, no obvious mass is identified in the nasopharynx (yellow star) or the Fossa of Rosenmüller (yellow arrow, right; yellow arrowhead, left) on naso-endoscopic examination (B).

associated for 1 month with abdominal distension, shortness of breath, loss of appetite and weight loss, intermittent fever, and night sweats. There was no nasal or otological symptoms. The full blood picture revealed hypochromic microcytic anemia (hemoglobin 6.4 g/dL), leukocytosis with neutrophilia (white blood cell count 34.2 × 10^9/L, absolute neutrophil count 26 × 10^9/L), and thrombocytopenia (platelet count 87 × 10^9/L). The patient was admitted to the hematology ward with an impression of lymphoma, and CT scans of the neck, thorax, abdomen, and pelvis were performed. The CT scan demonstrated mild thickening of the left torus tubarius, compared with the right side, and effacement of the left FOR, with no enhancing lesion seen (Figure 5A). There were multiple enlarged LN in the cervical, axillary, mediastinal, abdominal, and pelvic regions (Figures 5B, 5C and 5D), as well as hepatosplenomegaly and a right lung nodule. The subsequent patient was referred to the ORL team for an excision biopsy. Upon examination, the patient was febrile, tachypneic, with multiple enlarged LNs in the neck bilaterally (Figure 6A), axillae, and inguinal regions. There was prominence of the left torus tubarius compared with the right side; however, no obvious mass was identified in the nasopharynx or the FOR regions on naso-endoscopy (Figure 6B). Other head neck examinations were unremarkable. The abdomen was distended, and hepatosplenomegaly was present. A tru-cut biopsy of the left cervical LN was performed. HPE and IHC studies showed metastatic squamous cell carcinoma. A biopsy from the left FOR confirmed non-keratinizing NPC. The patient was not fit for palliative chemotherapy; subsequently, her condition deteriorated, and the patient died during the same admission.

DISCUSSION

NPC is a rare malignant lesion in Western countries but is highly prevalent in Asia (1,3,4). East and Southeast Asia are classified as endemic areas for NPC, with 70% of new cases reported in 2018 originating from these areas, and NPC was listed as the eighth leading cause of cancer deaths in Southeast Asia (3,4). Middle-aged men with a positive family history and a history of Epstein–Barr virus (EBV) infection, smoking, and consumption of preserved food or salted fish are the group most frequently affected in endemic areas (1,4,5).

The most common presenting symptom is neck swelling, followed by nasal and ear symptoms (1,5,6). Level II cervical LN is the most common site followed by level III, V and IV, while level I, VI and supraclavicular regions are rarely involved (8). Based on the literature and to the best of our knowledge, generalized LN involvement is more suggestive of lymphoproliferative or hematological malignancies, such as lymphoma, and is extremely rarely associated with NPC. The association between generalized lymphadenopathy and the prognosis of NPC has not been described in the literature. In this case series, all patients had distant metastases and were thus stage IVB; we believed that generalized lymphadenopathy could be a poor prognostic indicator.

Pre-treatment hemoglobin, white blood cell, and platelet levels have been investigated in solid tumors, including NPC, and have shown prognostic significance (7,9). A study conducted in China with a total of 658 patients showed that 3.3%, 9.1%, and 2.7% of patients had anemia, leukocytosis, and thrombocytosis, respectively (9). Another study in Indonesia with a smaller sample size (48 patients) showed
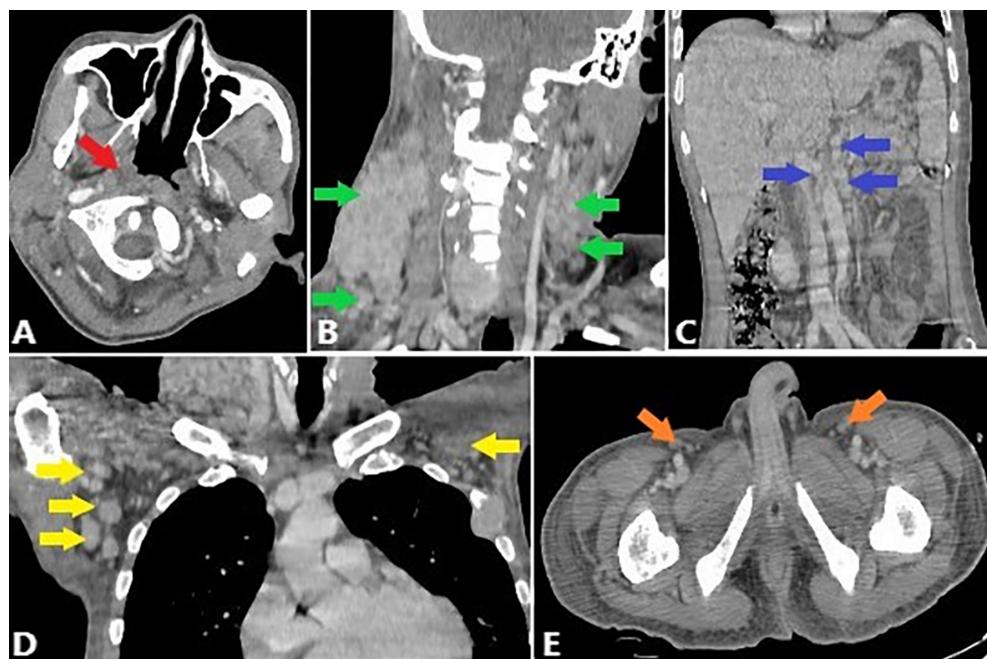
Figure 4. Contrast-enhanced CT scan of neck, thorax, abdomen, and pelvis. An axial image at the level of the nasopharynx shows mild thickening of the right torus tubarius compared with the left side and effacement of the right FOR (red arrow), with no enhancing lesion seen (A). A coronal image of the neck shows bilateral cervical nodes at levels II, III, IV, and V (green arrow; B). A coronal image of the abdominal region shows multiple enlarged para-aortic LNs (blue arrow; C). A coronal image of the thorax shows multiple enlarged axillary LNs (yellow arrow) (D). The axial image of the pelvis (E) depicts bilateral inguinal LN enlargement (orange arrowhead).

*CT: Computed tomography, LN: Lymph node, FOR: Fossa of Rosenmüller*
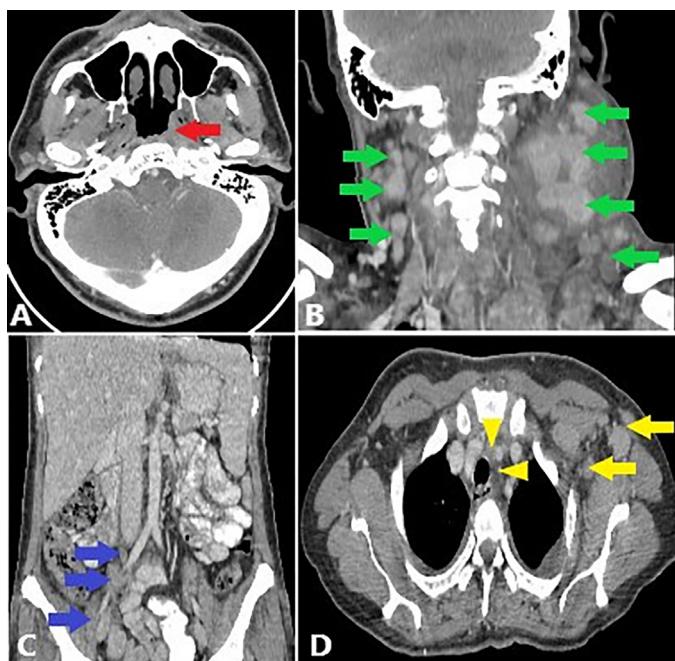
Figure 5. Contrast-enhanced CT scan of neck, thorax, abdomen and pelvis. Axial image at the level of the nasopharynx shows mild thickening of the left torus tubarius compared with the right side, with effacement of the left FOR (red arrow), without any enhancing lesion seen (A). Coronal image of the neck shows bilateral cervical nodes at levels II, III, IV and V (green arrow) (B). Coronal image of the abdomen and pelvis shows multiple enlarged LNs surrounding the right common and external iliac vessels (blue arrow; C). An axial image of the thorax shows multiple enlarged left axillary and paratracheal LNs (yellow arrow and yellow arrowhead, respectively) (D).

CT: Computed tomography, LN: Lymph node, FOR: Fossa of Rosenmüller

a higher percentage of patients with anemia, leukocytosis, and thrombocytosis: 52.1%, 29.2%, and 43.8%, respectively (7). These discrepancies could be due to many factors, such as the sample sizes of the studies, the stages of the disease at presentation, and the cutoff values used. Thrombocytopenia is rarely investigated and is less frequently associated with NPC compared with thrombocytosis. Chen et al. (10) reported that 10.1% and 15.8% of NPC patients had thrombocytopenia and thrombocytosis, respectively. Another study by Susilawati et al. (7) showed that 6.2% of NPC patients had thrombocytopenia, while 43.8% of patients had thrombocytosis. Anemia, leukocytosis, and thrombocytosis are well-established poor prognostic factors for NPC (7,9,11,12). Although a small number of studies investigated thrombocytopenia, they consistently showed an unfavorable prognosis in this patient category (7,10).

According to the United States National Cancer Institute (7), severe and extremely severe anemia are defined as hemoglobin levels of 6.5–7.9 g/dL and <6.5 g/dL, respectively. In this case series, one patient presented with severe anemia and two patients with extremely severe anemia. The causes of anemia in NPC patients are complex and multifactorial. It could be due to poor oral intake and nutrition in cancer patients, reduced hemoglobin production or hemolysis, and bleeding from the tumor. Tumor cells secrete the hormones serotonin and bombesin, which result in poor appetite, leading to poor nutrition (7). The tumor cells may also induce cytokine production, which can suppress erythropoiesis and the response of erythroid progenitor cells to erythropoietin and can cause hemolysis (9). An enlarging tumor is prone to bleeding due to the formation of neovessels that lack smooth muscle and contractile properties. Tumor hypoxia secondary to severe anemia may activate hypoxia-inducible factor-1, thereby promoting tumor metastasis (9).

Leukocytosis is often associated with neutrophilia, as observed in the present cases, and both indicate a poor prognosis in NPC patients (11,13). Leukocytosis and neutrophilia are defined as leukocyte count more than 10×10^9/L and 8×10^9/L respectively in most of the studies (11). The underlying inflammation, immune response, and cytokine release within the tumor microenvironment stimulate leukocyte and neutrophil proliferation (9,13). This chronic inflammatory process in malignancy is of paramount importance
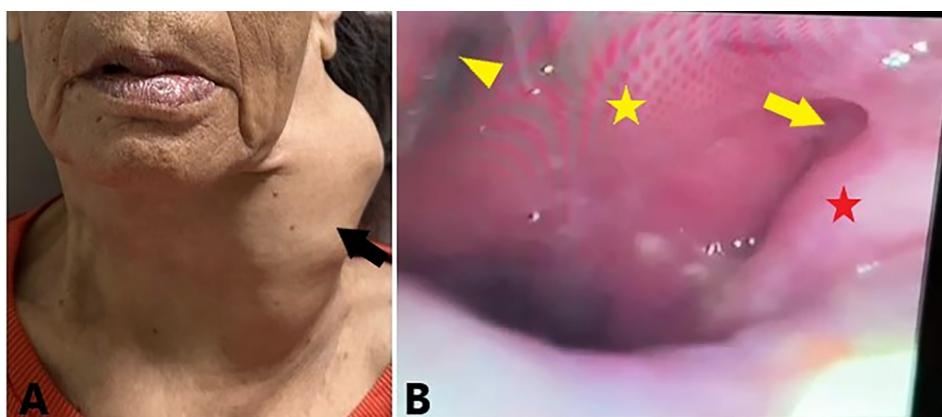

Figure 6. Huge left neck swelling with matted cervical LN (A). The left torus tubarius (red star) was prominent compared with the right side; however, no obvious mass was identified in the nasopharynx (yellow star) or Fossa of Rosenmüller (yellow arrow, left; yellow arrowhead, right) on nasoendoscopic examination (B).

LN: Lymph node

and has been found to promote tumor invasion, progression, and metastasis (13). Apart from this process, leukocytosis in solid tumors could be due to infection, use of corticosteroids, intoxication, severe hemorrhage, bone marrow metastases, paraneoplastic leukemoid syndrome, and use of granulocyte colony-stimulating factor (11,14).

Thrombocytosis in patients with NPC has been defined differently in the literature. Chen et al. (10) and Gao et al. (12) defined thrombocytosis as a platelet count greater than 300×10^9/L; Susilawati et al. (7) defined thrombocytosis as a platelet count greater than 380×10^9/L (7), while Qiu et al. (9) defined thrombocytosis as a platelet count greater than 400×10^9/L. In contrast, the definition of thrombocytopenia is more consistently defined as a platelet count less than 150×10^9/L (10,12). The cause of platelet proliferation in malignancy is still unclear, but it is believed to be secondary to the production of cytokines, such as interleukin 6 and thrombopoietin (10,12). Platelets secrete proangiogenic cytokines, vascular endothelial growth factor and thymidine phosphorylase, which are important in tumor invasion and progression (10). Thrombocytopenia may develop in patients with NPC secondary to diffuse infiltration of tumor cells into the bone marrow or spleen, immune-mediated mechanisms, EBV infection, or paraneoplastic syndrome (7,10,15). Thrombocytopenia secondary to bone marrow infiltration and bony metastases, as observed in the cases at presentation, categorized patients as having advanced disease (stage IVB) and significantly reduced the survival rate. A study conducted by Chen et al (10). showed that thrombocytopenia, compared with a moderate platelet count, was an unfavorable prognostic factor for overall survival in patients receiving concurrent chemoradiotherapy and had a greater negative effect than the thrombocytosis group.

In addition to prognostic significance, combinations of generalized lymphadenopathy, severe anemia, leukocytosis, and thrombocytopenia in the cases had misdirected us toward the diagnosis of lymphoma at the initial presentation. This atypical presentation of NPC significantly delays diagnosis and treatment and is generally associated with an unfavorable prognosis. Another challenge in the diagnosis of the presenting cases was the submucosal location of the tumor and the absence of an obvious mass in the nasopharynx or the FOR on naso-endoscopy and CT scan. A prominent unilateral torus tubarius, as seen in our cases 2 and 3, may suggest the presence of a submucosal tumor, and a deep biopsy should be performed in suspected cases. The nasal biopsy was not performed at the initial presentation in our cases because the patients' general clinical presentations were more suggestive of lymphoma. MRI is an excellent investigation for submucosal NPC because it can delineate soft tissue better than a CT scan (3), but it is not available at our center. Another imaging modality that helps localize the primary tumor is the combination of positron emission tomography and CT scan, which shows high uptake of the radioactive tracer (fluorodeoxyglucose) by the highly metabolic malignant cells. This imaging is currently considered the gold standard for cancer of unknown origin and should be performed prior to biopsy; however, it is not available in many centers, including ours.

Fine Needle Aspiration Cytology (FNAC) should be the first investigation of choice in patients with suspected head and neck malignancy to avoid the risk of tumor seeding to the skin and upstaging the cancer. However, in cases with suspected lymphoma, excisional or tru-cut biopsies are preferred because FNAC cannot provide sufficient tissue for diagnosis and subtype determination. In this case series, we performed excisional biopsies in two patients and a through-cut biopsy in one patient. All HPE results showed metastatic squamous cell carcinoma, whereas the IHC study had a limited role in determining the primary site. Special stains for NPC, such as EBV-encoded non-polyadenylated RNAs, EBV nuclear antigen 1, and latent membrane protein 1 and 2, are considered helpful (16), but they were not available at our center.

All patients in these cases were at stage IVB and were indicated for palliative chemotherapy. All of them had poor ECOG performance status at diagnosis and died within 4 months of diagnosis. Clinicians should be aware of these atypical presentations, and a prompt diagnosis should be made to avoid delays in treatment.

CONCLUSION

NPC is a rare cancer globally but is highly prevalent and endemic in East and Southeast Asia. The patients may present with atypical features that can mimic other malignant lesions. Generalized lymphadenopathy, severe anemia, leukocytosis, and thrombocytopenia are typical presentations of lymphoma but are atypical of NPC. These presentations not only cause diagnostic confusion but also are associated with significant poor prognostic indicators. Awareness of these atypical presentations is of paramount importance to avoid delays in management and worsening of overall survival.

Ethics

Footnotes

References

1. Tsang RKY, Kwong DLW. Nasopharyngeal carcinoma. In: Watkinson JC, Clarke RW, editors. Scott-Brown's otorhinolaryngology: head and neck surgery. 8th ed. USA: Taylor & Francis Group; 2019. p. 93-110. Available from: https://www.taylorfrancis.com/chapters/edit/10.1201/9780203731000-9/nasopharyngeal-carcinoma

2. Sharif SET, Zawawi N, Yajid AI, Shukri NM, Mohamad I. Pathology classification of nasopharyngeal carcinoma. In: Abdullah B, Balasubramanian A, Lazim NM, editors. An evidence-based approach to the management of nasopharyngeal cancer. 1st ed. UK: Academic Press; 2020. p. 73-92. Available from: https://www.elsevier.com/books/an-evidence-based-approach-to-the-management-of-nasopharyngeal-cancer/abdullah/978-0-12-814403–9.

3. Chen YP, Chan ATC, Le QT, Blanchard P, Sun Y, Ma J. Nasopharyngeal carcinoma. Lancet. 2019; 394: 64–80.

4. Chang ET, Ye W, Zeng YX, Adami HO. The Evolving Epidemiology of nasopharyngeal carcinoma. Cancer Epidemiol Biomarkers Prev. 2021; 30: 1035–47.

5. Suzina SA, Hamzah M. Clinical presentation of patients with nasopharyngeal carcinoma. Med J Malaysia. 2003; 58: 539–45.

6. Tiong TS, Selva KS. Clinical presentation of nasopharyngeal carcinoma in Sarawak Malaysia. Med J Malaysia. 2005; 60: 624–8.

7. Susilawati S, Kadriyan H, Sutirtayasa WP. Hematologic profile in patients with nasopharyngeal carcinoma. Adv Health Sci Res. 2021; 46: 110–5.

8. Ho FC, Tham IW, Earnest A, Lee KM, Lu JJ. Patterns of regional lymph node metastasis of nasopharyngeal carcinoma: a meta-analysis of clinical evidence. BMC Cancer. 2012; 12: 98.

9. Qiu MZ, Xu RH, Ruan DY, Li ZH, Luo HY, Teng KY, et al. Incidence of anemia, leukocytosis, and thrombocytosis in patients with solid tumors in China. Tumour Biol. 2010; 31: 633–41.

10. Chen YP, Chen C, Mai ZY, Gao J, Shen LJ, Zhao BC, et al. Pretreatment platelet count as a predictor for survival and distant metastasis in nasopharyngeal carcinoma patients. Oncol Lett. 2015; 9: 1458–66.

11. Su Z, Mao YP, OuYang PY, Tang J, Xie FY. Initial hyperleukocytosis and neutrophilia in nasopharyngeal carcinoma: incidence and prognostic impact. PLoS One. 2015; 10: e0136752.

12. Gao J, Zhang HY, Xia YF. Increased platelet count is an indicator of metastasis in patients with nasopharyngeal carcinoma. Tumour Biol. 2013; 34: 39–45.

13. He JR, Shen GP, Ren ZF, Qin H, Cui C, Zhang Y, et al. Pretreatment levels of peripheral neutrophils and lymphocytes as independent prognostic factors in patients with nasopharyngeal carcinoma. Head Neck. 2012; 34: 1769–76.

14. Lee DW, Teoh DC, Chong FL. A Case of nasopharyngeal carcinoma with paraneoplastic leukemoid reaction: a case report. Med J Malaysia. 2015; 70: 110–1.

15. Yang K, Zhang T, Chen J, Fan L, Yin Z, Hu Y, et al. Immune thrombocytopenia as a paraneoplastic syndrome in patients with nasopharyngeal cancer. Head Neck. 2012; 34: 127–30.

16. Ke K, Wang H, Fu S, Zhang Z, Duan L, Liu D, et al. Epstein-Barr virus-encoded RNAs as a survival predictor in nasopharyngeal carcinoma. Chin Med J (Engl). 2014; 127: 294–9.

Masson's Tumour of Parotid: A Case Report and Literature Review

Parotis Bezinin Masson Tümörü: Olgu Sunumu ve Literatür Derlemesi

◉ V Sha Kri Eh Dam[1], ◉ Ong Wee Kee[2], ◉ Lee Sen Lin[3]

[1]Department of Otorhinolaryngology–Head and Neck Surgery, Hospital Lahad Datu, Sabah, Malaysia
[2]Department of Radiology, Hospital Lahad Datu, Sabah, Malaysia
[3]Department of Pathology, Hospital Queen Elizabeth 1, Sabah, Malaysia

ABSTRACT

Masson's tumour is a rare non-neoplastic vascular lesion characterized by a reactive proliferation of endothelial cells with papillary growth secondary to intravascular thrombosis or vascular stasis. It most commonly affects medium-sized veins and mainly involves the skin and subcutaneous tissues of the head and neck region, trunk, and extremities. Parotid gland involvement is extremely rare, with only four cases reported worldwide to date. The preoperative diagnosis is challenging, and the condition is usually misdiagnosed as another more common benign lesion. Histopathological examination and immunohistochemical studies are considered the gold standard for the diagnosis and exclusion of malignant lesions that may resemble Masson's tumour. The extent of surgical resection, either superficial or total parotidectomy, depends on preoperative imaging and intraoperative findings. The prognosis is favourable with a low recurrence rate if the surgical margin is negative.

Keywords: Masson's tumour, intravascular papillary endothelial hyperplasia, parotid gland, parotidectomy

ÖZ

Masson tümörü, intravasküler tromboz veya vasküler staza sekonder olarak papiller büyüme gösteren reaktif endotelyal hücre proliferasyonu ile karakterize, nadir görülen ve neoplastik olmayan bir vasküler lezyondur. En sık orta büyüklükteki venleri etkiler ve baş-boyun bölgesi, gövde ve ekstremitelerin deri ile subkutan dokularını tutar. Parotis bezi tutulumu son derece nadirdir ve günümüze kadar dünya çapında yalnızca dört vaka bildirilmiştir. Preoperatif tanı güç olup, genellikle daha yaygın görülen başka bir benign lezyon olarak yanlış değerlendirilir. Histopatolojik inceleme ve immünohistokimyasal çalışmalar, Masson tümörüne benzer malign lezyonların ayırıcı tanısı ve doğrulanmasında altın standarttır. Cerrahi rezeksiyonun kapsamı, yüzeyel veya total parotidektomi olmasına dayalı olarak preoperatif görüntüleme ve intraoperatif bulgulara bağlıdır. Cerrahi sınır negatif olduğunda prognoz olumludur ve nüks oranı düşüktür.

Anahtar Sözcükler: Masson tümörü, intravasküler papiller endotelyal hiperplazi, parotis bezi, parotidektomi

Gazi Med J 2026;37(1):118-122

Dam et al. Masson's Tumour of Parotid

INTRODUCTION

Masson's tumour, also known as intravascular papillary endothelial hyperplasia (IPEH), is a rare, non-neoplastic lesion of vascular origin, characterized by reactive proliferation of endothelial cells with papillary growth (1,2). Pierre Masson, a French pathologist, first described this disease in 1923 as "vegetant intravascular hemangioendothelioma" (3).

The most common sites of involvement are the skin and subcutis and comprises around 2% of vascular tumours of the skin and subcutaneous tissue (4-6). It can occur in any blood vessel but has a predilection for the skin and subcutaneous tissues of the head and neck region, trunk, and extremities (5-7). The skin and subcutaneous tissue of the face and scalp are the most commonly affected sites in the head and neck region (7). Parotid gland involvement is extremely rare, with only four cases reported worldwide to date (5,6,8,9).

CASE REPORT

A 50-year-old male with underlying diabetes mellitus and hypertension presented with a one-year history of painless right parotid swelling that had gradually increased in size. There were no other locoregional symptoms, such as facial weakness, trismus, dysphagia, voice changes, or neck swelling. He has no risk factors for malignancy, such as smoking, alcohol consumption, a family history of malignancy, or a history of head and neck radiation. In addition, he denied any constitutional symptoms.

On examination, there was a diffuse swelling in the right parotid region, which had a smooth surface, was firm in consistency, non-tender, and immobile but not fixed to the overlying skin (Figure 1). The facial nerve was intact, with no medialisation of the lateral pharyngeal wall and no palpable cervical lymph nodes. Other head and neck examinations were unremarkable.

A computed tomography scan of the neck was performed and showed a well-circumscribed, heterogeneously enhancing solid lesion within the deep lobe of the right parotid gland, measuring 2.7 × 3.2 × 3.9 cm (Figure 2). There was no calcification, bony erosion, or cervical lymph node enlargement, and the superficial lobe appeared normal. A through-cut biopsy was performed, which

revealed normal salivary gland tissue. This finding likely represented the normal superficial lobe of the parotid gland rather than the deep lobe lesion.

The patient subsequently underwent a total parotidectomy. Intraoperatively, the mass was confirmed to arise from the deep lobe of the parotid gland, whereas the superficial lobe appeared normal (Figure 3). Postoperatively, the patient recovered well without any complications. Histopathological examination (HPE) of the deep lobe revealed an intrasalivary gland lesion, surrounded by a pseudofibrous capsule and composed of variably sized vascular spaces, with some areas exhibiting papillary structures within (Figure 4A). The papillae are lined by a single layer of plump endothelial cells (Figure 4B). No nuclear atypia or mitotic figures seen. Most areas exhibit organised
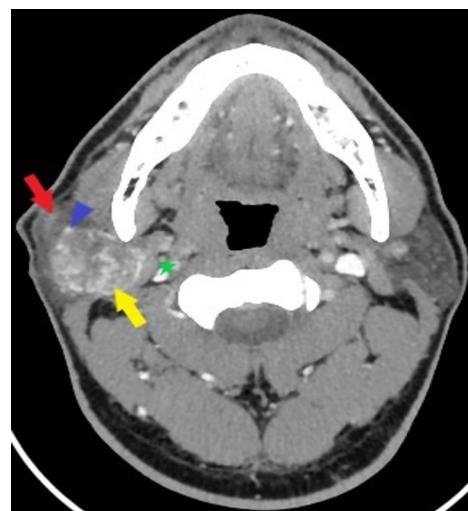
Figure 2. Contrasted axial view computerized tomography scan shows a well circumscribed heterogeneously enhancing solid lesion seen within the deep lobe of the right parotid gland (yellow arrow), without extension into the parapharyngeal space (green star). The lateral lobe appeared normal (red arrow). Blue arrowhead – retromandibular vein.

Figure 1. Diffused swelling at the right parotid region.
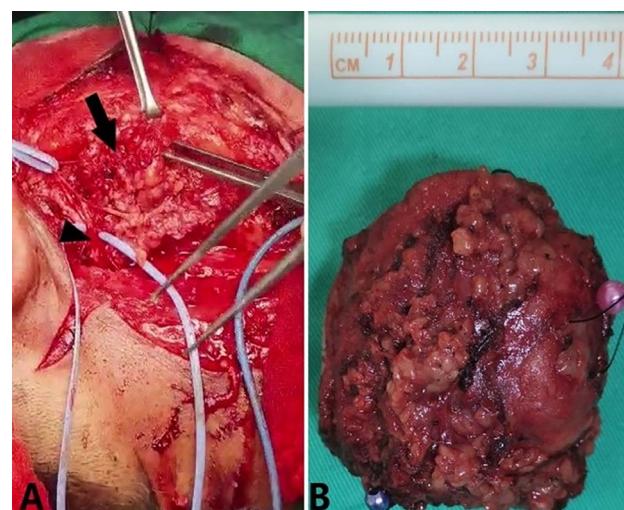
Figure 3. Mass arises from the deep lobe of parotid gland (arrow), deeper to facial nerve (arrowhead – main trunk of facial nerve) (A). A 4cm x 4cm mass with deep lobe of parotid gland was completely excised (B).

Gazi Med J 2026;37(1):118-122

Dam et al. Masson's Tumour of Parotid
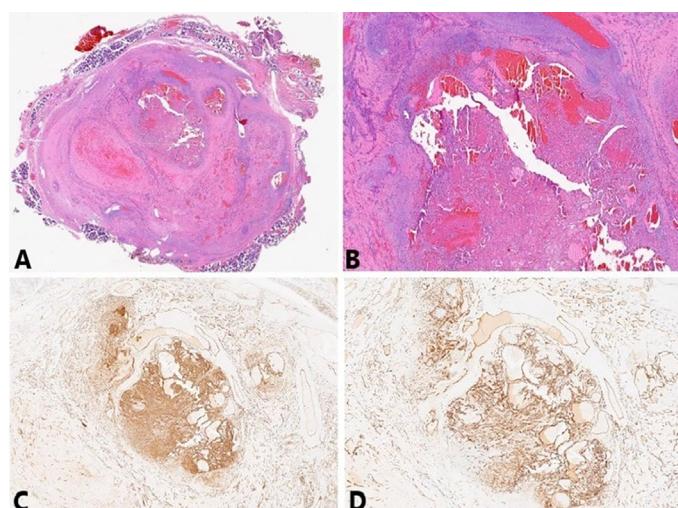
Figure 4. An intra-salivary gland lesion, surrounded by pseudo-fibrous capsule, composed of variable sizes of vascular spaces, with areas of papillary structures within that are lined by single layer endothelial cells (A, H&E x 40). Focal areas with papillary structures lined by endothelial cells (B, H&E x 400). CD31 immunostaining (C, x 200) and CD34 immunostaining (D, x 200) highlighting the endothelial cells lining the vessel wall.

thrombi associated with stromal haemorrhage, hyalinisation, myxoid change, and aggregates of haemosiderin-laden pigments. The endothelial cells lining the vascular channels are immunoreactive for CD31 and CD34 (Figure 4C and 4D) and negative for CK7, CK20, p63, and HHV8. These findings are suggestive of Masson's tumour. The HPE of the superficial lobe was normal.

DISCUSSION

Masson's tumour is a rare vascular lesion that mostly affects medium-sized veins but may occur in veins of any size and, rarely, in arteries (5,9). It was first described by Pierre Masson in 1923, who used the term vegetant intravascular hemangioendothelioma when he discovered intravascular papillary proliferation in a male patient with an inflamed hemorrhoidal plexus (3). It is also known as IPEH, a term highlighted by Clearkin and Enzinger (10) in 1976 to emphasize the non-neoplastic nature of the disease. Other terms used in the past to describe this disease entity include intravascular angiomatosis, intravenous atypical vascular proliferation, intravascular endothelial proliferation, reactive papillary endothelial hyperplasia, Masson's pseudoangiosarcoma, and Masson's intravascular hemangioendothelioma (1,6,7).

Generally, the skin and subcutis are the most commonly affected sites (4-6), while the face and scalp are the most frequently reported sites in the head and neck region (7). Oral cavity, lateral neck, mandible, thyroid, orbit, internal auditory canal, pharynx, larynx, maxillary sinus, and intracranium are among the reported sites of involvement in the head and neck region (1,6,7). Based on a literature review, salivary gland involvement is extremely rare, with only four cases reported in the parotid gland and one case in the submandibular gland (Table 1) (1,5,6,8,9). A case reported by Corio et al. (11) in 1982 was excluded due to the absence of clinical details, and another case reported by Kim et al. (12) in 2007 was also excluded because the mass was separate and located outside the submandibular gland.

Masson's tumour commonly occurred in adults without a distinct age, sex, or racial predilection (2,4). Incidence in children is very low, but it can occur as early as 9 months of age (7). Some studies suggest a slight female predominance, with a female-to-male ratio of 1.3:1.0 (1,6). It is a generally slow-growing tumour and usually presents

Table 1. Review of reported cases of salivary gland Masson's tumour

Author	Year	Age	Sex	Location	Presentation	Imaging	Biopsy/FNAC	Clinical impression	Treatment
Mokhtari et al. (8)	2011	39-year-old	M	Left parotid gland	Painless swelling for 1 year	NA	NA	Pleomorphic adenoma	Partial resection of the parotid gland
Mignogna et al. (6)	2016	70-year-old	F	Right parotid gland	Painless swelling for 5 years	MRI	NA	Pleomorphic adenoma	Extracapsular dissection
Carta et al. (9)	2018	43-year-old	F	Right parotid gland (superficial lobe)	Mild painful swelling for 4 years	MRI	NA	A hyper vascularized benign lesion	Subtotal parotidectomy
Cho et al. (1)	2021	37-year-old	F	Right submandibular gland	Painless swelling for 2 months	US and CT scan	Presence of some fibrinous material and mixed inflammatory cells	Sialadenitis secondary to sialolithiasis with intraglandular abscess or submandibular gland tumour	Ablation of the submandibular gland
Mohebbi et al. (5)	2023	29-year-old	F	Right parotid gland (superficial lobe)	Painless swelling (duration not mentioned)	MRI	NA	A vascular mass	Total parotidectomy

M: Male, F: Female, US: Ultrasound, CT: Computerised tomography, FNAC: Fine needle aspiration cytology, MRI: Magnetic resonance imaging, NA: Not available

Gazi Med J 2026;37(1):118-122

Dam et al. Masson's Tumour of Parotid

with painless swelling (7). The aetiology and pathogenesis are poorly understood, with various theories having been hypothesised. The aetiology is believed to be multifactorial, with approximately 30% of cases triggered by local trauma and vascular anomalies (2,4,5). Intravascular thrombus formation is the key factor in several theories of pathogenesis. Masson first described the disease as a neoplasm characterised by endothelial proliferation which results in thrombosis (3). Fifty-three years later, Clearkin and Enzinger (10) proposed a more widely accepted theory that explained that the formation of thrombosis leads to reactive proliferation of endothelial cells and papillary formation. This finding emphasized that the lesion is a reactive process rather than a neoplasm. Another theory by Levere et al. (13) is that the release of basic fibroblast growth factor by macrophages in response to traumatic vascular stasis stimulates endothelial cell proliferation. Additionally, Irey and Noris (14) suggested that hormones may play a role in the pathogenesis due to the female predilection in some studies.

Hashimoto et al. (15) classified Masson's tumour into 3 types based on aetiology. The pure type is the most common and arises de novo in a dilated vessel; the mixed type is associated with a pre-existing vascular anomaly; the extravascular type is associated with trauma-induced hematoma formation. Preoperative diagnosis is challenging. Fine-needle aspiration cytology is usually non-diagnostic or results in misdiagnosis in the majority of cases (7). Our present case underwent a Tru-Cut biopsy; however, the sample was not representative of the lesion. Imaging studies, whether computed tomography or magnetic resonance imaging, are non-specific but may be helpful in surgical planning (16). In the parotid gland, imaging features may resemble benign lesions such as pleomorphic adenoma, Warthin's tumour, or vascular tumours.

The diagnosis of Masson's tumour is usually made after HPE and immunohistochemistry (IHC) studies of the excised specimen. They are considered the gold standard for the diagnosis of Masson's tumour and the exclusion of malignant lesions that may resemble Masson's tumour, such as angiosarcoma and Kaposi sarcoma. The typical histopathological findings of Masson's tumour are proliferation of papillary structures within the blood vessel, thrombus formation, coverage by fewer than three layers of endothelial cells, and positive CD31 and CD34 immunohistochemical markers (1). On the other hand, proliferation of cells outside the vessel, papillae covered by more than two endothelial cell layers, and a positive CD105 immunohistochemical marker are more suggestive of angiosarcoma (1).

The treatment of Masson's tumour is complete excision with negative margins. The extent of surgical resection depends on the evaluation of preoperative imaging and intraoperative findings. A superficial parotidectomy is sufficient if the lesion is confined to the superficial lobe of the parotid without features suggestive of malignancy. However, if the lesion is located in the deep lobe of the parotid gland, total parotidectomy is usually required, as observed in the present case. The prognosis is good, with a low recurrence rate, if the margin is negative (1).

CONCLUSION

Masson's tumour is extremely rare occurred in parotid gland and usually misdiagnosed as another more common benign lesion.

Preoperative diagnosis is challenging, and most cases are diagnosed after HPE and IHC studies of the excised specimen. It is important to exclude other more serious conditions that may resemble Masson's tumour, such as angiosarcoma and Kaposi sarcoma. The treatment consists of complete excision with negative margins, and the prognosis is generally good, with a low recurrence rate.

Ethics

Informed Consent: Informed consent was obtained for publication.

Footnotes

Authorship Contributions

REFERENCES

1. Cho CF, Liu YH, Lin JC. Intravascular papillary endothelial hyperplasia (Masson's tumor) of the submandibular gland: a case report. Ear Nose Throat J. 2023; 102: 640–4.

2. da Silva Leal M, Amado C, Paracana B, Gonçalves G, Sousa M. Masson's tumour: a rare cause of cervical mass. Eur J Case Rep Intern Med. 2021; 8: 003078.

3. Díaz-Flores L, Gutiérrez R, Madrid JF, García-Suárez MP, González-Álvarez MP, Díaz-Flores L Jr, et al. Intravascular papillary endothelial hyperplasia (IPEH): evidence supporting a piecemeal mode of angiogenesis from vein endothelium, with vein wall neovascularization and papillary formation. Histol Histopathol. 2016; 31: 1271–9.

4. M Abdo E, Farouk N, E Elshinawy W, Mohamed Ahmed E, A Raafat M, Husien Abdo W, et al. Masson's tumor as an uncommon cause of neck mass: a case presentation. Vasc Endovascular Surg. 2024; 58: 405–9.

5. Mohebbi S, Zohourian Shahzadi S, Jamshidi Naeini A. Parotid Masson's tumor in a 29-years-old woman: a case report. Iran J Otorhinolaryngol. 2023; 35: 165–8.

6. Mignogna C, Barca I, Di Vito A, Puleo F, Malara N, Giudice A, et al. Extravascular type of intravascular papillary endothelial hyperplasia mimicking parotid gland neoplasia and the possible role of ferritin in the pathogenesis: A case report. Mol Clin Oncol. 2017; 6: 193–6.

7. Sarode GS, Sarode SC, Karmarkar SP. Oral intravascular papillary endothelial hyperplasia (Masson's tumor): a review of literature. J Oral Maxillofac Surg Med Pathol. 2014; 26: 73–9.

8. Mokhtari M, Azarpira N, Rasolmali R. Intravascular papillary endothelial hyperplasia (Masson's tumor) of the parotid gland. Indian J Pathol Microbiol. 2011; 54: 226–8.

9. Carta F, Sionis S, Ledda V, Gerosa C, Puxeddu R. Parotid Masson's tumor: case report. Braz J Otorhinolaryngol. 2018; 84: 523–5.

10. Clearkin KP, Enzinger FM. Intravascular papillary endothelial hyperplasia. Arch Pathol Lab Med. 1976; 100: 441–4.

11. Corio RL, Brannon RB, Tarpley TM. Intravascular papillary endothelial hyperplasia of the head and neck. Ear Nose Throat J. 1982; 61:88–91.

Gazi Med J 2026;37(1):118-122

Dam et al. Masson's Tumour of Parotid

12. Kim D, Israel H, Friedman M, Kuhel W, Langevin CJ, Plansky T. Intravascular papillary endothelial hyperplasia manifesting as a submandibular mass: an unusual presentation in an uncommon location. J Oral Maxillofac Surg. 2007; 65: 786–90.

13. Levere SM, Barsky SH, Meals RA. Intravascular papillary endothelial hyperplasia: a neoplastic "actor" representing an exaggerated attempt at recanalization mediated by basic fibroblast growth factor. J Hand Surg Am. 1994; 19: 559–64.

14. Irey NS, Norris HJ. Intimal vascular lesions associated with female reproductive steroids. Arch Pathol. 1973; 96: 227–34.

15. Hashimoto H, Daimaru Y, Enjoji M. Intravascular papillary endothelial hyperplasia. A clinicopathologic study of 91 cases. Am J Dermatopathol. 1983; 5: 539–46.

16. Giannitto C, Mercante G, Spriano G, Natoli R, Gaino F, Lofino L, et al. CT and MRI findings of head and neck masson's tumor: a rare case report and systematic review of the literature. Reports in Medical Imaging. 2021; 14: 53–64.

Cauliflower Ear Caused by *Pseudomonas aeruginosa* After "High" Ear Piercing

Yüksek Yerleşimli Kulak Piercingi Sonrası Pseudomonas aeruginosa'ya Bağlı Karnabahar Kulak Gelişimi

Ⓘ Yusuf Çağdaş Kumbul[1], Ⓘ Yusuf Tuncel[1], Ⓘ Furkan Yeşilkuş[1], Ⓘ Hasan Yasan[1], Ⓘ Onur Ünal[2]

[1]Department of Otorhinolaryngology, Süleyman Demirel University Faculty of Medicine, Isparta, Türkiye
[2]Department of Infectious Diseases and Clinical Microbiology, Süleyman Demirel University Faculty of Medicine, Isparta, Türkiye

ABSTRACT

Although piercing has become increasingly common, the lobule and auricular cartilage are among the most frequent sites. If this procedure is performed by untrained personnel, it increases the risk of perichondritis in the auricular cartilage. When perichondritis develops, increased local temperature, erythema, and pain in the auricle are warning signs for early diagnosis; if an abscess is present, drainage and antibiotic therapy are essential.

Keywords: Ear, piercing, perichondritis, Pseudomonas Aeruginosa

ÖZ

Piercing işlemi giderek yaygınlaşsa da, en sık uygulanan bölgeler arasında kulak lobülü ve aurikula kıkırdağı yer almaktadır. Bu işlem tecrübesiz kişiler tarafından yapılırsa, aurikula kıkırdağında perikondrit riskini artırır. Perikondrit geliştiğinde, aurikulada lokal olarak artmış sıcaklık, kızarıklık ve ağrı erken teşhis için uyarı işaretleridir; apse varsa drenaj ve antibiyotik tedavisi şarttır.

Anahtar Sözcükler: Kulak, piercing, perikondrit, Pseudomonas Aeruginos

INTRODUCTION

Piercing may result in health consequences, ranging from minor problems to potentially life-threatening situations (1). One of these problems is the development of cauliflower ear. Cauliflower ear results in an irregular ear shape, loss of natural contours, decreased cartilaginous support, and permanent aesthetic deformity (2). Cauliflower ear can be caused by infections that develop after piercings of the auricular cartilage performed under inappropriate conditions (3).

In this case report, the management of a patient who developed an auricular abscess after piercing is reviewed in light of the literature.

CASE REPORT

The female patient presented to our clinic with recurrent swelling of the right auricle for approximately 20 days following auricle piercing. In her past medical history, she presented to an otolaryngology clinic at an external center and was hospitalized there before being admitted to us. During this period, the patient's auricular abscess was drained with a syringe, and a silicone material, shaped to apply pressure to the anterior and posterior portions of the auricle, was sutured; 2 x 1 g ceftriaxone disodium (Eqiceft iv, Tüm*Ekip İlaç) and 3 x 500 mg metronidazole (Fladazol iv, Koçak Farma İlaç) were prescribed. After a 3-day hospital stay, the patient was discharged with a prescription for 1 x 600 mg of cefdinir (Cempes, po, Sanovel İlaç) and 3 x 500 mg of metronidazole (Flagyl, po, Sanofi). Three days later, she was recalled

Cite this article as: Kumbul YÇ, Tuncel Y, Yeşilkuş F, Yasan H, Ünal O. Cauliflower ear caused by *Pseudomonas aeruginosa* after "high" ear piercing. Gazi Med J. 2026;37(1):123-125

Address for Correspondence/Yazışma Adresi: Furkan Yeşilkuş, Department of Otorhinolaryngology, Suleyman Demirel University Faculty of Medicine, Isparta, Türkiye
E-mail / E-posta: furkanyesilkus@gmail.com
ORCID ID: orcid.org/0009-0008-4871-0200

for an outpatient clinic follow-up. During outpatient clinic follow-up, swelling exceeding the boundaries of the silicone material was observed, and the abscess was drained again using a syringe, without dislodging the silicone material. The patient, who showed insufficient clinical improvement (fever of 38.5 degrees and worsening otalgia), was referred to us the same day without removal of the silicone material from her ear (Figure 1a).

Removal of the silicone material sutured to the superior region of the right auricle in the external center resulted in hyperemia, increased temperature, and swelling of the auricle. When the swollen area was punctured using a syringe, pus emerged; incision and drainage were performed. During the drainage procedure, deformation of the cartilaginous structure was observed at the abscess drainage site. Notably, the anterior and posterior surfaces of the skin in that area were in contact. A Penrose drain was inserted along the incision line and a pressure dressing was applied (Figure 1b). The patient was informed that a deformity may develop of the auricle. A specimen of the drained abscess pus was sent for culture. Intravenous antibiotic therapy was planned for the patient, and she was admitted to our service for close observation. In the patient's complete blood count, white blood cells were 9.8 mg/dL, neutrophils were 7.9 mg/dL, and C-reactive protein was 6 mg/dL. The patient was referred to the infectious diseases clinic and was empirically started on 3 × 4.5 g piperacillin sodium/tazobactam sodium (Tazoject IV, Tüm*Ekip İlaç). The next day, a button was sewn in place to apply pressure to the superior aspect of the right auricle (Figure 1c). When *Pseudomonas aeruginosa* was isolated from the abscess culture on day 4, the patient was referred again to the infectious diseases clinic. The patient's antibiotic therapy was changed to meropenem trihydrate, 3 × 500 mg (Merosid iv, Koçak Farma İlaç). The patient's Penrose drain was removed on the same day. On the 5th day, the button in the auricle was removed. After the patient had received meropenem trihydrate for a total of 5 days, because the complete blood count was unremarkable and auricular findings on examination had regressed (Figure 1d). At discharge, the patient was prescribed 2 x 750 mg ciprofloxacin hydrochloride (Cipro po, Biofarma); 2 x 1 g amoxicillin + clavulanic acid (Augmentin po, GlaxoSmithKline); and 2 x 1 bacitracin + neomycin sulfate skin pomade (Thiochilline, Abdi İbrahim İlaç). At the 1-week and 3-month follow-up visits, cauliflower deformity of the auricle was observed, but there were no signs of inflammation (Figure 1e and 1f). Informed consent was obtained from the patient for presentation of this case report.

DISCUSSION

Piercing the cartilage in the upper third of the auricle, known as "high ear piercing", has become increasingly common. Infection involving the cartilage in this area, called perichondritis, can often lead to cartilage loss, resulting in an unsightly deformity known as "cauliflower ear" (1). An Auricular abscess may develop secondary to untreated or inadequately treated perichondritis. In our case, there was a piercing located high on the right auricle. The presence of swelling on physical examinationat the time of application made us suspect that there might be an abscess developing on the basis of perichondritis. The quickest way to confirm the diagnosis of an abscess is to aspirate the pus with a syringe. In this case, aspiration of pus with a syringe confirmed the diagnosis of an abscess. To prevent auricular perichondritis or abscess, it is imperative to maintain strict
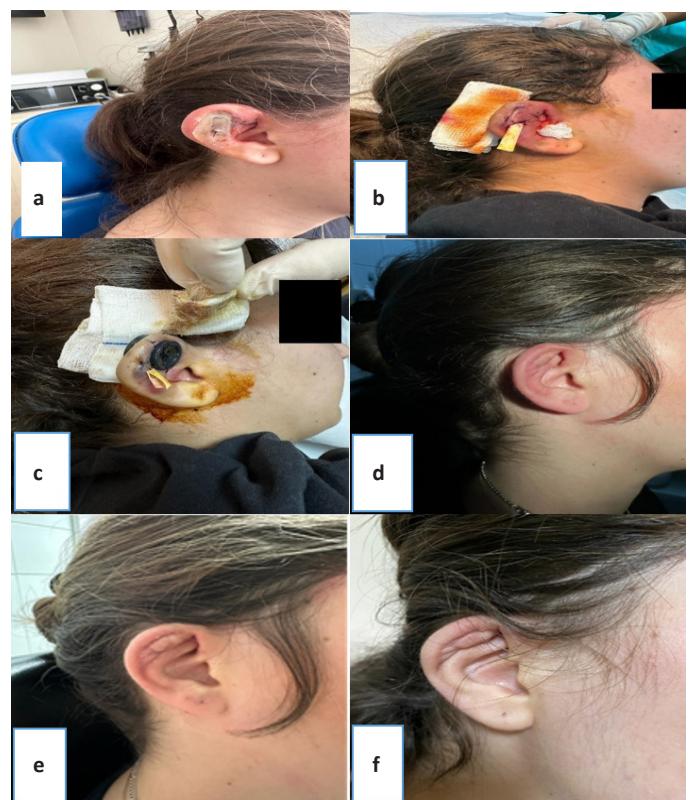
Figure 1. Image of the patient at the time of admission (a), confirmation of diagnosis after drainage (b), button sewed to the auricle on the 2nd day of admission (c), image of the auricle at discharge from hospital (d), image of the auricle in the 1st week (e), image of the auricle in the 3rd month (f).

hygiene during piercing. A common feature of patients who develop perichondritis and abscess is that they have had piercings performed in unregulated settings, as in our patient.

Pseudomonas aeruginosa is common in nature, and moist surfaces are suitable environments for its proliferation. It can cause otitis externa, keratitis, folliculitis, postoperative abscesses, and burn infections in immunocompetent individuals. *Pseudomonas aeruginosa* is a common causative agent in cases of perichondritis with abscess. In infections without abscess formation, *Staphylococcus aureus* is the predominant pathogen (4). Our patient was empirically started on piperacillin–tazobactam because she had previously received multiple antibiotic regimens without clinical response. However, because the patient's clinical condition did not improve sufficiently and the culture results showed only moderate susceptibility to piperacillin-tazobactam, the antibiotic treatment was changed to meropenem, to which the isolate was susceptible.

In our case, *Pseudomonas aeruginosa* was isolated from the abscess culture, and the antibiogram showed I (susceptible, increased exposure) for piperacillin-tazobactam and ciprofloxacin and S (susceptible, standard dosing regimen) for meropenem, according to European Committee on Antimicrobial Susceptibility Testing (EUCAST) criteria. The patient demonstrated clinical and laboratory improvement following intravenous piperacillin-tazobactam and meropenem therapy. According to the current EUCAST definition, category "I" antibacterial activity is assigned only when the drug

attains increased tissue or serum exposure (5). Therefore, high-dose ciprofloxacin (750 mg twice daily) was preferred during the sequential oral treatment phase to achieve adequate tissue concentrations against *Pseudomonas aeruginosa*. Although *Pseudomonas* was the only pathogen isolated, the patient's prior outpatient empirical antibiotic exposure may have suppressed the growth of certain bacteria in culture, such as Gram-positive or anaerobic bacteria. Anaerobic bacteria are difficult to isolate under routine clinical laboratory conditions because of their specific transport and culture requirements, which can lead to under-detection of these organisms, particularly in infections such as abscesses, where low oxygen tension favors polymicrobial growth. Therefore, amoxicillin-clavulanic acid was added to the treatment following parenteral therapy to maintain efficacy against *Pseudomonas* and to ensure coverage of possible concomitant anaerobic or gram-positive cocci that were not demonstrated in culture.

The auricular cartilage does not have a specific blood supply, and its nutrition is provided by the perichondrium immediately superficial to it. Any subperichondrial bleeding that occurs during cartilage piercing further reduces blood flow to the cartilage and increases the likelihood of infection. The resulting abscess hydrostatically lifts the perichondrium and the skin, thereby further limiting blood flow to the cartilage. Once an infection begins, antibiotics have a limited effect on cartilage that is no longer nourished; therefore, incision and drainage procedures are required for treatment (6). The culture of material obtained during drainage guides treatment. Specifically, from culture, the pathogenic microorganism that grows is identified and the antibiotics to which it is susceptible are determined. In this way, the patient receives the most effective antibiotic treatment. Even with antibiotic treatment, drainage, and debridement, a deformity ("cauliflower ear") may occur (1). This rate is much higher, especially among patients whose treatment was delayed, as in the case we presented.

Aggressive treatment initiated early in cases of suspected perichondritis is imperative to prevent irreversible ear deformity. Although antibiotics are started in almost every case, caution should be exercised if an abscess develops in patients who do not respond to antibiotics. If an abscess has developed, local wound care, incision and drainage, irrigation, tamponade, and dressing application should be added to the treatment steps (7). Before the patient in the present case presented to us, abscess drainage had been attempted using an injector, but the patient's treatment was unsuccessful. We recommend using syringes in such cases only to confirm the diagnosis when clinical findings are present. Incision with drain placement for therapeutic purposes seems to be a more suitable option for the treatment of an auricular abscess. In addition, attention to primary health care is an important factor in reducing these infections. For this reason, we recommend that businesses that perform under-the-counter piercings be closed down, and that establishments that operate professionally in this area be regularly inspected to ensure hygienic practices.

CONCLUSION

Early diagnosis of ear perichondritis is important, and aggressive treatment should be initiated promptly to prevent abscess formation. Incision and drainage are essential if an abscess develops. Antibiotic therapy should initially be targeted against *Pseudomonas aeruginosa*, and an abscess culture should be obtained. Antibiotic therapy may be revised based on culture results.

Ethics

Informed Consent: Informed consent was obtained from the patient for presentation of this case report.

Footnotes

Authorship Contributions

Surgical and Medical Practices: Y.Ç.K., Y.T., F.Y., H.Y., O.Ü., Concept: Y.Ç.K., Y.T., F.Y., H.Y., O.Ü., Design: Y.Ç.K., Y.T., F.Y., H.Y., O.Ü., Data Collection or Processing: Y.Ç.K., Y.T., F.Y., H.Y., O.Ü., Analysis or Interpretation: Y.Ç.K., Y.T., F.Y., Literature Search: Y.Ç.K., Y.T., F.Y., H.Y., Writing: Y.Ç.K., Y.T., F.Y.

Conflict of Interest: No conflict of interest was declared by the authors.

Financial Disclosure: The authors declared that this study received no financial support.

REFERENCES

1. Smith RA, Wang J, Sidal T. Complications and implications of body piercing in the head and neck. Current opinion in otolaryngology & head and neck surgery. 2002; 10: 199–205.

2. Jones SE, Mahendran S. Interventions for acute auricular haematoma. Cochrane Database Syst Rev. 2004; 2004: CD004166.

3. Binkhamis K, Habib HA, Alkahtani MK, Alrasheed DA, Barakeh MM, Alohali LM, et al. Cartilage ear piercing probable infections among females between 18 and 28 years old in Riyadh. Journal of Nature and Science of Medicine. 2022; 5: 182–7.

4. Klug TE, Holm N, Greve T, Ovesen T. Perichondritis of the auricle: bacterial findings and clinical evaluation of different antibiotic regimens. European Archives of Oto-Rhino-Laryngology. 2019; 276: 2199–203.

5. European Committee on Antimicrobial Susceptibility Testing (EUCAST). EUCAST: clinical breakpoints and dosing of antibiotics [Internet]. 2024 [cited 2026 Jan 7]. Available from: https://www.eucast.org/fileadmin/src/media/PDFs/EUCAST_files/Breakpoint_tables/v_14.0_Breakpoint_Tables.pdf

6. Perry AW, Sosin M. Reconstruction of ear deformity from post-piercing perichondritis. Arch Plast Surg. 2014; 41: 609–12.

7. Stewart GM, Thorp A, Brown L. Perichondritis--a complication of high ear piercing. Pediatr Emerg Care. 2006; 22: 804–6.

Developmental Perspective on Management of Childhood Chronic Diseases in Pediatric Practices

Pediatri Uygulamalarında Çocukluk Çağı Kronik Hastalıklarının Yönetimine İlişkin Gelişimsel Perspektif

Ⓘ Tuba Çelen Yoldaş

Department of Pediatrics, Division of Developmental Pediatrics, Gazi University Faculty of Medicine, Ankara, Türkiye

ABSTRACT

Management of chronic health conditions in pediatric practice requires a holistic and systematic approach for optimal development. Although a substantial body of literature exists on chronic disease and health management across various chronic health conditions, there is a need for holistic approaches to achieving the optimal developmental potential of these vulnerable groups of children. This article reviews the developmental and behavioral effects, the hospitalization process, and the clinical management of chronic health conditions in children and provides specific recommendations. Chronic health conditions both affect and are affected by the development and behavior of children. Clinicians should be aware that chronic conditions affect all family members. To minimize the adverse effects of the disease, the unmet needs of children and their families should be identified, and supportive approaches should be implemented throughout illness and hospitalization. Specific pediatric roles, including coordination of care, identification of developmental-behavioral functioning, assessment of family strengths, education about the disease, and planning for schooling, should be integrated into standard pediatric care for effective management of chronic conditions.

Keywords: Chronic diseases, child development, pediatric practices, hospitalization, clinical management

ÖZ

Pediatri uygulamalarında kronik sağlık sorunlarının yönetimi, optimum gelişim için bütüncül ve sistematik bir yaklaşım gerektirir. Çeşitli kronik sağlık sorunlarına ilişkin kronik hastalık ve sağlık yönetimi üzerine önemli bir literatür bulunmasına rağmen, bu savunmasız çocuk gruplarının en iyi gelişim potansiyeline ulaşması için bütüncül yaklaşıma ihtiyaç vardır. Bu makale, çocuklarda kronik sağlık sorunlarının gelişimsel ve davranışsal etkilerini, hastaneye yatış sürecini ve klinik yönetimini incelemekte ve özgül öneriler sunmaktadır. Kronik sağlık sorunları, çocukların gelişimini ve davranışlarını hem etkiler hem de bunlardan etkilenir. Klinisyenler, kronik sorunların tüm aile üyelerini etkilediğinin bilincinde olmalıdır. Hastalığın olumsuz etkilerini en aza indirmek için, çocukların ve ailelerinin karşılanmamış ihtiyaçları belirlenmeli ve hastalık ve hastanede yatış süresince destekleyici yaklaşımlar uygulanmalıdır. Bakım koordinasyonu, gelişimsel-davranışsal işlevselliğin belirlenmesi, ailenin güçlü yönlerinin değerlendirilmesi, hastalık hakkında eğitim ve okul planlaması gibi belirli pediatrik roller, kronik sorunların etkili yönetimi için standart pediatrik bakıma entegre edilmelidir.

Anahtar Sözcükler: Kronik hastalıklar, çocuk gelişimi, pediatri uygulamaları, hastaneye yatış, klinik yönetim

Gazi Med J 2026;37(1):126-134

Çelen Yoldaş. Management of Chronic Diseases in Pediatric Practices

INTRODUCTION

The prevalence of chronic diseases in children has increased over recent decades owing to advances in treatments and care for life-threatening pediatric conditions and increased survival among children with serious congenital or acquired diseases (1). Chronic diseases comprise a wide variety of conditions in childhood and are typically defined by two main criteria. The first is the duration of the disease, which is usually 3-12 months or permanent. The second is severity, indicated by limitations in age-appropriate activities, prolonged or recurrent hospitalizations, or the need for special care (2). The term "chronic health condition" refers to both diseases and disabilities within the context of children's developmental and behavioral functions (DBF), as affected by multiple factors, including age, duration, limitations in age-appropriate activities, visibility, progression, and physiological, psychological, and social characteristics. The World Health Organization has also introduced the International Classification of Functioning, Disability, and Health to identify chronic health conditions at the levels of body structures and functions, activities and limitations, and participation and restrictions, considering a variety of facilitating or limiting environmental factors (2,3).

Chronic conditions themselves have a significant impact on children and their families due to pain, caregiving responsibilities, and financial burdens. Concurrent effects of DBF pose additional challenges for affected children and their families. Children with chronic health conditions must cope with the disease itself and its impact on emotional, behavioral, and developmental functioning. Distress experienced by family members disturbs family functioning and influences an affected child's emotional state (4).

Chronic health conditions commonly originate from multiple integrated constitutional and psychosocial factors. Although most diseases have biological etiologies, such as metabolic or genetic abnormalities, some conditions reflect primarily environmental and social factors, such as lead poisoning or preventable home accidents. Psychosocial factors also affect the course and severity of chronic disease. Children living in poverty have difficulty accessing coordinated health care (1,2). Previous research has shown that children with special health care needs in low-income families have substantially higher unmet health needs than those in high-income families (5).

Community factors, as facilitators and barriers, also influence families' ability to normalize life while caring for a child with a chronic disease or disability and working toward independent living (6). Chronic stressors experienced by the affected child and family members may lead to conflicts; therefore, they develop many individual coping strategies to regulate their emotions and solve problems (7). Clinicians should consider the preferred coping strategy rather than ignore it. If coping repertoires are restricted or their adaptive mechanisms are poor, clinicians should know how to support them in coping with the disease (6-8).

Management of chronic health conditions in pediatric practice requires a holistic and systematic approach to achieve optimal developmental and health outcomes (4). Although there is a large body of literature on chronic diseases and the management of many chronic conditions, there is a need for more research on the holistic clinical management of these vulnerable groups to achieve optimal developmental potential (1,2,4). This paper aims to review developmental and behavioral effects, the hospitalization process, and the clinical management of chronic health conditions in children and provide specific recommendations.

Developmental and Behavioral Effects

The effect of chronic disease on the child's DBF depends on multiple, interrelated variables, including disease characteristics, such as whether it is congenital, as well as child, family, and social factors (2,4). For optimal health outcomes, clinicians should thoroughly understand the integrated factors that influence the DBF of children with chronic health conditions (Figure 1). The appropriate attitudes of parents and clinicians are of great importance to the development of positive outcomes in children during adaptation to the disease and treatment (9). Chronic health conditions are associated with a wide range of DBF problems (4,10). A national survey in the United States (US) conducted by the Centers for Disease Control and Prevention reported that parents of children with chronic health conditions were 2-30 times more likely to report attention-deficit/hyperactivity disorder, learning problems, and emotional and behavioral problems, with the highest rates among conditions involving the nervous or sensory systems (10).

Developmental Effects of Chronic Condition

Although development is a continuous, dynamic process, there are characteristic, age-specific developmental tasks, and chronic conditions may interfere with these tasks (2). The age at disease onset and the child's developmental stage particularly affect coping and adjustment (11). The more pervasive a chronic health condition, the more functioning is affected and the greater the challenge for the child and family. Progressive conditions pose significant challenges for family adaptation and expectations. Conditions with unpredictable courses are sources of chronic stress and maladjustment in the child and the caregivers. Conditions requiring frequent or prolonged hospitalization or isolation lead to parent-child attachment problems, unschooling, and difficulties with socialization and community participation. Children with a stable congenital condition, such as limb deficiency or hearing or vision deficits, commonly experience their condition as a difference rather than as a disease (2).

The factors that determine a child's reaction to a disease may be specific to the condition, treatment, family, and the child himself/herself; they interact with each other in a complex way (12). Developmental periods should be considered in order to understand the child's reactions to and understanding of the disease (9):

Infancy: The disease may adversely affect growth and pose caregiving challenges. The accompanying physical discomfort and changes in daily routines jeopardize the consistency and reliability of the baby's environment and undermine the development of basic trust (2,9).

Toddlerhood: They are prone to be more independent and curious, exploring their environment. Chronic diseases may delay the acquisition of developmental skills. The disease can create significant problems with parental competence and confidence, which may cause parents to exhibit overprotective or unfair attitudes that conflict with the toddler's or older child's increasing need for

Gazi Med J 2026;37(1):126-134

Çelen Yoldaş. Management of Chronic Diseases in Pediatric Practices
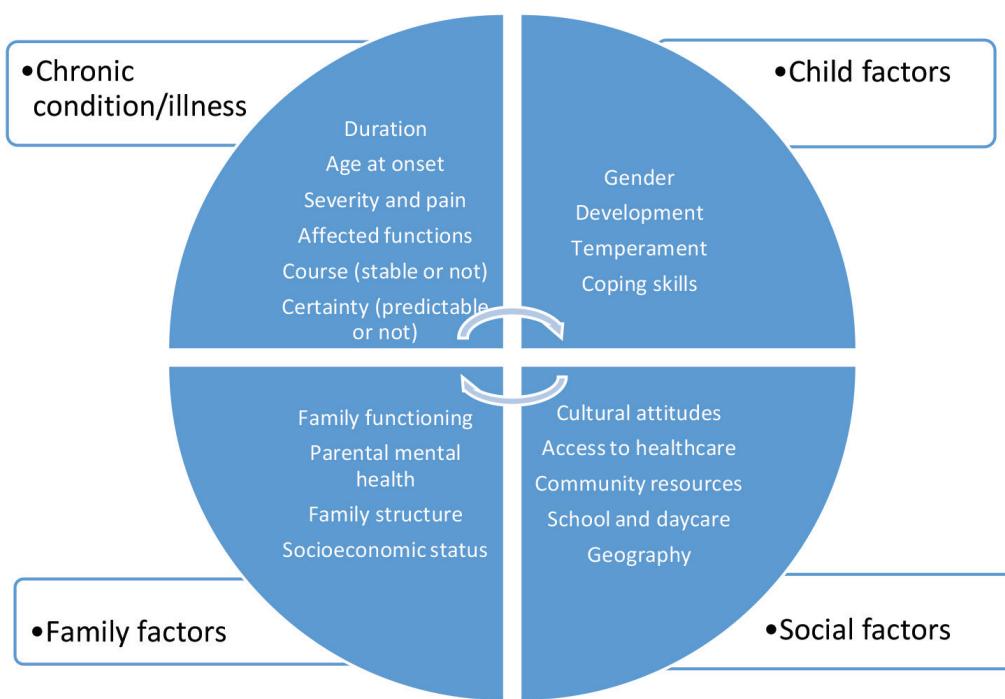
Figure 1. Integrated factors affecting the development and behavior of children with chronic health conditions.

independence, and these can undermine children's sense of self-control and autonomy (2,9).

Preschool period: Anxiety about separation from their parents and about physical harm is common. Egocentricity predominates, and they may perceive the disease as a consequence of bad behavior. Therefore, concerns about whether they will lose their parents' love or be separated from them take precedence over concerns about the name and nature of the disease. Distress may cause developmental regression in the child. The restrictions that parents impose on their children may make them fearful, passive, and dependent. Young children can reveal their feelings through behavior, play, or drawings (2,9).

School-aged children: Frequent absences due to the disease interfere with opportunities for learning and socialization. Children with physical differences must navigate peer acceptance while accepting their self-image. Restrictions due to disease or medical treatments cause fear of loss of control during this period. They can accept necessary procedures due to their increased comprehension and can describe specific complaints of their diseases. They may need to inquire about or discuss the condition. Therefore, brief and accurate information should be provided in an age-appropriate manner (2,9).

Adolescents: They must work to develop their identities and to maintain their educational and vocational goals while continuously managing their chronic condition. The limitations imposed by the chronic condition conflict with the increasing need for independence, which can negatively impact peer relationships and the development of secure sexual and physical identities. Gradual attainment of adult levels of disease understanding occurs during this period. Since many chronic diseases require dependence on caregivers, such

diseases are perceived as a loss of independence and a disruption of future plans. In addition, physical changes and disruption of school life constitute sources of psychological problems during this period. Informing adolescents about the disease and treatment, as well as sharing their feelings and thoughts, will help them adapt more readily (2,9).

Difficulties experienced by children with chronic diseases across different developmental periods are presented in Figure 2.

Importantly, chronic diseases may prevent the development of an appropriate individual identity in any child or adolescent. The presence of a disease may be more apparent than the presence of other individual characteristics. Adolescents themselves or clinicians often label those individuals as "diabetic" or "leukemic". Clinicians should use "people-first" language rather than "disease-first" language to encourage all involved (2).

Behavioral Effects of Chronic Condition

Community-based studies and meta-analyses commonly indicate an increased risk of behavioral and emotional problems in children with chronic conditions compared with healthy children, with an approximately twofold increase in risk (4,10). Overall adjustment problems, with increased rates of internalizing (anxiety, depression, withdrawal), externalizing (attention, hyperactivity, oppositional defiant disorder, conduct disorder), and low self-esteem, have been reported, regardless of the specific diagnosis (2). Parental adjustment is a determinant of the effect of chronic stress on the child. Many studies have shown a strong correlation between maternal mental health, particularly maternal depression and anxiety, and a child's emotional status (12-14). In a recent national study conducted among preschool children with chronic rheumatological diseases,

Gazi Med J 2026;37(1):126-134

Çelen Yoldaş. Management of Chronic Diseases in Pediatric Practices

Infancy/toddler	Preschool	School ages	Adolesants
•**Sense of trust** •Chronic disease/pain •Hospitalization and painful procedures •Changes in eating habits •Decreased growth •Restrictions in movement •Parent's sadness	•**Autonomy** •Need for adult supervision and control •Repeated separations •Restrictions on movement and diet •Decreased parental limit settings •Restrictions on social settings with peers	•**Sense of competence** •Need for adult supervision •Limited independence •Dependence on medical care •Medical and dietary needs •Activity restriction •School absence •Differences from peers	•**Identity development** •Need for medical supervision •Permanent dependency on parents •Changes in body appearance •Need for ongoing treatment or diet •Occupational limitations •Problems in sexuality

Figure 2. Difficulties of children with chronic diseases in different developmental periods.

maternal anxiety scores were positively associated with children's behavioral problems among those with familial mediterranean fever, a disease characterized by an unpredictable course. Internalizing problem scores were higher in children with chronic rheumatic diseases than in healthy children, suggesting the need for early childhood screening for developmental and behavioral problems to manage any chronic conditions (14).

The factors that positively affect the child's behavioral and emotional response to chronic disease are the following (12):

1) Dependence on family age-appropriately

2) Minimum need for secondary gains from the disease

3) Ability to withstand restrictions and responsibilities

4) Ability to develop satisfactory relaxing resources

Family Effects of Chronic Condition

The perception of the child as vulnerable is common among families who care for a child with a chronic health condition, and they usually act with varying degrees of protection, sometimes restricting the child's individual development (2). Each family develops their own coping strategies to adapt to the disease. Social and cultural factors influence their adaptation and are shaped by the context of family beliefs, myths, expectations, and roles (2,8,11).

Families whose child diagnosed with a chronic disease pass through a commonly predictable sequence of emotional reactions such as shock, denial, anger, stabilizing, and acceptance. However, these stages are not exclusive, crises may cause setbacks, and family members may go through different phases (12). Substantial hours of nursing care at home may affect family functioning, parenting attitudes, and individual independence. Although parents are generally willing to monitor their children's health, administer

medications, provide physical therapy, etc., they often report stress, fatigue, depression, and social isolation (7). Community-based studies have shown increased rates of mental health problems among parents, particularly high rates of depression or anxiety in mothers of children with chronic health conditions (13,15). Because caregiving tasks are usually attributed to mothers in families caring for a child with a chronic disease, mothers are less likely to work outside the home (12).

Parents also face economic burdens such as additional medical care costs, home environment requirements, transportation costs, and additional childcare needs. Lost income due to a parent's absence from work or missed career opportunities increase financial burden (16). Parents' economic problems may lead to marital tension. However, despite the stressful situations experienced by families caring for a child with a chronic disease, the frequency of divorce is no higher than that in the general population (17).

The parents' multiple tasks often limit the time available to siblings in families. Previous literature has yielded controversial results regarding sibling adjustment. Some have reported that living with a sibling who has chronic health conditions enhances maturity and skills and improves their resilience (18,19). Others have noted that siblings experience parental neglect, depressive symptoms, aggressive behavior, and academic failure (2,9,20). A recent meta-analysis has reported that siblings of children with chronic conditions have higher scores on depression rating scales compared with siblings of healthy children (20). Parental mental health and the family environment are the particular determinants of sibling adjustment. Clinical guidance emphasizes the importance of considering siblings and of encouraging a supportive family environment when caring for children with chronic diseases (18).

Gazi Med J 2026;37(1):126-134

Çelen Yoldaş. Management of Chronic Diseases in Pediatric Practices

Families need multidimensional social support to cope better with their chronic conditions. Effective community resources, such as advocacy groups and condition-specific societies, may help parents obtain information and tangible support, as well as foster a sense of worth. Clinicians should shift their focus from providing solely targeted treatment to fostering family partnership, given this population's complex needs within the individual's social context (2).

Recommendations for Management

Difficulties in DBF differ by the developmental age periods which should be considered to understand the reactions and comprehension of the disease of the child. Clinicians should know that all family members are affected by chronic conditions. Frequently encountered problems such as overprotective parental attitudes and non-compliance with the treatment process can be prevented by health personnel approaching the family and the child with open communication and understanding their needs, informing them about the disease or treatment, and also maintaining effective communication within the family. To minimize the adverse effects of the disease, the unmet needs of children and their families should be identified, supportive programs should be developed, and the quality and quantity of services provided to children and families, as well as research on these issues, should be increased.

Hospitalization Process

Hospitalization is a universally significant source of stress due to separation anxiety, disruption of daily routines, unfamiliarity with the environment and people, and pain and fear associated with the disease and its treatment (21,22).

Both the child and the family require planning for hospitalization to enhance their ability to adapt by reducing their anxiety during hospitalization (22). Some innovative programs, techniques, and approaches have been developed to help children and families cope more effectively with the stress associated with hospitalization (23). Educational interventions for siblings of hospitalized children are also beneficial (24).

Children's Reactions to Hospitalization

Emotional difficulties are greatest among children aged 6 months to 6 years and increase particularly if hospitalization is long or recurs frequently. Separation from parents and other important family members is difficult for children because of their physical, social, and cognitive immaturity and their close, dependent relationships with their parents. In older children, it is perceived as a loss of independence; in adolescents, as a disruption of plans for the future. Some react verbally, whereas others react behaviorally (22).

The suggestions for all age groups include performing treatments at home whenever possible, using day-care units, limiting invasive, painful procedures, providing information according to the child's developmental level before procedures, and minimizing hospitalizations. Parents may also experience anxiety and a loss of control when their children are hospitalized, potentially affecting their children's responses (9). The following techniques can be used to reduce the stress of both the child and the parents (9,22):

The Techniques to Minimize the Stress Associated with the Hospitalization

Before hospitalization:

• Provide general education about child health and diseases through media and schools.

• Provide pre-hospitalization tours, videos, and educational materials (e.g., brochures and coloring books).

• Include the child and parents in decisions and discussions about procedures and hospitalization.

During the hospitalization:

• Minimize the length and number of hospital stays.

• Encourage and facilitate the visits by family members and friends.

• Provide child-life programs (fun and therapeutic play) and hospital school programs.

• Ensure continuity of care and minimize changes in doctors, nurses, and other healthcare staff.

• Provide family-centered care, parents accompany and support the child.

• Provide pain control, a limited number of procedures, and maximal mobility.

• Support personal care and the child's sense of self-control.

• Encourage ongoing interest from the peer group.

Hospital structure:

• Cheerful and child-oriented decor

• Developmentally appropriate toys and objects, play spaces to support cognitive and emotional well-being

• Comfortable accommodation for parents to facilitate family-centered care

• Waiting areas for parents near the operating or recovery rooms to reduce anxiety

Developmental Supportive Approaches for Pediatric Patients During Hospitalization

In addition to the psychological stress caused by hospitalization, biological stress resulting from the effects of disease and treatment on the central nervous system may lead to negative developmental trajectories in hospitalized children (25). Both biological and psychological risk factors increase cortisol secretion. Long-term high cortisol levels affect the function of the nervous system and cause structural changes in brain regions related to learning and memory, thus negatively affecting development (26).

The patient- and family-centered care approach, therapeutic play, child life services, hospital schools and educational activities, and pain control are recommended to prevent or reduce the negative effects of hospitalization on child development (23).

Patient and Family Centered Care Approach: Within this approach, healthcare professionals collaborate with the family to make joint decisions regarding disease treatment and related health processes. Involving families in their children's medical interventions or postoperative care reduces anxiety among children and families, reduces the need for analgesics, and accelerates postoperative recovery (27). Although the family-centered approach is well known,

Gazi Med J 2026;37(1):126-134

Çelen Yoldaş. Management of Chronic Diseases in Pediatric Practices

its implementation is limited even in developed countries. In five years of national survey data from the US comprising responses from 36,675 parents of children with developmental or chronic health conditions, these parents were less likely to report that their healthcare provider always demonstrated the family-centered approach than parents whose children did not have any health conditions (28).

Therapeutic play: Play is vital for all children to cope more effectively with chronic stressful conditions. Through play, children re-enact daily life experiences and have the opportunity to participate in these experiences; thus, they reduce stress by developing a sense of internal control. Therapeutic play methods can transform the child's helpless and passive feelings into active feelings of control by creating scenarios in which anticipated sources of stress are managed (for example, by allowing the child to administer an injection to a doll). In these plays, the expression of feelings is encouraged, education about the hospital experience is provided, and physiological benefits are conferred (such as through the blow-out game to improve lung function) (29).

Child life services: Specially trained child life specialists provide an organized service known as "child life" in health centers in developed countries. These services aim to support child development through therapeutic play, educational activities, and other supportive activities during hospitalization (30).

Educational activities - Hospital schools: It is difficult for children with chronic diseases to attend school regularly due to long treatment periods and frequent hospitalizations. This restricts their opportunities for social development, disrupts school adaptation and success, and thus adversely affects children's developmental outcomes. Educational programs, called "hospital school programs", that follow the curriculum with professional teachers in hospitals have been initiated to support children's development during hospitalization in many countries (31).

Pain control: Management and treatment of pain should be the primary goal of pediatric care. Pain is a biological and psychosocial stressor that affects the development of hospitalized children. The perception of pain and its stress increase over time if adequate pain control is not provided. Children with chronic pain report higher levels of physical disability, anxiety, depression, and sleep problems as well as poorer academic performance and lower quality of life, compared with their peers (32).

Recommendations for Hospitalization

Clinicians should aim to promote optimal functioning in everyone involved in the process and to restore the family to normalcy as much as possible. Preparation for hospitalization is important for managing the condition. It is recommended that all family members involved in the process be informed about the disease, the evaluation, and the treatment. Information should be tailored to the developmental level of the child. Defenses such as denial and reflection should be expected. Open and sufficient communication establishes a sense of trust and competence in the child and the family, thereby increasing self-esteem, coping skills, and treatment adherence during hospitalization. The child should be allowed to express his/her feelings about the disease. What will be done should be explained before the procedures; however, it is necessary

to avoid unnecessary medical details and to be aware that anxiety and stress can impair the ability to understand what is heard. Many healthcare professionals underestimate young children's capabilities and do not attempt to communicate with them. It is also necessary to be available to listen to the child and family. Children whose parents have depression or anxiety and who receive less family support are considered at risk and should be referred to mental health services. The development of hospitalized children can be supported by reducing both biological and psychosocial stressors. The clinician's role during hospitalization is to minimize the distress and trauma while maximizing the benefits of care coordination (21).

Clinical Management of Chronic Health Conditions

The effective management of chronic conditions in children requires specific pediatric roles, including coordination of care, identification of DBF, assessment of family strengths, education about the disease, and school planning (2). Figure 3 presents the recommended pediatric management for children with chronic health conditions in clinical practice.

Coordination of Care

The medical home concept has been widely embraced as a primary care model for all children, initially to ensure coordinated care for those with chronic conditions. This model transforms the healthcare delivery system by avoiding fragmented care, overuse, or underuse; promoting interagency cooperation; alleviating stress for families;

Coordination of Care
- Preventive and medical care
- Chronic illness care, medical home model
- Collaborative care with other services and subspecialists

Identification of Developmental-Behavioral Functions
- Periodic assessment
- Monitoring and referral
- Supporting strategies

Assessment of Family Strengths and Difficulties
- Knowledge of family
- Social support
- Coping strategies
- Psychological status

Education about Illness
- Developmentally appropriate education
- Ongoing education
- Decision making

Planning for School Education
- Treatment plans
- Emergency plans
- Implications for participation in classes and outside activities
- Individual evaluation and support for education

Figure 3. Recommended clinical pediatric management of children with chronic health conditions.

Gazi Med J 2026;37(1):126-134

Çelen Yoldaş. Management of Chronic Diseases in Pediatric Practices

and ultimately improving outcomes such as health status, quality of life, and participation in school and the community. Following the registration of children with chronic health conditions, medical home providers, in addition to implementing standard medical care, provide children and families with access to educational materials and partner with families in decision-making, often in collaboration with other services and subspecialists (33).

Coordination of care entails developing an up-to-date family-centered care plan; helping the family learn about their child's care; facilitating access to needed services; establishing a network that connects all care providers, including social and educational services; and helping resolve conflicts among all parties. Social and emotional support for the family is also an integral part of care (34). Families usually need care coordination during the first year after diagnosis, during the adaptation process at discharge, and during particular transitional periods, such as schooling or transition to adulthood. They usually feel more competent in managing their child's needs and services as they acquire experience over time (11).

Identification of Developmental and Behavioral Functions

Children with chronic health conditions and their families require a wide range of services to meet their special needs. Through periodic assessments, clinicians can inform families about or help families access preventive mental health care, appropriate home nursing, educational and social services, and other specialized therapies (34). Healthy siblings of children with chronic health conditions are also at risk; therefore, the needs of other family members should be considered. Clinicians should ensure that all family members receive developmental monitoring and health supervision to prevent, identify, and manage the risks (27). Because of the high cost of health care for many chronic conditions, clinicians should also be familiar with both private and public referral sources in their region (33,34).

The clinician should be aware of the problems associated with DBF in children with chronic conditions and assess functioning and the need for referral (4,10). Developmentally supportive strategies should be discussed with families at every opportunity (14). Although most clinicians are willing to identify DBF in their patients with chronic conditions, they face multiple barriers, including a lack of time, training, and resources for referral. Therefore, a high proportion of children and families have unidentified developmental, behavioral, and mental health needs (35).

Assessment of Family Strengths and Difficulties

Clinicians should identify families' knowledge, social support, and coping strategies; help them increase support, if necessary; recognize difficulties and unmet needs; and strengthen skills for coping with and nurturing their child. If coping strategies are inadequate, clinicians should direct them toward strategies such as empowerment, self-management skills, and task sharing to help them cope with their diseases. Additionally, clinicians should be sensitive to maternal depression and marital dysfunction and know how to identify these problems and provide referrals when necessary. Telehealth, respite care, socio-emotional support, insurance and employment benefits, and parenting support are promising approaches to reduce stress and improve parental health and well-being in the clinical management of chronic health conditions. Parents are likely to

benefit from interventions tailored to their needs at different time points along their child's chronic disease trajectory (36).

Education about disease

Patient education is a key component of patient engagement, supporting them in managing their lives with chronic conditions. Structured educational programs enhance knowledge, self-management skills, and autonomy. In a scoping review on children, patient education was found to be beneficial in terms of decreased use of emergency care, hospitalizations, and visits to general practitioners, as well as fewer missed school days (37). Education about the disease and treatment should be given according to the developmental level of the child and the comprehension abilities of the parent. Education for the child is a continuing process as the child develops cognitively. On the other hand, families may receive much confusing information from different providers; clinicians can clarify knowledge for the families. Clinicians should communicate effectively with families and other providers and remain current on the related health condition (27).

Partnership in decision-making has expanded tremendously during the last decades. Parents accept more responsibilities in care now. Through the transition to adulthood, children take more responsibility to learn self-management of their chronic condition. When children and adolescents are actively involved in decision-making in their health care, they are usually better informed, thereby facilitating and benefiting the work of the health professionals (38).

Planning for School Education

Many children with chronic health conditions need satisfactory planning for school education. Due to school being the main workplace of children, clinicians should consider the school requirements. Some families need the support of their doctors to adjust school needs for their children. Some children need special education services because of the impact of their diseases on social and cognitive development. Some children with chronic health conditions cannot participate in standard education curriculums, requiring modifications of school days or class environment. Some require planning for medication or emergency care at school. School staff often need education about the disease and the necessity and results of schooling in the context of chronic conditions. Clinicians should work in collaboration with schools and families to ensure the best school placement (2).

CONCLUSION

Chronic health conditions both affect and are affected by DBF in children. Clinicians should know that all family members are affected by chronic conditions. Therefore, the unmet needs of children and their families should be determined, and supportive approaches should be implemented during illness and hospitalization. Specific pediatric roles, such as coordination of care, identification of DBF, assessment of family strengths, education about the disease, and school education planning, should be integrated into standard pediatric care for effective management of chronic conditions in children. Given the complexity of managing chronic health conditions for children and their families, holistic pediatric involvement with interdisciplinary collaboration and care coordination is necessary.

Gazi Med J 2026;37(1):126-134

Çelen Yoldaş. Management of Chronic Diseases in Pediatric Practices

REFERENCES

1. van der Lee JH, Mokkink LB, Grootenhuis MA, Heymans HS, Offringa M. Definitions and measurement of chronic health conditions in childhood: a systematic review. JAMA. 2007; 297: 2741–51.

2. Thyen U, Perrin JM. Chronic health conditions. In: Carey WB, Crocker AC, Elias ER, Feldman HM, Coleman WL, editors. Developmental and Behavioral Pediatrics. 4th ed. Philadelphia: Saunders Elsevier; 2009. Available from: https://www.elsevier.com/books/developmental-and-behavioral-pediatrics/9781416033707.

3. World Health Organization. International classification of functioning, disability and health: ICF. Geneva: World Health Organization; 2001. Available from: https://www.who.int/standards/classifications/international-classification-of-functioning-disability-and-health.

4. Blackman JA, Gurka MJ, Gurka KK, Oliver MN. Emotional, developmental and behavioural co-morbidities of children with chronic health conditions. J Paediatr Child Health. 2011; 47: 742–7.

5. van Dyck PC, Kogan MD, McPherson MG, Weissman GR, Newacheck PW. Prevalence and characteristics of children with special health care needs. Arch Pediatr Adolesc Med. 2004; 158: 884–90.

6. Macdonald M, Lang A, Savage E, Chappe V, Murphy A, Gosse F, et al. Working to have a normal life with cystic fibrosis in an adherence-driven health care system. Respir Care. 2019; 64: 945–52.

7. Smith S, Tallon M, Clark C, Jones L, Morelius E. "You never exhale fully because you're not sure what's next": parents' experiences of stress caring for children with chronic conditions. Front Pediatr. 2022; 10: 902655.

8. Rinaldi Carpenter D, Narsavage GL. One breath at a time: living with cystic fibrosis. J Pediatr Nurs. 2004; 19: 25–32.

9. Özmert EN. Gelişimsel pediatri. In: Yurdakök M, editor. Yurdakök Pediatri. Ankara: Güneş Tıp Kitabevi; 2017. Available from: https://www.guneskitabevi.com/yurdakok-pediatri.

10. Blackman JA, Conaway MR. Developmental, emotional and behavioral co-morbidities across the chronic health condition spectrum. J Pediatr Rehabil Med. 2013; 6: 63–71.

11. Tluczek A, Grob R, Warne E, Van Gorp S, Greene L, Homa K. Parenting children with cystic fibrosis: developmental acquisition of expertise. J Dev Behav Pediatr. 2022; 43: 463–72.

12. İnal N, Pekcanlar A. Chronic illness, hospitalization and child. DEÜ Tıp Fakültesi Dergisi. 2008;22(2):99–105. Available from: https://dergipark.org.tr/en/pub/deutipfak/issue/4683/64162.

13. Fraser LK, Murtagh FE, Aldridge J, Sheldon T, Gilbody S, Hewitt C. Health of mothers of children with a life-limiting condition: a comparative cohort study. Arch Dis Child. 2021; 106: 987–93.

14. Çelen Yoldaş T, Özdel S, Karakaya J, Bülbül M. Developmental and behavioral problems of preschool-age children with chronic rheumatic diseases. J Dev Behav Pediatr. 2022; 43: e162–9.

15. Barker MM, Beresford B, Fraser LK. Incidence of anxiety and depression in children and young people with life-limiting conditions. Pediatr Res. 2023; 93: 2081–90.

16. Fitzgerald C, George S, Somerville R, Linnane B, Fitzpatrick P. Caregiver burden of parents of young children with cystic fibrosis. J Cyst Fibros. 2018; 17: 125–31.

17. Sabbeth BF, Leventhal JM. Marital adjustment to chronic childhood illness: a critique of the literature. Pediatrics. 1984; 73: 762–8.

18. Deavin A, Greasley P, Dixon C. Children's perspectives on living with a sibling with a chronic illness. Pediatrics. 2018; 142: e20174151.

19. Woodgate RL, Edwards M, Ripat JD, Rempel G, Johnson SF. Siblings of children with complex care needs: their perspectives and experiences of participating in everyday life. Child Care Health Dev. 2016; 42: 504–12.

20. Martinez B, Pechlivanoglou P, Meng D, Traubici B, Mahood Q, Korczak D, et al. Clinical health outcomes of siblings of children with chronic conditions: a systematic review and meta-analysis. J Pediatr. 2022; 250: 83–92.

21. Rauch DA; Committee on Hospital Care; Section on Hospital Medicine. Physician's role in coordinating care of hospitalized children. Pediatrics. 2018; 142: e20181503.

22. Perrin EC, Shipman D. Hospitalization, surgery, and medical and dental procedures. In: Carey WB, Crocker AC, Elias ER, Feldman HM, Coleman WL, editors. Developmental and Behavioral Pediatrics. 4th ed. Philadelphia: Saunders Elsevier; 2009. Available from: https://www.elsevier.com/books/developmental-and-behavioral-pediatrics/9781416033707.

23. Atay G, Eras Z, Ertem İ. Developmental support of children during their hospitalizations. J Child. 2011; 11: 1–4.

24. Gursky B. The effect of educational interventions with siblings of hospitalized children. J Dev Behav Pediatr. 2007; 28: 392–8.

25. Armstrong FD. Neurodevelopment and chronic illness: mechanisms of disease and treatment. Ment Retard Dev Disabil Res Rev. 2006; 12: 168–73.

26. Mueller SC, Maheu FS, Dozier M, Peloso E, Mandell D, Leibenluft E, et al. Early-life stress is associated with impairment in cognitive control in adolescence: an fMRI study. Neuropsychologia. 2010; 48: 3037–44.

27. Committee on Hospital Care; Institute for Patient- and Family-Centered Care. Patient- and family-centered care and the pediatrician's role. Pediatrics. 2012; 129: 394–404.

28. Brannon GE, Ray MR, Lark P, Kindratt TB. Influence of pediatric patients' developmental or chronic health condition status as a predictor of parents' perceptions of patient- and family-centered care. Health Commun. 2022; 37: 880–8.

29. Nijhof SL, Vinkers CH, van Geelen SM, Duijff SN, Achterberg EJM, van der Net J, et al. Healthy play, better coping: the importance of play for the development of children in health and disease. Neurosci Biobehav Rev. 2018; 95: 421–9.

30. Romito B, Jewell J, Jackson M; AAP Committee on hospital care; association of child life professionals. Child life services. Pediatrics. 2021; 147: e2020040261.

31. Caggiano G, Brunetti LIG, Ho K, Piovani A, Quaranta A. Hospital school program: the right to education for long-term care children. Int J Environ Res Public Health. 2021; 18: 11435.

32. World Health Organization. WHO issues new guidelines on the management of chronic pain in children. Geneva: World Health Organization; 2021. Available from: https://www.who.int/news/item/01-02-2021-who-issues-new-guidelines-on-the-management-of-chronic-pain-in-children

33. Lerner CF, Klitzner TS. The medical home at 50: are children with medical complexity the key to proving its value? Acad Pediatr. 2017; 17: 581–8.

34. Council on Children with Disabilities; Medical Home Implementation Project Advisory Committee. Patient- and family-centered care coordination: a framework for integrating care for children and youth across multiple systems. Pediatrics. 2014; 133: e1451–60.

35. Rhodes A, Sciberras E, Oberklaid F, South M, Davies S, Efron D. Unmet developmental, behavioral, and psychosocial needs in

Gazi Med J 2026;37(1):126-134

Çelen Yoldaş. Management of Chronic Diseases in Pediatric Practices

children attending pediatric outpatient clinics. J Dev Behav Pediatr. 2012; 33: 469–78.

36. Bradshaw S, Bem D, Shaw K, Taylor B, Chiswell C, Salama M, et al. Improving health, wellbeing and parenting skills in parents of children with special health care needs and medical complexity - a scoping review. BMC Pediatr. 2019; 19: 301.

37. Stenberg U, Haaland-Øverby M, Koricho AT, Trollvik A, Kristoffersen LR, Dybvig S, et al. How can we support children, adolescents and young adults in managing chronic health challenges? A scoping review on the effects of patient education interventions. Health Expect. 2019; 22: 849–62.

38. Quaye AA, Coyne I, Söderbäck M, Hallström IK. Children's active participation in decision-making processes during hospitalisation: an observational study. J Clin Nurs. 2019; 28: 4525–37.

Leptin as a Biomarker of Cancer Prognosis: A Friend of Colorectal Cancer

Kanser Prognozunun Biyobelirteci Olarak Leptin: Kolorektal Kanserin Bir Dostu

Elisha Apatewen Akanbong[1], Ali Şenol[2], Özkan Duru[2], Miyase Çınar[2], Haceli Öcal[2]

[1]Department of Veterinary Biochemistry, Kırıkkale University Institute of Health Sciences, Kırıkkale, Türkiye
[2]Department of Veterinary Biochemistry, Kırıkkale University Faculty of Veterinary Medicine, Kırıkkale, Türkiye

ABSTRACT

This review aims to evaluate the role of the peptide hormone leptin in the initiation and progression of cancer, with a particular focus on colorectal cancer (CRC). A comprehensive literature search was conducted in Google Scholar and PubMed databases to identify relevant studies published from 2020 and 2025. Articles investigating the influence of leptin and its receptors on cancer development and progression, particularly in CRC, were included without language restrictions. This review highlights that leptin promotes cancer progression by abrogating the efficacy of chemotherapeutic agents. Additionally, across the reviewed articles, some studies reported no causal relationship no statistically significant association between leptin and CRC. Although some articles report that leptin and its receptor have no association with the development and progression of cancer, the majority of articles implicate leptin in the development and progression of cancer, mainly in CRC. Due to these discrepancies, there is an urgent need for additional studies employing meticulously designed, standardized methodologies and rigorous control measures to annihilate potential confounding factors. These conflicting findings may be explained by differences in study designs and confounding factors, such as obesity. Obesity is a major risk factor for various forms of cancer and can trigger CRC by causing cellular changes such as mitochondrial dysfunction. In such cases, increased leptin levels may not directly mean that leptin causes CRC. Although evidence suggests a potential role for leptin in the development and progression of CRC, inconsistencies in the literature underscore the need for further research. Future studies should employ standardized methodologies and rigorous control for confounders to clarify leptin's mechanistic and clinical relevance in colorectal carcinogenesis.

Keywords: Leptin, leptin and colorectal cancer, leptin and cancer, leptin and anticancer agents, colorectal cancer

ÖZ

Bu derleme, peptit hormonu leptinin kanserin başlaması ve ilerlemesindeki rolünü, özellikle kolorektal kanser (CRC) üzerinde yoğunlaşarak değerlendirmeyi amaçlamaktadır. 2020 ve 2025 yılları arasında yayınlanmış ilgili çalışmaları belirlemek için Google Akademik ve PubMed veri tabanları kullanılarak kapsamlı bir literatür araştırması yürütülmüştür. Leptinin ve reseptörlerinin kanser gelişimi ve ilerlemesi, özellikle de CRC üzerindeki etkisini araştıran makaleler dil kısıtlaması olmaksızın dahil edilmiştir. Bu derleme makalesi, leptinin kemoterapötik ajanların etkinliğini ortadan kaldırarak kanser ilerlemesini desteklediğini vurgulamaktadır. Ayrıca, incelenen makalelerden bazı çalışmalar leptin ve CRC arasında nedensel bir korelasyon olmadığını ve leptin ve CRC arasında istatistiksel olarak anlamlı bir ilişki olmadığını bildirmiştir. Bazı makaleler leptinin ve reseptörünün kanser gelişimi ve ilerlemesi ile bir ilişkisi olmadığını bildirmesine rağmen, makalelerin çoğu leptinin kanser gelişimi ve ilerlemesinde, özellikle CRC'de rol oynadığını belirtmektedir. Bu tutarsızlıklar nedeniyle, potansiyel karıştırıcı faktörleri ortadan kaldırmak için daha titizlikle tasarlanmış standartlaştırılmış metodolojiler ve titiz kontrol önlemleri içeren daha fazla çalışmaya acil ihtiyaç vardır. Bu çelişkili bulgular, çalışma tasarımlarındaki farklılıklar ve obezite gibi karıştırıcı faktörlerin varlığı ile açıklanabilir. Obezite, çeşitli kanser türleri için önemli bir risk faktörüdür ve mitokondriyal disfonksiyon gibi hücresel değişikliklere neden olarak CRC'yi tetikleyebilir. Bu gibi durumlarda, artan leptin seviyeleri doğrudan leptinin CRC'ye neden olduğu anlamına gelmeyebilir. Kanıtlar, CRC'nin gelişimi ve ilerlemesinde leptinin potansiyel bir rolü olduğunu gösterse de, literatürdeki tutarsızlıklar daha fazla araştırmaya ihtiyaç olduğunu vurgulamaktadır. Gelecekteki çalışmalar, leptinin kolorektal karsinogenezdeki mekanistik ve klinik önemini açıklığa kavuşturmak için standartlaştırılmış metodolojiler ve karıştırıcı faktörlerin titiz kontrolünü kullanmalıdır.

Anahtar Sözcükler: Leptin, leptin ve kolorektal kanser, leptin ve kanser, leptin ve kanser önleyici ilaçlar, kolorektal kanser

Gazi Med J 2026;37(1):135-140

Akanbong et al. Leptin as a Prognostic Biomarker in Colorectal Cancer

INTRODUCTION

Leptin, a 16 kDa peptide hormone composed of 167 amino acids and expressed mainly by adipocytes, was discovered in 1994 in leptin-deficient (ob/ob) and leptin receptor-deficient (db/db) mice. This hormone, which was later referred to as a product of the *obese (ob)* gene in vertebrates, shows structural differences in its primary amino acid sequence, but secondary and tertiary structures are the same and similar to the long-chain helical cytokines, including interleukin (IL) 6, IL-11, and IL-12 (1). The leptin hormone plays a crucial role in regulating body weight and energy expenditure. Circulating leptin levels reflect the amount of energy stored in adipose tissue and correlate with the occurrence and degree of obesity. In other words, a higher circulating leptin level indicates greater energy storage (Figure 1) (2). Although it is expressed primarily in adipose tissue, it has also been found in other tissues, such as muscle, the brain, and the gastrointestinal system. Its expression is regulated by IL-1β during inflammation, insulin, and cortisol (1).

Aside from the pivotal role of leptin in obesity by regulating food intake and basal metabolism, its influence extends to various tissues and systems, including its interactions with the immune system and implications for cancer initiation and progression. The hormone leptin has been implicated in the initiation and progression of many types of cancer. However, evidence has suggested that leptin has a beneficial and possibly antitumoral role. The first anticancer effect of leptin treatment in human cancer cell lines was reported in the Michigan Adenocarcinoma Pancreatic Cancer-2 and Pancreatic Carcinoma-1 pancreatic cancer cell lines. Low serum leptin levels have been correlated with pancreatic cancer, and high expression of leptin has been associated with better survival in patients with colorectal cancer (CRC) (1). Nonetheless, due to the paradoxical effect of leptin, pre-exposure of colon cancer cells to leptin inhibited tumour necrosis factor alpha (TNF-α)-induced apoptosis. However, its knockdown enhanced TNF-α-induced apoptosis by upregulating the p53-upregulated modulator of apoptosis (PUMA). That is, the expression of functional leptin and/or leptin receptors inhibits TNF-α-induced apoptosis in colon cancer cells (3). Excessive systemic and pulmonary leptin levels have also been linked to an increased risk of lung cancer (4).

Since leptin is produced in adipose tissue, understanding its relationship with adipose tissue mass is essential for exploring its potential correlation with the risk of colon cancer (3). With more than 1 million new cases diagnosed annually, CRC is the third most prevalent cancer in men, the second most prevalent cancer in women, and the primary cause of cancer-related mortality (5). While its risk factors include germline mutations, alcohol, and tobacco, obesity is also a significant risk factor for CRC (3). Considering the role of leptin in the initiation and progression of cancer, as well as its significant impact in mitigating obesity, a primary risk factor for colon cancer, this review aims to determine whether leptin is a friend or foe of colon cancer by examining publications from 2020 to date using Google Scholar and PubMed databases.

Literature Search

This review was conducted by searching the Google Scholar and PubMed electronic databases for relevant literature using keywords such as leptin, colon cancer, leptin and colon cancer, and leptin and cancer. Of the articles obtained, only those published in 2020 or later were considered in this work. Considering the topics discussed in this review, Research articles, meta-analyses, and reviews that did not pertain to the topics of this review were considered irrelevant and excluded from the study. No language limitation was applied in the literature search. Moreover, the reference lists of review papers were further searched to identify potentially more relevant research articles.

Leptin and Cancer

Leptin exhibits proliferative activity in tumour cells of various cancer types (Figure 2), such as breast, gastric, endometrial, and prostate cancers. In vitro experiments have shown that leptin, through the phosphoinositide 3-kinase/protein kinase B (PI3K/AKT), janus kinase/signal transducer and activator of transcription 3 (JAK/STAT3), and extracellular signal-regulated kinase 1 and 2 (ERK1/2) signalling pathways, can exert its proliferative effect in cancer cells (7). Leptin does not influence carcinogenesis via proliferation alone; it may also influence carcinogenesis by suppressing apoptosis in cancer cells. This may be achieved by upregulating the expression of anti-apoptotic genes such as B-cell lymphoma-x-long, B-cell lymphoma 2, and survivin. According to Ayed et al. (7), leptin has been reported to reduce apoptosis in cancer cells by inhibiting the expression of many pro-apoptotic genes, including TNFR1, FADD, Caspase 3, 6, 7, 9, and 10, CAD, ICAD, BAX, BAD, BAK1, BID, BOK, APAF1, TRAF-interacting protein, TRAIL, IGF1R, and TRADD.
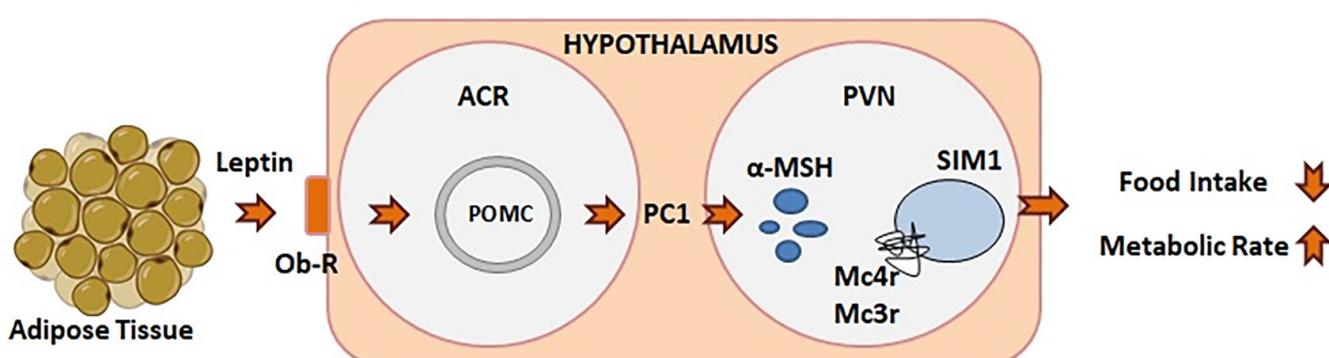

Figure 1. Adipose tissue responds to higher energy levels by producing leptin. This was adapted from Reference 6.

Gazi Med J 2026;37(1):135-140

Akanbong et al. Leptin as a Prognostic Biomarker in Colorectal Cancer
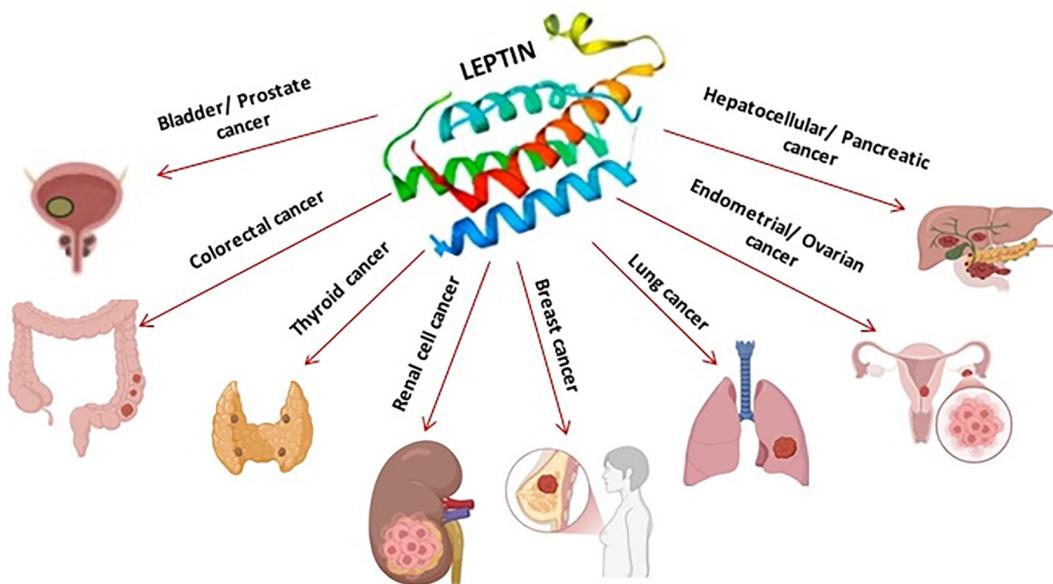
Figure 2. Leptin is associated with various types of tumours. This was adapted from Reference 1.

Chronically elevated leptin levels (hyperleptinemia), characteristic of obesity, may increase cancer susceptibility and progression, as the antitumor immune response is impaired in such cases. For instance, it may result in complete paralysis of the cellular metabolism and cytotoxic machinery in natural killer cells, driven by lipid accumulation (7).

Leptin and Breast Cancer

Studies on leptin and cancer have shown that leptin is involved in the occurrence and progression of breast cancer. Leptin and its receptor can be used in the diagnosis and prognosis of breast cancer (8). According to Ayed et al. (7), leptin promotes cell cycle progression in cancer cells by upregulating the cell cycle progression genes CCND1, CCNA2, PCNA, and E2F3, and downregulating the cell cycle inhibitor genes p21WAF1/CIP1, p27KIP1, and GADD45A. Leptin enhances fatty acid synthesis and oxidation in oestrogen receptor-positive breast cancer cells. These metabolic changes, which are necessary for leptin-stimulated tumour growth, are caused by activation of autophagy and of the sterol regulatory element-binding protein 1 (9).

Leptin and Gastric Cancer

Leptin facilitates the metastasis and invasion of cancer cells. In a previous study, leptin induced migration and invasion of gastric cancer cells by activating AKT and andextracellular ERK pathways and upregulating vascular endothelial growth factor (10).

Leptin and Endometrial Cancer

Endometrial cancer is not excluded from the influence of leptin. Leptin plays a role in invasion and distant metastasis of endometrial cancer and, in fact, is responsible for its proliferation (11). In a study conducted among 30 endometrial cancer patients, it was reported that leptin and its receptors were overexpressed and that the elevated levels of leptin and its receptors were the potential reason for the progression of endometrial cancer (12).

Leptin and Prostate Cancer

The expressions of leptin and its receptors could also serve as potential biomarkers for assessing the risk and severity of prostate cancer. In a study, it was reported that leptin and its receptors were overexpressed in patients with prostate cancer, with higher expression in the severe and metastatic group than in patients with confined tumours (13).

Leptin and Gall bladder Cancer

Exosomes derived from gallbladder cancer cells have been shown to polarize macrophages toward the M2 phenotype via activation of the STAT pathway. The study also reported that leptin was present in exosomes produced by gallbladder cancer cells and that increased leptin levels facilitated the invasion and migration of gallbladder cancer cells. The researchers indicated that blocking leptin reduces the polarization effect (14).

Leptin and Anticancer Drugs

In a study, a drug was designed, and its anticancer and cytotoxic effects were evaluated. According to the researchers, the drug suppressed the expression of leptin and its receptor genes and could significantly increase the efficiency of targeted drug delivery in cancer treatment (4). Increasing evidence suggests that obesity, aside from being a major predisposing factor for cancer, is associated with resistance to anticancer chemotherapy, and this is probably driven by leptin. Inferring from obesity's role in chemoresistance, recent studies have further reported on leptin's specific roles in various cancers. Ayed et al. (7) reported that a study found patients with pancreatic adenocarcinoma who did not respond to gemcitabine-based chemotherapy had significantly higher serum leptin levels compared to those who were responsive. This lack of responsiveness to chemotherapy may be linked to elevated leptin levels, which are associated with obesity.

Gazi Med J 2026;37(1):135-140

Akanbong et al. Leptin as a Prognostic Biomarker in Colorectal Cancer

A study investigating survival and chemoresistance in patients with estrogen-receptor-negative breast cancer reported that the expression of the leptin receptor and leptin-targeted genes is associated with poorer survival. In addition, increased expression of these genes (*ABCB1, WNT4, ADHFE1, TBC1D3, LL22NC03, RDH5*, and *ITGB3*), which are chemoresistance-related genes, was associated with tumorigenesis and chemotherapeutic failure. Thus, targeting leptin receptor signalling during chemotherapy could improve chemotherapeutic efficacy (15), and this has been demonstrated in a study in which metformin and silibinin synergistically suppressed lung cancer growth, possibly through regulation of the gene expression of leptin and its receptor. In the study, the synergistic effect of metformin and silibinin considerably reduced the expression of leptin and of its receptor gene, thereby providing a more promising and safer treatment strategy for cancer, especially lung cancer (16).

In addition, leptin's influence on chemoresistance in mesenchymal cells has been demonstrated in a study in which a leptin-conditioned medium from human mesenchymal cells promoted resistance to cisplatin in cultured human osteosarcoma cells. According to the study, leptin upregulated transforming growth factor-β (TGF-β) expression in mesenchymal cells, an effect that was suppressed by knockdown of the leptin receptor. The suppression of TGF-β expression in the mesenchymal cells due to leptin receptor knockdown also ameliorated the chemoresistance of osteosarcoma cells to cisplatin (17). Additionally, leptin has been suggested to influence the growth and drug resistance of cancer cells; however, its mechanism by which it induces drug resistance in gallbladder cancer cells has not been fully elucidated. Given this, leptin-induced drug resistance in gallbladder cancer cells was investigated in vivo. The study found that leptin reduced the efficacy of gemcitabine by activating myeloid cell leukaemia 1 (MCL-1), thereby promoting resistance to gemcitabine. Upon treatment with leptin, a chain reaction was observed in which activated pSTAT3, in turn, activated the transcription factor CEBPD, which subsequently increased MCL1 levels, thereby contributing to drug resistance in gallbladder cancer cells. In other words, targeting the pSTAT3/CEBPD/MCL1 axis could help improve the efficacy of gemcitabine in cancer patients, specifically gallbladder cancer patients (18). Leptin increases AXL expression by inhibiting the AMPK pathway, thereby increasing activation and nuclear translocation of yes-associated protein. This process ultimately increased resistance to the chemotherapy drug 5-fluorouracil (5-FU) in the CRC tumours from mice fed a high-fat diet. However, when leptin levels were neutralised, the sensitivity of CRC tumours to 5-FU was restored (19). This further demonstrates leptin's interference with chemotherapy in favour of cancer cells.

Overall, the gene expression of leptin and its receptor could affect the success of cancer therapy by promoting drug resistance or reducing the efficacy of therapeutic agents. The reviewed studies consistently demonstrate that leptin contributes to chemoresistance in various cancers by affecting gene expression and signalling pathways. Therefore, targeting either these leptin-mediated mechanisms or leptin and its receptor gene expression could enhance chemotherapy outcomes.

Leptin and Colon Cancer

Leptin's Influence and Biochemical Mechanisms in Colorectal Cancer

CRC is associated with obesity, and available data suggest that CRC is positively correlated with many factors, including metabolic syndrome and serum leptin levels (1,20). Leptin is thought to be involved in the development and progression of CRC (21). Some studies have reported no association between circulating or high serum leptin levels and CRC (1,18). The majority of studies have reported that the overexpression of leptin and its receptor is correlated with tumour progression (1,22,23). Colectomy has been reported to decrease serum leptin levels, supporting the correlation between leptin and CRC. Thus, targeting leptin and its receptor is essential for the prevention and treatment of CRC (1).

Singh et al. (3) also demonstrated that TNF-α induces p53-independent apoptosis of colon cancer cells through the upregulation of PUMA. However, pre-exposure of the colon cancer cells to leptin inhibited TNF-α–induced PUMA. In other words, it can be inferred that leptin promotes the growth of colon cancer cells by inhibiting apoptosis. Because of leptin's mitogenic, antiapoptotic, and tumorigenic effects, significantly higher leptin levels observed in 32 CRC patients were associated with an increased risk of CRC (23). In addition, leptin was considered a candidate gene for further analysis after assessing The Cancer Genome Atlas (TCGA) to identify expressed genes with prognostic value in CRC. The researchers then investigated its expression in 206 CRC patients without liver metastasis and 201 CRC patients with liver metastasis. Based on TCGA data, they concluded that leptin overexpression indicates a poorer overall survival prognosis in CRC patients. It was also reported that leptin expression is significantly correlated with the stage of metastasis and is a valuable marker for predicting outcomes in CRC patients (22). Erkasap et al. (24) noted that leptin could play a significant role in the initiation and/or development of CRC. Their research revealed significantly increased mRNA expression of leptin, its receptor, Notch, and IL-1 in human CRC specimens.

Leptin may also contribute to the survival and progression of CRC by reducing the efficacy of colorectal anticancer drugs. Leptin, by inhibiting the AMPK pathway, increased AXL expression, subsequently increasing YAP activation and nuclear translocation, culminating in increased resistance to 5-FU in CRC cells in high-fat-fed mice; when leptin levels were neutralised, the sensitivity of CRC cells to the chemotherapy drug 5-FU was restored (19). This illustrates the chemoresistant and antiapoptotic nature of leptin in promoting CRC cell survival.

CRC Therapeutic Approaches

Due to leptin's role in CRC progression, there is a critical need for interventions, and this could be addressed by leveraging its relevance. To further demonstrate that leptin and its receptors are essential in the development and progression of CRC and play a role in CRC chemoresistance, leptin's unique ability to target its receptor was leveraged to enhance drug delivery in CRC. PEGylated liposomal doxorubicin was functionalized with a leptin-derived peptide (Lp31), resulting in improved uptake and cytotoxicity in C26 colon cancer cells. The study found that doxorubicin inhibited tumour growth in a

Gazi Med J 2026;37(1):135-140

Akanbong et al. Leptin as a Prognostic Biomarker in Colorectal Cancer

concentration-dependent manner (25). Similarly, the leptin-derived peptide was used to suppress tumour growth in a tumour-bearing mouse model of colon carcinoma (26). The suppression of tumour growth and angiogenesis, promotion of apoptosis, in a human colon cancer cell subcutaneous xenograft mouse model by Weichang'an Formula, a traditional Chinese medicine (herbal preparation), through decreased leptin mRNA expression, was attributed to leptin/STAT3 signal transduction (27).

Epidemiological Evidence

Epidemiologically, studies exploring a related factor, such as adipose tissue, have reported that adipose tissue mass, especially visceral adipose tissue mass, is directly correlated with the risk of colon adenoma and cancer. In the case of excess adipose tissue mass (obesity), the functional roles of adipose tissue are disrupted, which could cause inflammation and altered secretion of pro- and anti-inflammatory cytokines. Additionally, excess adipose tissue mass leads to increased levels of leptin, which have been associated with an increased risk of colon cancer (3).

Contrasting Views and Future Directions

Although leptin is implicated and reported to be essential in CRC progression, a case-control study involving 955 CRC patients, 497 colon adenoma patients, and 911 healthy individuals that investigated the causal association between circulating leptin levels and the risk of colon adenoma, CRC, and the progression of colon adenoma to CRC reported otherwise. According to the case-control study, circulating leptin levels probably correlate with the risk of colon adenoma, CRC, and progression from colon adenoma to CRC. However, the Mendelian randomisation analysis found no evidence of a causal association between circulating leptin levels and the risk of colon adenoma, CRC, and progression from colon adenoma to CRC (28). The expression levels of leptin and its receptor were evaluated in 46 healthy individuals and 44 CRC patients. No statistically significant differences were observed between the normal group and the CRC group in the expression of leptin and its receptor. Thus, leptin and its receptor would not be useful biomarkers for CRC. However, according to the study, the CRC cases showed an insignificantly higher expression of the leptin receptor (29).

Overall, leptin and its receptors are involved in the initiation and progression of CRC. However, investigating the mRNA expression of leptin and its receptor within in vivo CRC-induced model-based studies, independent of obesity, would provide further essential data on its role. Moreover, the prognosis of CRC treatment could be improved by leveraging the leptin signalling pathway or its derived peptides in a case of CRC.

CONCLUSION

Based on the reviewed papers from 2020 to date, leptin may be involved in the development and progression of CRC. Additionally, targeting leptin and its receptor during chemotherapy could contribute to a favorable prognosis, as it has the potential to induce chemoresistance. However, other studies have reported neither a causal correlation between leptin and CRC nor a statistically significant association. Given these discrepancies, there is an urgent need for additional studies with more meticulously designed, standardised methods and rigorous control measures to eliminate

potential confounding factors. For instance, obesity, the major risk factor for various forms of cancer, causes several changes, including mitochondrial dysfunction, which can also induce CRC. Thus, the increased level of leptin in such circumstances may not necessarily indicate that leptin is the cause of CRC. This review also highlights the necessity for additional clarification of and research into the mechanisms and clinical implications of leptin's effects on CRC.

REFERENCES

1. Jiménez-Cortegana C, López-Saavedra A, Sánchez-Jiménez F, Pérez-Pérez A, Castiñeiras J, Virizuela-Echaburu JA, et al. Leptin, both bad and good actor in cancer. Biomolecules. 2021; 11: 913.

2. Pérez-Pérez A, Sánchez-Jiménez F, Vilariño-García T, Sánchez-Margalet V. Role of leptin in inflammation and vice versa. Int J Mol Sci. 2020; 21: 5887.

3. Singh S, Mayengbam SS, Chouhan S, Deshmukh B, Ramteke P, Athavale D, et al. Role of TNFα and leptin signaling in colon cancer incidence and tumor growth under obese phenotype. Biochim Biophys Acta Mol Basis Dis. 2020; 1866: 165660.

4. Alagheband Y, Jafari-gharabaghlou D, Imani M, Mousazadeh H, Dadashpour M, Firouzi-Amandi A et al. Design and fabrication of a dual-drug loaded nano-platform for synergistic anticancer and cytotoxicity effects on the expression of leptin in lung cancer treatment. J Drug Delivery Sci Tech. 2022; 73:103389.

5. Wang Y, Li J, Fu X, Li J, Liu L, Alkohlani A, et al. Association of circulating leptin and adiponectin levels with colorectal cancer risk: a systematic review and meta-analysis of case-control studies. Cancer Epidemiol. 2021; 73: 101958.

6. Albosta M, Bakke J. Intermittent fasting: is there a role in the treatment of diabetes? A review of the literature and guide for primary care physicians. Clin Diabetes Endocrinol. 2021; 7: 3.

7. Ayed K, Nabi L, Akrout R, Mrizak H, Gorrab A, Bacha D, et al. Obesity and cancer: focus on leptin. Mol Biol Rep. 2023; 50: 6177–89.

8. Al-Hussaniy HA, Alburghaif AH, Naji MA. Leptin hormone and its effectiveness in reproduction, metabolism, immunity, diabetes, hopes and ambitions. J Med Life. 2021; 14: 600–5.

9. Pham DV, Tilija Pun N, Park PH. Autophagy activation and SREBP-1 induction contribute to fatty acid metabolic reprogramming by leptin in breast cancer cells. Mol Oncol. 2021; 15: 657–78.

10. Park KB, Kim EY, Chin H, Yoon DJ, Jun KH. Leptin stimulates migration and invasion and maintains cancer stem like properties in gastric cancer cells. Oncol Rep. 2022; 48: 162.

11. Słabuszewska-Jóźwiak A, Lukaszuk A, Janicka-Kośnik M, Wdowiak A, Jakiel G. Role of leptin and adiponectin in endometrial cancer. Int J Mol Sci. 2022; 23: 5307.

Gazi Med J 2026;37(1):135-140

Akanbong et al. Leptin as a Prognostic Biomarker in Colorectal Cancer

12. Boroń D, Nowakowski R, Grabarek BO, Zmarzły N, Opławski M. Expression pattern of leptin and its receptors in endometrioid endometrial cancer. J Clin Med. 2021; 10: 2787.

13. Kamel HFM, Nassir AM, Al Refai AA. Assessment of expression levels of leptin and leptin receptor as potential biomarkers for risk of prostate cancer development and aggressiveness. Cancer Med. 2020; 9: 5687–96.

14. Zhao S, Liu Y, He L, Li Y, Lin K, Kang Q, et al. Gallbladder cancer cell-derived exosome-mediated transfer of leptin promotes cell invasion and migration by modulating STAT3-mediated M2 macrophage polarization. Anal Cell Pathol (Amst). 2022; 2022: 9994906.

15. Lipsey CC, Harbuzariu A, Robey RW, Huff LM, Gottesman MM, Gonzalez-Perez RR. Leptin signaling affects survival and chemoresistance of estrogen receptor negative breast cancer. Int J Mol Sci. 2020; 21: 3794.

16. Salmani Javan E, Lotfi F, Jafari-Gharabaghlou D, Mousazadeh H, Dadashpour M, Zarghami N. Development of a magnetic nanostructure for co-delivery of metformin and silibinin on growth of lung cancer cells: possible action through leptin gene and its receptor regulation. Asian Pac J Cancer Prev. 2022; 23: 519–27.

17. Feng H, Zhang Q, Zhao Y, Zhao L, Shan B. Leptin acts on mesenchymal stem cells to promote chemoresistance in osteosarcoma cells. Aging (Albany NY). 2020; 12: 6340–51.

18. Wang WJ, Lai HY, Zhang F, Shen WJ, Chu PY, Liang HY, et al. MCL1 participates in leptin-promoted mitochondrial fusion and contributes to drug resistance in gallbladder cancer. JCI Insight. 2021; 6: e135438.

19. Chen YC, Chien CY, Hsu CC, Lee CH, Chou YT, Shiah SG, et al. Obesity-associated leptin promotes chemoresistance in colorectal cancer through YAP-dependent AXL upregulation. Am J Cancer Res. 2021; 11: 4220–40.

20. Lee J, Lee KS, Kim H, Jeong H, Choi MJ, Yoo HW, et al. The relationship between metabolic syndrome and the incidence of colorectal cancer. Environ Health Prev Med. 2020; 25: 6.

21. Chludzińska-Kasperuk S, Lewko J, Sierżantowicz R, Krajewska-Kułak E, Reszeć-Giełażyn J. The effect of serum leptin concentration and leptin receptor expression on colorectal cancer. Int J Environ Res Public Health. 2023; 20: 4951.

22. Li C, Quan J, Wei R, Zhao Z, Guan X, Liu Z, et al. Leptin overexpression as a poor prognostic factor for colorectal cancer. Biomed Res Int. 2020; 2020: 7532514.

23. Mhaidat NM, Alzoubi KH, Kubas MA, Banihani MN, Hamdan N, Al-Jaberi TM. High levels of leptin and non-high molecular weight-adiponectin in patients with colorectal cancer: Association with chemotherapy and common genetic polymorphisms. Biomed Rep. 2021; 14: 13.

24. Erkasap N, Ozyurt R, Ozkurt M, Erkasap S, Yasar F, Ihtiyar E, et al. Role of Notch, IL-1 and leptin expression in colorectal cancer. Exp Ther Med. 2021; 21: 600.

25. Shahraki N, Mehrabian A, Amiri-Darban S, Moosavian SA, Jaafari MR. Preparation and characterization of PEGylated liposomal Doxorubicin targeted with leptin-derived peptide and evaluation of their anti-tumor effects, *in vitro* and *in vivo* in mice bearing C26 colon carcinoma. Colloids Surf B Biointerfaces. 2021; 200: 111589.

26. Lin TC, Hsiao M. Leptin and cancer: updated functional roles in carcinogenesis, therapeutic niches, and developments. Int J Mol Sci. 2021; 22: 2870.

27. Pan CF, Zhang X, Wang JW, Yang T, Zhong LLD, Shen KP. Weichang'an Formula inhibits tumor growth in combination with bevacizumab in a murine model of colon cancer-making up for the deficiency of bevacizumab by inhibiting VEGFR-1. Front Pharmacol. 2020; 11: 512598.

28. Zhao H, Ling Y, Mi S, Zhu J, Fan J, Yang Y, et al. [Associations of circulating leptin levels with colorectal adenoma and colorectal cancer: a case-control and Mendelian randomization study]. Nan Fang Yi Ke Da Xue Xue Bao. 2023; 43: 1989–97.

29. Mahmoudi-Nesheli M, Alizadeh-Navaei R, Vahedi L, Amjadi O, Taghvaei T, Maleki I, et al. Evaluation of circulating leptin and its receptor (Ob-R) tissue expression in colorectal cancer, a report from North of Iran. Iran J Pathol. 2023; 18: 299–305.

Histopathological and Clinical Examination of Spinal Tumors: A Single-Center Experience and Literature Review

Spinal Tümörlerinin Histopatolojik ve Klinik İncelemesi: Tek Merkez Deneyimi ve Literatür Taraması

⦿ Tolga Türkmen[1], ⦿ Öykü Öztürk[2], ⦿ Zaur Güliyev[2], ⦿ Pelin Kuzucu[2], ⦿ Mesut Emre Yaman[2], ⦿ Gökhan Kurt[2],
⦿ Fikret Hüseyin Doğulu[2], ⦿ Ahmet Memduh Kaymaz[2], ⦿ Ömer Hakan Emmez[1], ⦿ Aydemir Kale[2]

[1]Güven Health Group Hospital, Ankara, Türkiye
[2] Clinic of Neurology, Department of Neurosurgery, Gazi University Faculty of Medicine, Ankara, Türkiye

ABSTRACT

Spinal tumors are distributed across various anatomical compartments and include diverse histopathological subtypes. However, most studies in the current literature focus on a limited range of tumor types or specific subgroups. This study aims to provide a comprehensive analysis of spinal tumors, offering a broader perspective on their clinical and pathological characteristics. We retrospectively reviewed clinical data from patients who underwent surgery for spinal tumors arising from the spinal cord or spinal column between 2010 and 2023. Clinical characteristics such as age, gender, presenting symptoms, histopathological features, tumor location, and anatomical compartment were evaluated. Approximately half of the spinal tumors in our series were located in the extradural compartment. Among these, metastatic tumors accounted for 68% of cases, representing 31% of all spinal tumors. Intradural pathological subtypes, in decreasing order of frequency, were: schwannoma, meningioma, ependymoma, and astrocytic tumors; primary spinal column tumors included chordoma, hemangioma, and chondrosarcoma. Local pain was the most common initial symptom, particularly in ependymomas (47.8%). Motor deficits were most frequently associated with glial tumors (17%). This study demonstrates the broad pathological spectrum of surgically treated spinal tumors. Despite an accelerating diagnostic trend, the findings indicate only a modest increase in the need for surgical intervention in spinal metastases.

Keywords: Chordoma, extradural tumors, initial symptoms of spinal tumors, intradural tumors, primary spinal tumors, spinal metastases

ÖZ

Spinal tümörleri farklı anatomik kompartmanlarda gözlenir ve birçok histopatolojik alt tip içermektedir. Ancak mevcut literatürdeki çoğu çalışma, sınırlı sayıda tümör tipine veya belirli alt gruplara odaklanmaktadır. Bu çalışma, spinal tümörlerinin kapsamlı bir analizini sunmayı ve klinik ve patolojik özelliklerine daha geniş bir bakış açısı sunmayı amaçlamaktadır. 2010 ile 2023 yılları arasında omurilik veya vertebral kolondan köken alan spinal tümörler nedeniyle opere edilen hastaların klinik verileri retrospektif olarak incelenmiştir. Yaş, cinsiyet, ilk semptomları, histopatolojik özellikler, tümörün lokalizasyonu ve anatomik kompartmanları gibi karakteristik özellikler değerlendirilmiştir. Serimizdeki spinal tümörlerinin yaklaşık yarısı ekstradural kompartmanda yer almaktadır. Bunların arasında metastatik tümörler vakaların %68'ini oluşturmaktadır ve tüm spinal tümörlerinin %31'ini temsil etmektedir. İntradural kompartmandaki patolojik alt tipler, sıklık sırası azalan şekilde: schwannoma, menenjioma, ependiyoma ve astrositik tümörler; primer vertebral kolon tümörleri arasında kordoma, hemanjiyom ve kondrosarkom yer almaktadır. Lokal ağrı, özellikle metastazlarda (%75,2) en sık görülen başlangıç semptomuydu. Motor defisit ise en sık glial tümörlerle (%63,0) gözlemlenmiştir. Bu çalışma, cerrahi olarak tedavi edilen spinal tümörlerin geniş bir patolojik spektrumda olduğunu göstermektedir. Artan tanı oranlarına rağmen, bu bulgular spinal metastazlarda cerrahi müdahalede gerekliliğinde ılımlı bir artış olduğunu göstermektedir.

Anahtar Sözcükler: Kordoma, ekstradural tümörler, intradural tümörler, primer spinal tümörler, spinal metastazlar

Gazi Med J 2026;37(1):141-146

Türkmen et al. Spinal Tumors -A Single-Center Experience

INTRODUCTION

The term "spinal tumors" refers to neoplasms arising from the spinal cord, the vertebral column, or the surrounding structures. They are commonly classified according to their anatomical compartment as intramedullary–intradural, extramedullary–intradural, and extradural. The most frequently affected compartment is the extradural space. Within this region, metastatic spinal tumors (MSTs) (e.g., multiple myeloma, prostate, breast, thyroid, and lung) are the most frequently observed, whereas primary spinal osseous tumors (e.g., chordoma, haemangioma, and osteoblastoma) are rare (1-3). Within the intradural space, the most common subtypes are meningiomas, schwannomas, and ependymomas (4,5).

Given that localized spinal pain is an almost universal human experience, the increasing use of imaging techniques, along with their expanding indications, has led to an increase in incidental detection of spinal column-related neoplasms, although less frequently than other incidental pathologies (6,7). Despite the increasing prevalence of spinal neoplasms and advances in diagnostic and therapeutic capabilities, accurate incidence data for spinal tumor subtypes remain scarce. The main reasons for this include the heterogeneity of data sources across existing studies, the inclusion of cases treated with specific therapeutic approaches, and the focus on particular histopathological subtypes. Because spinal tumors are diverse, the incidence and characteristics of specific subgroups are often reported. Consequently, the accurate incidence of pathologies involving all compartments relevant to spinal surgery has yet to be established.

The clinical presentation of spinal tumors ranges from local and radicular pain to neurological deficits of varying severity due to compression of the spinal neural elements (8,9). In terms of treatment, the primary surgical principle for benign tumors is to employ techniques that allow maximum exposure and resection while minimizing damage to spinal stability. With the increasing adoption of minimally invasive approaches in spinal surgery, hemilaminectomy—once avoided due to the risk of inadequate decompression and unintended spinal cord injury—has now become more widely accepted (10,11). A multidisciplinary approach is generally the most appropriate choice for MSTs. Surgical intervention for metastatic tumors aims to relieve spinal cord compression, reduce tumor burden as much as possible, separate the tumor from critical tissues, and allow time for adjunctive treatments. It is also crucial to protect patients with active oncological conditions from the risks and complications of major surgeries.

In this study, conducted at one of the largest neurosurgery centers in Türkiye, we retrospectively reviewed the records of 407 patients with spinal tumors who underwent surgery from 2010 onward. Based on this review, we present our clinical experience in light of current literature.

MATERIALS AND METHODS

The routinely collected prospective electronic medical records of all operations for the treatment of spinal column tumors were retrospectively evaluated. Gazi University Ethics Committee reviewed and approved the research protocol for this study (approval number: 2023-1351, date: 18.04.20239). Patients who underwent surgery between 2010 and 2023 were included in the cohort. Various surgeons from the spine team at our clinic performed all operations. Baseline medical data, such as age, gender, presenting symptoms, and pathology, were included.

The tumors were classified as cervical, cervicothoracic, thoracic, thoracolumbar, lumbar, and sacral based on their level. Tumors involving the C7-T1 and T12-L1 segments were classified as cervicothoracic and thoracolumbar junctions, respectively. The cohort was segmented into axial anatomical compartments using magnetic resonance imaging and classified as intramedullary, intradural-extramedullary (ID-EM), or extradural tumors according to axial location within the spinal column. We excluded cases in which biopsy or vertebral augmentation had been performed, cases with relapses, and patients under 18 years of age. Data from cases with at least two years of radiological follow-up were evaluated to assess spinal alignment.

Since this study did not involve a defined cohort, statistical tests were unnecessary. Instead, the findings were evaluated descriptively, focusing on clinical observations and histopathological characteristics.

Results

A total of 491 patients who underwent surgery were considered for inclusion in the study, of whom 84 were excluded due to relapsed tumors or biopsy. Finally, 407 patients were enrolled: 198 females and 209 males, with a mean age of 50.2 ± 16.2 years.

The most common histological types were metastases (n = 129, 31.7%), schwannoma (n = 59, 14.5%), meningioma (n = 52, 12.8%), and ependymoma (n = 46, 11.3%). The gender distribution and median age varied by histological type (Table 1). Histological examination revealed the presence of various tumors in the other group, including five arachnoid cysts, four cavernomas, two angiosarcomas, five Ewing sarcomas, three hemangioblastomas, one lipoma, one medulloblastoma, one osteoblastoma, two osteofibromas, and one subependymoma. According to the axial location of the tumors within the spinal cord, 21.4% (n = 87) of the tumors were intramedullary, 27.3% (n = 111) were ID-EM 46.2% (n = 188) were extradural, involving the vertebral bone, while the remaining 5.1% (n = 21) exhibited a multicomponent pattern. Five metastases and three Ewing sarcomas were ID-EM, whereas two metastases were intramedullary.

The distribution of clinical symptoms was as follows: local pain (n = 241; 59.2%), motor deficit (n = 183; 45%), and sensory deficit (n = 143; 35.1%). Local pain was the most common clinical symptom across all histological subtypes. It was most frequently observed in metastases (n = 97; 75.2%), meningiomas (n = 32; 61.5%), schwannomas (n = 33; 55.9%), and ependymomas (n = 22; 47.8%). Glial tumors were most commonly associated with motor deficits at presentation (n = 17, 63.0%), while sensory deficits were most frequently observed in metastases. All clinical symptoms are summarized in Table 2. Regarding tumor location, 16.5% (n = 67) were in the cervical region, 3.7% (n = 15) in the cervicothoracic region, 39% (n = 159) in the thoracic region, 4.7% (n = 19) in the thoracolumbar region, 31% (n = 126) in the lumbar region, and 5.1% (n = 21) in the sacral region (Table 3).

Eight cases were operated on via an anterior approach, while the others were operated on via a posterolateral approach.

Gazi Med J 2026;37(1):141-146

Türkmen et al. Spinal Tumors -A Single-Center Experience

Table 1. Demographic information and gender distribution of histopathological subtypes.

	Female		Male		Total		The median age
	n	%	n	%	n	%	
Meningioma	40	20.2	12	5.7	52	12.8	58.9 ± 17
Schwannoma	31	15.7	28	13.4	59	14.5	42.2 ± 13
Ependymoma	21	10.6	25	12.0	46	11.3	42.2 ± 14
Astrocytic tumors	20	10.1	7	3.3	27	6.6	40.4 ± 15
Epidermoid tumors	2	1.0	5	2.4	7	1.7	41.1 ± 8
Dermoid tumors	2	1.0	5	2.4	7	1.7	33.7 ± 10
Other intradural tumors	7	3.5	8	3.8	15	3.7	-
Metastases	46	23.2	83	39.7	129	31.7	59.1 ± 13
Chordoma	6	3.0	11	5.3	17	4.2	58.2 ± 10
Hemangioma	8	4.0	2	1.0	10	2.5	51.5 ± 13
Chondrosarcoma	5	2.5	1	0.5	6	1.5	35.3 ± 14
Osteosarcoma			5	2.4	5	1.2	46.2 ± 24
Aneurysmal bone cyst	1	0.5	3	1.4	4	1.0	40.0 ± 11
Giant cell tumor	2	1.0	1	0.5	3	0.7	47.3 ± 23
Ewing sarcoma	3	1.5	2	1.0	5	1.2	34.2 ± 10
Other mesenchymal tumors	3	1.5	6	2.9	9	2.2	-
Unclassified	1	0.5	5	2.4	6	1.5	-
Total	198		209		407		

Table 2. Distribution of common symptoms by axial location.

	Local pain		Motor deficits		Sensory deficits	
	n	%	n	%	n	%
Intramedullary	50	57.5%	36	41.4%	28	32.2%
Ependymoma	22	47.8%	14	30.4%	15	32.6%
Astrocytic tumors	15	55.6%	17	63.0%	7	25.9%
Intradural-extramedullary	66	59.5%	57	51.4%	46	41.4%
Meningioma	32	61.5%	24	46.2%	24	46.2%
Schwannoma	33	55.9%	26	44.1%	19	32.2%
Extradural	125	63.5%	90	45.7%	69	35%
Metastases	97	75.2%	74	57.4%	50	38.8%
Chordoma	7	41.2%	5	29.4%	7	41.2%
Other primary bone tumors*	18	42.9%	9	21.4%	11	26.2%

*Hemangioma, chondrosarcoma, osteosarcoma, aneurysmal bone cyst, giant cell tumor, Ewing sarcoma, other mesenchymal tumors.

Hemilaminectomy was performed in 103 cases. Among the 143 bilateral laminectomy cases with at least two years of follow-up after surgery, 23% showed a radiological increase in the local kyphosis angle; however, none required reconstruction with instrumentation. A total of 16 patients (4%) underwent posterior instrumentation during the initial surgery. Among them, 9 had metastases, 6 had tumors of bone origin, and 1 had a schwannoma with extradural extension.

DISCUSSION

This study focused on the histological distribution, demographic characteristics, and epidemiological features of all spinal neoplasms treated surgically. The cases had a mean age of 50 ± 16 years, with an equal gender distribution. The mean age was higher in cases of metastasis, meningioma, and chordoma than in other pathologies, consistent with previous reports. Data analysis revealed that spinal tumors were most frequently located in the extradural compartment (46.2%), a proportion that although slightly lower than figures reported in the literature, is within a comparable range (12).

Gazi Med J 2026;37(1):141-146

Türkmen et al. Spinal Tumors -A Single-Center Experience

Table 3. Distribution of histopathological subtypes by spinal level.

	Cervical		Cervicothoracic		Thoracic		Thoracolumbar		Lumbar		Sacrum	
	n	%	n	%	n	%	n	%	n	%	n	%
Meningioma	6	11.5	2	3.8	39	75.0	2	3.8	3	5.8	-	-
Ependymoma	14	30.4	4	8.7	7	15.2	3	6.5	18	39.1	-	-
Schwannoma	13	22.0	2	3.4	15	25.4	2	3.4	26	44.1	1	1.7
Astrocytic tumors	7	25.9	2	7.4	10	37.0	3	11.1	3	11.1	2	7.4
Metastases	9	7.0	4	3.1	59	45.7	4	3.1	45	34.9	8	6.2
Hemangioma	0	-	-	-	8	80.0	-	0.0	2	20.0	-	-
Chordoma	5	29.4	-	-	2	11.8	1	5.9	1	5.9	8	47.1
Chondrosarcoma	0	-	-	-	1	16.7	-	0.0	5	83.3	-	-
Total	67	16.5	15	3.7	159	39	19	4.7	126	31	21	5.1

Metastases accounted for 68% of lesions in the extradural compartment and 31% of all spinal tumors, representing the most common subtype of spinal neoplasms, as reported in previous studies. Among primary bone tumors located in the extradural compartment, chordoma (9%) and haemangioma (5%) were the most frequently observed. Contrary to the commonly held view, primary spinal tumors constituted 10% of spinal tumors, a relatively high proportion (3,6).

Intradural tumors are among the rarest tumor types, comprising 4–8% of central nervous system tumors (13,14). Extramedullary lesions are the most common intradural lesions. The most frequently observed tumors within the ID-EM category are meningiomas, which account for 16–25% of cases (5,14,15). These tumors typically occur in women and are most often found in the thoracic vertebrae. In our series, meningiomas comprised 22% of ID-EM tumors, with a female-to-male ratio of 3.5:1. In only one case, the tumor extended from the dural defect into the epidural space rather than the intradural space. Extradural meningiomas can also mimic schwannomas (16,17). Despite the relatively advanced mean age at diagnosis (58.9 ± 17 years), they generally show a good prognosis, provided there is no invasion of the arachnoid or pia mater (18,19).

Although schwannomas are reported as the second most common tumor in ID-EM, epidemiological studies report that schwannomas are more common than meningiomas (15). They are mainly located intradurally, originating from the dorsal root, but 10–15% extend extradurally. They are observed at roughly equal frequency in both sexes, and the average age at diagnosis is 47 years. Our findings are consistent with those reported in the literature and with findings from our series. Schwannomas can occur as solitary or multiple lesions at any spinal level, but despite numerous series in the literature, there is no consensus regarding the most commonly affected spinal level. In their recent meta-analysis, Alvarez-Crespo et al. (20) reported that the cervical region is the most common segment. Contrary to what has been reported in the literature, we found that the lumbar region was the most common site in our series, accounting for 44.1% of cases. Schwannomas are known to be slow-growing tumors and generally present with radicular pain and myelopathic findings; however, in our series, local pain was the most frequently observed symptom (21,22).

Ependymomas are usually benign lesions, most commonly occurring in the cervical region. The incidence is slightly male-predominant, and in our series males accounted for 54%. The bimodal age distribution of ependymomas is a recognised feature; the mean age in our series is 42.0 ± 1.9 years. The relatively high mean age in our cohort may result from including only adult patients. The most common symptoms at diagnosis are local pain and sensory deficits. However, owing to the greater accessibility of radiological imaging, diagnoses are made earlier; therefore, sensory deficit complaints are more frequently observed (23). In our series, local pain was observed in 47.8% of patients, while a sensory deficit was present in 32.2%.

In our series, astrocytomas accounted for 42% of primary intramedullary tumors, with a mean patient age of 40.2 years. Contrary to the literature, a female predominance (64.3%) was observed in our study. Motor and sensory deficits are more frequently observed in spinal cord astrocytomas than in other intradural tumors (24,25). In our series, the most commonly observed symptom was motor deficit. This finding may be attributed to increased edema caused by early changes in the tumor microenvironment of astrocytomas (24,26). Compared with childhood, spinal astrocytomas in adults are associated with a worse prognosis (27). Tumor grade and histological type play a crucial role in determining prognosis. In particular, a well-defined surgical dissection plane in pilocytic lesions increases the likelihood of total resection (28,29). Although intraoperative neuromonitoring has been observed to encourage more extensive surgical resection in anaplastic astrocytomas, studies have shown that even gross total resection does not contribute to survival in glioblastomas (30,31).

Spinal column lesions, the majority of which are bone metastases, are increasingly encountered owing to improved survival among patients with primary malignancies (32,33). Extradural lesions account for approximately 60% of spinal oncological cases (12). In our series, 46.2% of spinal tumors were extradural, with the thoracic region the most commonly involved site. MSTs are the most frequently observed extradural lesions. Approximately 10–30% of cancer patients develop spinal metastases; however, it is estimated that only 10–20% of these cases become symptomatic (2,34,35). Consistent with the literature, three-quarters of the

Gazi Med J 2026;37(1):141-146

Türkmen et al. Spinal Tumors -A Single-Center Experience

cases in our series were located in this anatomical region; only four were intradural. MSTs typically spread hematogenously through the extensive venous plexus of the vertebrae. Anatomically, they tend to extend posteriorly to involve the pedicle. Despite their high prevalence, MSTs often present with minimal clinical symptoms. This highlights the importance of routine metastasis screening and early detection programs (36). During our screening, localized pain was detected in three-quarters of MST cases, whereas sensory or motor deficits were observed in half of cases. The inclusion of only surgically treated patients in our series may have influenced these findings.

Primary bone tumors of the spine (PSTs) are rare and mostly benign lesions (6). This group includes hemangiomas, osteoid osteomas, aneurysmal bone cysts, osteochondromas, neurofibromas, giant cell tumors of bone, and eosinophilic granulomas. Benign primary bone tumors account for approximately 41% of all bone tumors. However, conflicting reports exist regarding which primary bone tumor is most frequently observed. Dang et al. (6) reported giant cell tumors as the most common PST in their series, whereas Kelley et al. (37) identified multiple myeloma as the most frequently observed PST. This discrepancy arises from differences in the theoretical classification of myeloma, as many studies consider it a metastatic, rather than a primary, spinal tumor. In our series, the proportion of benign lesions was low, and the most frequently observed tumor was chordoma. This result appears lower than those reported in the literature, likely due to the high number of chordoma cases in our series. The role of the center where the study was conducted as a referral center for complex spinal tumors may have contributed to this finding. Benign lesions are often diagnosed incidentally, as their clinical presentation tends to be non-specific and subtle. In most cases, observation is the preferred treatment approach. However, in patients with persistent pain or neurological compression, surgical intervention may become necessary (38).

Primary malignant spinal tumors generally exhibit locally aggressive behavior (6). The most common subtypes include chordoma, chondrosarcoma, Ewing sarcoma, and osteosarcoma. Although these tumors can develop at any vertebral segment, they most frequently occur at the cranial and caudal ends of the spine. The sacrum and cervical spine were the most common locations in our series, with prevalence rates of 47% and 29%, respectively. The age at diagnosis of chordomas varies widely; consistent with the literature, the mean age in our series was 58.1 ± 9.37 years, with a male predominance. Surgery is the primary treatment modality; however, defining the tumor margins intraoperatively remains challenging. Currently, maximal surgical resection followed by adjuvant therapy is the most effective approach for local disease control.

Posterior approaches are used in nearly all surgical procedures for intradural tumors. The techniques most commonly used are hemilaminectomy and laminectomy. In spinal surgery, there is a growing trend toward minimally invasive techniques to preserve stability and minimize muscle damage. In line with this trend, the literature suggests an increasing preference for hemilaminectomy in tumor resection (10,39). Although unilateral hemilaminectomy offers theoretical advantages such as reduced blood loss, earlier discharge, and faster recovery, cohort studies have shown no significant superiority over laminectomy in these aspects (39). In our series, protective laminectomy preserving the facet joints was the predominant approach for intradural tumors (168/226). Despite an increased kyphotic angle observed radiologically during follow-up, no patients exhibited clinical symptoms requiring reconstruction. Among the cases that underwent bilateral laminectomy, 25 of involved the junctional region. Midline bilateral laminectomies, performed while preserving the facet joints, can be considered reliable methods for tumor resection because of their extensive exposure.

Study Limitions

Our study has limitations owing to its retrospective design. First, because our cohort included only surgically treated patients, those managed conservatively were not evaluated. Secondly, some spinal tumor subtypes had small sample sizes, which may have led to discrepancies in incidence rates compared with those reported in the literature. Additionally, this study may be criticized for relying on data from a single institution, which could introduce selection bias. Another limitation is the incomplete follow-up data for some cases. Nevertheless, data obtained from a national referral center will contribute to the epidemiological and descriptive literature.

Conclusion

This study has established a comprehensive database on spinal tumors by analyzing data from 407 patients with various tumor types. The primary aim is to reveal the true prevalence of spinal neoplasms requiring surgical intervention. Although metastases constitute the majority of diagnostically identified spinal tumors, their proportion in surgical series does not markedly differ from that of other spinal pathologies.

Ethics

Footnotes

Authorship Contributions

Surgical and Medical Practices: T.T., M.E.Y., G.K., F.H.D., A.M.K., Ö.H.E., A.K., Concept: T.T., P.K., A.K., Design: T.T., P.K., A.M.K., Ö.H.E., A.K., Data Collection or Processing: Ö.Ö., Z.G., F.H.D., A.M.K., Analysis or Interpretation: Ö.Ö., G.K., Literature Search: T.T., Ö.Ö., Z.G., G.K., Writing: T.T., Ö.Ö., P.K., M.E.Y., A.K.

REFERENCES

1. Bollen L, van der Linden YM, Pondaag W, Fiocco M, Pattynama BP, Marijnen CA, et al. Prognostic factors associated with survival in patients with symptomatic spinal bone metastases: a retrospective cohort study of 1,043 patients. Neuro Oncol. 2014; 16: 991–8.

Gazi Med J 2026;37(1):141-146

Türkmen et al. Spinal Tumors -A Single-Center Experience

2. Wang F, Zhang H, Yang L, Yang XG, Zhang HR, Li JK, et al. Epidemiological characteristics of 1196 patients with spinal metastases: a retrospective study. Orthop Surg. 2019; 11: 1048–53.

3. Zhou Z, Wang X, Wu Z, Huang W, Xiao J. Epidemiological characteristics of primary spinal osseous tumors in Eastern China. World J Surg Oncol. 2017; 15: 73.

4. Duong LM, McCarthy BJ, McLendon RE, Dolecek TA, Kruchko C, Douglas LL, et al. Descriptive epidemiology of malignant and nonmalignant primary spinal cord, spinal meninges, and cauda equina tumors, United States, 2004-2007. Cancer. 2012; 118: 4220–7.

5. Ottenhausen M, Ntoulias G, Bodhinayake I, Ruppert FH, Schreiber S, Förschler A, et al. Intradural spinal tumors in adults-update on management and outcome. Neurosurg Rev. 2019; 42: 371–88.

6. Dang L, Liu X, Dang G, Jiang L, Wei F, Yu M, et al. Primary tumors of the spine: a review of clinical features in 438 patients. J Neurooncol. 2015; 121: 513–20.

7. Hall H. Effective spine triage: patterns of pain. Ochsner J. 2014; 14: 88–95.

8. Cole JS, Patchell RA. Metastatic epidural spinal cord compression. Lancet Neurol. 2008; 7: 459–66.

9. Patchell RA, Tibbs PA, Regine WF, Payne R, Saris S, Kryscio RJ, et al. Direct decompressive surgical resection in the treatment of spinal cord compression caused by metastatic cancer: a randomised trial. Lancet. 2005; 366: 643–8.

10. Liao D, Li D, Wang R, Xu J, Chen H. Hemilaminectomy for the removal of the spinal tumors: an analysis of 901 patients. Front Neurol. 2023; 13: 1094073.

11. Pompili A, Caroli F, Crispo F, Giovannetti M, Raus L, Vidiri A, et al. Unilateral laminectomy approach for the removal of spinalmeningiomas and schwannomas: impact on pain, spinal stability, and neurologic results. World Neurosurg. 2016; 85: 282–91.

12. Kumar N, Tan WLB, Wei W, Vellayappan BA. An overview of the tumors affecting the spine-inside to out. Neurooncol Pract. 2020; 7: i10–7.

13. Engelhard HH, Villano JL, Porter KR, Stewart AK, Barua M, Barker FG, et al. Clinical presentation, histology, and treatment in 430 patients with primary tumors of the spinal cord, spinal meninges, or cauda equina. J Neurosurg Spine. 2010; 13: 67–77.

14. Schellinger KA, Propp JM, Villano JL, McCarthy BJ. Descriptive epidemiology of primary spinal cord tumors. J Neurooncol. 2008; 87: 173–9.

15. Jung KW, Park KH, Ha J, Lee SH, Won YJ, Yoo H. Incidence of primary spinal cord, spinal meninges, and cauda equina tumors in Korea, 2006-2010. Cancer Res Treat. 2015; 47: 166–72.

16. Nakamizo A, Suzuki SO, Shimogawa T, Amano T, Mizoguchi M, Yoshimoto K, et al. Concurrent spinal nerve root schwannoma and meningioma mimicking single-component schwannoma. Neuropathology. 2012; 32: 190–5.

17. Garaud S, Boto J, Egervari K, Vargas MI. Extradural spinal meningioma mimicking a schwannoma: magnetic resonance imaging findings. Can J Neurol Sci. 2022; 49: 467–9.

18. Sacko O, Rabarijaona M, Loiseau H. La chirurgie des méningiomes rachidiens après 75 ans. Neurochirurgie. 2008; 54: 512–6.

19. Setzer M, Vatter H, Marquardt G, Seifert V, Vrionis FD. Management of spinal meningiomas: surgical results and a review of the literature. Neurosurg Focus. 2007; 23: E14.

20. Alvarez-Crespo DJ, Conlon M, Kazim SF, Skandalakis GP, Bowers CA, Chhabra K, et al. Clinical characteristics and surgical outcomes of 2542 patients with spinal schwannomas: a systematic review and meta-analysis. World Neurosurg. 2024; 182: 165–83.

21. Chen P, Guo Y, Huang R, Xiao J, Cheng Z. Spinal schwannoma causes acute subarachnoid haemorrhage: a case report and literature review. Neurochirurgie. 2021; 67: 495–9.

22. Jenkins AL 3rd, Ahuja A, Oliff AH, Sobotka S. Spinal Schwannoma presenting due to torsion and hemorrhage: case report and review of literature. Spine J. 2015; 15: e1–4.

23. Klekamp J. Spinal ependymomas. Part 1: Intramedullary ependymomas. Neurosurg Focus. 2015; 39: E6.

24. Abd-El-Barr MM, Huang KT, Chi JH. Infiltrating spinal cord astrocytomas: Epidemiology, diagnosis, treatments and future directions. J Clin Neurosci. 2016; 29: 15–20.

25. Beyer S, von Bueren AO, Klautke G, Guckenberger M, Kortmann RD, Pietschmann S, et al. A systematic review on the characteristics, treatments and outcomes of the patients with primary spinal glioblastomas or gliosarcomas reported in literature until march 2015. PLoS One. 2016; 11: e0148312.

26. Pang B, An S, Liu Y, Jiang T, Jia W, Chai R, et al. Understanding spinal cord astrocytoma: Molecular mechanism, therapy, and comprehensive management. Cancer Lett. 2024; 601: 217154.

27. Bagley CA, Wilson S, Kothbauer KF, Bookland MJ, Epstein F, Jallo GI. Long term outcomes following surgical resection of myxopapillary ependymomas. Neurosurg Rev. 2009; 32: 321–34.

28. Minehan KJ, Shaw EG, Scheithauer BW, Davis DL, Onofrio BM. Spinal cord astrocytoma: pathological and treatment considerations. J Neurosurg. 1995; 83: 590–5.

29. Raco A, Esposito V, Lenzi J, Piccirilli M, Delfini R, Cantore G. Long-term follow-up of intramedullary spinal cord tumors: a series of 202 cases. Neurosurgery. 2005; 56: 972–81.

30. McGirt MJ, Chaichana KL, Atiba A, Bydon A, Witham TF, Yao KC, et al. Incidence of spinal deformity after resection of intramedullary spinal cord tumors in children who underwent laminectomy compared with laminoplasty. J Neurosurg Pediatr. 2008; 1: 57–62.

31. Adams H, Avendaño J, Raza SM, Gokaslan ZL, Jallo GI, Quiñones-Hinojosa A. Prognostic factors and survival in primary malignant astrocytomas of the spinal cord: a population-based analysis from 1973 to 2007. Spine (Phila Pa 1976). 2012; 37: E727–35.

32. Macedo F, Ladeira K, Pinho F, Saraiva N, Bonito N, Pinto L, et al. Bone metastases: an overview. Oncol Rev. 2017; 11: 321.

33. Saad F, Ivanescu C, Phung D, Loriot Y, Abhyankar S, Beer TM, et al. Skeletal-related events significantly impact health-related quality of life in metastatic castration-resistant prostate cancer: data from PREVAIL and AFFIRM trials. Prostate Cancer Prostatic Dis. 2017; 20: 110-6.

34. Fridley JS, Syed S, Niu T, Leary OP, Gokaslan ZL. Presentation of spinal cord and column tumors. Neurooncol Pract. 2020; 7: i18–24.

35. Sutcliffe P, Connock M, Shyangdan D, Court R, Kandala NB, Clarke A. A systematic review of evidence on malignant spinal metastases: natural history and technologies for identifying patients at high risk of vertebral fracture and spinal cord compression. Health Technol Assess. 2013; 17: 1–274.

36. Sciubba DM, Petteys RJ, Dekutoski MB, Fisher CG, Fehlings MG, Ondra SL, et al. Diagnosis and management of metastatic spine disease. A review. J Neurosurg Spine. 2010; 13: 94–108.

37. Kelley SP, Ashford RU, Rao AS, Dickson RA. Primary bone tumours of the spine: a 42-year survey from the Leeds Regional Bone Tumour Registry. Eur Spine J. 2007; 16: 405–9.

38. Boriani S, Weinstein JN, Biagini R. Primary bone tumors of the spine. Terminology and surgical staging. Spine (Phila Pa 1976). 1997; 22: 1036–44.

39. Gu R, Liu JB, Xia P, Li C, Liu GY, Wang JC. Evaluation of hemilaminectomy use in microsurgical resection of intradural extramedullary tumors. Oncol Lett. 2014; 7: 1669–72.